Non-Linear and Linear System Identification of Debutanizer Column

by

Mohamad Razlan bin Md Radzi
13545

Dissertation submitted in partial fulfilment of
the requirements for the
Bachelor of Engineering (Hons)
(Chemical Engineering)

May 2014

Universiti Teknologi PETRONAS
Bandar Seri Iskandar
31750 Tronoh
Perak Darul Ridzuan

CERTIFICATION

CERTIFICATION OF APPROVAL

Linear and Nonlinear System Identification of Debutanizer Column

by

Mohamad Razlan bin Md Radzi
13545

A project dissertation submitted to the

Chemical Engineering Programme

Universiti Teknologi PETRONAS

in partial fulfilment of the requirement for the

BACHELOR OF ENGINEERING (Hons)

(CHEMICAL ENGINEERING)

Approved by,

_____

(Nasser bin Mohamed Ramli)

UNIVERSITI TEKNOOGI PETRONAS

TRONOH, PERAK

May 2014

CERTIFICATION OF ORIGINALITY

This is to certify that I am responsible for the work submitted in this project, that the original work is my own except as specified in the references and acknowledgements, and that the original work contained herein have not been undertaken or done by unspecified sources or persons.

_____

MOHAMAD RAZLAN BIN MD RADZI

ABSTRACT

Debutanizer column is one of the common unit operation in a chemical industry. The column is complex and unpredictable in nature, making them difficult to be handled. Hence, system identification is used in identifying and estimate mathematical models of dynamic systems of the debutanizer column from measured data. The identification was done to achieve stability of the debutanizer column through simulation through obtaining linear and non-linear process models using System Identification Toolbox.

In this simulation, process model or polynomial model tool will be used to identify linear system and as for nonlinear system, nonlinear model tool is the tool of choice. Based on results obtained from linear system identification, the system is unstable under linear condition. As for nonlinear system identification, the system is stable at certain parameter and unstable at the rest. Further work needs to be done to improve the result.

ACKNOWLEDGEMENT

In completion of this final year project, I would like to thank Universiti Teknologi PETRONAS for providing me with the opportunity to conduct this study. I would also like to express my gratitude to my supervisor, Mr Nasser bin Mohamed Ramli for his continuous support and motivation throughout the project. Finally, I would like to thank my parents for their continuous support and encouragement which driven me to complete this project.

TABLE OF CONTENTS

TABLE OF FIGURES

CHAPTER 1

INTRODUCTION

1.1 Background of Study

Debutanizer column is one of the most common unit operations in the chemical industry especially the crude oil industry. It is a type of fractional distillation column that is used to separate butane from natural gas, especially during the refining process (wiseGEEK, n.d.). Debutanizer column is controlled usually by manipulating the top and bottom composition of the column, in order to attain the desired purity of products (Mohamed Ramli, Hussain, Mohamed Jan, & Abdullah, 2014). Hence, various methods are used to estimate and identify and predict this problem with high precision and accuracy; one of them is system identification.

System identification is a common method that is still widely used in identifying and estimate mathematical models of dynamic systems from measured data (Ljung & MathWorks, 2005). It can be used for creating and using models of dynamic systems easily, by using both time-domain and frequency-domain input-output data to recognize continuous-time and discrete-time transfer functions, process models, and state-space models (MathWorks, n.d.).

In this project, process modelling of debutanizer column will be identified using the System Identification Toolbox in MATLAB program. The data for this simulation project is taken from a debutanizer column located in a crude oil industry.

1.2 Problem Statement

Debutanizer column is a complex unit operation that is unpredictable in nature, making them difficult to be handled by engineers. Most of the complexity of the process of controlling the column comes from unique characteristics of the column itself, such as complex dynamics, high nonlinearity and interaction between the control loops (Gupta, Ray, & Samanta, 2009) (Mohamed Ramli et al., 2014).

However, based on researches, by identifying the transfer model and system model, behaviour of the debutanizer column can be known, making stabilizing the column possible.

1.3 Objectives

The objectives of this project are:

i. To achieve stability of the debutanizer column through simulation.
ii. To obtain linear and non-linear process models using System Identification Toolbox.
iii. To analyse the data obtained and plot required charts.

1.4 Scope of Study

Despite the broad methods in determining the process models of debutanizer column, the scope of this study the study is only limited to identifying process models for the overhead pressure of liquefied petroleum gas using linear and non-linear system identification. This project will only use System Identification Toolbox to identify the process models and MATLAB to plot graphs for data analysis, although there is other software various available to identify process model.

CHAPTER 2

LITERATURE REVIEW

2.1 Column Description

2.1.1 Crude Oil Distillation Column

In overall, crude oil distillation column consists of three sections, which receives crude oil to form liquefied petroleum gas as the main product which is produced at debutanizer column and other by-products such as petroleum products and naphtha. As stated by Mohamed Ramli et al. (2014) and Bousono Zavala (2011) distillation column consists of two parts, Catalytic Reforming Unit (CRU) or known as the front end, of which reactor-refrigerator and main fractionator is located, and Crude Distillation Unit (CDU), also known as the front end. The main focus is at Crude Distillation Unit (CDU), where debutanizer column was located.

2.1.2 Debutanizer Column

As for debutanizer column, it acts as the main column to produce the main product which is liquefied petroleum gas. The column is located at Crude Distillation Unit (CDU). The column first receives unstabilized naphtha as a feed from the crude distiller and start fractionating the naphtha into two parts, where light ends is removed at the top section and debutanized naphtha is removed from the bottom. The condensed liquid from overhead product from the top section will then be directed to liquefied petroleum gas (LPG) section where further processes will be done to further purify the product. Ansari and Tadé (1998), explains that there will be some of the condensed liquid being reflowed to control the product and bottom quality.

Based on Huang and Riggs (2002) and Gupta et al. (2009), most of the debutanizer column condenser operated as a flooded condenser and there is no liquid level indicator placed in the condenser. If overloaded, flooding on the column may occur.

Thus, overhead pressure is controlled by altering distillate product flow, which acts as an effective liquid level indicator in the condenser.

2.2 System Identification Toolbox

System can be defined as the overall behaviour that is studied while model can be defined as internal representation of the whole system that is used in order to study the system. That means system identification is the study of overall behaviour of the system using model as a representation (Pelckmans, 2012). System identification is also a process of gaining parameter estimation based on observations that originates from a dynamical system and it also deals with many restraints that surfaces in the process of designing, conducting and interpreting results (MathWorks, n.d.).

System Identification Toolbox is a program that is developed by MATLAB in order to assist in obtaining process models from a set of data accurately and precisely. It has various functions and models such as transfer function, process model, and state-space model identification. This can be done in either time-domain or frequency-domain response data. System Identification Toolbox can also perform model estimation using various models such as maximum likelihood. Finally, this toolbox is also able to perform delay estimation and reconstruction of missing data (MathWorks, n.d.).

There are various tools that is useful for both linear and nonlinear system identification. However, in this simulation, process model or polynomial model tool will be used to identify linear system and as for nonlinear system, nonlinear model tool is the tool of choice.

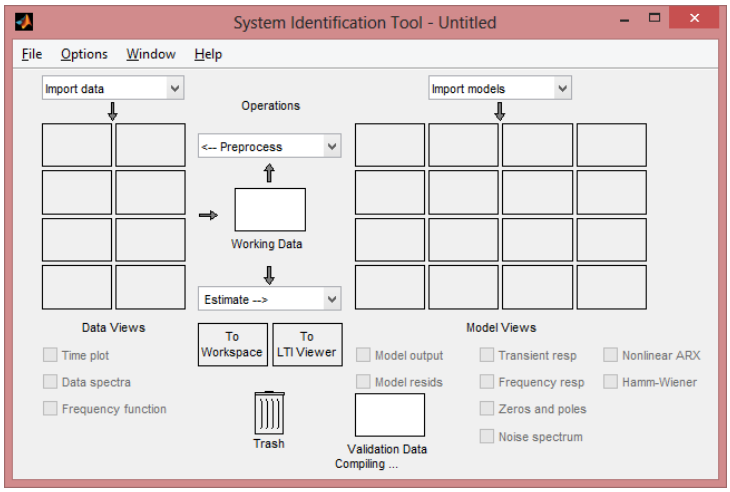

Figure 1: System Identification Toolbox

2.2.1 Linear System Identification

2.2.1.1 Process Model

Process model is one of the models available in System Identification Toolbox. It uses simple continuous-time transfer function to describe linear system dynamics. Among the elements that process modelling is able to identify is static gain, time constants, process zero, possible time delay or enforced integration. This process models is widely applied in many industries. This is due to its various advantages, which it is simple, it has ability to support transport delay in estimation and interpret model coefficients in a simple and easy manner. Process modelling is also able to specify model up to third order model, and poles can be either in real mode or in complex model. (Ljung & MathWorks, 2005)

2.2.1.2 Polynomial Model

Polynomial model is another model available in System Identification Toolbox. It is a mathematical model or equation in which the responses is as a function of input factors and input factors raised to integer exponents. It express the relationship between input, output and noise by making a generalized transfer function notion. In polynomial modelling, not all polynomials are simultaneously active as simpler forms are usually employed and integrator to the nose source may be added (Ljung & MathWorks, 2005) . Among polynomial model structures are ARX, ARIX, ARMAX, ARIMAX, Box-Jenkins (BJ) and lastly Output-Error (OE) (Zhu, 2001).

2.2.2 Non-linear System Identification

Linear model are not sufficient enough to capture system dynamics, hence nonlinear system identification is used to estimate nonlinear models. Among nonlinear model structures are nonlinear ARX and Hammerstein-Wiener. For nonlinear ARX, the model enable the user to model nonlinearities using various structures such as wavelet networks. As for Hammerstein-Weiner, static nonlinear distortions present at the input and output of linear system can be estimated. (Ljung & MathWorks, 2005)

CHAPTER 3

METHODOLOGY

3.1 Project Flow Chart

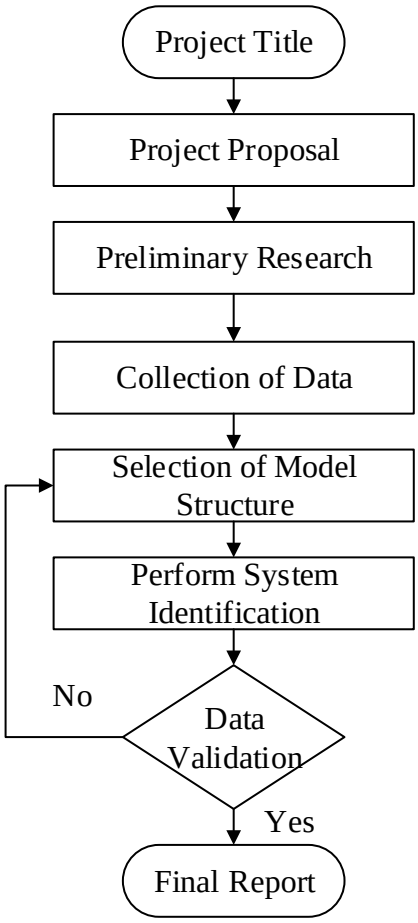

3.2 Project Activities

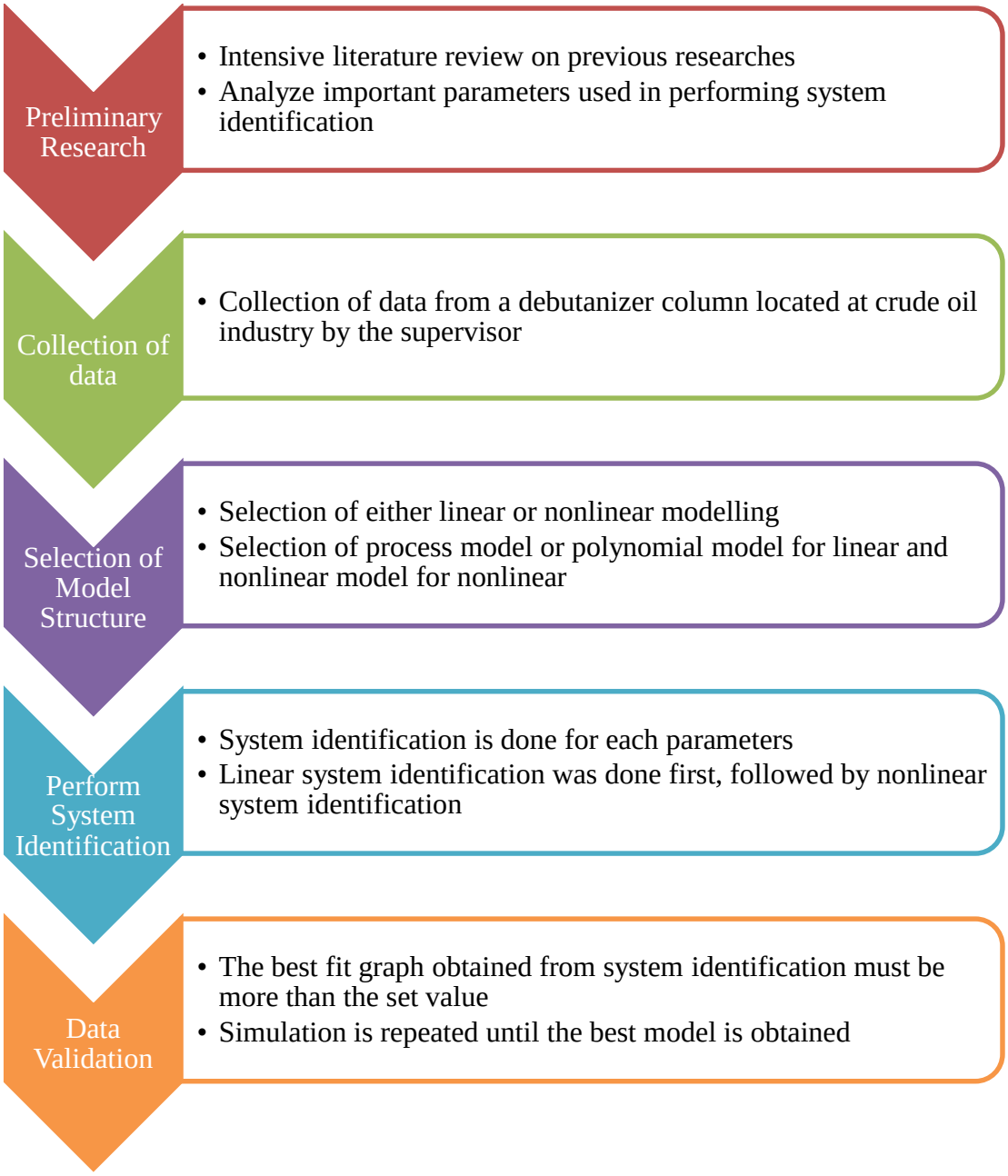

3.3 Gantt Chart

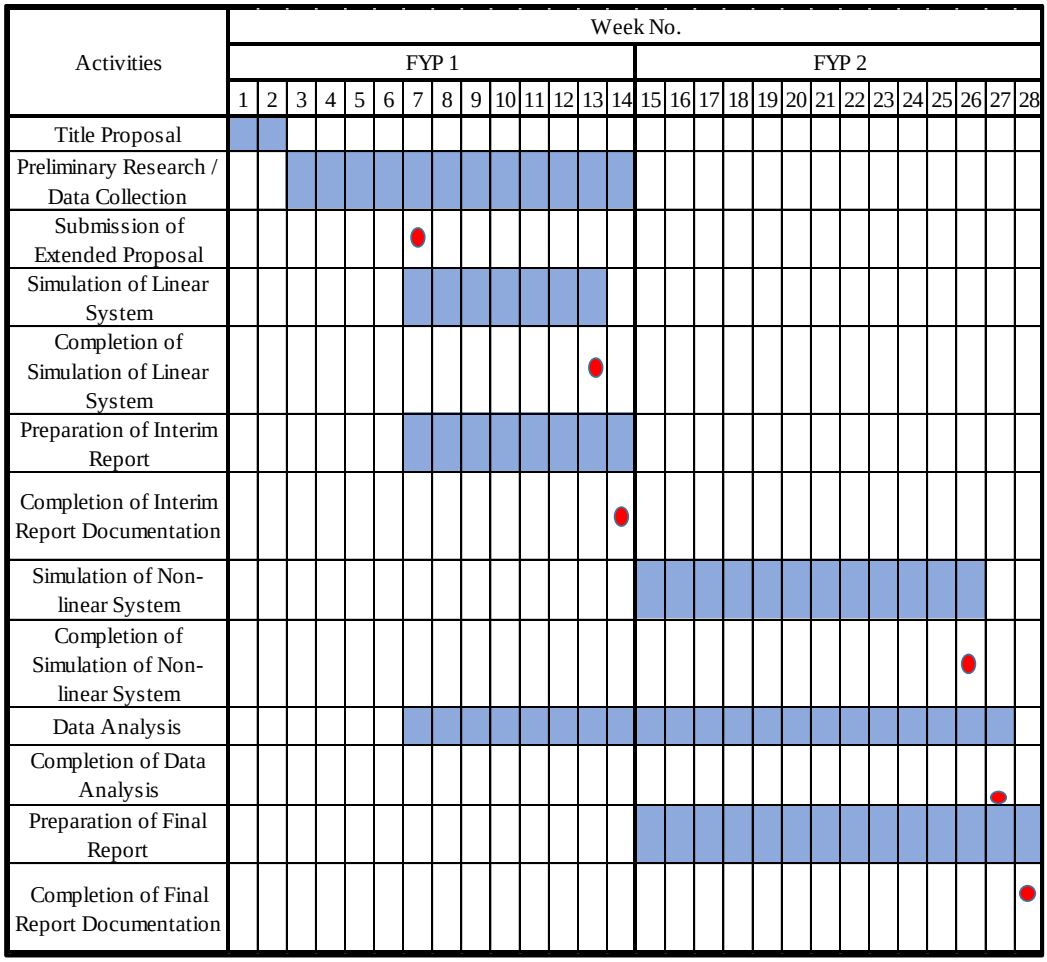

3.4 Project Key Milestones

Project Title Received	Week 1
Submission of Extended Proposal	Week 7
Linear System Identification Completed	Week 13
Submission of Interim Draft Report	Week 13
Submission of Interim Report	Week 14
Non-linear System Identification Completed	Week 27
Submission of Final Draft Report	Week 27
Submission of Final Report	Week 28

3.5 Research Methodology

The simulation will be done using System Identification Toolbox and MATLAB. The methodology used to conduct the simulation for linear and non-linear system identification of debutanizer column is stated below:

3.5.1 Linear

1. Collection of data from supervisor.
2. Transfer data collected into MATLAB.
3. Transfer the data from MATLAB into System Identification Toolbox.
4. Perform linear system identification on a variable by using either process model or polynomial model, using trial and error method until the best fit result of 80% and above is obtained.
5. Repeat step 3 until all the required process models for each variable has been identified.
6. Identify the transfer function of the model in transform z (discrete) or s model (continuous) for each model obtained. Convert model to s transform if z transform is obtained.
7. Plot step, Bode, Nyquist, Nichols and root locus plot for each of the model obtained.
8. Create separate m.file using all of the data obtained for each of the parameters.
9. Analyse the plots obtained.

3.5.2 Non-linear

1. Collection of data from supervisor.
2. Transfer data collected into MATLAB
3. Transfer the data from MATLAB into System Identification Toolbox.
4. Perform nonlinear system identification on a variable using nonlinear model, using trial and error method until the best fit result of 80% and above is obtained.
5. Transfer the selected model into Linear Time Invariant Viewer (LTI Viewer) to observe the plots obtained from the model. Plot step, impulse, Bode, Nyquist, Nichols and zero/pole plot for each of the model obtained.

6. Analyze the plots obtained.

3.6 List of Variables

Table 1: List of variables

Temperature	Level	Flow	Pressure
• Temperature 1 • Temperature 2 • Temperature 3 • Temperature 4 • Temperature 5 • Temperature 6	• Level 1 • Level 2 • Level 3 • Level 4	• Flow 1 • Flow 2	• Pressure 1

CHAPTER 4

RESULT AND DISCUSSION

4.1 Data Gathering, Result and Discussion

4.1.1 Linear System Identification

Below are the sample result obtained from variable Temperature 1. The remaining result for other variables are placed in the Appendix 1. First, the data obtained from system identification is in ARX model, then the model was transformed to transfer model in z transform (discrete). The new z transform model is then transformed to s transform (continuous).

4.1.1.1 Temperature 1

ARX Model

Fit to estimation data: 94.57%

A(z) = 1 - 0.7072 z^-1 + 0.1827 z^-2 - 0.5755 z^-3 + 0.285 z^-4 - 0.209 z^-5 - 0.2145 z^-6
- 0.07183 z^-7 + 0.2027 z^-8 + 0.2856 z^-9 - 0.07964 z^-10 - 0.05402 z^-11
+ 0.2555 z^-12 + 0.0665 z^-13 - 0.2131 z^-14 + 0.08394 z^-15 - 0.6418 z^-16
+ 0.2883 z^-17 - 0.5991 z^-18 + 0.5974 z^-19 - 0.1083 z^-20 + 0.3575 z^-21
- 0.09827 z^-22 + 0.035 z^-23 + 0.1045 z^-24 + 0.1242 z^-25 - 0.122 z^-26
- 0.09197 z^-27 + 0.09019 z^-28 + 0.3247 z^-29 - 0.05638 z^-30 - 0.4827 z^-31
+ 0.2856 z^-32 - 0.2823 z^-33 + 0.1276 z^-34 - 0.2617 z^-35 - 0.1318 z^-36
+ 0.6789 z^-37 + 0.09893 z^-38 + 0.06507 z^-39 - 0.5166 z^-40 + 0.0609 z^
-41 - 0.01328 z^-42 + 0.1646 z^-43 - 0.07834 z^-44 + 0.0169 z^-45 - 0.1691 z^-46
+ 0.06677 z^-47 - 0.02076 z^-48 - 0.04534 z^-49 + 0.1961 z^-50 - 0.3944 z^-51
+ 0.9019 z^-52 - 0.06574 z^-53 + 0.2934 z^-54 - 0.4097 z^-55 + 0.07873 z^
-56 + 0.2346 z^-57 - 0.002598 z^-58 + 0.1521 z^-59 - 0.4835 z^-60 + 0.2742 z^-61
- 0.03012 z^-62 - 0.108 z^-63 + 0.1949 z^-64 - 0.4765 z^-65 + 0.162 z^-66
- 0.2703 z^-67 + 0.3708 z^-68 - 0.09786 z^-69 - 0.2309 z^-70 - 0.08279 z^
-71 - 0.09435 z^-72 + 0.773 z^-73 + 0.09409 z^-74 + 0.1048 z^-75 - 0.5381 z^-76
+ 0.4308 z^-77 - 0.7016 z^-78 + 0.2815 z^-79 - 0.9166 z^-80 + 0.4305 z^-81
+ 0.02115 z^-82 + 0.1589 z^-83 + 0.3533 z^-84 + 0.1845 z^-85 + 0.3738 z^-86
- 0.3541 z^-87 - 0.07173 z^-88 - 0.06321 z^-89 - 0.1912 z^-90 - 0.1412 z^
-91 - 0.1886 z^-92 - 0.3705 z^-93 + 0.62 z^-94 - 0.1497 z^-95 + 0.1105 z^
-96 - 0.379 z^-97

B(z) = -0.5941 z^-1 - 0.2283 z^-2 + 1.413 z^-3 + 1.048 z^-4 - 0.1375 z^-5 - 0.3082 z^-6
- 0.7341 z^-7 + 0.5494 z^-8 - 0.799 z^-9 - 1.574 z^-10 - 0.1629 z^-11 - 0.1948 z^-12
+ 1.651 z^-13 - 0.6818 z^-14 + 0.04035 z^-15 - 0.4216 z^-16 + 1.387 z^-17
- 0.1973 z^-18 - 0.4975 z^-19 - 0.6937 z^-20 - 0.9858 z^-21 + 0.6846 z^-22

- 1.05 z^-23 + 0.6877 z^-24 + 0.6712 z^-25 + 1.784 z^-26 - 0.1502 z^-27 - 0.9273 z^-28
+ 1.077 z^-29 - 1.153 z^-30 + 1.262 z^-31 - 0.4228 z^-32 + 0.07666 z^-33
- 1.107 z^-34 + 0.3496 z^-35 + 0.3715 z^-36 + 1.305 z^-37 - 0.7904 z^-38
- 1.473 z^-39 + 0.1236 z^-40 + 1.114 z^-41 - 0.6073 z^-42 - 0.9796 z^-43
- 1.113 z^-44 + 0.08748 z^-45 + 1.493 z^-46 + 0.01542 z^-47 - 0.5829 z^-48
- 1.173 z^-49 + 1.285 z^-50 - 0.7411 z^-51 - 0.1767 z^-52 - 0.6666 z^-53
- 1.047 z^-54 + 2.793 z^-55 + 2.039 z^-56 + 0.03808 z^-57 - 0.3114 z^-58
- 1.186 z^-59 + 2.361 z^-60 - 0.9908 z^-61 + 2.261 z^-62 - 2.368 z^-63 + 1.305 z^-64
- 0.7806 z^-65 + 0.2317 z^-66 - 0.2581 z^-67 - 2.458 z^-68 + 0.5239 z^-69
- 0.7746 z^-70 + 1.743 z^-71 - 1.77 z^-72 + 0.9129 z^-73 - 0.8129 z^-74 + 1.833 z^-75
+ 0.1532 z^-76 - 0.7189 z^-77 + 0.467 z^-78 - 0.8076 z^-79 + 0.5918 z^-80
- 1.159 z^-81 + 0.4686 z^-82 - 1.877 z^-83 + 1.123 z^-84 + 0.2063 z^-85 + 1.041 z^-86
+ 0.3794 z^-87 + 0.8641 z^-88 + 1.374 z^-89 + 0.4645 z^-90 + 0.8685 z^-91
+ 0.64 z^-92 + 0.2453 z^-93 + 0.1179 z^-94 - 1.217 z^-95 - 1.402 z^-96 - 2.357 z^-97

Transfer model in z transform

-0.5941 z^-1 - 0.2283 z^-2 + 1.413 z^-3 + 1.048 z^-4 - 0.1375 z^-5 - 0.3082 z^-6
- 0.7341 z^-7 + 0.5494 z^-8 - 0.799 z^-9 - 1.574 z^-10 - 0.1629 z^-11
- 0.1948 z^-12 + 1.651 z^-13 - 0.6818 z^-14 + 0.04035 z^-15 - 0.4216 z^-16
+ 1.387 z^-17 - 0.1973 z^-18 - 0.4975 z^-19 - 0.6937 z^-20 - 0.9858 z^-21
+ 0.6846 z^-22 - 1.05 z^-23 + 0.6877 z^-24 + 0.6712 z^-25 + 1.784 z^-26
- 0.1502 z^-27 - 0.9273 z^-28 + 1.077 z^-29 - 1.153 z^-30 + 1.262 z^-31
- 0.4228 z^-32 + 0.07666 z^-33 - 1.107 z^-34 + 0.3496 z^-35 + 0.3715 z^-36
+ 1.305 z^-37 - 0.7904 z^-38 - 1.473 z^-39 + 0.1236 z^-40 + 1.114 z^-41
- 0.6073 z^-42 - 0.9796 z^-43 - 1.113 z^-44 + 0.08748 z^-45 + 1.493 z^-46
+ 0.01542 z^-47 - 0.5829 z^-48 - 1.173 z^-49 + 1.285 z^-50 - 0.7411 z^-51
- 0.1767 z^-52 - 0.6666 z^-53 - 1.047 z^-54 + 2.793 z^-55 + 2.039 z^-56
+ 0.03808 z^-57 - 0.3114 z^-58 - 1.186 z^-59 + 2.361 z^-60 - 0.9908 z^-61
+ 2.261 z^-62 - 2.368 z^-63 + 1.305 z^-64 - 0.7806 z^-65 + 0.2317 z^-66
- 0.2581 z^-67 - 2.458 z^-68 + 0.5239 z^-69 - 0.7746 z^-70 + 1.743 z^
-71 - 1.77 z^-72 + 0.9129 z^-73 - 0.8129 z^-74 + 1.833 z^-75 + 0.1532 z^-76
- 0.7189 z^-77 + 0.467 z^-78 - 0.8076 z^-79 + 0.5918 z^-80 - 1.159 z^
-81 + 0.4686 z^-82 - 1.877 z^-83 + 1.123 z^-84 + 0.2063 z^-85 + 1.041 z^-86
+ 0.3794 z^-87 + 0.8641 z^-88 + 1.374 z^-89 + 0.4645 z^-90 + 0.8685 z^-91
+ 0.64 z^-92 + 0.2453 z^-93 + 0.1179 z^-94 - 1.217 z^-95 - 1.402 z^-96
- 2.357 z^-97

---

1 - 0.7072 z^-1 + 0.1827 z^-2 - 0.5755 z^-3 + 0.285 z^-4 - 0.209 z^-5 - 0.2145 z^-6
- 0.07183 z^-7 + 0.2027 z^-8 + 0.2856 z^-9 - 0.07964 z^-10 - 0.05402 z^-11
+ 0.2555 z^-12 + 0.0665 z^-13 - 0.2131 z^-14 + 0.08394 z^-15 - 0.6418 z^-16
+ 0.2883 z^-17 - 0.5991 z^-18 + 0.5974 z^-19 - 0.1083 z^-20 + 0.3575 z^-21
- 0.09827 z^-22 + 0.035 z^-23 + 0.1045 z^-24 + 0.1242 z^-25 - 0.122 z^-26
- 0.09197 z^-27 + 0.09019 z^-28 + 0.3247 z^-29 - 0.05638 z^-30 - 0.4827 z^-31
+ 0.2856 z^-32 - 0.2823 z^-33 + 0.1276 z^-34 - 0.2617 z^-35 - 0.1318 z^-36
+ 0.6789 z^-37 + 0.09893 z^-38 + 0.06507 z^-39 - 0.5166 z^-40 + 0.0609 z^-41
- 0.01328 z^-42 + 0.1646 z^-43 - 0.07834 z^-44 + 0.0169 z^-45 - 0.1691 z^-46
+ 0.06677 z^-47 - 0.02076 z^-48 - 0.04534 z^-49 + 0.1961 z^-50 - 0.3944 z^-51
+ 0.9019 z^-52 - 0.06574 z^-53 + 0.2934 z^-54 - 0.4097 z^-55 + 0.07873 z^-56
+ 0.2346 z^-57 - 0.002598 z^-58 + 0.1521 z^-59 - 0.4835 z^-60 + 0.2742 z^-61
- 0.03012 z^-62 - 0.108 z^-63 + 0.1949 z^-64 - 0.4765 z^-65 + 0.162 z^-66
- 0.2703 z^-67 + 0.3708 z^-68 - 0.09786 z^-69 - 0.2309 z^-70 - 0.08279 z^-71
- 0.09435 z^-72 + 0.773 z^-73 + 0.09409 z^-74 + 0.1048 z^-75 - 0.5381 z^-76
+ 0.4308 z^-77 - 0.7016 z^-78 + 0.2815 z^-79 - 0.9166 z^-80 + 0.4305 z^-81
+ 0.02115 z^-82 + 0.1589 z^-83 + 0.3533 z^-84 + 0.1845 z^-85 + 0.3738 z^-86
- 0.3541 z^-87 - 0.07173 z^-88 - 0.06321 z^-89 - 0.1912 z^-90 - 0.1412 z^-91
- 0.1886 z^-92 - 0.3705 z^-93 + 0.62 z^-94 - 0.1497 z^-95 + 0.1105 z^
-96 - 0.379 z^-97

Transfer model in s transform

$$
\frac{-2.835 s^{98} + 4.841 s^{97} - 475.4 s^{96} + 793.5 s^{95} - 3.841e04 s^{94} + 6.262e04 s^{93} - 1.992e06 s^{92} + 3.17e06 s^{91} - 7.453e07 s^{90} + 1.157e08 s^{89} - 2.144e09 s^{88} + 3.244e09 s^{87} - 4.932e10 s^{86} + 7.272e10 s^{85} - 9.329e11 s^{84} + 1.339e12 s^{83} - 1.479e13 s^{82} + 2.066e13 s^{81} - 1.994e14 s^{80} + 2.71e14 s^{79} - 2.313e15 s^{78} + 3.055e15 s^{77} - 2.328e16 s^{76} + 2.988e16 s^{75} - 2.047e17 s^{74} + 2.551e17 s^{73} - 1.582e18 s^{72} + 1.913e18 s^{71} - 1.078e19 s^{70} + 1.266e19 s^{69} - 6.512e19 s^{68} + 7.411e19 s^{67} - 3.492e20 s^{66} + 3.853e20 s^{65} - 1.667e21 s^{64} + 1.782e21 s^{63} - 7.093e21 s^{62} + 7.347e21 s^{61} - 2.693e22 s^{60} + 2.702e22 s^{59} - 9.131e22 s^{58} + 8.869e22 s^{57} - 2.765e23 s^{56} + 2.599e23 s^{55} - 7.476e23 s^{54} + 6.802e23 s^{53} - 1.804e24 s^{52} + 1.588e24 s^{51} - 3.881e24 s^{50} + 3.304e24 s^{49} - 7.435e24 s^{48} + 6.119e24 s^{47} - 1.266e25 s^{46} + 1.007e25 s^{45} - 1.912e25 s^{44} + 1.469e25 s^{43} - 2.554e25 s^{42} + 1.895e25 s^{41} - 3.009e25 s^{40} + 2.155e25 s^{39} - 3.116e25 s^{38} + 2.151e25 s^{37} - 2.824e25 s^{36} + 1.877e25 s^{35} - 2.229e25 s^{34} + 1.425e25 s^{33} - 1.524e25 s^{32} + 9.35e24 s^{31} - 8.969e24 s^{30} + 5.267e24 s^{29} - 4.508e24 s^{28} + 2.527e24 s^{27} - 1.918e24 s^{26} + 1.022e24 s^{25} - 6.841e23 s^{24} + 3.447e23 s^{23} - 2.02e23 s^{22} + 9.556e22 s^{21} - 4.864e22 s^{20} + 2.142e22 s^{19} - 9.386e21 s^{18} + 3.801e21 s^{17} - 1.419e21 s^{16} + 5.201e20 s^{15} - 1.634e20 s^{14} + 5.303e19 s^{13} - 1.381e19 s^{12} + 3.845e18 s^{11} - 8.145e17 s^{10} + 1.857e17 s^{9} - 3.122e16 s^{8} + 5.406e15 s^{7} - 6.979e14 s^{6} + 7.999e13 s^{5} - 7.591e12 s^{4} + 4.347e11 s^{3} - 2.777e10 s^{2} + 4.473e07 s - 1.71e06}{s^{99} + 0.992 s^{98} + 168.5 s^{97} + 163 s^{96} + 1.368e04 s^{95} + 1.289e04 s^{94} + 7.131e05 s^{93} + 6.541e05 s^{92} + 2.681e07 s^{91} + 2.392e07 s^{90} + 7.746e08 s^{89} + 6.718e08 s^{88} + 1.791e10 s^{87} + 1.508e10 s^{86} + 3.403e11 s^{85} + 2.781e11 s^{84} + 5.421e12 s^{83} + 4.294e12 s^{82} + 7.344e13 s^{81} + 5.633e13 s^{80} + 8.559e14 s^{79} + 6.351e14 s^{78} + 8.656e15 s^{77} + 6.208e15 s^{76} + 7.649e16 s^{75} + 5.296e16 s^{74} + 5.94e17 s^{73} + 3.967e17 s^{72} + 4.072e18 s^{71} + 2.619e18 s^{70} + 2.472e19 s^{69} + 1.53e19 s^{68} + 1.334e20 s^{67} + 7.931e19 s^{66} + 6.404e20 s^{65} + 3.655e20 s^{64} + 2.742e21 s^{63} + 1.5e21 s^{62} + 1.048e22 s^{61} + 5.488e21 s^{60} + 3.579e22 s^{59} + 1.791e22 s^{58} + 1.092e23 s^{57} + 5.214e22 s^{56} + 2.977e23 s^{55} + 1.354e23 s^{54} + 7.246e23 s^{53} + 3.134e23 s^{52} + 1.573e24 s^{51} + 6.46e23 s^{50} + 3.044e24 s^{49} + 1.184e24 s^{48} + 5.24e24 s^{47} + 1.927e24 s^{46} + 8.007e24 s^{45} + 2.776e24 s^{44} + 1.084e25 s^{43} + 3.531e24 s^{42} + 1.295e25 s^{41} + 3.954e24 s^{40} + 1.361e25 s^{39} + 3.882e24 s^{38} + 1.255e25 s^{37} + 3.325e24 s^{36} + 1.009e25 s^{35} + 2.471e24 s^{34} + 7.047e24 s^{33} + 1.583e24 s^{32} + 4.245e24 s^{31} + 8.671e23 s^{30} + 2.192e24 s^{29} + 4.022e23 s^{28} + 9.618e23 s^{27} + 1.561e23 s^{26} + 3.555e23 s^{25} + 4.989e22 s^{24} + 1.095e23 s^{23} + 1.288e22 s^{22} + 2.776e22 s^{21} + 2.607e21 s^{20} + 5.704e21 s^{19} + 3.956e20 s^{18} + 9.332e20 s^{17} + 4.118e19 s^{16} + 1.189e20 s^{15} + 2.242e18 s^{14} + 1.147e19 s^{13} - 6.217e16 s^{12} + 8.066e17 s^{11} - 2.191e16 s^{10} + 3.932e16 s^{9} - 1.745e15 s^{8} + 1.233e15 s^{7} - 6.755e13 s^{6} + 2.223e13 s^{5} - 1.232e12 s^{4} + 1.927e11 s^{3} - 8.269e09 s^{2} + 5.329e08 s - 2.201e05}
$$

After the transfer model was transformed into s model, step response, Bode plot, Nyquist plot, root locus and lastly Nichols plot was plotted to analyse the stability of the system in linear condition.

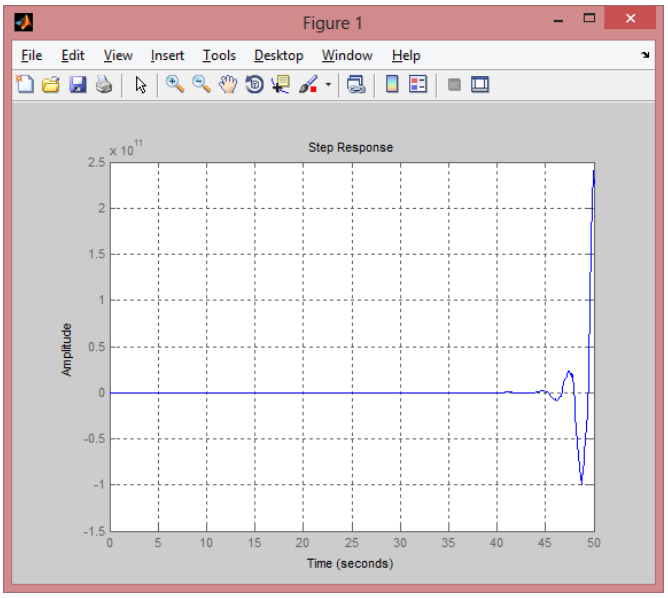

Figure 2: Step response (Temperature 1 - Linear)

Based on observation from Figure 2, the step response plot shows that the system is unstable under linear condition. The response plot shows sudden increasing oscillation as time approaches the end which indicates unstable system (Ogata, 2007). For a system to be declared stable, there must not be any increasing oscillation in the plot.

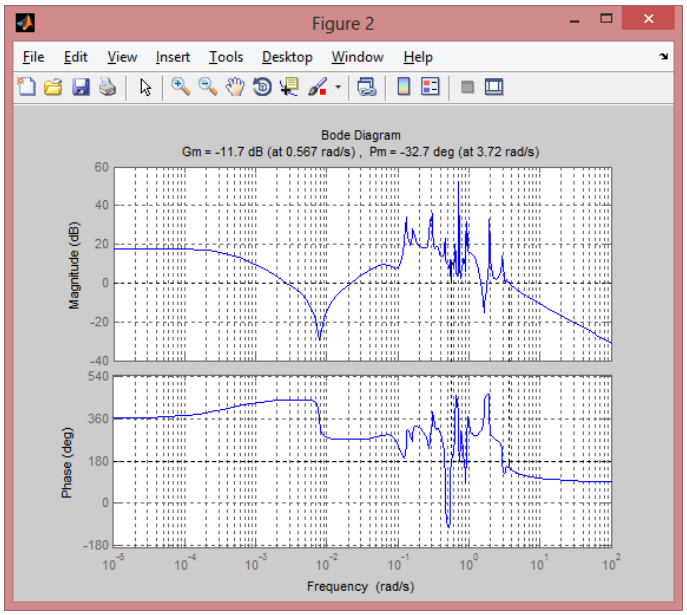

Figure 3: Bode plot (Temperature 1 - Linear)

Moving on to Figure 3, it is shown that the from Bode plot that the stability of the system, based on the phase margin and gain margin obtained, which is -11.7dB and -32.7 degrees, indicates that the system is unstable during under linear condition. For a system to be declared stable, it must have positive gain margin of values at least 10dB

and phase margin of values at least 40 degrees. (Massachusetts Institute of Technology, 2000).

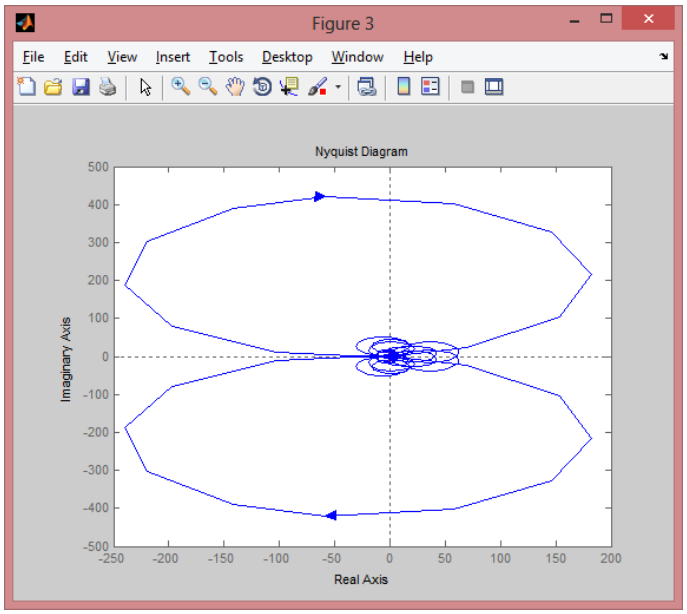

Figure 4: Nyquist plot (Temperature 1 - Linear)

Based on the Nyquist plot obtained in Figure 4, it is shown that the system is unstable under linear condition. This is due to that the Nyquist plot satisfy the requirement the system to be able to be declared stable. This is because the Nyquist plot obtained has clockwise encirclements at the -1+j0 point, which indicates that the system is unstable. As stated by (Ogata, 2007), for a system to be declared unstable, there must be no clockwise encirclement at the -1+j0 point.

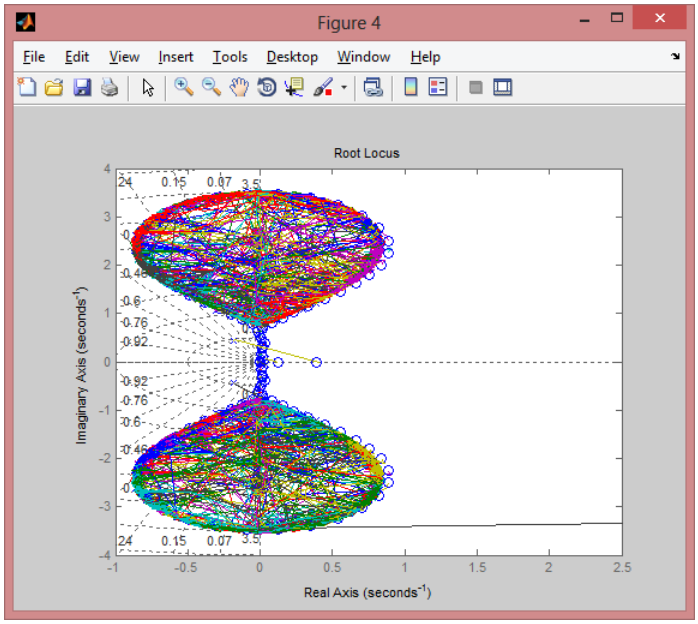

Figure 5: Root locus plot (Temperature 1 - Linear)

The root locus shows that the system is unstable under linear condition. This is due to the presence of complex roots with positive real parts. This causes the system to have increasing oscillation, proven by the step response plot in Figure 2. For the system to be stable, there must not be any roots with positive real parts present. (Claymore, n.d.)

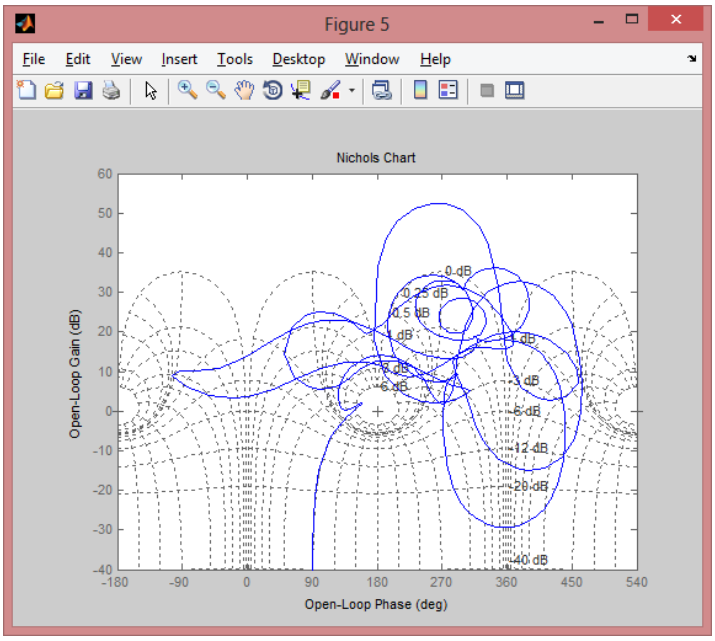

Figure 6: Nichols Plot (Temperature 1 - Linear)

Lastly, based on the Nichols plot in Figure 6, it is observed that the gain margin is -3dB as the open-loop locus intersect with 0dB axis. The phase margin is also proven to be infinite as there is no intersection of open-loop locus with -180 degrees line. Based on the gain and phase margin, it is observed that the system is unstable under linear condition due to the value of the gain is less than 0dB. In order for the system to be declared stable, the gain margin must be more than 0dB (Chen, 1997).

4.1.1.2 Temperature 2

Based on Figure 7 in Appendix 1, the step response shows that the system is unstable in linear condition due to the sudden increasing oscillation as time approaches the ending. As for Figure 8 in Appendix 1, it is shown that the from Bode plot that the stability of the system, based on the phase margin and gain margin obtained, which is -6.8dB and 33.6 degrees, indicates that the system is unstable during under linear condition. Moving on to Figure 9 in Appendix 1, the Nyquist plot shows that the system is unstable under linear condition. This is due to there are poles present on the right-half s-plane. For the system to be declared stable, there must not be any poles in

the right-half s-plane (Ogata, 2007). Next, based on Figure 10 in Appendix 1, the root locus plot shows that the system is unstable as there is complex roots with positive real parts present. This causes the system to have increasing oscillation, proven by the step response plot on Figure 7 in Appendix 1. Lastly, on the Nichols plot on Figure 11 in Appendix 1, it is observed that the gain margin is -6dB as the open-loop locus intersect with 0dB axis. The phase margin observed is around -40 degrees. Hence, the system is unstable under linear condition.

4.1.1.3 Temperature 3

Based on Figure 12 in Appendix 1, the step response shows that the system is unstable in linear condition due to the sudden increasing oscillation as time approaches the ending. Next, for Figure 13 in Appendix 1, it is shown that the from Bode plot, that the stability of the system, based on the phase margin and gain margin obtained, which is -3.02dB and 10.8 degrees, indicates that the system is unstable during under linear condition. As for Figure 14 in Appendix 1, the Nyquist plot shows that the system is unstable under linear condition. This is due to there are poles present on the right-half s-plane. Based on Figure 15 in Appendix 1, the root locus plot shows that the system is unstable as there is complex roots with positive real parts present. This causes the system to have increasing oscillation, proven by the step response plot on Figure 12 in Appendix 1. Finally, on the Nichols plot on Figure 16 in Appendix 1, it is observed that the gain margin is around -3dB as the open-loop locus intersect with 0dB axis. Phase margin observed is 0 degrees. Hence, the system is unstable under linear condition.

4.1.1.4 Temperature 4

For Temperature 4, based on Figure 17 in Appendix 1, the step response shows that the system is unstable in linear condition due to the sudden increasing oscillation as time approaches the ending. Next, for Figure 18 in Appendix 1, it is shown that the from Bode plot, that the stability of the system, based on the phase margin and gain margin obtained, which is 0.587dB and 2.47 degrees, indicates that the system is unstable during under linear condition. As for Figure 19 in Appendix 1, the Nyquist plot shows that the system is unstable under linear condition. This is due to the presence of encirclement of -1 + j0 point. Based on Figure 20 in Appendix 1, the root

locus plot shows that the system is unstable as there is complex roots with positive real parts present. This causes the system to have increasing oscillation, proven by the step response plot on Figure 17 in Appendix 1. Finally, on the Nichols plot on Figure 21 in Appendix 1, it is observed that the gain margin is around -3dB as the open-loop locus intersect with 0dB axis. Phase margin observed is 0 degrees. Hence, the system is unstable under linear condition.

4.1.1.5 Temperature 5

For Temperature 5, based on Figure 22 in Appendix 1, the step response shows that the system is unstable in linear condition due to the sudden increasing oscillation as time approaches the ending. Next, for Figure 23 in Appendix 1, it is shown that the from Bode plot, that the stability of the system, based on the phase margin and gain margin obtained, which is -27dB and 92.8 degrees, indicates that the system is unstable during under linear condition. As for Figure 24 in Appendix 1, the system is unstable in linear condition. This is because the Nyquist plot obtained has clockwise encirclements at the -1+j0 point, which indicates that the system is unstable. Based on Figure 25 in Appendix 1, the root locus plot shows that the system is unstable as there is complex roots with positive real parts present. This causes the system to have increasing oscillation, proven by the step response plot on Figure 22 in Appendix 1. Finally, on the Nichols plot on Figure 26 in Appendix 1, it is observed that the gain margin is around -3dB as the open-loop locus intersect with 0dB axis. Phase margin observed is infinite. Hence, the system is unstable under linear condition.

4.1.1.6 Temperature 6

Moving on to Temperature 6, based on Figure 27 in Appendix 1, the step response shows that the system is unstable in linear condition due to the sudden increasing oscillation as time approaches the ending. Next, for Figure 28 in Appendix 1, it is shown that the from Bode plot, that the stability of the system, based on the phase margin and gain margin obtained, which is -3.74dB and 30.2 degrees, indicates that the system is unstable during under linear condition. Moving on, based on Figure 29 in Appendix 1, the system is unstable in linear condition. This is because the Nyquist plot obtained has clockwise encirclements at the -1+j0 point, which indicates that the system is unstable. Based on Figure 30 in Appendix 1, the root locus plot shows that

the system is unstable as there is complex roots with positive real parts present. This causes the system to have increasing oscillation, proven by the step response plot on Figure 27 in Appendix 1. Finally, on the Nichols plot on Figure 31 in Appendix 1, it is observed that the gain margin is around -40dB as the open-loop locus intersect with 0dB axis. Phase margin observed is infinite. Hence, the system is unstable under linear condition.

4.1.1.7 Level 1

As for Level 1, based on Figure 32 in Appendix 1, the step response shows that the system is unstable in linear condition due to the sudden increasing oscillation as time approaches the ending. Next, for Figure 33 in Appendix 1, it is shown that the from Bode plot, that the stability of the system, based on the phase margin and gain margin obtained, which is 6.69dB and 68.5 degrees, indicates that the system is unstable during under linear condition. As for Figure 34 in Appendix 1, the system is unstable in linear condition. This is because the Nyquist plot obtained has clockwise encirclements at the -1+j0 point, which indicates that the system is unstable. Based on Figure 35 in Appendix 1, the root locus plot shows that the system is unstable as there is complex roots with positive real parts present. This causes the system to have increasing oscillation, proven by the step response plot on Figure 32 in Appendix 1. Finally, on the Nichols plot on Figure 36 in Appendix 1, it is observed that the gain margin is around -20dB as the open-loop locus intersect with 0dB axis. Phase margin is observed to be around 0 degrees. Hence, the system is unstable under linear condition.

4.1.1.8 Level 2

Based on Figure 37 in Appendix 1, the step response shows that the system is unstable in linear condition due to the sudden increasing oscillation as time approaches the ending. Next, for Figure 38 in Appendix 1, it is shown that the from Bode plot, that the stability of the system, based on the phase margin and gain margin obtained, which is -2.58dB and -35.8 degrees, indicates that the system is unstable during under linear condition. As for Figure 39 in Appendix 1, the system is unstable in linear condition. This is because the Nyquist plot obtained has one or more counter-clockwise encirclements at the -1+j0 point with unequal number of poles in the right half s plane,

which indicates that the system is unstable. For a system to be declared stable, if there is one or more counter-clockwise encirclements at the -1+j0 point, the number of encirclements must be equal to number of poles in the right half s plane (Ogata, 2007). Based on Figure 40 in Appendix 1, the root locus plot shows that the system is unstable as there is complex roots with positive real parts present. This causes the system to have increasing oscillation, proven by the step response plot on Figure 32 in Appendix 1. Finally, on the Nichols plot on Figure 41 in Appendix 1, it is observed that the gain margin is around -6dB as the open-loop locus intersect with 0dB axis. Phase margin is observed to be around -15 degrees. Hence, the system is unstable under linear condition.

4.1.1.9 Level 3

As for Level 3 based on Figure 42 in Appendix 1, the step response shows that the system is unstable in linear condition due to the sudden increasing oscillation as time approaches the ending. Next, for Figure 43 in Appendix 1, it is shown that the from Bode plot, that the stability of the system, based on the phase margin and gain margin obtained, which is 0.31dB and -1.3 degrees, indicates that the system is unstable under linear condition. Moving on, based on Figure 44 in Appendix 1, the system is unstable in linear condition. This is because the Nyquist plot obtained clockwise encirclements at the -1+j0 point, which indicates that the system is unstable. Based on Figure 45 in Appendix 1, the root locus plot shows that the system is unstable as there is complex roots with positive real parts present. This causes the system to have increasing oscillation, proven by the step response plot on Figure 42 in Appendix 1. Finally, on the Nichols plot on Figure 46 in Appendix 1, it is observed that the gain margin is around -3dB as the open-loop locus intersect with 0dB axis. Phase margin is observed to be around 20 degrees. Hence, the system is unstable under linear condition.

4.1.1.10 Level 4

Based on Figure 47 in Appendix 1, the step response shows that the system is unstable in linear condition due to the sudden increasing oscillation as time approaches the ending. As for Figure 48 in Appendix 1, it is shown that the from Bode plot, that the stability of the system, based on the phase margin and gain margin obtained, which is -10.9dB and -13.3 degrees, indicates that the system is unstable under linear condition.

Moving on, based on Figure 49 in Appendix 1, Nyquist plot shows that the system is unstable under linear conditions, due to obtained clockwise encirclements at the -1+j0 point, which indicates that the system is unstable. Based on Figure 50 in Appendix 1, the root locus plot shows that the system is unstable as there is complex roots with positive real parts present. This causes the system to have increasing oscillation, proven by the step response plot on Figure 46 in Appendix 1. Finally, on the Nichols plot on Figure 51 in Appendix 1, it is observed that the gain margin is around -20dB as the open-loop locus intersect with 0dB axis. Phase margin is observed is infinite. Hence, the system is unstable under linear condition.

4.1.1.11 Flow 1

As for Flow 1, based on Figure 52 in Appendix 1, the step response shows that the system is unstable in linear condition due to the sudden increasing oscillation as time approaches the ending. Moving on to Figure 53 in Appendix 1, it is shown that the from Bode plot, that the stability of the system, based on the phase margin and gain margin obtained, which is -1.97dB and -72.4 degrees, indicates that the system is unstable under linear condition. Next, based on Figure 54 in Appendix 1, the system is unstable in linear condition. This is because the Nyquist plot obtained clockwise encirclements at the -1+j0 point, which indicates that the system is unstable. Based on Figure 55 in Appendix 1, the root locus plot shows that the system is unstable as there is complex roots with positive real parts present. This causes the system to have increasing oscillation, proven by the step response plot on Figure 52 in Appendix 1. Finally, on the Nichols plot on Figure 56 in Appendix 1, it is observed that the gain margin is around -6dB as the open-loop locus intersect with 0dB axis. Phase margin is observed to be around -6 degrees. Hence, the system is unstable under linear condition.

4.1.1.12 Flow 2

Based on Figure 57 in Appendix 1, the step response shows that the system is unstable in linear condition due to the sudden increasing oscillation as time approaches the ending. As for Figure 58 in Appendix 1, it is shown that the from Bode plot, that the stability of the system, based on the phase margin and gain margin obtained, which is 6.18dB and -13.2 degrees, indicates that the system is unstable under linear condition. Moving on, based on Figure 59 in Appendix 1, Nyquist plot shows that the system is

unstable under linear conditions, due to obtained clockwise encirclements at the -1+j0 point, which indicates that the system is unstable. Based on Figure 60 in Appendix 1, the root locus plot shows that the system is unstable as there is complex roots with positive real parts present. This causes the system to have increasing oscillation, proven by the step response plot on Figure 56 in Appendix 1. Finally, on the Nichols plot on Figure 61 in Appendix 1, it is observed that the gain margin is around -10dB as the open-loop locus intersect with 0dB axis. Phase margin is observed is infinite. Hence, the system is unstable under linear condition.

4.1.1.13 Pressure 1

For the last variable which is Pressure 1, based on Figure 62 in Appendix 1, the step response shows that the system is unstable in linear condition due to the sudden increasing oscillation as time approaches the ending. Moving on to Figure 63 in Appendix 1, it is shown that the from Bode plot, that the stability of the system, based on the phase margin and gain margin obtained, which is -16dB and -89.7 degrees, indicates that the system is unstable under linear condition. Next, based on Figure 64 in Appendix 1, the system is unstable in linear condition. This is because the Nyquist plot has encirclement at the -1+j0 point, which indicates that the system is unstable. Based on Figure 55 in Appendix 1, the root locus plot shows that the system is unstable as there is complex roots with positive real parts present. This causes the system to have increasing oscillation, proven by the step response plot on Figure 65 in Appendix 1. Finally, on the Nichols plot on Figure 66 in Appendix 1, it is observed that the gain margin is around -12dB as the open-loop locus intersect with 0dB axis. Phase margin is unknown. Hence, the system is unstable under linear condition.

4.1.2 Non-linear System Identification

As for non-linear system identification, only six plots for each variable are obtained from LTI Viewer tool. The equations are unable to be extracted from the System Identification Toolbox

4.1.2.1 Temperature 1

Based on the Figure 67 in Appendix 2, the step response plot shows that the plot stabilizes as time approaches the ending. This indicates that the system is stable in nonlinear condition (Ogata, 2007). For a system to be declared stable, the plot must not have increasing oscillation in the bode plot. As for Figure 68 in Appendix 2, impulse plot also shows that the amplitude slowly stables as time approaches the end. This shows that the system is stable at nonlinear condition (Ogata, 2007). Next, for Figure 69 in Appendix 2, the Bode plot shows that the system is stable due to no increasing oscillation observed in the plot. For a system to be declared stable, the plot must not have no increasing oscillation in the Bode plot (Massachusetts Institute of Technology, 2000). Moving on, the Nyquist plot shown at Figure 70 in Appendix 2 shows that there is no clockwise encirclements on the -1+j0 point This indicates that the system is stable (Ogata, 2007). Next, at Figure 71 in Appendix 2, the Nichols plot shows that based on the Nichols plot in Figure 6, it is observed that the gain margin is 1dB as the open-loop locus intersect with 0dB axis. The phase margin is also proven to be infinite as no open-loop locus intersect with -180 degrees line. Based on the gain and phase margin, it is observed that the system is stable under nonlinear condition due to the value of the gain is more than 0dB. In order for the system to be declared stable, the gain margin must be more than 0dB. (Chen, 1997). Lastly, for poles/zero plot shown at Figure 72 in Appendix 2, the plot shows that the system is unstable due to the presence of positive real roots (Claymore, n.d.).

4.1.2.2 Temperature 2

Based on Figure 73 in Appendix 2, the step response plot shows that the system is unstable at nonlinear condition. This is due to the constant decrease of the plot as time increases. Next, for Figure 74 in Appendix 2, the impulse plot shows that the system is critically stable due to the constant oscillation observed in the plot. Critically stable means that the system is at the middle of a stable or instable process (Ogata, 2007). Moving on to Figure 75 in Appendix 2, the Bode plot shows that the system is not stable due to the unstable oscillation towards the end of the plot. There must not be any sudden collation for the system to be labelled stable. The Nyquist plot at Figure 76 in Appendix 2 shows that the system is unstable due to the presence of the counter clockwise encirclements in the right side of the plane (Ogata, 2007). On the other hand, the Figure 77 in Appendix 2 shows that the system is unstable due to the phase margin is proven to be infinite as no open-loop locus intersect with -180 degrees line. As for gain margin, the gain margin is less than 0dB. Lastly, the pole/zero plot at Figure 78 in Appendix 2 shows that the system is unstable due to there are roots at right plane.

4.1.2.3 Temperature 3

Based on Figure 79 in Appendix 2, the step response plot shows that the system is critically stable at nonlinear condition. This is due to the constant oscillation of the plot as time increases. Next, for Figure 80 in Appendix 2, the impulse plot shows that the system is critically stable due to the constant oscillation observed in the plot. Moving on to Figure 81 in Appendix 2, the Bode plot shows that the system is not stable due to the unstable oscillation towards the end of the plot. There must not be any sudden collation for the system to be labelled stable. The Nyquist plot at Figure 82 in Appendix 2 shows that the system is unstable due to the presence of the counter clockwise encirclements in the right side of the plane. On the other hand, the Figure 83 in Appendix 2 shows that the system is unstable due to the phase margin is proven to be infinite as no open-loop locus intersect with -180 degrees line. As for gain margin, the gain margin is less than 0dB. Lastly, the pole/zero plot at Figure 84 in Appendix 2 shows that the system is unstable due to there are roots at positive real roots.

4.1.2.4 Temperature 4

Based on Figure 85 in Appendix 2, the step response plot shows that the system is unstable at nonlinear condition. This is due to the constant oscillating increase of the plot as time increases that shows no sign of stabilizing as time increases. Next, for Figure 86 in Appendix 2, the impulse plot shows that the system is unstable due to the inconstant oscillation observed in the plot. Moving on to Figure 87 in Appendix 2, the Bode plot shows that the system is not stable due to the unstable oscillation towards the end of the plot. The Nyquist plot at Figure 88 in Appendix 2 shows that the system is unstable due to the uneven number of encirclements at the both sides of the plane (Ogata, 2007). On the other hand, the Figure 89 in Appendix 2 shows that the system is unstable due to the phase margin is proven to be infinite as no open-loop locus intersect with -180 degrees line. As for gain margin, the gain margin is less than 0dB. Lastly, the pole/zero plot at Figure 90 in Appendix 2 shows that the system is unstable due to there are roots at right plane.

4.1.2.5 Temperature 5

Based on Figure 91 in Appendix 2, the step response plot shows that the system is unstable at nonlinear condition. This is due to the constant oscillating increase of the plot as time increases that shows no sign of stabilizing as time increases. Next, for Figure 92 in Appendix 2, the impulse plot shows that the system is unstable due to the inconstant oscillation observed in the plot. Moving on to Figure 93 in Appendix 2, the Bode plot shows that the system is not stable due to the unstable oscillation towards the end of the plot. The Nyquist plot at Figure 94 in Appendix 2 shows that the system is unstable due to the uneven number of encirclements at the both sides of the plane. On the other hand, the Figure 95 in Appendix 2 shows that the system is unstable due to the phase margin is proven to be infinite as no open-loop locus intersect with -180 degrees line. As for gain margin, the gain margin is less than 0dB. Lastly, the pole/zero plot at Figure 96 in Appendix 2 shows that the system is unstable due to there are roots at right plane.

4.1.2.6 Temperature 6

Based on Figure 97 in Appendix 2, the step response plot shows that the system is stable at nonlinear condition. This is due to the constant oscillating of the plot as time increases. Next, for Figure 98 in Appendix 2, the impulse plot shows that the system

is stable due to the oscillation slowly becoming stable as time increases. Moving on to Figure 99 in Appendix 2, the Bode plot shows that the system is stable due to the no unstable oscillation towards the end of the plot. The Nyquist plot at Figure 100 in Appendix 2 shows that the system is stable due to the no encirclements on the -1+j0 point. On the other hand, the Figure 101 in Appendix 2 shows that the system is stable due to the phase margin is proven to be infinite as no open-loop locus intersect with -180 degrees line. As for gain margin, the gain margin is more than 0dB. Lastly, the pole/zero plot at Figure 102 in Appendix 2 shows that the system is unstable due to there are roots at right plane.

4.1.2.7 Level 1

Based on Figure 103 in Appendix 2, the step response plot shows that the system is stable at nonlinear condition. This is due to the plot stabilizes as time increases. Next, for Figure 104 in Appendix 2, the impulse plot shows that the system is stable due to the constant oscillation observed in the plot towards the end of the time. Moving on to Figure 105 in Appendix 2, the Bode plot shows that the system is not stable due to the unstable oscillation towards the end of the plot. The Nyquist plot at Figure 106 in Appendix 2 shows that the system is unstable due to the uneven number of encirclements at the both sides of the plane. On the other hand, the Figure 107 in Appendix 2 shows that the system is unstable due to the phase margin is proven to be infinite as no open-loop locus intersect with -180 degrees line. As for gain margin, the gain margin is infinite and is less than 0dB. Lastly, the pole/zero plot at Figure 108 in Appendix 2 shows that the system is unstable due to there are roots at right plane.

4.1.2.8 Level 2

Based on Figure 109 in Appendix 2, the step response plot shows that the system is stable at nonlinear condition. This is due to the plot stabilizes at the end on the time. Next, for Figure 110 in Appendix 2, the impulse plot shows that the system is stable due to plot stabilizes towards the end of the time. Moving on to Figure 111 in Appendix 2, the Bode plot shows that the system is not stable due to the unstable oscillation towards the end of the plot. The Nyquist plot at Figure 112 in Appendix 2 shows that the system is unstable due to the uneven number of encirclements at the both sides of the plane. On the other hand, the Figure 113 in Appendix 2 shows that the system is

unstable due to the phase margin is proven to be infinite as no open-loop locus intersect with -180 degrees line. As for gain margin, the gain margin is infinite and is less than 0dB. Lastly, the pole/zero plot at Figure 114 in Appendix 2 shows that the system is unstable due to there are roots at right plane.

4.1.2.9 Level 3

Based on Figure 115 in Appendix 2, the step response plot shows that the system is unstable at nonlinear condition. This is due to the sudden increasing oscillation towards the end (Ogata, 2007). Next, for Figure 116 in Appendix 2, the impulse plot shows that the system is unstable due to sudden increasing oscillation towards the end. Moving on to Figure 117 in Appendix 2, the Bode plot shows that the system is not stable due to the unstable oscillation towards the end of the plot. The Nyquist plot at Figure 118 in Appendix 2 shows that the system is unstable due to the uneven number of encirclements at the both sides of the plane. On the other hand, the Figure 119 in Appendix 2 shows that the system is unstable due to the phase margin is proven to be infinite as no open-loop locus intersect with -180 degrees line. As for gain margin, the gain margin is infinite and is less than 0dB. Lastly, the pole/zero plot at Figure 120 in Appendix 2 shows that the system is unstable due to there are roots at right plane.

4.1.2.10 Level 4

Based on Figure 121 in Appendix 2, the step response plot shows that the system is stable at nonlinear condition. This is due to the plot slowly stabilizes towards the end. Next, for Figure 122 in Appendix 2, the impulse plot shows that the system is stable due to the plot slowly stabilizes as time increases oscillation towards the end. Moving on to Figure 123 in Appendix 2, the Bode plot shows that the system is not stable due to the unstable oscillation towards the end of the plot. The Nyquist plot at Figure 124 in Appendix 2 shows that the system is stable due to the even number of encirclements at the both sides of the plane. On the other hand, the Figure 125 in Appendix 2 shows that the system is unstable due to the phase margin is proven to be infinite as no open-loop locus intersect with -180 degrees line. As for gain margin, the gain margin is infinite and is less than 0dB. Lastly, the pole/zero plot at Figure 126 in Appendix 2 shows that the system is unstable due to there are roots at right plane.

4.1.2.11 Flow 1

Based on Figure 127 in Appendix 2, the step response plot shows that the system is unstable at nonlinear condition. This is due to the sudden increasing oscillation towards the end. Next, for Figure 128 in Appendix 2, the impulse plot shows that the system is unstable due to sudden increasing oscillation towards the end. Moving on to Figure 129 in Appendix 2, the Bode plot shows that the system is not stable due to the unstable oscillation towards the end of the plot. The Nyquist plot at Figure 130 in Appendix 2 shows that the system is unstable due to the uneven number of encirclements at the both sides of the plane. On the other hand, the Figure 131 in Appendix 2 shows that the system is unstable due to the phase margin is proven to be infinite as no open-loop locus intersect with -180 degrees line. As for gain margin, the gain margin is infinite and is less than 0dB. Lastly, the pole/zero plot at Figure 132 in Appendix 2 shows that the system is unstable due to there are roots at right plane.

4.1.2.12 Flow 2

Based on Figure 133 in Appendix 2, the step response plot shows that the system is unstable at nonlinear condition. This is due to the plot decreasing as time increases and shows no sign of stabilizing towards the end. Next, for Figure 134 in Appendix 2, the impulse plot shows that the system is stable due to the plot stabilizing as time increases. Moving on to Figure 135 in Appendix 2, the Bode plot shows that the system is not stable due to the unstable oscillation towards the end of the plot. The Nyquist plot at Figure 136 in Appendix 2 shows that the system is unstable due to the there is one or more clockwise encirclements present in the -1+j0 point. On the other hand, the Figure 137 in Appendix 2 shows that the system is unstable due to the phase margin is proven to be infinite as no open-loop locus intersect with -180 degrees line. As for gain margin, the gain margin is infinite and is less than 0dB. Lastly, the pole/zero plot at Figure 138 in Appendix 2 shows that the system is unstable due to there are roots at right plane.

4.1.2.13 Pressure 1

Based on Figure 139 in Appendix 2, the step response plot shows that the system is unstable at nonlinear condition. This is due to the sudden oscillation at the end of the plot. Next, for Figure 140 in Appendix 2, the impulse plot shows that the system is stable due to the sudden oscillation at the end of the plot. Moving on to Figure 141 in Appendix 2, the Bode plot shows that the system is not stable due to the unstable

oscillation towards the end of the plot. The Nyquist plot at Figure 142 in Appendix 2 shows that the system is unstable due to the there is one or more clockwise encirclements present in the -1+j0 point. On the other hand, the Figure 143 in Appendix 2 shows that the system is unstable due to the phase margin is proven to be infinite as no open-loop locus intersect with -180 degrees line. As for gain margin, the gain margin is infinite and is less than 0dB. Lastly, the pole/zero plot at Figure 144 in Appendix 2 shows that the system is unstable due to there are roots at right plane.

4.2 Overall Discussion

As of Final Year Project I, only linear system identification was simulated and completed. The simulation was done using trial and error method until the best fit of more than 80% is obtained. The model obtained from system identification, transfer models in z and s transform and plots obtained are presented. Based on the results obtained, all obtained model is based on ARX model structure.

For Final Year Project II, the project continues with non-linear system identification. The simulation was done also using trial and error method, until best fit of 80% is obtained. However, due to some unforeseen circumstances, there are some result obtained that is below 80% best fit. Further simulation will be done to improve the result. Based on result obtained, majority of the model is based on Hammerstein – Wiener model, only some are based on sigmoid network.

Below are the table for the best fit of the simulation:

Table 2: Best fit table

Parameter	**Linear (%)**	**Nonlinear (%)**
Temperature 1	94.57	72.97
Temperature 2	95.35	68.35
Temperature 3	92.95	60.52
Temperature 4	93.06	59.32
Temperature 5	97.32	85.74
Temperature 6	99.84	91.98
Level 1	84.5	100
Level 2	96.38	69
Level 3	96.56	100

Level 4	99.27	94.3
Flow 1	91.16	100
Flow 2	94.31	100
Pressure 1	90.04	100

Hence, the model obtained for nonlinear system identification may not be accurate enough due to some best fit obtained under 80%. As for linear system identification, the model obtained is accurate due to the high best fit %.

Based on the plots obtained, based on the simulation and analysis done, from the plotted charts, it shows that the system is unstable under linear condition and the simulation was done for various parameters. As for nonlinear, some of the parameters are stable and some are not stable when simulation was done. This is true due to the high nonlinearity of the column itself, which is already explained in the literature review.

CHAPTER 5

CONCLUSION AND RECOMMENDATION

5.1 Conclusion

As a conclusion, the project managed to reach its objective which is to perform linear and nonlinear system identification on debutanizer column. Based on the simulation and analysis done, from the plotted charts, it shows that the system is unstable under linear condition and the simulation was done for various parameters. As for nonlinear, some of the parameters are stable and some are not stable. Hence, it can be concluded that the system is nonlinear, hence good control strategy will be needed to ensure that the system can be controlled later.

5.2 Recommendations

Further research and work needs to be done with the simulation. One of the recommendation is that the data from the plant should be collected by the student itself. This is so that the student can at least have some experience with collection of data. The collection of data should also be more than once and at different time. This is to eliminate the probability of error.

It is also recommended that more plots is done, such as M and N circles to further investigate the stability of the system. Lastly, for further research, it is recommended to use other software other than MATLAB for system identification to compare the difference in terms of the model obtained from identification. MATLAB software also did not show and provide nonlinear transfer function equation of nonlinear system identification after modelling is done, hence, other robust software is recommended to be used to obtain the transfer equation.

REFERENCES

Ansari, R. M., & Tadé, M. O. (1998). Nonlinear model based multivariable control of a debutanizer. *Journal of Process Control, 8*(4), 279-286. doi: http://dx.doi.org/10.1016/S0959-1524(98)00003-1

Bousono Zavala, O. (2011). *Multivariable Model Predictive Control for optimal operation of a fluid catalytic cracking debutanizer distillation column.* (1534403 M.S.), University of Puerto Rico, Mayaguez (Puerto Rico), Ann Arbor. Retrieved from http://search.proquest.com/docview/1315766356?accountid=47520 ProQuest Dissertations & Theses Full Text: The Sciences and Engineering Collection database.

Chen, W. B., Donald. J. (1997). Stability Analysis On the Nichols Chart and Its Application in QFT. from http://citeseerx.ist.psu.edu/viewdoc/download;jsessionid=83F05890DBC8FAD13A31876BF1235B73?doi=10.1.1.35.1879&rep=rep1&type=pdf

Claymore. (n.d.). Root Locus Analysis. from http://claymore.engineer.gvsu.edu/~jackh/books/model/chapters/rootlocus.pdf

Gupta, S., Ray, S., & Samanta, A. N. (2009). Nonlinear control of debutanizer column using profile position observer. *Computers & Chemical Engineering, 33*(6), 1202-1211. doi: http://dx.doi.org/10.1016/j.compchemeng.2008.12.009

Huang, H., & Riggs, J. B. (2002). Comparison of PI and MPC for control of a gas recovery unit. *Journal of Process Control, 12*(1), 163-173. doi: http://dx.doi.org/10.1016/S0959-1524(01)00004-X

Ljung, L., & MathWorks, I. (2005). *System Identification Toolbox for Use with MATLAB: User's Guide*: MathWorks, Incorporated.

Massachusetts Institute of Technology. (2000). Stability Criteria - (Gain Margin and Phase Margin). from

http://stuff.mit.edu/afs/athena/course/2/2.010/www_f00/psets/hw3_dir/tutor3_dir/tut3_g.html

MathWorks, I. (n.d.). System Identification Toolbox. from http://www.mathworks.com/products/sysid/

Mohamed Ramli, N., Hussain, M. A., Mohamed Jan, B., & Abdullah, B. (2014). Composition Prediction of a Debutanizer Column using Equation Based Artificial Neural Network Model. *Neurocomputing, 131*(0), 59-76. doi: http://dx.doi.org/10.1016/j.neucom.2013.10.039

Ogata, K. (2007). *Matlab for Control Engineers*: Prentice Hall.

Pelckmans, K. (2012). Lecture Notes for a course on System Identification, v2012. http://www.it.uu.se/edu/course/homepage/systemid/vt12/ch1.pdf

wiseGEEK. (n.d.). What is a debutanizer? , from http://www.wisegeek.com/what-is-a-debutanizer.htm

Zhu, Y. (2001). *Multivariable System Identification For Process Control*: Elsevier Science.

APPENDICES

APPENDIX 1

LINEAR SYSTEM IDENTIFICATION

Temperature 2

ARX Model

Fit to estimation data: 95.35%

A(z) = 1 - 0.5696 z^-1 - 0.02657 z^-2 - 0.3957 z^-3 + 0.2241 z^-4 + 0.3555 z^-5
- 0.1324 z^-6 + 0.1225 z^-7 - 0.2306 z^-8 - 0.3123 z^-9 + 0.2664 z^-10
+ 0.03602 z^-11 + 0.6742 z^-12 - 0.5282 z^-13 - 0.3053 z^-14 - 0.1089 z^-15
+ 0.6016 z^-16 + 0.3267 z^-17 - 0.353 z^-18 + 0.3949 z^-19 - 0.9479 z^-20
- 0.7422 z^-21 + 0.9478 z^-22 + 0.5304 z^-23 + 0.4442 z^-24 - 0.2384 z^
-25 - 0.5165 z^-26 - 0.4078 z^-27 - 0.4994 z^-28 + 0.5935 z^-29 + 0.1268 z^-30
+ 0.4999 z^-31 - 0.3978 z^-32 + 0.3786 z^-33 - 0.3542 z^-34 - 0.0657 z^
-35 - 0.187 z^-36 - 0.478 z^-37 + 0.3034 z^-38 - 0.1344 z^-39 + 0.291 z^-40
+ 0.9884 z^-41 - 0.7539 z^-42 - 0.1112 z^-43 - 0.3682 z^-44 - 0.03629 z^-45
- 0.07217 z^-46 + 0.2605 z^-47 + 0.2965 z^-48 + 0.282 z^-49 - 0.708 z^-50
- 0.3303 z^-51 + 0.383 z^-52 - 0.6547 z^-53 + 0.9683 z^-54 - 0.02071 z^
-55 - 0.07672 z^-56 - 0.6064 z^-57 - 0.07626 z^-58 + 0.1833 z^-59 - 0.3308 z^-60
+ 0.7839 z^-61 + 0.1565 z^-62 + 0.0545 z^-63 - 0.3646 z^-64 + 0.06855 z^-65
- 0.1268 z^-66 + 0.002604 z^-67 + 0.2998 z^-68 - 0.1294 z^-69 - 0.5756 z^-70
+ 0.3768 z^-71 - 0.0002049 z^-72 + 0.04997 z^-73 + 0.4092 z^-74 - 0.08036 z^-75
- 0.112 z^-76 - 0.1527 z^-77 - 0.08999 z^-78 + 0.07614 z^-79 + 0.1966 z^-80
- 0.3376 z^-81 - 0.1179 z^-82 + 0.04947 z^-83 + 0.4421 z^-84 - 0.2646 z^-85
+ 0.3541 z^-86 - 0.03492 z^-87 - 0.4243 z^-88 - 0.4125 z^-89 - 0.2705 z^-90
+ 0.8904 z^-91 - 0.6428 z^-92 + 0.6263 z^-93 + 0.05975 z^-94 - 0.3167 z^-95
- 0.09775 z^-96 + 0.03556 z^-97 + 0.2625 z^-98

B(z) = 1.368 z^-1 - 0.7038 z^-2 + 0.8748 z^-3 + 0.211 z^-4 - 0.9802 z^-5 - 1.347 z^-6
+ 0.07037 z^-7 + 0.006908 z^-8 + 0.3513 z^-9 + 0.4587 z^-10 + 0.2475 z^
-11 + 0.5504 z^-12 - 1.177 z^-13 + 0.8949 z^-14 - 0.2254 z^-15 - 0.7176 z^-16
+ 0.3824 z^-17 - 0.3541 z^-18 + 1.201 z^-19 + 0.07092 z^-20 + 0.1443 z^
-21 - 0.782 z^-22 - 3.235 z^-23 + 1.537 z^-24 - 0.5804 z^-25 + 1.217 z^
-26 + 2.242 z^-27 - 1.032 z^-28 - 1.485 z^-29 - 0.7344 z^-30 - 0.8937 z^-31
+ 1.253 z^-32 - 0.2932 z^-33 + 2.328 z^-34 - 1.181 z^-35 + 0.82 z^-36 - 1.269 z^-37
+ 0.3525 z^-38 - 1.011 z^-39 - 0.13 z^-40 - 0.0499 z^-41 - 0.1663 z^-42
+ 3.431 z^-43 - 1.516 z^-44 + 0.005022 z^-45 - 0.7235 z^-46 + 0.2722 z^
-47 - 1.894 z^-48 + 0.2629 z^-49 + 1.845 z^-50 - 0.2073 z^-51 - 0.08982 z^-52
- 1.289 z^-53 + 2.024 z^-54 - 2.374 z^-55 + 0.7663 z^-56 + 1.808 z^-57
- 1.073 z^-58 - 1.157 z^-59 + 1.299 z^-60 - 1.783 z^-61 + 0.3728 z^-62
+ 0.9129 z^-63 + 0.4118 z^-64 + 2.233 z^-65 - 1.564 z^-66 + 1.399 z^-67
- 2.932 z^-68 + 1.113 z^-69 - 1.298 z^-70 + 0.378 z^-71 - 0.06832 z^-72
+ 0.3323 z^-73 + 0.5154 z^-74 - 0.2318 z^-75 + 1.319 z^-76 + 0.8994 z^-77
- 2.744 z^-78 + 2.259 z^-79 - 1.615 z^-80 - 0.7833 z^-81 + 2.739 z^-82
- 1.822 z^-83 - 0.03042 z^-84 - 0.8841 z^-85 + 0.7018 z^-86 + 0.2208 z^
-87 + 2.219 z^-88 - 1.517 z^-89 + 2.002 z^-90 - 3.437 z^-91 - 0.3842 z^
-92 - 0.0993 z^-93 + 0.05629 z^-94 + 2.918 z^-95 - 0.1703 z^-96 - 0.4787 z^-97

Transfer model in z transform

1.368 z^-1 - 0.7038 z^-2 + 0.8748 z^-3 + 0.211 z^-4 - 0.9802 z^-5 - 1.347 z^-6

+ 0.07037 z^-7 + 0.006908 z^-8 + 0.3513 z^-9 + 0.4587 z^-10 + 0.2475 z^
-11 + 0.5504 z^-12 - 1.177 z^-13 + 0.8949 z^-14 - 0.2254 z^-15 - 0.7176 z^-16
+ 0.3824 z^-17 - 0.3541 z^-18 + 1.201 z^-19 + 0.07092 z^-20 + 0.1443 z^
-21 - 0.782 z^-22 - 3.235 z^-23 + 1.537 z^-24 - 0.5804 z^-25 + 1.217 z^
-26 + 2.242 z^-27 - 1.032 z^-28 - 1.485 z^-29 - 0.7344 z^-30 - 0.8937 z^-31
+ 1.253 z^-32 - 0.2932 z^-33 + 2.328 z^-34 - 1.181 z^-35 + 0.82 z^-36 - 1.269 z^-37
+ 0.3525 z^-38 - 1.011 z^-39 - 0.13 z^-40 - 0.0499 z^-41 - 0.1663 z^-42
+ 3.431 z^-43 - 1.516 z^-44 + 0.005022 z^-45 - 0.7235 z^-46 + 0.2722 z^
-47 - 1.894 z^-48 + 0.2629 z^-49 + 1.845 z^-50 - 0.2073 z^-51 - 0.08982 z^-52
- 1.289 z^-53 + 2.024 z^-54 - 2.374 z^-55 + 0.7663 z^-56 + 1.808 z^-57
- 1.073 z^-58 - 1.157 z^-59 + 1.299 z^-60 - 1.783 z^-61 + 0.3728 z^-62
+ 0.9129 z^-63 + 0.4118 z^-64 + 2.233 z^-65 - 1.564 z^-66 + 1.399 z^-67
- 2.932 z^-68 + 1.113 z^-69 - 1.298 z^-70 + 0.378 z^-71 - 0.06832 z^-72
+ 0.3323 z^-73 + 0.5154 z^-74 - 0.2318 z^-75 + 1.319 z^-76 + 0.8994 z^-77
- 2.744 z^-78 + 2.259 z^-79 - 1.615 z^-80 - 0.7833 z^-81 + 2.739 z^-82
- 1.822 z^-83 - 0.03042 z^-84 - 0.8841 z^-85 + 0.7018 z^-86 + 0.2208 z^
-87 + 2.219 z^-88 - 1.517 z^-89 + 2.002 z^-90 - 3.437 z^-91 - 0.3842 z^
-92 - 0.0993 z^-93 + 0.05629 z^-94 + 2.918 z^-95 - 0.1703 z^-96 - 0.4787 z^-97

---

1 - 0.5696 z^-1 - 0.02657 z^-2 - 0.3957 z^-3 + 0.2241 z^-4 + 0.3555 z^-5 - 0.1324 z^-6
+ 0.1225 z^-7 - 0.2306 z^-8 - 0.3123 z^-9 + 0.2664 z^-10 + 0.03602 z^-11
+ 0.6742 z^-12 - 0.5282 z^-13 - 0.3053 z^-14 - 0.1089 z^-15 + 0.6016 z^
-16 + 0.3267 z^-17 - 0.353 z^-18 + 0.3949 z^-19 - 0.9479 z^-20 - 0.7422 z^-21
+ 0.9478 z^-22 + 0.5304 z^-23 + 0.4442 z^-24 - 0.2384 z^-25 - 0.5165 z^
-26 - 0.4078 z^-27 - 0.4994 z^-28 + 0.5935 z^-29 + 0.1268 z^-30 + 0.4999 z^-31
- 0.3978 z^-32 + 0.3786 z^-33 - 0.3542 z^-34 - 0.0657 z^-35 - 0.187 z^-36
- 0.478 z^-37 + 0.3034 z^-38 - 0.1344 z^-39 + 0.291 z^-40 + 0.9884 z^-41
- 0.7539 z^-42 - 0.1112 z^-43 - 0.3682 z^-44 - 0.03629 z^-45 - 0.07217 z^-46
+ 0.2605 z^-47 + 0.2965 z^-48 + 0.282 z^-49 - 0.708 z^-50 - 0.3303 z^-51
+ 0.383 z^-52 - 0.6547 z^-53 + 0.9683 z^-54 - 0.02071 z^-55 - 0.07672 z^-56
- 0.6064 z^-57 - 0.07626 z^-58 + 0.1833 z^-59 - 0.3308 z^-60 + 0.7839 z^-61
+ 0.1565 z^-62 + 0.0545 z^-63 - 0.3646 z^-64 + 0.06855 z^-65 - 0.1268 z^-66
+ 0.002604 z^-67 + 0.2998 z^-68 - 0.1294 z^-69 - 0.5756 z^-70 + 0.3768 z^-71
- 0.0002049 z^-72 + 0.04997 z^-73 + 0.4092 z^-74 - 0.08036 z^-75 - 0.112 z^-76
- 0.1527 z^-77 - 0.08999 z^-78 + 0.07614 z^-79 + 0.1966 z^-80 - 0.3376 z^-81
- 0.1179 z^-82 + 0.04947 z^-83 + 0.4421 z^-84 - 0.2646 z^-85 + 0.3541 z^-86
- 0.03492 z^-87 - 0.4243 z^-88 - 0.4125 z^-89 - 0.2705 z^-90 + 0.8904 z^-91
- 0.6428 z^-92 + 0.6263 z^-93 + 0.05975 z^-94 - 0.3167 z^-95 - 0.09775 z^-96
+ 0.03556 z^-97 + 0.2625 z^-98

Transfer model in s transform

1.549 s^99 + 4.649 s^98 + 261.9 s^97 + 761.7 s^96 + 2.134e04 s^95 + 6.007e04 s^94
+ 1.116e06 s^93 + 3.038e06 s^92 + 4.209e07 s^91 + 1.107e08 s^90 + 1.221e09 s^89
+ 3.1e09 s^88 + 2.832e10 s^87 + 6.936e10 s^86 + 5.403e11 s^85 + 1.274e12 s^84
+ 8.642e12 s^83 + 1.96e13 s^82 + 1.176e14 s^81 + 2.562e14 s^80 + 1.377e15 s^79
+ 2.878e15 s^78 + 1.399e16 s^77 + 2.802e16 s^76 + 1.243e17 s^75 + 2.382e17 s^74
+ 9.712e17 s^73 + 1.777e18 s^72 + 6.699e18 s^71 + 1.169e19 s^70 + 4.095e19 s^69
+ 6.81e19 s^68 + 2.224e20 s^67 + 3.52e20 s^66 + 1.076e21 s^65 + 1.619e21 s^64
+ 4.645e21 s^63 + 6.636e21 s^62 + 1.79e22 s^61 + 2.427e22 s^60 + 6.166e22 s^59
+ 7.93e22 s^58 + 1.898e23 s^57 + 2.315e23 s^56 + 5.223e23 s^55 + 6.04e23 s^54
+ 1.283e24 s^53 + 1.408e24 s^52 + 2.813e24 s^51 + 2.931e24 s^50 + 5.495e24 s^49
+ 5.442e24 s^48 + 9.545e24 s^47 + 9.004e24 s^46 + 1.471e25 s^45 + 1.325e25 s^44
+ 2.007e25 s^43 + 1.73e25 s^42 + 2.415e25 s^41 + 2e25 s^40 + 2.554e25 s^39
+ 2.039e25 s^38 + 2.363e25 s^37 + 1.826e25 s^36 + 1.903e25 s^35 + 1.43e25 s^34
+ 1.326e25 s^33 + 9.744e24 s^32 + 7.942e24 s^31 + 5.734e24 s^30 + 4.055e24 s^29
+ 2.893e24 s^28 + 1.748e24 s^27 + 1.239e24 s^26 + 6.292e23 s^25 + 4.461e23 s^24

+ 1.866e23 s^23 + 1.332e23 s^22 + 4.484e22 s^21 + 3.249e22 s^20 + 8.557e21 s^19
+ 6.36e21 s^18 + 1.263e21 s^17 + 9.771e20 s^16 + 1.391e20 s^15 + 1.146e20 s^14
+ 1.085e19 s^13 + 9.928e18 s^12 + 5.491e17 s^11 + 6.064e17 s^10 + 1.456e16 s^9
+ 2.455e16 s^8 + 4.212e12 s^7 + 5.993e14 s^6 - 1.063e13 s^5 + 7.489e12 s^4
- 2.479e11 s^3 + 3.437e10 s^2 - 1.682e09 s + 2.169e07

---

s^100 + 1.643 s^99 + 172.2 s^98 + 272.3 s^97 + 1.428e04 s^96 + 2.174e04 s^95
+ 7.604e05 s^94 + 1.114e06 s^93 + 2.921e07 s^92 + 4.118e07 s^91 + 8.624e08 s^90
+ 1.17e09 s^89 + 2.038e10 s^88 + 2.658e10 s^87 + 3.958e11 s^86 + 4.965e11 s^85
+ 6.445e12 s^84 + 7.772e12 s^83 + 8.928e13 s^82 + 1.035e14 s^81 + 1.064e15 s^80
+ 1.185e15 s^79 + 1.101e16 s^78 + 1.177e16 s^77 + 9.96e16 s^76 + 1.021e17 s^75
+ 7.919e17 s^74 + 7.786e17 s^73 + 5.56e18 s^72 + 5.24e18 s^71 + 3.459e19 s^70
+ 3.123e19 s^69 + 1.913e20 s^68 + 1.653e20 s^67 + 9.425e20 s^66 + 7.79e20 s^65
+ 4.142e21 s^64 + 3.272e21 s^63 + 1.627e22 s^62 + 1.227e22 s^61 + 5.709e22 s^60
+ 4.11e22 s^59 + 1.792e23 s^58 + 1.23e23 s^57 + 5.031e23 s^56 + 3.288e23 s^55
+ 1.262e24 s^54 + 7.848e23 s^53 + 2.829e24 s^52 + 1.671e24 s^51 + 5.655e24 s^50
+ 3.171e24 s^49 + 1.007e25 s^48 + 5.353e24 s^47 + 1.595e25 s^46 + 8.024e24 s^45
+ 2.241e25 s^44 + 1.065e25 s^43 + 2.786e25 s^42 + 1.249e25 s^41 + 3.055e25 s^40
+ 1.289e25 s^39 + 2.944e25 s^38 + 1.166e25 s^37 + 2.483e25 s^36 + 9.212e24 s^35
+ 1.824e25 s^34 + 6.318e24 s^33 + 1.161e25 s^32 + 3.74e24 s^31 + 6.358e24 s^30
+ 1.897e24 s^29 + 2.977e24 s^28 + 8.184e23 s^27 + 1.181e24 s^26 + 2.973e23 s^25
+ 3.934e23 s^24 + 8.999e22 s^23 + 1.087e23 s^22 + 2.24e22 s^21 + 2.457e22 s^20
+ 4.515e21 s^19 + 4.468e21 s^18 + 7.239e20 s^17 + 6.406e20 s^16 + 9.037e19 s^15
+ 7.053e19 s^14 + 8.557e18 s^13 + 5.765e18 s^12 + 5.953e17 s^11 + 3.344e17 s^10
+ 2.92e16 s^9 + 1.293e16 s^8 + 9.534e14 s^7 + 3.029e14 s^6 + 1.88e13 s^5
+ 3.674e12 s^4 + 1.816e11 s^3 + 1.676e10 s^2 + 4.307e08 s + 1.249e06

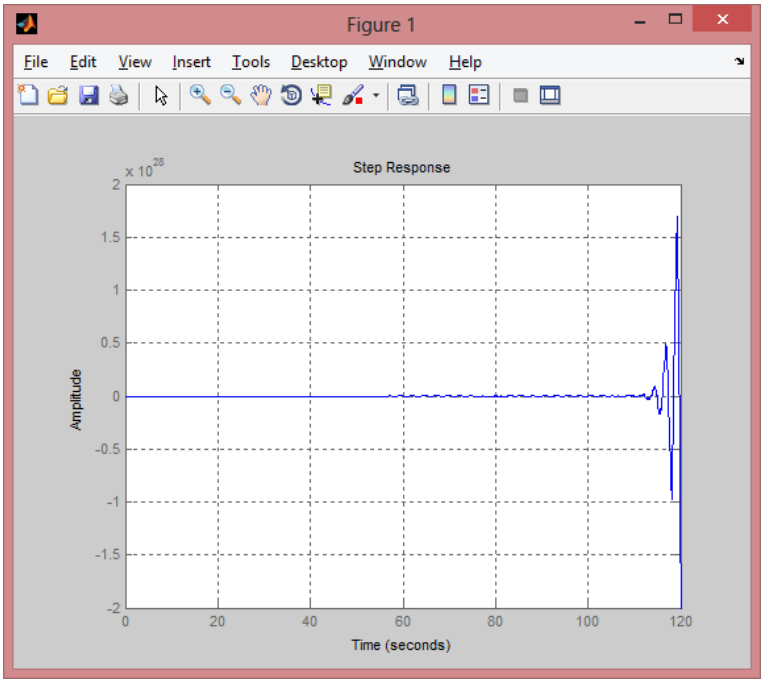

Figure 7: Step response (Temperature 2 – Linear)

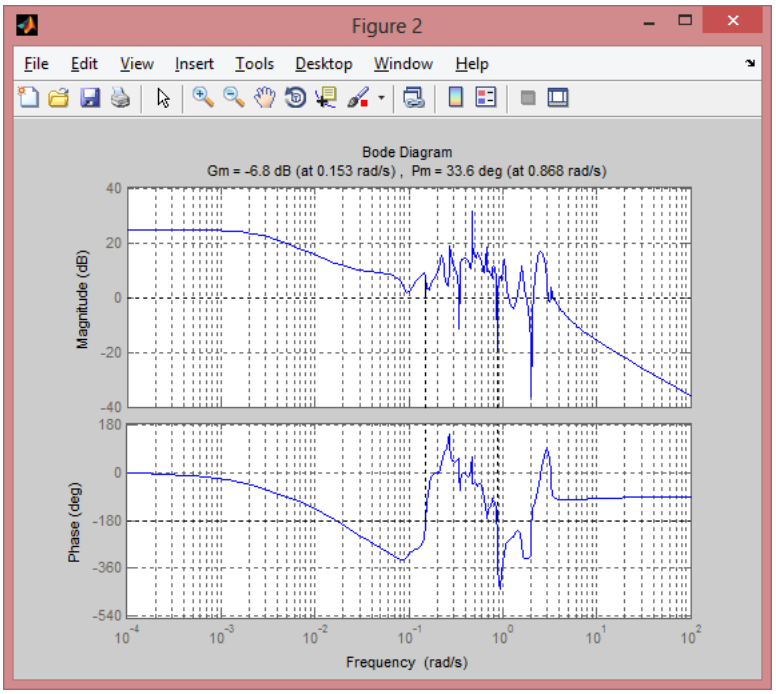

Figure 8: Bode plot (Temperature 2 - Linear)

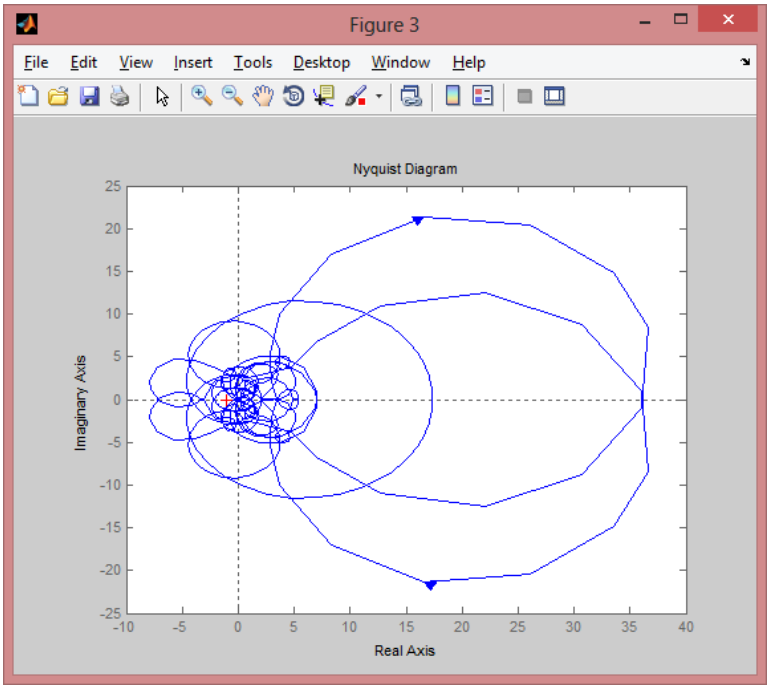

Figure 9: Nyquist plot (Temperature 2 - Linear)

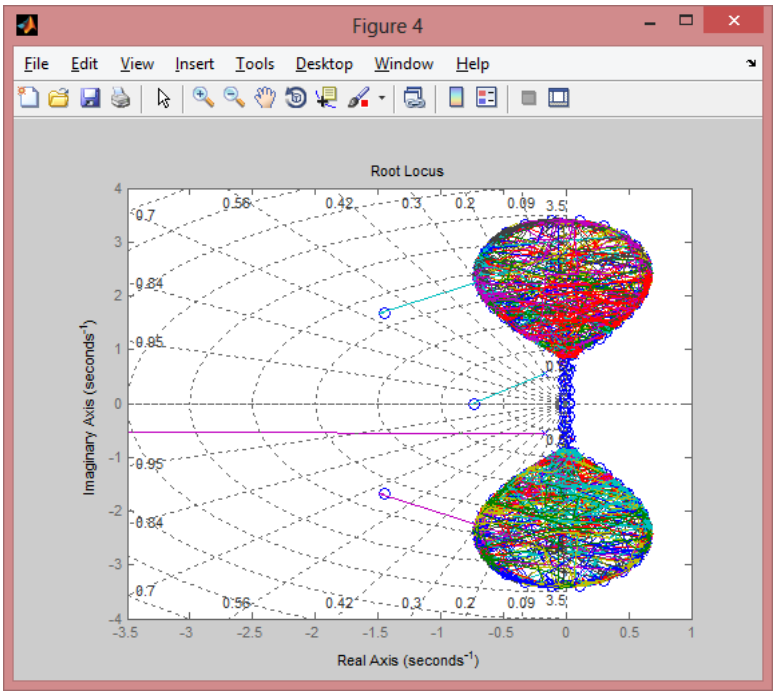

Figure 10: Root locus plot (Temperature 2 - Linear)

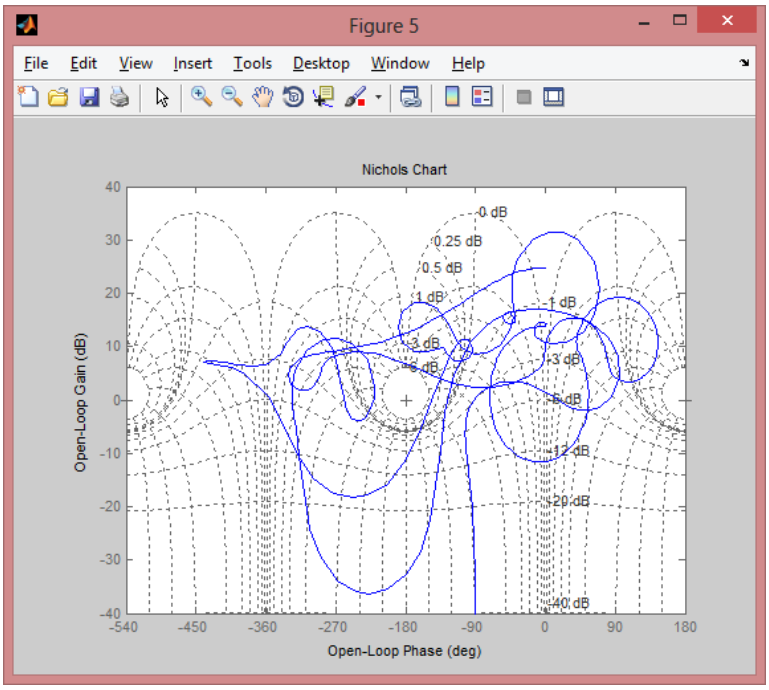

Figure 11: Nichols plot (Temperature 2 - Linear)

Temperature 3

ARX Model

Fit to estimation data: 92.95%

A(z) = 1 - 1.333 z^-1 - 0.1003 z^-2 + 0.04838 z^-3 + 1.31 z^-4 - 1.188 z^-5 + 0.641 z^-6
- 0.5738 z^-7 + 0.603 z^-8 - 0.5069 z^-9 + 0.06223 z^-10 - 0.8508 z^-11 + 1.541 z^-12
+ 0.08293 z^-13 - 0.4284 z^-14 - 0.975 z^-15 + 0.455 z^-16 + 0.06784 z^-17
+ 0.467 z^-18 + 0.7372 z^-19 - 1.151 z^-20 + 0.2842 z^-21 - 0.5076 z^-22
+ 0.4634 z^-23 - 0.03397 z^-24 + 0.4784 z^-25 - 0.7735 z^-26 + 0.9629 z^-27
- 0.6093 z^-28 + 0.2928 z^-29 - 1.208 z^-30 + 1.337 z^-31 - 0.6492 z^-32
+ 0.9216 z^-33 - 0.7676 z^-34 + 0.01774 z^-35 - 0.07515 z^-36 - 0.007522 z^-37
+ 0.0503 z^-38 + 0.0724 z^-39 + 0.1101 z^-40 - 0.3051 z^-41 + 0.8424 z^-42
- 0.153 z^-43 - 0.945 z^-44 - 0.4963 z^-45 + 1.164 z^-46 + 0.3493 z^-47 - 0.3428 z^-48
- 0.4663 z^-49 + 0.4478 z^-50 - 0.5343 z^-51 + 0.3504 z^-52 - 0.4879 z^-53
+ 0.7327 z^-54 + 0.2129 z^-55 + 0.02298 z^-56 - 0.1926 z^-57 - 0.07282 z^
-58 - 0.7216 z^-59 + 0.1083 z^-60 + 1.423 z^-61 - 0.1255 z^-62 - 0.5066 z^-63
- 0.7891 z^-64 + 0.8035 z^-65 - 0.09392 z^-66 + 0.6109 z^-67 - 0.7393 z^-68
+ 0.4189 z^-69 - 0.5429 z^-70 + 0.8597 z^-71 + 0.2438 z^-72 - 1.093 z^-73
- 0.1302 z^-74 - 0.005411 z^-75 + 1.452 z^-76 - 0.3493 z^-77 - 0.5465 z^-78
- 0.3775 z^-79 + 0.4557 z^-80 + 0.1364 z^-81 - 0.174 z^-82 + 0.02438 z^-83
+ 0.2256 z^-84 + 0.3779 z^-85 - 0.2637 z^-86 - 0.5845 z^-87 - 0.3038 z^-88
+ 1.005 z^-89 - 0.005901 z^-90 - 0.3504 z^-91 + 0.4036 z^-92 - 0.5665 z^-93
- 0.3265 z^-94 + 0.4575 z^-95 + 0.5773 z^-96 - 0.4181 z^-97 - 0.9443 z^-98
+ 1.108 z^-99 - 0.4177 z^-100

B(z) = 1.184 z^-1 + 0.09413 z^-2 - 1.469 z^-3 - 0.4548 z^-4 + 1.052 z^-5 + 1.303 z^-6
- 0.2926 z^-7 - 0.1603 z^-8 - 0.3721 z^-9 + 0.2598 z^-10 + 0.8072 z^-11 + 0.03714 z^-12
- 0.2193 z^-13 + 0.7016 z^-14 + 0.9661 z^-15 - 0.01371 z^-16 - 0.6395 z^-17
- 0.4298 z^-18 + 0.697 z^-19 + 0.4649 z^-20 + 0.1945 z^-21 - 0.2075 z^-22
- 0.1751 z^-23 - 0.6862 z^-24 - 0.1515 z^-25 + 0.2482 z^-26 - 0.01193 z^-27
+ 1.192 z^-28 + 0.551 z^-29 - 1.545 z^-30 - 0.5726 z^-31 - 1.4 z^-32 + 0.005766 z^-33
+ 1.385 z^-34 + 0.5085 z^-35 - 1.35 z^-36 - 0.8893 z^-37 - 0.5811 z^-38 - 1.016 z^-39
+ 0.1423 z^-40 + 1.011 z^-41 + 0.4317 z^-42 - 1.702 z^-43 - 0.2908 z^-44
- 0.05609 z^-45 + 0.2293 z^-46 - 0.2646 z^-47 + 0.05649 z^-48 + 0.6031 z^
-49 + 0.1451 z^-50 - 0.1004 z^-51 - 0.281 z^-52 + 0.1574 z^-53 - 0.5276 z^-54
+ 0.05882 z^-55 + 1.185 z^-56 - 0.005859 z^-57 - 0.6561 z^-58 - 0.03779 z^-59
- 0.4374 z^-60 + 0.1964 z^-61 + 0.4151 z^-62 - 1.309 z^-63 + 0.03076 z^-64
+ 1.6 z^-65 - 0.1283 z^-66 - 0.5845 z^-67 + 0.1543 z^-68 + 0.8191 z^-69 + 0.5102 z^-70
+ 0.4684 z^-71 + 0.2716 z^-72 - 0.05741 z^-73 + 0.6398 z^-74 + 0.7102 z^-75
+ 1.144 z^-76 + 0.3582 z^-77 + 0.1661 z^-78 - 0.1259 z^-79 + 0.6666 z^-80
+ 0.3473 z^-81 + 0.1981 z^-82 + 0.206 z^-83 - 0.4264 z^-84 - 0.1567 z^-85
+ 0.3969 z^-86 - 0.08814 z^-87 - 0.3226 z^-88 + 0.269 z^-89 - 0.1478 z^-90
+ 0.2392 z^-91 - 0.3298 z^-92 - 1.04 z^-93 + 0.4532 z^-94 + 0.4489 z^-95
- 0.757 z^-96 + 0.0998 z^-97 + 0.3961 z^-98 - 0.4763 z^-99 - 0.9415 z^-100

Transfer model in z transform

1.184 z^-1 + 0.09413 z^-2 - 1.469 z^-3 - 0.4548 z^-4 + 1.052 z^-5 + 1.303 z^-6
- 0.2926 z^-7 - 0.1603 z^-8 - 0.3721 z^-9 + 0.2598 z^-10 + 0.8072 z^-11
+ 0.03714 z^-12 - 0.2193 z^-13 + 0.7016 z^-14 + 0.9661 z^-15 - 0.01371 z^-16
- 0.6395 z^-17 - 0.4298 z^-18 + 0.697 z^-19 + 0.4649 z^-20 + 0.1945 z^-21
- 0.2075 z^-22 - 0.1751 z^-23 - 0.6862 z^-24 - 0.1515 z^-25 + 0.2482 z^-26

- 0.01193 z^-27 + 1.192 z^-28 + 0.551 z^-29 - 1.545 z^-30 - 0.5726 z^
-31 - 1.4 z^-32 + 0.005766 z^-33 + 1.385 z^-34 + 0.5085 z^-35 - 1.35 z^-36
- 0.8893 z^-37 - 0.5811 z^-38 - 1.016 z^-39 + 0.1423 z^-40 + 1.011 z^
-41 + 0.4317 z^-42 - 1.702 z^-43 - 0.2908 z^-44 - 0.05609 z^-45 + 0.2293 z^-46
- 0.2646 z^-47 + 0.05649 z^-48 + 0.6031 z^-49 + 0.1451 z^-50 - 0.1004 z^-51
- 0.281 z^-52 + 0.1574 z^-53 - 0.5276 z^-54 + 0.05882 z^-55 + 1.185 z^-56
- 0.005859 z^-57 - 0.6561 z^-58 - 0.03779 z^-59 - 0.4374 z^-60 + 0.1964 z^-61
+ 0.4151 z^-62 - 1.309 z^-63 + 0.03076 z^-64 + 1.6 z^-65 - 0.1283 z^-66
- 0.5845 z^-67 + 0.1543 z^-68 + 0.8191 z^-69 + 0.5102 z^-70 + 0.4684 z^-71
+ 0.2716 z^-72 - 0.05741 z^-73 + 0.6398 z^-74 + 0.7102 z^-75 + 1.144 z^-76
+ 0.3582 z^-77 + 0.1661 z^-78 - 0.1259 z^-79 + 0.6666 z^-80 + 0.3473 z^-81
+ 0.1981 z^-82 + 0.206 z^-83 - 0.4264 z^-84 - 0.1567 z^-85 + 0.3969 z^-86
- 0.08814 z^-87 - 0.3226 z^-88 + 0.269 z^-89 - 0.1478 z^-90 + 0.2392 z^-91
- 0.3298 z^-92 - 1.04 z^-93 + 0.4532 z^-94 + 0.4489 z^-95 - 0.757 z^-96
+ 0.0998 z^-97 + 0.3961 z^-98 - 0.4763 z^-99 - 0.9415 z^-100

---

1 - 1.333 z^-1 - 0.1003 z^-2 + 0.04838 z^-3 + 1.31 z^-4 - 1.188 z^-5 + 0.641 z^-6
- 0.5738 z^-7 + 0.603 z^-8 - 0.5069 z^-9 + 0.06223 z^-10 - 0.8508 z^-11
+ 1.541 z^-12 + 0.08293 z^-13 - 0.4284 z^-14 - 0.975 z^-15 + 0.455 z^
-16 + 0.06784 z^-17 + 0.467 z^-18 + 0.7372 z^-19 - 1.151 z^-20 + 0.2842 z^-21
- 0.5076 z^-22 + 0.4634 z^-23 - 0.03397 z^-24 + 0.4784 z^-25 - 0.7735 z^-26
+ 0.9629 z^-27 - 0.6093 z^-28 + 0.2928 z^-29 - 1.208 z^-30 + 1.337 z^
-31 - 0.6492 z^-32 + 0.9216 z^-33 - 0.7676 z^-34 + 0.01774 z^-35 - 0.07515 z^-36
- 0.007522 z^-37 + 0.0503 z^-38 + 0.0724 z^-39 + 0.1101 z^-40 - 0.3051 z^-41
+ 0.8424 z^-42 - 0.153 z^-43 - 0.945 z^-44 - 0.4963 z^-45 + 1.164 z^-46
+ 0.3493 z^-47 - 0.3428 z^-48 - 0.4663 z^-49 + 0.4478 z^-50 - 0.5343 z^-51
+ 0.3504 z^-52 - 0.4879 z^-53 + 0.7327 z^-54 + 0.2129 z^-55 + 0.02298 z^-56
- 0.1926 z^-57 - 0.07282 z^-58 - 0.7216 z^-59 + 0.1083 z^-60 + 1.423 z^-61
- 0.1255 z^-62 - 0.5066 z^-63 - 0.7891 z^-64 + 0.8035 z^-65 - 0.09392 z^-66
+ 0.6109 z^-67 - 0.7393 z^-68 + 0.4189 z^-69 - 0.5429 z^-70 + 0.8597 z^-71
+ 0.2438 z^-72 - 1.093 z^-73 - 0.1302 z^-74 - 0.005411 z^-75 + 1.452 z^-76
- 0.3493 z^-77 - 0.5465 z^-78 - 0.3775 z^-79 + 0.4557 z^-80 + 0.1364 z^-81
- 0.174 z^-82 + 0.02438 z^-83 + 0.2256 z^-84 + 0.3779 z^-85 - 0.2637 z^-86
- 0.5845 z^-87 - 0.3038 z^-88 + 1.005 z^-89 - 0.005901 z^-90 - 0.3504 z^-91
+ 0.4036 z^-92 - 0.5665 z^-93 - 0.3265 z^-94 + 0.4575 z^-95 + 0.5773 z^-96
- 0.4181 z^-97 - 0.9443 z^-98 + 1.108 z^-99 - 0.4177 z^-100

Transfer model in s transform

-0.2225 s^100 + 3.516 s^99 - 35.46 s^98 + 580.2 s^97 - 2720 s^96 + 4.612e04 s^95
- 1.338e05 s^94 + 2.353e06 s^93 - 4.748e06 s^92 + 8.658e07 s^91 - 1.294e08 s^90
+ 2.449e09 s^89 - 2.821e09 s^88 + 5.541e10 s^87 - 5.052e10 s^86 + 1.03e12 s^85
- 7.585e11 s^84 + 1.605e13 s^83 - 9.688e12 s^82 + 2.128e14 s^81 - 1.065e14 s^80
+ 2.425e15 s^79 - 1.017e15 s^78 + 2.397e16 s^77 - 8.499e15 s^76 + 2.071e17 s^75
- 6.256e16 s^74 + 1.571e18 s^73 - 4.077e17 s^72 + 1.052e19 s^71 - 2.363e18 s^70
+ 6.24e19 s^69 - 1.224e19 s^68 + 3.286e20 s^67 - 5.677e19 s^66 + 1.54e21 s^65
- 2.368e20 s^64 + 6.434e21 s^63 - 8.901e20 s^62 + 2.399e22 s^61 - 3.023e21 s^60
+ 7.986e22 s^59 - 9.287e21 s^58 + 2.375e23 s^57 - 2.584e22 s^56 + 6.309e23 s^55
- 6.512e22 s^54 + 1.496e24 s^53 - 1.485e23 s^52 + 3.164e24 s^51 - 3.062e23 s^50
+ 5.961e24 s^49 - 5.691e23 s^48 + 9.991e24 s^47 - 9.506e23 s^46 + 1.486e25 s^45
- 1.422e24 s^44 + 1.959e25 s^43 - 1.896e24 s^42 + 2.28e25 s^41 - 2.244e24 s^40
+ 2.336e25 s^39 - 2.344e24 s^38 + 2.099e25 s^37 - 2.149e24 s^36 + 1.647e25 s^35
- 1.719e24 s^34 + 1.124e25 s^33 - 1.192e24 s^32 + 6.625e24 s^31 - 7.105e23 s^30
+ 3.353e24 s^29 - 3.615e23 s^28 + 1.447e24 s^27 - 1.554e23 s^26 + 5.275e23 s^25
- 5.588e22 s^24 + 1.609e23 s^23 - 1.659e22 s^22 + 4.06e22 s^21 - 4.005e21 s^20

+ 8.354e21 s^19 - 7.721e20 s^18 + 1.379e21 s^17 - 1.161e20 s^16 + 1.789e20 s^15
- 1.32e19 s^14 + 1.778e19 s^13 - 1.087e18 s^12 + 1.308e18 s^11 - 6.046e16 s^10
+ 6.797e16 s^9 - 1.987e15 s^8 + 2.319e15 s^7 - 2.406e13 s^6 + 4.558e13 s^5
+ 4.706e11 s^4 + 3.798e11 s^3 + 1.238e10 s^2 + 1.343e08 s + 2.094e07

---

s^101 + 0.8719 s^100 + 166.5 s^99 + 144.3 s^98 + 1.336e04 s^97 + 1.15e04 s^96
+ 6.881e05 s^95 + 5.888e05 s^94 + 2.558e07 s^93 + 2.174e07 s^92 + 7.31e08 s^91
+ 6.173e08 s^90 + 1.672e10 s^89 + 1.402e10 s^88 + 3.145e11 s^87 + 2.618e11 s^86
+ 4.959e12 s^85 + 4.097e12 s^84 + 6.654e13 s^83 + 5.453e13 s^82 + 7.682e14 s^81
+ 6.243e14 s^80 + 7.7e15 s^79 + 6.2e15 s^78 + 6.747e16 s^77 + 5.38e16 s^76
+ 5.197e17 s^75 + 4.101e17 s^74 + 3.536e18 s^73 + 2.758e18 s^72 + 2.132e19 s^71
+ 1.643e19 s^70 + 1.143e20 s^69 + 8.685e19 s^68 + 5.455e20 s^67 + 4.086e20 s^66
+ 2.324e21 s^65 + 1.713e21 s^64 + 8.845e21 s^63 + 6.408e21 s^62 + 3.01e22 s^61
+ 2.14e22 s^60 + 9.162e22 s^59 + 6.377e22 s^58 + 2.494e23 s^57 + 1.697e23 s^56
+ 6.072e23 s^55 + 4.027e23 s^54 + 1.321e24 s^53 + 8.519e23 s^52 + 2.564e24 s^51
+ 1.604e24 s^50 + 4.435e24 s^49 + 2.683e24 s^48 + 6.828e24 s^47 + 3.978e24 s^46
+ 9.332e24 s^45 + 5.217e24 s^44 + 1.13e25 s^43 + 6.033e24 s^42 + 1.207e25 s^41
+ 6.128e24 s^40 + 1.136e25 s^39 + 5.447e24 s^38 + 9.367e24 s^37 + 4.216e24 s^36
+ 6.742e24 s^35 + 2.826e24 s^34 + 4.214e24 s^33 + 1.631e24 s^32 + 2.274e24 s^31
+ 8.04e23 s^30 + 1.052e24 s^29 + 3.357e23 s^28 + 4.144e23 s^27 + 1.175e23 s^26
+ 1.377e23 s^25 + 3.407e22 s^24 + 3.823e22 s^23 + 8.055e21 s^22 + 8.756e21 s^21
+ 1.524e21 s^20 + 1.632e21 s^19 + 2.247e20 s^18 + 2.43e20 s^17 + 2.494e19 s^16
+ 2.832e19 s^15 + 1.969e18 s^14 + 2.512e18 s^13 + 9.957e16 s^12 + 1.635e17 s^11
+ 2.389e15 s^10 + 7.43e15 s^9 - 2.444e13 s^8 + 2.191e14 s^7 - 2.414e12 s^6
+ 3.722e12 s^5 - 1.801e10 s^4 + 2.859e10 s^3 + 5.874e08 s^2 + 2.509e07 s
+ 4.953e06

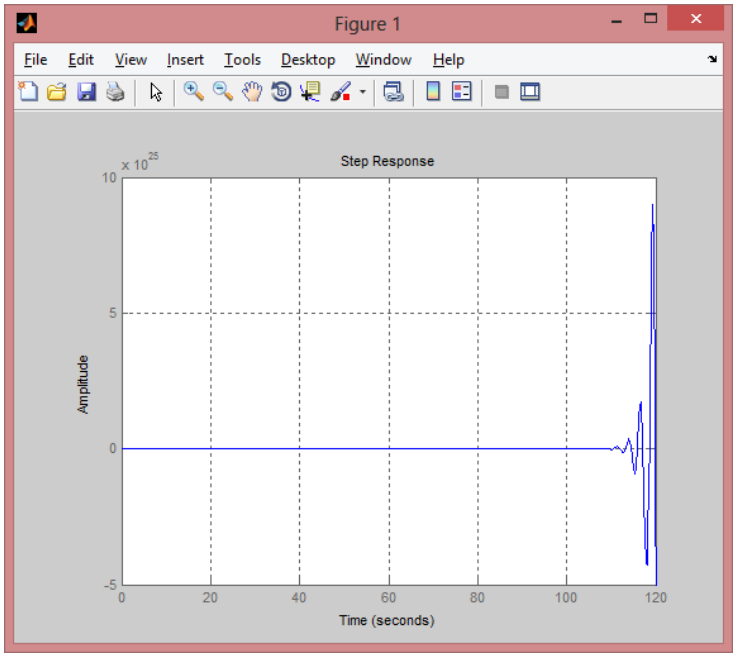

Figure 12: Step response (Temperature 3 - Linear)

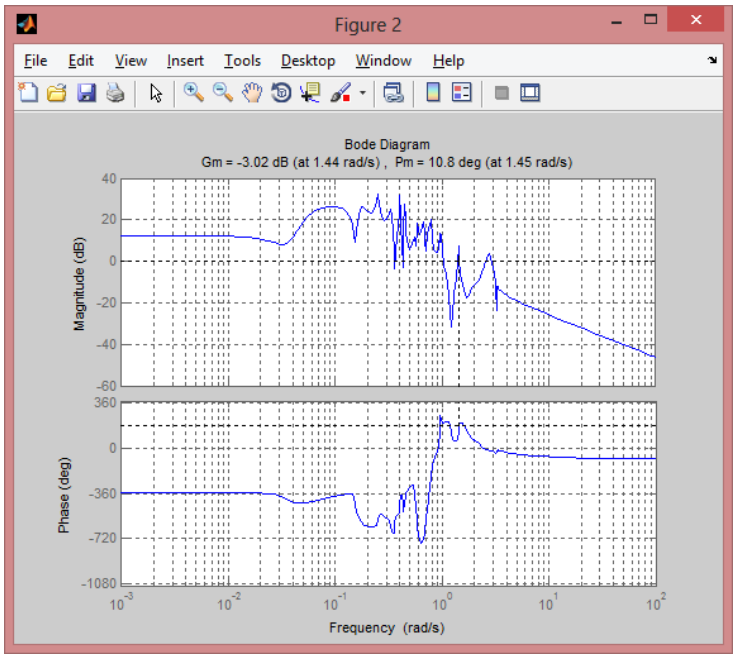

Figure 13: Bode plot (Temperature 3 - Linear)

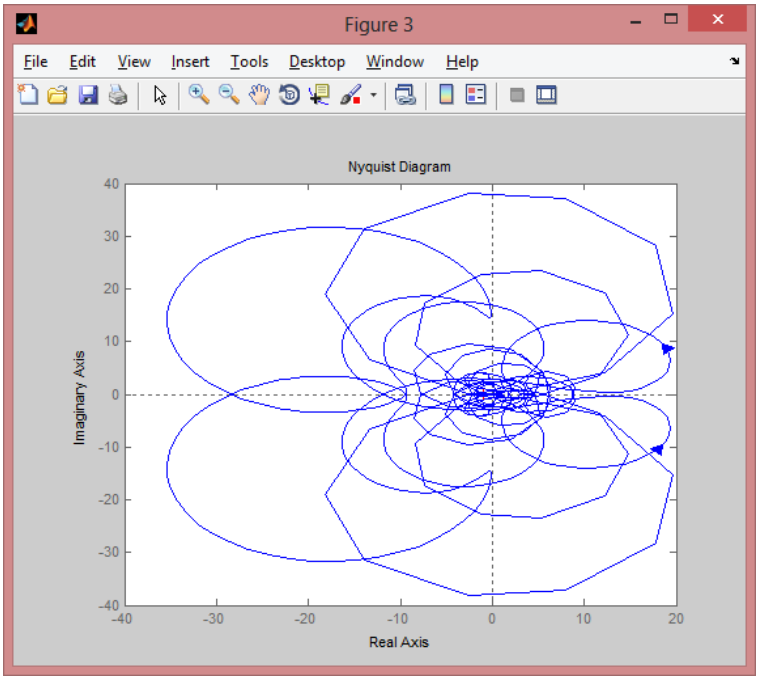

Figure 14: Nyquist plot (Temperature 3 - Linear)

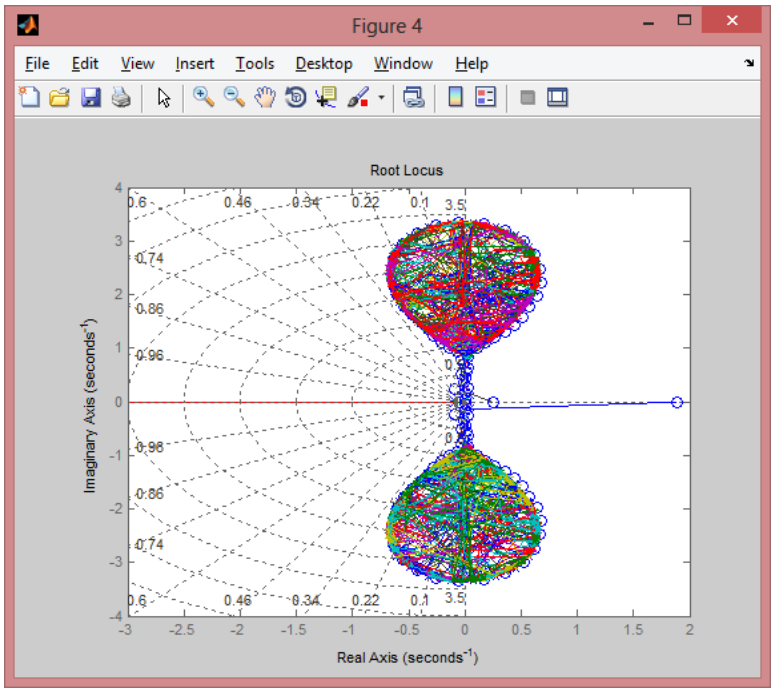

Figure 15: Root locus plot (Temperature 3 - Linear)

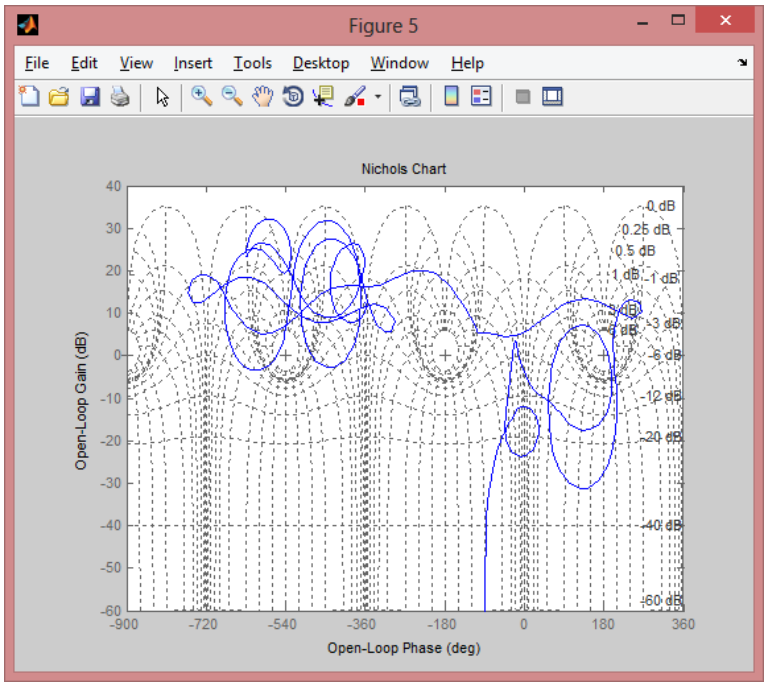

Figure 16: Nichols plot (Temperature 3 - Linear)

Temperature 4

ARX Model

Fit to estimation data: 93.06%

A(z) = 1 - 0.9571 z^-1 - 0.07967 z^-2 + 0.4984 z^-3 + 0.0102 z^-4 - 0.01262 z^-5
+ 0.03243 z^-6 + 0.06358 z^-7 - 0.4081 z^-8 + 0.1529 z^-9 - 0.02169 z^-10
+ 0.1059 z^-11 + 0.1146 z^-12 - 0.2823 z^-13 - 0.04716 z^-14 + 0.06066 z^
-15 + 0.04609 z^-16 - 0.07193 z^-17 - 0.03622 z^-18 + 0.1903 z^-19 - 0.5132 z^-20
+ 0.4182 z^-21 + 0.1599 z^-22 + 0.01222 z^-23 + 0.1044 z^-24 - 0.1768 z^-25
- 0.2639 z^-26 + 0.1086 z^-27 + 0.3359 z^-28 - 0.03718 z^-29 - 0.2967 z^-30
+ 0.163 z^-31 - 0.5229 z^-32 + 0.08248 z^-33 + 0.00762 z^-34 + 0.4459 z^-35
- 0.4288 z^-36 - 0.03854 z^-37 - 0.1585 z^-38 + 0.2843 z^-39 - 0.1576 z^-40
+ 0.05709 z^-41 - 0.03076 z^-42 + 0.1954 z^-43 - 0.0995 z^-44 - 0.1305 z^
-45 + 0.2874 z^-46 - 0.1075 z^-47 - 0.4611 z^-48 + 0.6987 z^-49 - 0.1247 z^-50
- 0.4716 z^-51 + 0.2458 z^-52 + 0.1029 z^-53 - 0.1002 z^-54 - 0.2108 z^-55
+ 0.615 z^-56 - 0.452 z^-57 + 0.06085 z^-58 + 0.09419 z^-59 - 0.2098 z^-60
+ 0.3281 z^-61 - 0.1801 z^-62 - 0.01367 z^-63 - 0.1201 z^-64 + 0.1299 z^-65
+ 0.01567 z^-66 - 0.4242 z^-67 + 0.2484 z^-68 - 0.1435 z^-69 + 0.3694 z^-70
- 0.2878 z^-71 + 0.2952 z^-72 - 0.2605 z^-73 - 0.1496 z^-74 + 0.2314 z^-75
- 0.2482 z^-76 + 0.7306 z^-77 - 0.4793 z^-78 + 0.01753 z^-79 - 0.009507 z^-80
+ 0.02006 z^-81 + 0.02768 z^-82 + 0.1768 z^-83 - 0.04696 z^-84 - 0.4351 z^-85
+ 0.4876 z^-86 - 0.395 z^-87 - 0.002345 z^-88 + 0.3605 z^-89 - 0.2503 z^-90
+ 0.1064 z^-91 - 0.333 z^-92 + 0.336 z^-93 + 0.2048 z^-94 - 0.3413 z^-95
+ 0.1731 z^-96 - 0.2256 z^-97 + 0.333 z^-98

B(z) = 0.5208 z^-2 - 0.601 z^-3 + 1.426 z^-4 - 0.414 z^-5 + 0.6452 z^-6 - 0.5911 z^-7
- 0.2324 z^-8 - 0.3309 z^-9 + 0.2932 z^-10 + 1.035 z^-11 - 1.479 z^-12 + 0.5842 z^-13
- 1.062 z^-14 - 0.5577 z^-15 + 0.8929 z^-16 + 0.3071 z^-17 + 0.1447 z^-18
- 0.258 z^-19 - 0.4163 z^-20 - 0.2011 z^-21 + 0.6595 z^-22 + 0.4344 z^-23
- 0.8023 z^-24 + 0.1333 z^-25 - 1.127 z^-26 + 2.214 z^-27 - 0.4743 z^-28
+ 0.02089 z^-29 + 0.3344 z^-30 - 2.028 z^-31 + 2.422 z^-32 - 1.799 z^-33
+ 1.335 z^-34 - 0.61 z^-35 + 0.008766 z^-36 - 2.018 z^-37 + 0.3374 z^-38
+ 0.006561 z^-39 + 1.916 z^-40 - 1.02 z^-41 + 0.1702 z^-42 + 0.252 z^-43
- 0.751 z^-44 - 0.4213 z^-45 + 1.128 z^-46 + 0.2053 z^-47 + 0.0593 z^-48
+ 0.1642 z^-49 - 0.6273 z^-50 - 0.2376 z^-51 + 0.0346 z^-52 + 0.9548 z^-53
+ 0.2205 z^-54 - 0.9026 z^-55 - 0.08852 z^-56 + 1.429 z^-57 - 1.505 z^-58
- 0.7844 z^-59 + 1.632 z^-60 - 0.373 z^-61 - 0.2838 z^-62 - 0.5104 z^-63
+ 0.9094 z^-64 - 0.9805 z^-65 + 0.9765 z^-66 - 0.878 z^-67 - 0.1751 z^-68
+ 0.5588 z^-69 + 0.1413 z^-70 - 0.4234 z^-71 - 0.7016 z^-72 + 1.09 z^-73
- 1.498 z^-74 + 1.535 z^-75 + 0.3228 z^-76 + 0.7943 z^-77 - 0.7464 z^-78
- 0.9992 z^-79 + 0.5553 z^-80 - 0.01365 z^-81 + 0.1792 z^-82 - 0.002713 z^-83
- 0.3175 z^-84 - 0.2181 z^-85 - 1.233 z^-86 + 1.7 z^-87 + 0.1374 z^-88 + 0.9672 z^-89
- 1.803 z^-90 + 1.006 z^-91 - 0.881 z^-92 - 0.5767 z^-93 + 1.067 z^-94 + 0.07597 z^-95
+ 0.08479 z^-96 + 0.3872 z^-97

Transfer model in z transform

0.5208 z^-1 - 0.601 z^-2 + 1.426 z^-3 - 0.414 z^-4 + 0.6452 z^-5 - 0.5911 z^-6
- 0.2324 z^-7 - 0.3309 z^-8 + 0.2932 z^-9 + 1.035 z^-10 - 1.479 z^-11
+ 0.5842 z^-12 - 1.062 z^-13 - 0.5577 z^-14 + 0.8929 z^-15 + 0.3071 z^-16
+ 0.1447 z^-17 - 0.258 z^-18 - 0.4163 z^-19 - 0.2011 z^-20 + 0.6595 z^-21
+ 0.4344 z^-22 - 0.8023 z^-23 + 0.1333 z^-24 - 1.127 z^-25 + 2.214 z^-26
- 0.4743 z^-27 + 0.02089 z^-28 + 0.3344 z^-29 - 2.028 z^-30
+ 2.422 z^-31 - 1.799 z^-32 + 1.335 z^-33 - 0.61 z^-34 + 0.008766 z^-35
- 2.018 z^-36 + 0.3374 z^-37 + 0.006561 z^-38 + 1.916 z^-39

- 1.02 z^-40 + 0.1702 z^-41 + 0.252 z^-42 - 0.751 z^-43 - 0.4213 z^-44
+ 1.128 z^-45 + 0.2053 z^-46 + 0.0593 z^-47 + 0.1642 z^-48 - 0.6273 z^-49
- 0.2376 z^-50 + 0.0346 z^-51 + 0.9548 z^-52 + 0.2205 z^-53
- 0.9026 z^-54 - 0.08852 z^-55 + 1.429 z^-56 - 1.505 z^-57 - 0.7844 z^-58
+ 1.632 z^-59 - 0.373 z^-60 - 0.2838 z^-61 - 0.5104 z^-62 + 0.9094 z^-63
- 0.9805 z^-64 + 0.9765 z^-65 - 0.878 z^-66 - 0.1751 z^-67 + 0.5588 z^-68
+ 0.1413 z^-69 - 0.4234 z^-70 - 0.7016 z^-71 + 1.09 z^-72 - 1.498 z^-73
+ 1.535 z^-74 + 0.3228 z^-75 + 0.7943 z^-76 - 0.7464 z^-77 - 0.9992 z^-78
+ 0.5553 z^-79 - 0.01365 z^-80 + 0.1792 z^-81 - 0.002713 z^-82
- 0.3175 z^-83 - 0.2181 z^-84 - 1.233 z^-85 + 1.7 z^-86 + 0.1374 z^-87
+ 0.9672 z^-88 - 1.803 z^-89 + 1.006 z^-90 - 0.881 z^-91 - 0.5767 z^-92
+ 1.067 z^-93 + 0.07597 z^-94 + 0.08479 z^-95 + 0.3872 z^-96

z^(-1) * ----------

1 - 0.9571 z^-1 - 0.07967 z^-2 + 0.4984 z^-3 + 0.0102 z^-4 - 0.01262 z^-5
+ 0.03243 z^-6 + 0.06358 z^-7 - 0.4081 z^-8 + 0.1529 z^-9 - 0.02169 z^-10
+ 0.1059 z^-11 + 0.1146 z^-12 - 0.2823 z^-13 - 0.04716 z^-14
+ 0.06066 z^-15 + 0.04609 z^-16 - 0.07193 z^-17 - 0.03622 z^
-18 + 0.1903 z^-19 - 0.5132 z^-20 + 0.4182 z^-21 + 0.1599 z^
-22 + 0.01222 z^-23 + 0.1044 z^-24 - 0.1768 z^-25 - 0.2639 z^-26
+ 0.1086 z^-27 + 0.3359 z^-28 - 0.03718 z^-29 - 0.2967 z^-30
+ 0.163 z^-31 - 0.5229 z^-32 + 0.08248 z^-33 + 0.00762 z^-34
+ 0.4459 z^-35 - 0.4288 z^-36 - 0.03854 z^-37 - 0.1585 z^-38
+ 0.2843 z^-39 - 0.1576 z^-40 + 0.05709 z^-41 - 0.03076 z^-42
+ 0.1954 z^-43 - 0.0995 z^-44 - 0.1305 z^-45 + 0.2874 z^-46
- 0.1075 z^-47 - 0.4611 z^-48 + 0.6987 z^-49 - 0.1247 z^-50
- 0.4716 z^-51 + 0.2458 z^-52 + 0.1029 z^-53 - 0.1002 z^-54
- 0.2108 z^-55 + 0.615 z^-56 - 0.452 z^-57 + 0.06085 z^-58 + 0.09419 z^-59
- 0.2098 z^-60 + 0.3281 z^-61 - 0.1801 z^-62 - 0.01367 z^-63
- 0.1201 z^-64 + 0.1299 z^-65 + 0.01567 z^-66 - 0.4242 z^-67
+ 0.2484 z^-68 - 0.1435 z^-69 + 0.3694 z^-70 - 0.2878 z^-71
+ 0.2952 z^-72 - 0.2605 z^-73 - 0.1496 z^-74 + 0.2314 z^-75
- 0.2482 z^-76 + 0.7306 z^-77 - 0.4793 z^-78 + 0.01753 z^-79
- 0.009507 z^-80 + 0.02006 z^-81 + 0.02768 z^-82 + 0.1768 z^
-83 - 0.04696 z^-84 - 0.4351 z^-85 + 0.4876 z^-86 - 0.395 z^
-87 - 0.002345 z^-88 + 0.3605 z^-89 - 0.2503 z^-90 + 0.1064 z^-91
- 0.333 z^-92 + 0.336 z^-93 + 0.2048 z^-94 - 0.3413 z^-95 + 0.1731 z^-96
- 0.2256 z^-97 + 0.333 z^-98

Transfer model in s transform

0.1654 s^99 + 1.438 s^98 + 30.88 s^97 + 233.4 s^96 + 2735 s^95 + 1.824e04 s^94
+ 1.536e05 s^93 + 9.141e05 s^92 + 6.158e06 s^91 + 3.303e07 s^90
+ 1.882e08 s^89 + 9.17e08 s^88 + 4.571e09 s^87 + 2.036e10 s^86
+ 9.072e10 s^85 + 3.713e11 s^84 + 1.501e12 s^83 + 5.675e12 s^82
+ 2.104e13 s^81 + 7.376e13 s^80 + 2.527e14 s^79 + 8.245e14 s^78
+ 2.624e15 s^77 + 7.998e15 s^76 + 2.375e16 s^75 + 6.782e16 s^74
+ 1.884e17 s^73 + 5.054e17 s^72 + 1.316e18 s^71 + 3.327e18 s^70
+ 8.132e18 s^69 + 1.941e19 s^68 + 4.456e19 s^67 + 1.007e20 s^66
+ 2.171e20 s^65 + 4.658e20 s^64 + 9.422e20 s^63 + 1.924e21 s^62
+ 3.648e21 s^61 + 7.103e21 s^60 + 1.261e22 s^59 + 2.348e22 s^58
+ 3.896e22 s^57 + 6.95e22 s^56 + 1.075e23 s^55 + 1.843e23 s^54
+ 2.651e23 s^53 + 4.375e23 s^52 + 5.835e23 s^51 + 9.294e23 s^50
+ 1.146e24 s^49 + 1.765e24 s^48 + 2.003e24 s^47 + 2.993e24 s^46
+ 3.114e24 s^45 + 4.522e24 s^44 + 4.294e24 s^43 + 6.071e24 s^42
+ 5.239e24 s^41 + 7.226e24 s^40 + 5.636e24 s^39 + 7.596e24 s^38
+ 5.325e24 s^37 + 7.024e24 s^36 + 4.4e24 s^35 + 5.685e24 s^34
+ 3.162e24 s^33 + 4.006e24 s^32 + 1.965e24 s^31 + 2.441e24 s^30
+ 1.048e24 s^29 + 1.277e24 s^28 + 4.758e23 s^27 + 5.678e23 s^26

+ 1.821e23 s^25 + 2.126e23 s^24 + 5.811e22 s^23 + 6.617e22 s^22
+ 1.524e22 s^21 + 1.687e22 s^20 + 3.23e21 s^19 + 3.461e21 s^18
+ 5.419e20 s^17 + 5.59e20 s^16 + 7.001e19 s^15 + 6.916e19 s^14
+ 6.713e18 s^13 + 6.325e18 s^12 + 4.534e17 s^11 + 4.077e17 s^10
+ 1.992e16 s^9 + 1.734e16 s^8 + 4.931e14 s^7 + 4.407e14 s^6
+ 4.719e12 s^5 + 5.71e12 s^4 - 2.244e10 s^3 + 2.65e10 s^2
- 3.642e08 s + 1.003e07

exp(-1*s) * ----------

s^100 + 1.086 s^99 + 170.4 s^98 + 181 s^97 + 1.398e04 s^96 + 1.453e04 s^95
+ 7.369e05 s^94 + 7.479e05 s^93 + 2.802e07 s^92 + 2.776e07 s^91
+ 8.189e08 s^90 + 7.914e08 s^89 + 1.915e10 s^88 + 1.804e10 s^87
+ 3.684e11 s^86 + 3.377e11 s^85 + 5.939e12 s^84 + 5.296e12 s^83
+ 8.146e13 s^82 + 7.058e13 s^81 + 9.613e14 s^80 + 8.084e14 s^79
+ 9.848e15 s^78 + 8.029e15 s^77 + 8.817e16 s^76 + 6.962e16 s^75
+ 6.94e17 s^74 + 5.3e17 s^73 + 4.823e18 s^72 + 3.558e18 s^71
+ 2.97e19 s^70 + 2.114e19 s^69 + 1.626e20 s^68 + 1.115e20 s^67
+ 7.926e20 s^66 + 5.229e20 s^65 + 3.447e21 s^64 + 2.185e21 s^63
+ 1.339e22 s^62 + 8.143e21 s^61 + 4.651e22 s^60 + 2.708e22 s^59
+ 1.444e23 s^58 + 8.042e22 s^57 + 4.011e23 s^56 + 2.132e23 s^55
+ 9.956e23 s^54 + 5.041e23 s^53 + 2.207e24 s^52 + 1.063e24 s^51
+ 4.367e24 s^50 + 1.995e24 s^49 + 7.696e24 s^48 + 3.331e24 s^47
+ 1.206e25 s^46 + 4.934e24 s^45 + 1.678e25 s^44 + 6.47e24 s^43
+ 2.065e25 s^42 + 7.491e24 s^41 + 2.244e25 s^40 + 7.633e24 s^39
+ 2.143e25 s^38 + 6.82e24 s^37 + 1.793e25 s^36 + 5.321e24 s^35
+ 1.308e25 s^34 + 3.606e24 s^33 + 8.268e24 s^32 + 2.112e24 s^31
+ 4.505e24 s^30 + 1.062e24 s^29 + 2.101e24 s^28 + 4.545e23 s^27
+ 8.312e23 s^26 + 1.643e23 s^25 + 2.764e23 s^24 + 4.963e22 s^23
+ 7.64e22 s^22 + 1.237e22 s^21 + 1.731e22 s^20 + 2.506e21 s^19
+ 3.16e21 s^18 + 4.049e20 s^17 + 4.558e20 s^16 + 5.1e19 s^15
+ 5.06e19 s^14 + 4.858e18 s^13 + 4.178e18 s^12 + 3.363e17 s^11
+ 2.452e17 s^10 + 1.602e16 s^9 + 9.6e15 s^8 + 4.836e14 s^7
+ 2.28e14 s^6 + 8.112e12 s^5 + 2.812e12 s^4 + 5.731e10 s^3
+ 1.266e10 s^2 + 3.783e07 s + 2.014e06

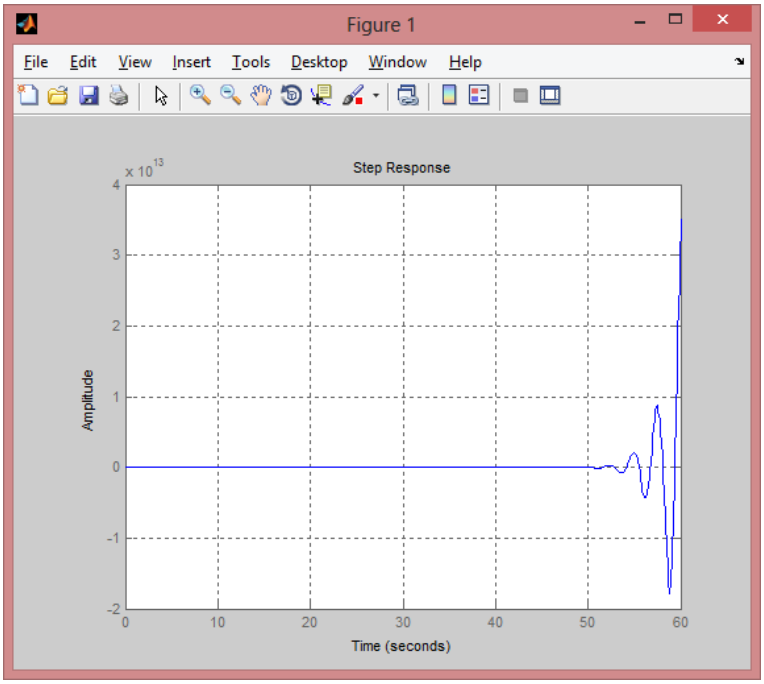

Figure 17: Step response (Temperature 4 - Linear)

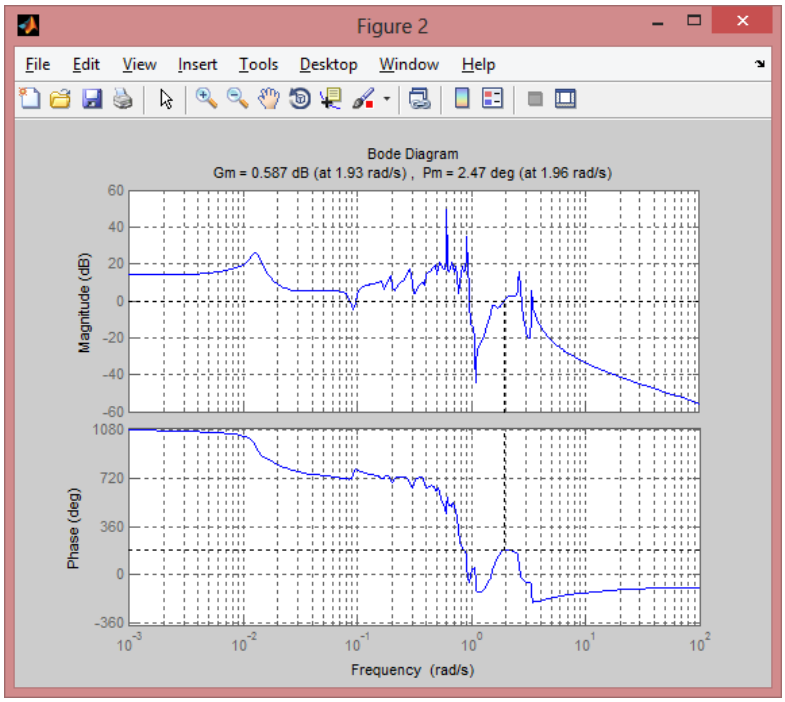

Figure 18: Bode plot (Temperature 4 - Linear)

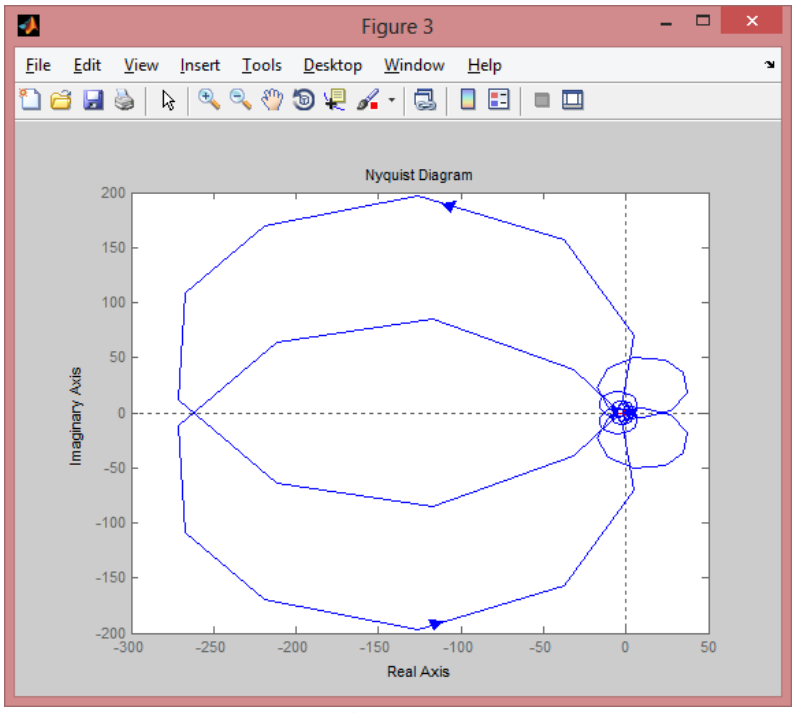

Figure 19: Nyquist plot (Temperature 4 - Linear)

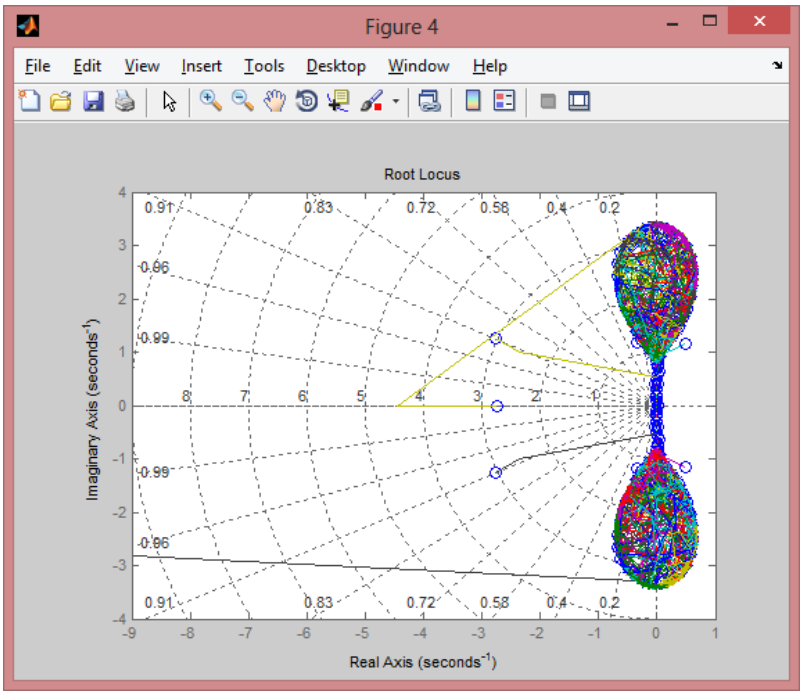

Figure 20: Root locus (Temperature 4 - Linear)

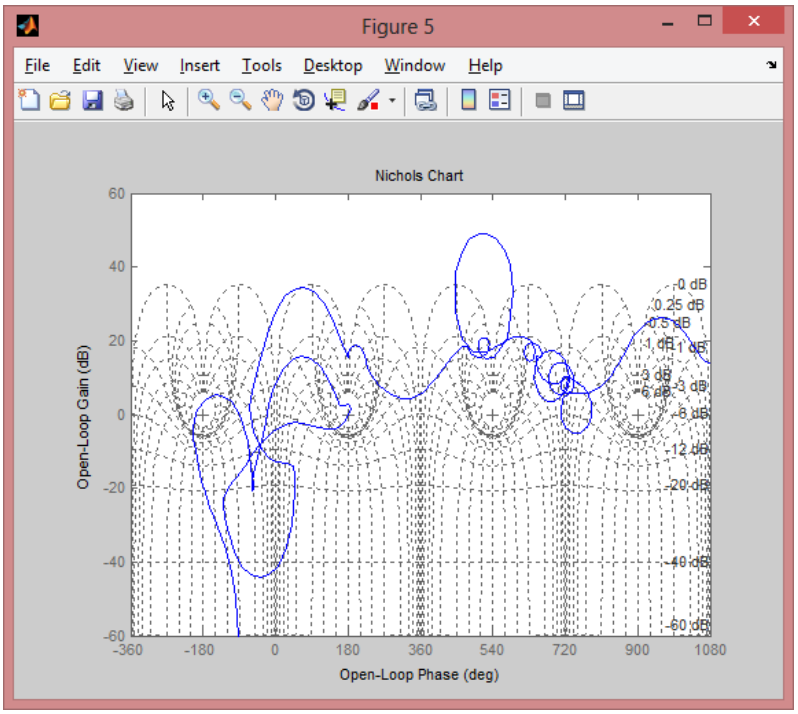

Figure 21: Nichols plot (Temperature 4 - Linear)

Temperature 5

ARX Model

Fit to estimation data: 97.32%

A(z) = 1 + 0.07149 z^-1 - 0.2553 z^-2 - 0.05937 z^-3 + 0.4757 z^-4 + 0.3646 z^-5
+ 0.2535 z^-6 - 0.08232 z^-7 - 0.06597 z^-8 - 0.2419 z^-9 - 0.1366 z^-10
+ 0.06196 z^-11 - 0.1098 z^-12 + 0.2227 z^-13 - 0.07965 z^-14 - 0.01827 z^-15
- 0.3924 z^-16 - 0.02913 z^-17 - 0.1851 z^-18 - 0.1918 z^-19 + 0.02176 z^
-20 + 0.2656 z^-21 - 0.1233 z^-22 + 0.2404 z^-23 - 0.2064 z^-24 - 0.6244 z^-25
- 0.3994 z^-26 + 0.2137 z^-27 + 0.5666 z^-28 - 0.3544 z^-29 + 0.6412 z^-30
- 0.6546 z^-31 - 0.3958 z^-32 - 0.1644 z^-33 + 0.653 z^-34 + 0.02264 z^-35
- 0.367 z^-36 + 0.839 z^-37 - 0.06427 z^-38 - 0.8889 z^-39 - 0.4882 z^-40
+ 0.4347 z^-41 - 0.4256 z^-42 + 0.3595 z^-43 + 0.5926 z^-44 + 0.4118 z^-45
- 1.074 z^-46 - 0.3005 z^-47 + 0.8887 z^-48 + 0.1931 z^-49 + 0.1119 z^-50
+ 1.029 z^-51 - 0.1852 z^-52 - 0.9658 z^-53 + 0.2809 z^-54 + 0.3366 z^-55
- 0.05334 z^-56 - 0.07579 z^-57 + 0.8653 z^-58 - 0.9396 z^-59 - 0.2161 z^
-60 + 0.3258 z^-61 + 0.24 z^-62 - 0.1354 z^-63 + 0.5863 z^-64 + 0.3438 z^
-65 - 0.672 z^-66 + 0.06192 z^-67 + 0.1559 z^-68 + 1.203 z^-69 - 1.157 z^
-70 + 0.5472 z^-71 - 0.1878 z^-72 - 0.3875 z^-73 + 0.3709 z^-74 + 0.9904 z^-75
- 1.06 z^-76 + 0.09107 z^-77 + 1.56 z^-78 - 0.7143 z^-79 - 0.6731 z^-80 + 0.1791 z^-81
+ 0.6699 z^-82 - 0.1219 z^-83 + 0.6969 z^-84 - 0.02402 z^-85 + 0.03959 z^
-86 - 0.8526 z^-87 + 0.3658 z^-88 - 0.6231 z^-89 + 0.1441 z^-90 + 0.6657 z^-91
- 0.2122 z^-92 - 1.772 z^-93 - 0.1056 z^-94 + 1.15 z^-95 - 0.3376 z^-96 - 1.31 z^-97
+ 0.06934 z^-98 + 0.2038 z^-99

B(z) = -27.92 z^-1 + 106.4 z^-2 + 75.26 z^-3 - 37.53 z^-4 - 62.13 z^-5 + 44.92 z^
-6 + 32.01 z^-7 + 8.775 z^-8 + 41.29 z^-9 - 11.16 z^-10 - 66.78 z^-11 - 39.03 z^-12
- 0.9028 z^-13 - 32.04 z^-14 - 1.465 z^-15 + 39.52 z^-16 + 43.31 z^-17 - 59.66 z^-18
- 37.35 z^-19 + 37.76 z^-20 - 39.67 z^-21 - 44.92 z^-22 + 80.36 z^-23 + 34.46 z^-24
+ 45.22 z^-25 - 8.947 z^-26 - 103.3 z^-27 - 114.8 z^-28 + 52.2 z^-29 + 142.8 z^-30
- 53.51 z^-31 + 54.47 z^-32 - 152.7 z^-33 + 13.29 z^-34 - 22.32 z^-35 + 70.61 z^-36
+ 4.455 z^-37 - 62.51 z^-38 + 78.93 z^-39 - 33.67 z^-40 - 126.3 z^-41 - 92.31 z^-42
+ 81.37 z^-43 - 32.9 z^-44 + 46.81 z^-45 + 4.341 z^-46 + 71.02 z^-47 - 177.6 z^-48
- 25.06 z^-49 + 152.2 z^-50 + 6.482 z^-51 - 11.4 z^-52 + 163.7 z^-53 - 78.65 z^-54
- 119.1 z^-55 + 88.01 z^-56 + 88.83 z^-57 - 31.24 z^-58 - 36.75 z^-59 + 152.4 z^-60
- 108.7 z^-61 - 9.287 z^-62 + 36.19 z^-63 + 93.19 z^-64 - 29.4 z^-65 + 65.47 z^-66
+ 26.38 z^-67 - 68.86 z^-68 - 24.08 z^-69 + 71.64 z^-70 + 171.8 z^-71 - 183.7 z^-72
+ 73.53 z^-73 - 30.83 z^-74 - 74.77 z^-75 + 86.97 z^-76 + 131.7 z^-77 - 170.2 z^-78
+ 20.53 z^-79 + 189.5 z^-80 - 151 z^-81 - 69.73 z^-82 - 21.21 z^-83 + 129.1 z^-84
+ 46.26 z^-85 + 36.26 z^-86 - 48.22 z^-87 + 27.49 z^-88 - 111.1 z^-89 + 52.85 z^-90
- 48.68 z^-91 + 36.4 z^-92 + 125.3 z^-93 - 109.5 z^-94 - 257 z^-95 + 25.05 z^-96

Transfer model in z transform

-27.92 z^-1 + 106.4 z^-2 + 75.26 z^-3 - 37.53 z^-4 - 62.13 z^-5 + 44.92 z^-6
+ 32.01 z^-7 + 8.775 z^-8 + 41.29 z^-9 - 11.16 z^-10 - 66.78 z^-11 - 39.03 z^-12
- 0.9028 z^-13 - 32.04 z^-14 - 1.465 z^-15 + 39.52 z^-16 + 43.31 z^-17
- 59.66 z^-18 - 37.35 z^-19 + 37.76 z^-20 - 39.67 z^-21 - 44.92 z^-22
+ 80.36 z^-23 + 34.46 z^-24 + 45.22 z^-25 - 8.947 z^-26 - 103.3 z^-27
- 114.8 z^-28 + 52.2 z^-29 + 142.8 z^-30 - 53.51 z^-31 + 54.47 z^-32
- 152.7 z^-33 + 13.29 z^-34 - 22.32 z^-35 + 70.61 z^-36 + 4.455 z^-37
- 62.51 z^-38 + 78.93 z^-39 - 33.67 z^-40 - 126.3 z^-41 - 92.31 z^-42
+ 81.37 z^-43 - 32.9 z^-44 + 46.81 z^-45 + 4.341 z^-46 + 71.02 z^-47
- 177.6 z^-48 - 25.06 z^-49 + 152.2 z^-50 + 6.482 z^-51 - 11.4 z^-52
+ 163.7 z^-53 - 78.65 z^-54 - 119.1 z^-55 + 88.01 z^-56 + 88.83 z^-57

- 31.24 z^-58 - 36.75 z^-59 + 152.4 z^-60 - 108.7 z^-61 - 9.287 z^-62
+ 36.19 z^-63 + 93.19 z^-64 - 29.4 z^-65 + 65.47 z^-66 + 26.38 z^-67
- 68.86 z^-68 - 24.08 z^-69 + 71.64 z^-70 + 171.8 z^-71 - 183.7 z^-72
+ 73.53 z^-73 - 30.83 z^-74 - 74.77 z^-75 + 86.97 z^-76 + 131.7 z^-77
- 170.2 z^-78 + 20.53 z^-79 + 189.5 z^-80 - 151 z^-81 - 69.73 z^-82 - 21.21 z^-83
+ 129.1 z^-84 + 46.26 z^-85 + 36.26 z^-86 - 48.22 z^-87 + 27.49 z^-88
- 111.1 z^-89 + 52.85 z^-90 - 48.68 z^-91 + 36.4 z^-92 + 125.3 z^-93
- 109.5 z^-94 - 257 z^-95 + 25.05 z^-96 + 161.7 z^-97 - 27.19 z^-98 - 168.4 z^-99

---

1 + 0.07149 z^-1 - 0.2553 z^-2 - 0.05937 z^-3 + 0.4757 z^-4 + 0.3646 z^-5 + 0.2535 z^-6
- 0.08232 z^-7 - 0.06597 z^-8 - 0.2419 z^-9 - 0.1366 z^-10 + 0.06196 z^-11
- 0.1098 z^-12 + 0.2227 z^-13 - 0.07965 z^-14 - 0.01827 z^-15 - 0.3924 z^-16
- 0.02913 z^-17 - 0.1851 z^-18 - 0.1918 z^-19 + 0.02176 z^-20 + 0.2656 z^-21
- 0.1233 z^-22 + 0.2404 z^-23 - 0.2064 z^-24 - 0.6244 z^-25 - 0.3994 z^-26
+ 0.2137 z^-27 + 0.5666 z^-28 - 0.3544 z^-29 + 0.6412 z^-30 - 0.6546 z^-31
- 0.3958 z^-32 - 0.1644 z^-33 + 0.653 z^-34 + 0.02264 z^-35 - 0.367 z^-36
+ 0.839 z^-37 - 0.06427 z^-38 - 0.8889 z^-39 - 0.4882 z^-40 + 0.4347 z^-41
- 0.4256 z^-42 + 0.3595 z^-43 + 0.5926 z^-44 + 0.4118 z^-45 - 1.074 z^-46
- 0.3005 z^-47 + 0.8887 z^-48 + 0.1931 z^-49 + 0.1119 z^-50 + 1.029 z^-51
- 0.1852 z^-52 - 0.9658 z^-53 + 0.2809 z^-54 + 0.3366 z^-55 - 0.05334 z^-56
- 0.07579 z^-57 + 0.8653 z^-58 - 0.9396 z^-59 - 0.2161 z^-60 + 0.3258 z^-61
+ 0.24 z^-62 - 0.1354 z^-63 + 0.5863 z^-64 + 0.3438 z^-65 - 0.672 z^-66
+ 0.06192 z^-67 + 0.1559 z^-68 + 1.203 z^-69 - 1.157 z^-70 + 0.5472 z^-71
- 0.1878 z^-72 - 0.3875 z^-73 + 0.3709 z^-74 + 0.9904 z^-75 - 1.06 z^
-76 + 0.09107 z^-77 + 1.56 z^-78 - 0.7143 z^-79 - 0.6731 z^-80 + 0.1791 z^-81
+ 0.6699 z^-82 - 0.1219 z^-83 + 0.6969 z^-84 - 0.02402 z^-85 + 0.03959 z^-86
- 0.8526 z^-87 + 0.3658 z^-88 - 0.6231 z^-89 + 0.1441 z^-90 + 0.6657 z^-91
- 0.2122 z^-92 - 1.772 z^-93 - 0.1056 z^-94 + 1.15 z^-95 - 0.3376 z^-96
- 1.31 z^-97 + 0.06934 z^-98 + 0.2038 z^-99

Transfer model in s transform

167 s^99 - 971.9 s^98 + 2.833e04 s^97 - 1.564e05 s^96 + 2.314e06 s^95 - 1.212e07 s^94
+ 1.213e08 s^93 - 6.028e08 s^92 + 4.585e09 s^91 - 2.161e10 s^90 + 1.332e11 s^89
- 5.95e11 s^88 + 3.096e12 s^87 - 1.31e13 s^86 + 5.912e13 s^85 - 2.369e14 s^84
+ 9.461e14 s^83 - 3.588e15 s^82 + 1.288e16 s^81 - 4.619e16 s^80 + 1.507e17 s^79
- 5.109e17 s^78 + 1.531e18 s^77 - 4.898e18 s^76 + 1.358e19 s^75 - 4.099e19 s^74
+ 1.059e20 s^73 - 3.011e20 s^72 + 7.285e20 s^71 - 1.949e21 s^70 + 4.439e21 s^69
- 1.116e22 s^68 + 2.403e22 s^67 - 5.671e22 s^66 + 1.158e23 s^65 - 2.561e23 s^64
+ 4.975e23 s^63 - 1.029e24 s^62 + 1.908e24 s^61 - 3.684e24 s^60 + 6.538e24 s^59
- 1.176e25 s^58 + 2.002e25 s^57 - 3.347e25 s^56 + 5.476e25 s^55 - 8.491e25 s^54
+ 1.338e26 s^53 - 1.919e26 s^52 + 2.918e26 s^51 - 3.859e26 s^50 + 5.673e26 s^49
- 6.897e26 s^48 + 9.817e26 s^47 - 1.093e27 s^46 + 1.509e27 s^45 - 1.535e27 s^44
+ 2.057e27 s^43 - 1.902e27 s^42 + 2.479e27 s^41 - 2.075e27 s^40 + 2.633e27 s^39
- 1.986e27 s^38 + 2.457e27 s^37 - 1.661e27 s^36 + 2.005e27 s^35 - 1.209e27 s^34
+ 1.424e27 s^33 - 7.613e26 s^32 + 8.755e26 s^31 - 4.126e26 s^30 + 4.631e26 s^29
- 1.911e26 s^28 + 2.092e26 s^27 - 7.511e25 s^26 + 7.997e25 s^25 - 2.482e25 s^24
+ 2.562e25 s^23 - 6.823e24 s^22 + 6.793e24 s^21 - 1.542e24 s^20 + 1.469e24 s^19
- 2.824e23 s^18 + 2.545e23 s^17 - 4.115e22 s^16 + 3.451e22 s^15 - 4.666e21 s^14
+ 3.558e21 s^13 - 3.998e20 s^12 + 2.682e20 s^11 - 2.488e19 s^10 + 1.401e19 s^9
- 1.061e18 s^8 + 4.685e17 s^7 - 2.836e16 s^6 + 8.841e15 s^5 - 4.047e14 s^4
+ 7.342e13 s^3 - 2.167e12 s^2 + 9.553e10 s + 1.718e08

---

s^100 + 2.468 s^99 + 171.7 s^98 + 401.7 s^97 + 1.419e04 s^96 + 3.152e04 s^95

+ 7.524e05 s^94 + 1.588e06 s^93 + 2.877e07 s^92 + 5.777e07 s^91 + 8.453e08 s^90
+ 1.616e09 s^89 + 1.986e10 s^88 + 3.621e10 s^87 + 3.836e11 s^86 + 6.672e11 s^85
+ 6.207e12 s^84 + 1.031e13 s^83 + 8.54e13 s^82 + 1.357e14 s^81 + 1.011e15 s^80
+ 1.538e15 s^79 + 1.037e16 s^78 + 1.514e16 s^77 + 9.303e16 s^76 + 1.303e17 s^75
+ 7.33e17 s^74 + 9.872e17 s^73 + 5.097e18 s^72 + 6.608e18 s^71 + 3.139e19 s^70
+ 3.924e19 s^69 + 1.717e20 s^68 + 2.072e20 s^67 + 8.363e20 s^66 + 9.758e20 s^65
+ 3.631e21 s^64 + 4.103e21 s^63 + 1.407e22 s^62 + 1.543e22 s^61 + 4.873e22 s^60
+ 5.19e22 s^59 + 1.508e23 s^58 + 1.563e23 s^57 + 4.168e23 s^56 + 4.212e23 s^55
+ 1.029e24 s^54 + 1.016e24 s^53 + 2.268e24 s^52 + 2.189e24 s^51 + 4.455e24 s^50
+ 4.213e24 s^49 + 7.789e24 s^48 + 7.23e24 s^47 + 1.21e25 s^46 + 1.104e25 s^45
+ 1.666e25 s^44 + 1.497e25 s^43 + 2.028e25 s^42 + 1.797e25 s^41 + 2.175e25 s^40
+ 1.904e25 s^39 + 2.048e25 s^38 + 1.774e25 s^37 + 1.686e25 s^36 + 1.448e25 s^35
+ 1.208e25 s^34 + 1.03e25 s^33 + 7.484e24 s^32 + 6.345e24 s^31 + 3.986e24 s^30
+ 3.368e24 s^29 + 1.81e24 s^28 + 1.528e24 s^27 + 6.95e23 s^26 + 5.874e23 s^25
+ 2.231e23 s^24 + 1.894e23 s^23 + 5.915e22 s^22 + 5.063e22 s^21 + 1.274e22 s^20
+ 1.105e22 s^19 + 2.186e21 s^18 + 1.935e21 s^17 + 2.914e20 s^16 + 2.657e20 s^15
+ 2.914e19 s^14 + 2.781e19 s^13 + 2.081e18 s^12 + 2.135e18 s^11 + 9.811e16 s^10
+ 1.139e17 s^9 + 2.627e15 s^8 + 3.903e15 s^7 + 2.419e13 s^6 + 7.534e13 s^5
- 3.302e11 s^4 + 6.333e11 s^3 - 5.035e09 s^2 + 1.028e09 s + 1.227e07

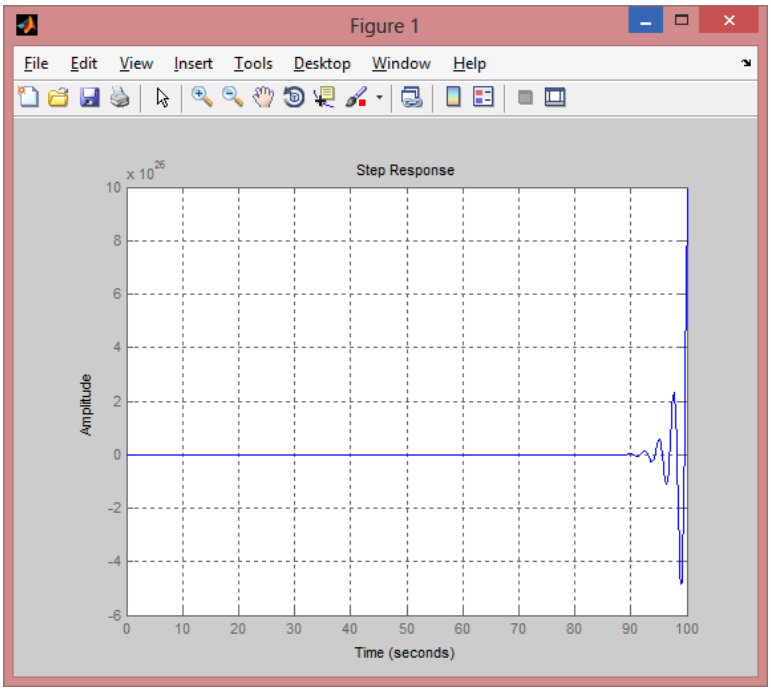

Figure 22: Step response (Temperature 5 - Linear)

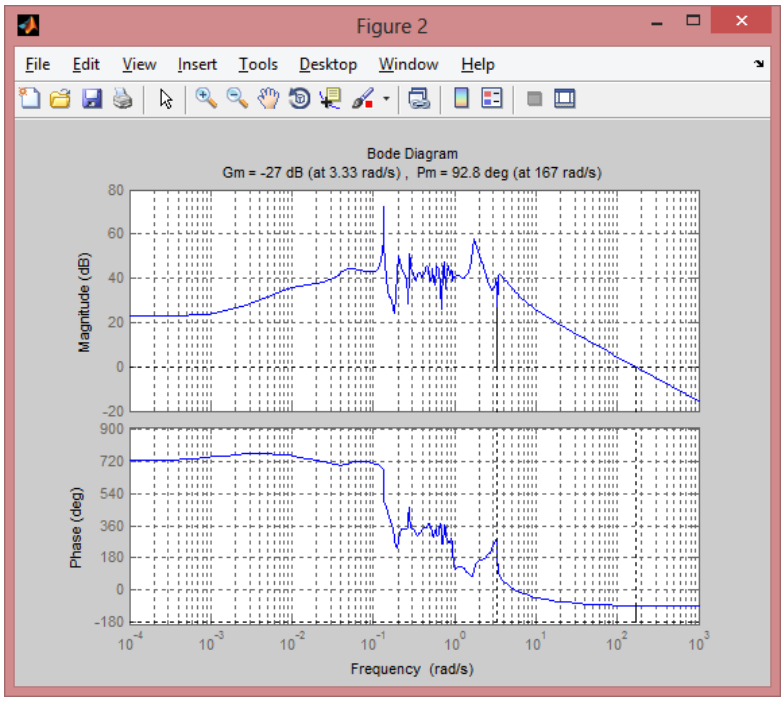

Figure 23: Bode plot (Temperature 5 - Linear)

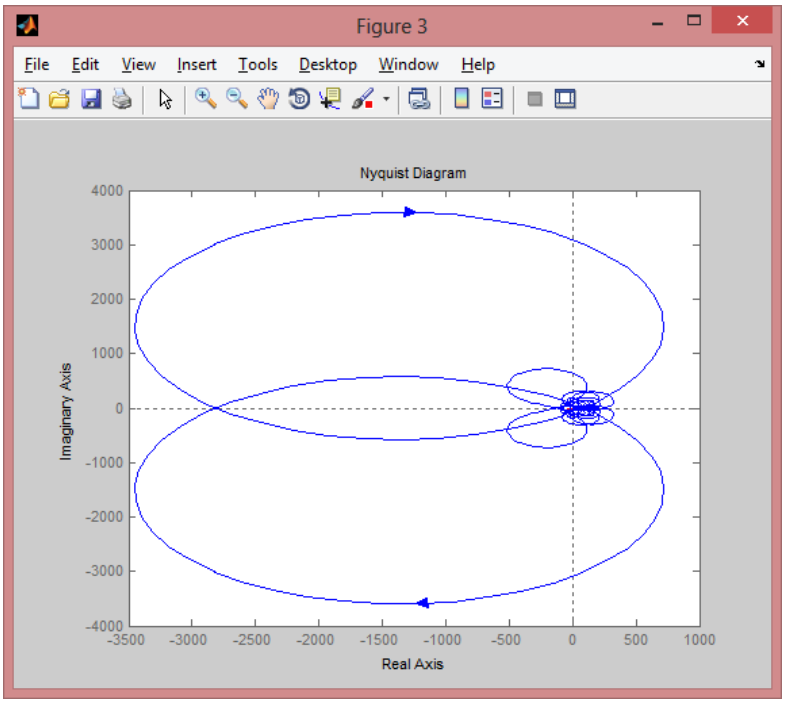

Figure 24: Nyquist plot (Temperature 5 - Linear)

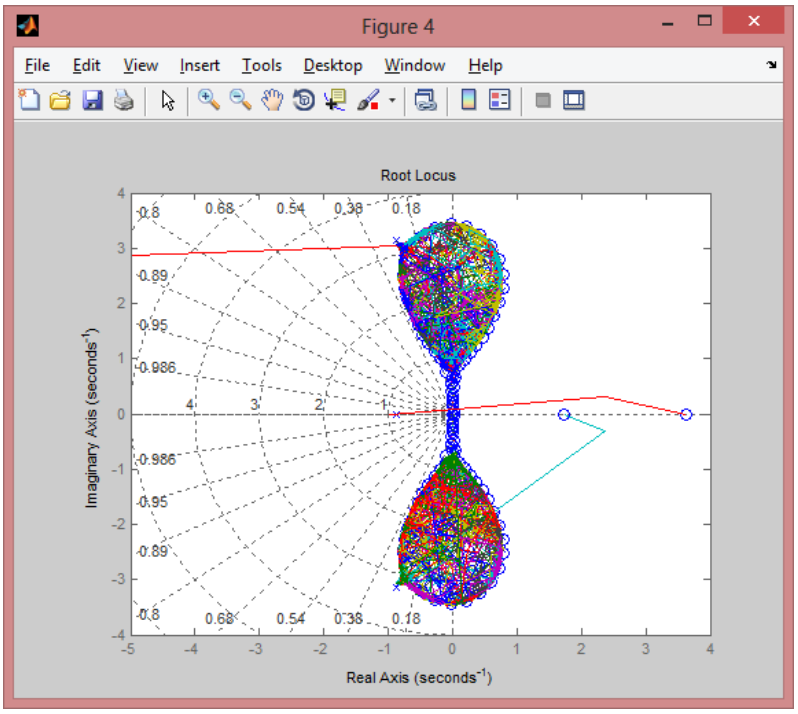

Figure 25: Root locus plot (Temperature 5 - Linear)

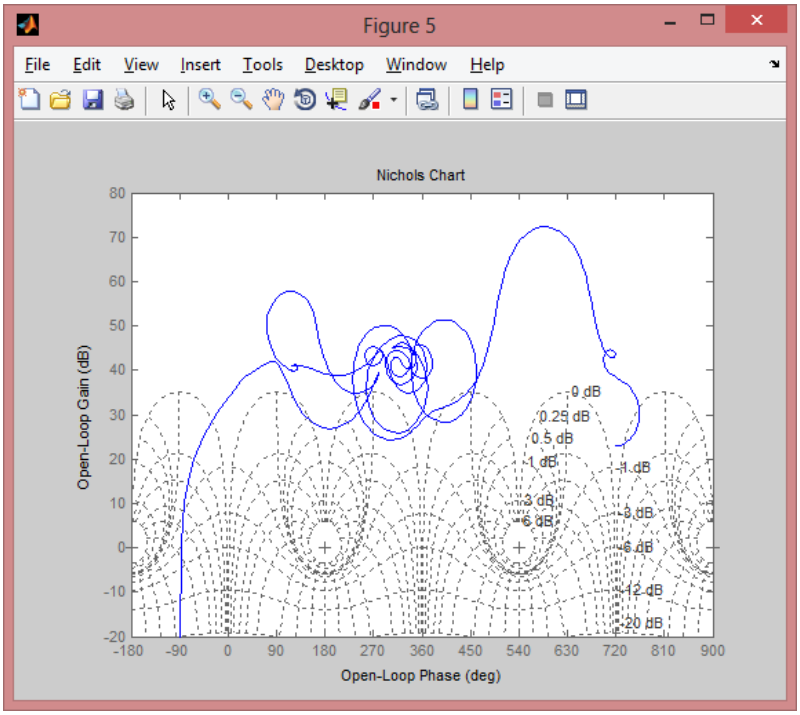

Figure 26: Nyquist plot (Temperature 5 - Linear)

Temperature 6

ARX Model

Fit to estimation data: 99.84%

A(z) = 1 - 1.877 z^-1 + 1.137 z^-2 - 0.3809 z^-3 + 0.6007 z^-4 - 0.5496 z^-5 + 0.1551 z^-6
- 0.1755 z^-7 + 0.3993 z^-8 - 0.4431 z^-9 + 0.5573 z^-10 - 0.4267 z^-11 - 0.07666 z^-12
+ 0.3071 z^-13 - 0.6443 z^-14 + 1.281 z^-15 - 1.248 z^-16 + 0.7427 z^-17
- 0.946 z^-18 + 1.149 z^-19 - 0.7094 z^-20 + 0.5369 z^-21 - 0.8407 z^-22
+ 1.082 z^-23 - 1.141 z^-24 + 1.398 z^-25 - 1.416 z^-26 + 1.027 z^-27 - 0.4261 z^-28
+ 0.02314 z^-29 + 0.131 z^-30 + 0.2755 z^-31 - 0.4873 z^-32 + 0.242 z^-33
- 0.4302 z^-34 + 0.6776 z^-35 - 0.5149 z^-36 + 0.4558 z^-37 - 0.4981 z^-38
+ 0.04034 z^-39 + 0.4048 z^-40 - 0.3009 z^-41 + 0.5253 z^-42 - 0.8893 z^-43
+ 0.7044 z^-44 - 0.3838 z^-45 + 0.2375 z^-46 + 0.2469 z^-47 - 0.9729 z^-48
+ 1.352 z^-49 - 1.139 z^-50 + 0.3789 z^-51 + 0.418 z^-52 - 0.7557 z^-53 + 1.194 z^-54
- 1.613 z^-55 + 1.407 z^-56 - 0.8038 z^-57 + 0.2398 z^-58 + 0.0344 z^-59
- 0.1051 z^-60 + 0.1206 z^-61 - 0.124 z^-62 + 0.04574 z^-63 + 0.06628 z^-64
- 0.2565 z^-65 + 0.5435 z^-66 - 0.6764 z^-67 + 0.1695 z^-68 + 0.6074 z^-69
- 0.843 z^-70 + 1.077 z^-71 - 1.253 z^-72 + 0.8258 z^-73 - 0.5902 z^-74 + 0.5486 z^-75
- 0.3411 z^-76 + 0.3682 z^-77 - 0.5347 z^-78 + 0.4267 z^-79 - 0.42 z^-80
+ 0.6232 z^-81 - 0.4483 z^-82 + 0.4603 z^-83 - 0.5354 z^-84 + 0.02642 z^-85
+ 0.5704 z^-86 - 0.5435 z^-87 + 0.09007 z^-88 + 0.2694 z^-89 - 0.7428 z^-90
+ 1.136 z^-91 - 1.195 z^-92 + 1.264 z^-93 - 1.081 z^-94 + 0.6538 z^-95 - 0.9798 z^-96
+ 1.356 z^-97 - 0.4934 z^-98 - 0.1929 z^-99

B(z) = 0.496 z^-1 - 0.09315 z^-2 - 0.509 z^-3 + 0.3132 z^-4 - 0.001518 z^-5 - 0.01894 z^-6
- 0.2764 z^-7 - 0.1626 z^-8 - 0.4697 z^-9 + 0.372 z^-10 - 0.1585 z^-11 - 0.3596 z^-12
+ 0.5015 z^-13 - 0.7424 z^-14 + 0.4641 z^-15 - 0.2467 z^-16 + 0.164 z^-17
+ 0.1131 z^-18 - 0.8258 z^-19 + 0.341 z^-20 - 0.6136 z^-21 + 0.3763 z^-22
+ 0.03135 z^-23 - 0.2318 z^-24 - 0.2688 z^-25 + 0.5291 z^-26 + 0.2313 z^-27
+ 0.1843 z^-28 + 1.138 z^-29 + 0.2685 z^-30 - 0.9961 z^-31 - 0.08249 z^-32
+ 0.86 z^-33 - 0.1554 z^-34 - 0.3204 z^-35 - 0.276 z^-36 - 0.3999 z^-37 + 0.539 z^-38
- 0.37 z^-39 - 0.8843 z^-40 - 0.1569 z^-41 + 0.08812 z^-42 + 0.1056 z^-43
- 0.1487 z^-44 - 0.11 z^-45 + 0.1531 z^-46 - 0.2366 z^-47 - 0.09483 z^-48
- 0.1484 z^-49 + 0.8246 z^-50 - 0.4767 z^-51 + 1.093 z^-52 - 0.1691 z^-53
+ 0.4991 z^-54 + 0.5329 z^-55 + 0.00232 z^-56 + 0.7313 z^-57 + 0.2734 z^-58
+ 0.5629 z^-59 + 0.1327 z^-60 + 0.1673 z^-61 - 0.09032 z^-62 + 0.1176 z^-63
+ 0.3078 z^-64 - 0.5765 z^-65 + 0.133 z^-66 + 0.2672 z^-67 - 0.2965 z^-68
+ 0.2283 z^-69 - 0.4849 z^-70 + 0.06278 z^-71 - 0.1478 z^-72 + 0.3488 z^-73
+ 0.7028 z^-74 - 0.2043 z^-75 + 0.03211 z^-76 - 0.5211 z^-77 - 0.09338 z^
-78 + 0.05116 z^-79 - 0.02149 z^-80 - 0.3389 z^-81 + 0.3835 z^-82 - 0.2685 z^-83
- 0.6977 z^-84 + 1.153 z^-85 - 0.4881 z^-86 + 0.1561 z^-87 - 0.1016 z^-88
+ 0.1982 z^-89 + 0.7392 z^-90 - 0.391 z^-91 - 0.1047 z^-92 - 0.2925 z^-93
+ 0.441 z^-94 + 0.5471 z^-95 - 0.6214 z^-96 + 0.2739 z^-97 + 0.4358 z^-98
- 0.651 z^-99

Transfer model in z transform

0.496 z^-1 - 0.09315 z^-2 - 0.509 z^-3 + 0.3132 z^-4 - 0.001518 z^-5 - 0.01894 z^-6
- 0.2764 z^-7 - 0.1626 z^-8 - 0.4697 z^-9 + 0.372 z^-10 - 0.1585 z^-11
- 0.3596 z^-12 + 0.5015 z^-13 - 0.7424 z^-14 + 0.4641 z^-15 - 0.2467 z^-16
+ 0.164 z^-17 + 0.1131 z^-18 - 0.8258 z^-19 + 0.341 z^-20 - 0.6136 z^
-21 + 0.3763 z^-22 + 0.03135 z^-23 - 0.2318 z^-24 - 0.2688 z^-25 + 0.5291 z^-26
+ 0.2313 z^-27 + 0.1843 z^-28 + 1.138 z^-29 + 0.2685 z^-30 - 0.9961 z^-31
- 0.08249 z^-32 + 0.86 z^-33 - 0.1554 z^-34 - 0.3204 z^-35 - 0.276 z^
-36 - 0.3999 z^-37 + 0.539 z^-38 - 0.37 z^-39 - 0.8843 z^-40 - 0.1569 z^-41

+ 0.08812 z^-42 + 0.1056 z^-43 - 0.1487 z^-44 - 0.11 z^-45 + 0.1531 z^-46
- 0.2366 z^-47 - 0.09483 z^-48 - 0.1484 z^-49 + 0.8246 z^-50 - 0.4767 z^-51
+ 1.093 z^-52 - 0.1691 z^-53 + 0.4991 z^-54 + 0.5329 z^-55 + 0.00232 z^-56
+ 0.7313 z^-57 + 0.2734 z^-58 + 0.5629 z^-59 + 0.1327 z^-60 + 0.1673 z^-61
- 0.09032 z^-62 + 0.1176 z^-63 + 0.3078 z^-64 - 0.5765 z^-65 + 0.133 z^-66
+ 0.2672 z^-67 - 0.2965 z^-68 + 0.2283 z^-69 - 0.4849 z^-70 + 0.06278 z^-71
- 0.1478 z^-72 + 0.3488 z^-73 + 0.7028 z^-74 - 0.2043 z^-75 + 0.03211 z^-76
- 0.5211 z^-77 - 0.09338 z^-78 + 0.05116 z^-79 - 0.02149 z^-80 - 0.3389 z^-81
+ 0.3835 z^-82 - 0.2685 z^-83 - 0.6977 z^-84 + 1.153 z^-85 - 0.4881 z^-86
+ 0.1561 z^-87 - 0.1016 z^-88 + 0.1982 z^-89 + 0.7392 z^-90 - 0.391 z^-91
- 0.1047 z^-92 - 0.2925 z^-93 + 0.441 z^-94 + 0.5471 z^-95 - 0.6214 z^-96
+ 0.2739 z^-97 + 0.4358 z^-98 - 0.651 z^-99

---

1 - 1.877 z^-1 + 1.137 z^-2 - 0.3809 z^-3 + 0.6007 z^-4 - 0.5496 z^-5 + 0.1551 z^-6
- 0.1755 z^-7 + 0.3993 z^-8 - 0.4431 z^-9 + 0.5573 z^-10 - 0.4267 z^-11
- 0.07666 z^-12 + 0.3071 z^-13 - 0.6443 z^-14 + 1.281 z^-15 - 1.248 z^-16
+ 0.7427 z^-17 - 0.946 z^-18 + 1.149 z^-19 - 0.7094 z^-20 + 0.5369 z^
-21 - 0.8407 z^-22 + 1.082 z^-23 - 1.141 z^-24 + 1.398 z^-25 - 1.416 z^-26
+ 1.027 z^-27 - 0.4261 z^-28 + 0.02314 z^-29 + 0.131 z^-30 + 0.2755 z^-31
- 0.4873 z^-32 + 0.242 z^-33 - 0.4302 z^-34 + 0.6776 z^-35 - 0.5149 z^-36
+ 0.4558 z^-37 - 0.4981 z^-38 + 0.04034 z^-39 + 0.4048 z^-40 - 0.3009 z^-41
+ 0.5253 z^-42 - 0.8893 z^-43 + 0.7044 z^-44 - 0.3838 z^-45 + 0.2375 z^-46
+ 0.2469 z^-47 - 0.9729 z^-48 + 1.352 z^-49 - 1.139 z^-50 + 0.3789 z^
-51 + 0.418 z^-52 - 0.7557 z^-53 + 1.194 z^-54 - 1.613 z^-55 + 1.407 z^-56
- 0.8038 z^-57 + 0.2398 z^-58 + 0.0344 z^-59 - 0.1051 z^-60 + 0.1206 z^-61
- 0.124 z^-62 + 0.04574 z^-63 + 0.06628 z^-64 - 0.2565 z^-65 + 0.5435 z^-66
- 0.6764 z^-67 + 0.1695 z^-68 + 0.6074 z^-69 - 0.843 z^-70 + 1.077 z^
-71 - 1.253 z^-72 + 0.8258 z^-73 - 0.5902 z^-74 + 0.5486 z^-75 - 0.3411 z^-76
+ 0.3682 z^-77 - 0.5347 z^-78 + 0.4267 z^-79 - 0.42 z^-80 + 0.6232 z^
-81 - 0.4483 z^-82 + 0.4603 z^-83 - 0.5354 z^-84 + 0.02642 z^-85 + 0.5704 z^-86
- 0.5435 z^-87 + 0.09007 z^-88 + 0.2694 z^-89 - 0.7428 z^-90 + 1.136 z^-91
- 1.195 z^-92 + 1.264 z^-93 - 1.081 z^-94 + 0.6538 z^-95 - 0.9798 z^-96
+ 1.356 z^-97 - 0.4934 z^-98 - 0.1929 z^-99

Transfer model in s transform

-0.1978 s^100 + 3.919 s^99 - 36.12 s^98 + 653.8 s^97 - 3146 s^96 + 5.252e04 s^95
- 1.744e05 s^94 + 2.707e06 s^93 - 6.923e06 s^92 + 1.006e08 s^91 - 2.1e08 s^90
+ 2.872e09 s^89 - 5.066e09 s^88 + 6.559e10 s^87 - 1e11 s^86 + 1.231e12 s^85
- 1.647e12 s^84 + 1.934e13 s^83 - 2.299e13 s^82 + 2.585e14 s^81 - 2.75e14 s^80
+ 2.97e15 s^79 - 2.845e15 s^78 + 2.959e16 s^77 - 2.565e16 s^76 + 2.575e17 s^75
- 2.026e17 s^74 + 1.969e18 s^73 - 1.409e18 s^72 + 1.327e19 s^71 - 8.656e18 s^70
+ 7.925e19 s^69 - 4.715e19 s^68 + 4.201e20 s^67 - 2.282e20 s^66 + 1.981e21 s^65
- 9.826e20 s^64 + 8.329e21 s^63 - 3.772e21 s^62 + 3.124e22 s^61 - 1.291e22 s^60
+ 1.046e23 s^59 - 3.944e22 s^58 + 3.129e23 s^57 - 1.075e23 s^56 + 8.355e23 s^55
- 2.615e23 s^54 + 1.992e24 s^53 - 5.668e23 s^52 + 4.234e24 s^51 - 1.094e24 s^50
+ 8.017e24 s^49 - 1.878e24 s^48 + 1.35e25 s^47 - 2.86e24 s^46 + 2.017e25 s^45
- 3.858e24 s^44 + 2.669e25 s^43 - 4.594e24 s^42 + 3.116e25 s^41 - 4.815e24 s^40
+ 3.201e25 s^39 - 4.423e24 s^38 + 2.882e25 s^37 - 3.545e24 s^36 + 2.263e25 s^35
- 2.466e24 s^34 + 1.541e25 s^33 - 1.48e24 s^32 + 9.046e24 s^31 - 7.604e23 s^30
+ 4.545e24 s^29 - 3.319e23 s^28 + 1.937e24 s^27 - 1.22e23 s^26 + 6.931e23 s^25
- 3.735e22 s^24 + 2.056e23 s^23 - 9.435e21 s^22 + 4.981e22 s^21 - 1.947e21 s^20
+ 9.661e21 s^19 - 3.254e20 s^18 + 1.462e21 s^17 - 4.39e19 s^16 + 1.667e20 s^15
- 4.794e18 s^14 + 1.354e19 s^13 - 4.27e17 s^12 + 7.083e17 s^11 - 3.104e16 s^10
+ 1.804e16 s^9 - 1.774e15 s^8 - 1.591e14 s^7 - 7.114e13 s^6 - 2.093e13 s^5
- 1.575e12 s^4 - 3.732e11 s^3 - 1.168e10 s^2 - 2.387e09 s + 7.696e07

---

s^101 + 3.094 s^100 + 174.6 s^99 + 502.7 s^98 + 1.468e04 s^97 + 3.934e04 s^96
+ 7.914e05 s^95 + 1.975e06 s^94 + 3.077e07 s^93 + 7.146e07 s^92 + 9.194e08 s^91
+ 1.987e09 s^90 + 2.197e10 s^89 + 4.417e10 s^88 + 4.314e11 s^87 + 8.066e11 s^86
+ 7.099e12 s^85 + 1.234e13 s^84 + 9.934e13 s^83 + 1.604e14 s^82 + 1.196e15 s^81
+ 1.792e15 s^80 + 1.249e16 s^79 + 1.736e16 s^78 + 1.139e17 s^77 + 1.468e17 s^76
+ 9.138e17 s^75 + 1.09e18 s^74 + 6.469e18 s^73 + 7.14e18 s^72 + 4.058e19 s^71
+ 4.137e19 s^70 + 2.262e20 s^69 + 2.127e20 s^68 + 1.123e21 s^67 + 9.724e20 s^66
+ 4.971e21 s^65 + 3.959e21 s^64 + 1.966e22 s^63 + 1.437e22 s^62 + 6.952e22 s^61
+ 4.653e22 s^60 + 2.198e23 s^59 + 1.344e23 s^58 + 6.214e23 s^57 + 3.465e23 s^56
+ 1.57e24 s^55 + 7.96e23 s^54 + 3.546e24 s^53 + 1.629e24 s^52 + 7.144e24 s^51
+ 2.965e24 s^50 + 1.283e25 s^49 + 4.791e24 s^48 + 2.048e25 s^47 + 6.861e24 s^46
+ 2.903e25 s^45 + 8.683e24 s^44 + 3.644e25 s^43 + 9.682e24 s^42 + 4.037e25 s^41
+ 9.481e24 s^40 + 3.934e25 s^39 + 8.12e24 s^38 + 3.36e25 s^37 + 6.054e24 s^36
+ 2.502e25 s^35 + 3.909e24 s^34 + 1.617e25 s^33 + 2.173e24 s^32 + 9.009e24 s^31
+ 1.033e24 s^30 + 4.3e24 s^29 + 4.164e23 s^28 + 1.744e24 s^27 + 1.412e23 s^26
+ 5.952e23 s^25 + 3.986e22 s^24 + 1.692e23 s^23 + 9.264e21 s^22 + 3.953e22 s^21
+ 1.75e21 s^20 + 7.48e21 s^19 + 2.65e20 s^18 + 1.125e21 s^17 + 3.163e19 s^16
+ 1.314e20 s^15 + 2.919e18 s^14 + 1.158e19 s^13 + 2.029e17 s^12 + 7.419e17 s^11
+ 1.023e16 s^10 + 3.281e16 s^9 + 3.553e14 s^8 + 9.301e14 s^7 + 8.179e12 s^6
+ 1.512e13 s^5 + 1.336e11 s^4 + 1.181e11 s^3 + 1.524e09 s^2 + 3.301e08 s

+ 5.526e06

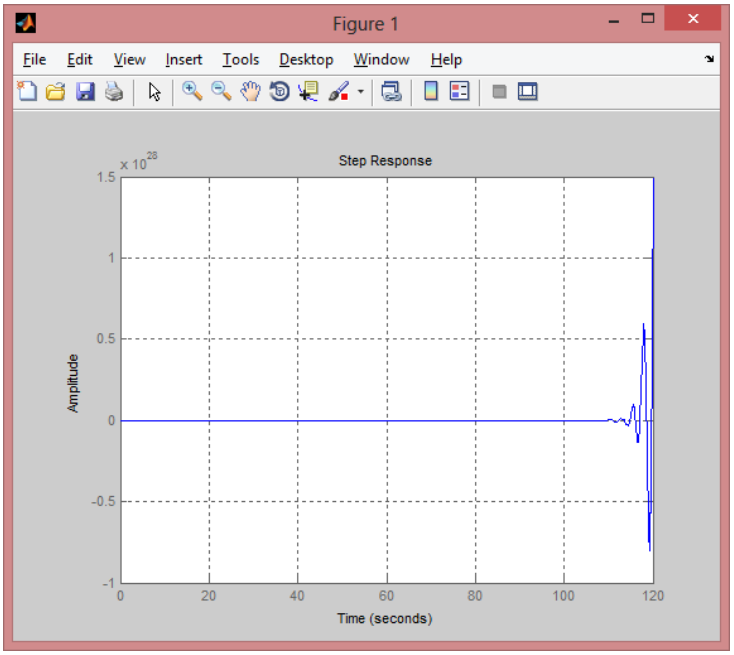

Figure 27: Step response (Temperature 6 - Linear)

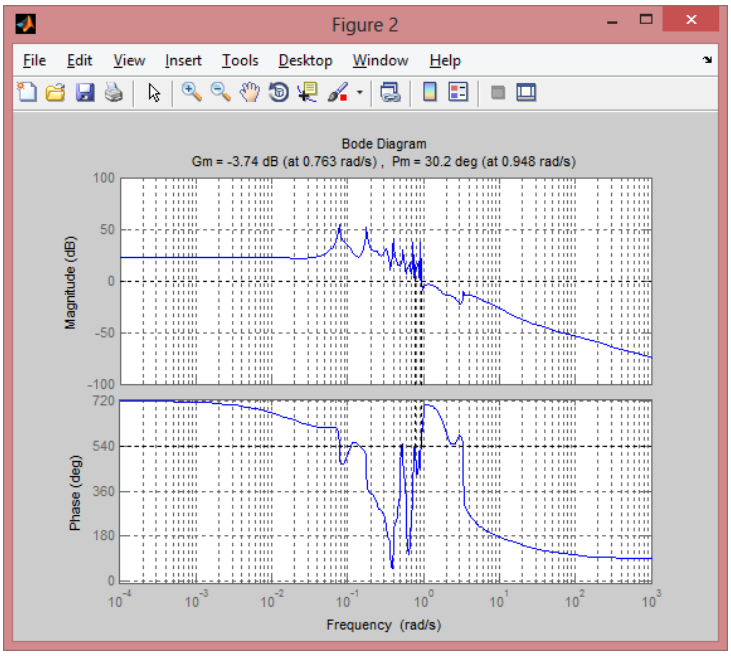

Figure 28: Bode plot (Temperature 6 - Linear)

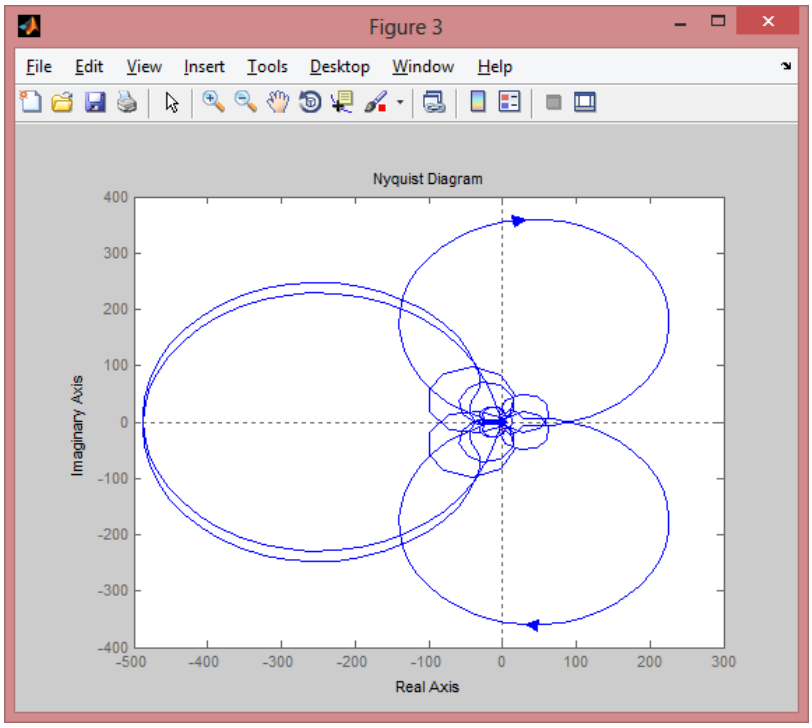

Figure 29: Nyquist plot (Temperature 6 - Linear)

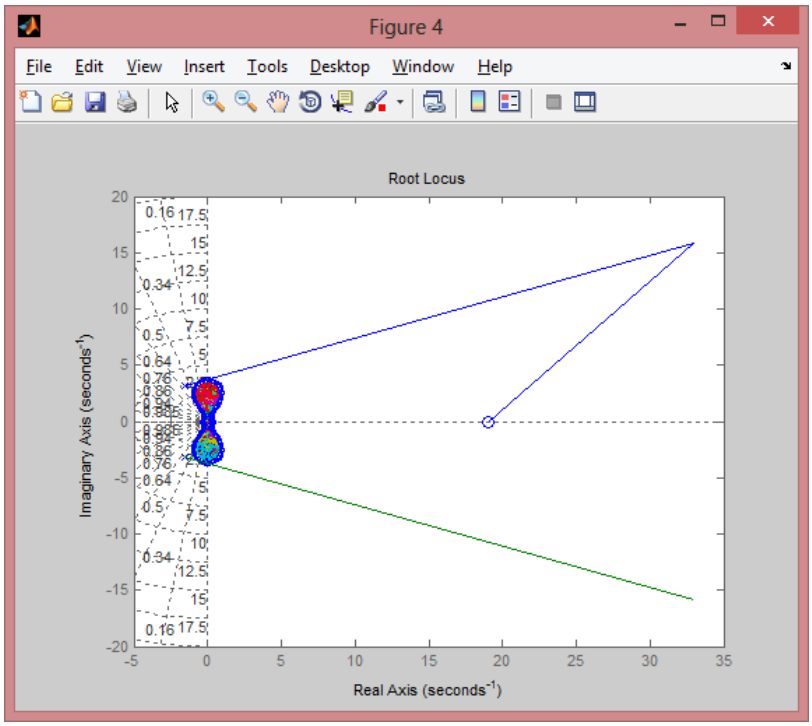

Figure 30: Root locus plot (Temperature 6 - Linear)

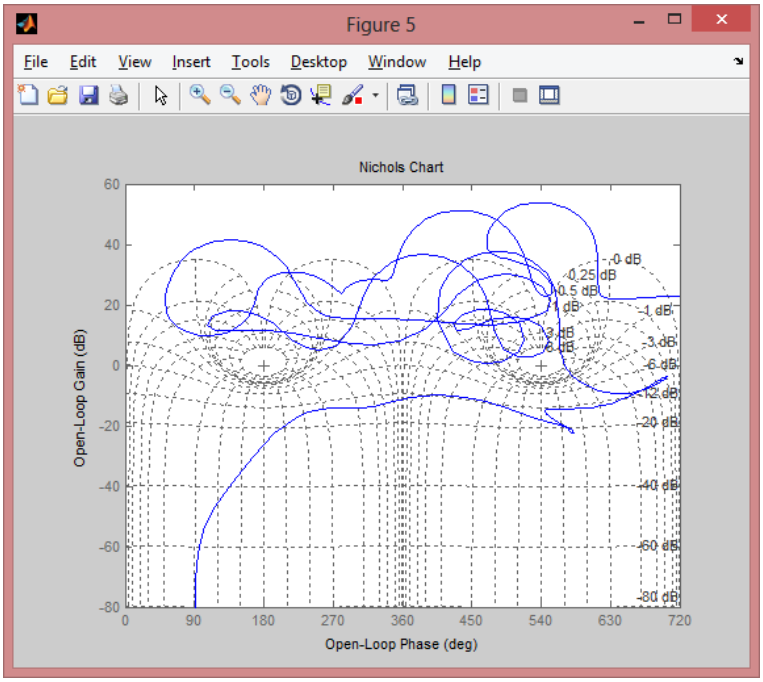

Figure 31: Nichols plot (Temperature 6 - Linear)

Level 1

ARX Model

Fit to estimation data: 84.5%

A(z) = 1 - 0.7313 z^-1 + 0.6747 z^-2 - 0.07717 z^-3 + 0.4125 z^-4 + 0.1185 z^-5 + 0.5476 z^-6
- 0.1168 z^-7 + 0.2645 z^-8 + 0.064 z^-9 + 0.4486 z^-10 + 0.1093 z^-11 + 0.2261 z^-12
+ 0.2727 z^-13 + 0.777 z^-14 - 0.2884 z^-15 + 0.9318 z^-16 - 0.1224 z^-17
+ 0.6684 z^-18 - 0.2651 z^-19 + 0.5452 z^-20 + 0.01442 z^-21 + 0.2391 z^-22
+ 0.1968 z^-23 - 0.2227 z^-24 + 0.5923 z^-25 - 0.2458 z^-26 + 0.0004188 z^-27
+ 0.04377 z^-28 + 0.2871 z^-29 - 0.4814 z^-30 + 0.1418 z^-31 + 0.2162 z^-32
- 0.2725 z^-33 + 0.1859 z^-34 - 0.2802 z^-35 + 0.2339 z^-36 + 0.1416 z^-37
+ 0.1764 z^-38 - 0.2862 z^-39 + 0.04004 z^-40 + 0.08527 z^-41 - 0.157 z^-42
+ 0.2651 z^-43 - 0.3554 z^-44 + 0.3377 z^-45 - 0.5968 z^-46 + 0.1829 z^-47
- 0.06365 z^-48 - 0.1697 z^-49 - 0.3472 z^-50 + 0.2315 z^-51 - 0.4388 z^-52
- 0.01694 z^-53 - 0.2347 z^-54 - 0.002039 z^-55 + 0.03309 z^-56 - 0.09773 z^-57
+ 0.06969 z^-58 + 0.1614 z^-59 - 0.2326 z^-60 + 0.2576 z^-61 - 0.1355 z^-62
+ 0.22 z^-63 - 0.1962 z^-64 + 0.1745 z^-65 - 0.1875 z^-66 + 0.1123 z^-67
- 0.2706 z^-68 + 0.02671 z^-69 - 0.1323 z^-70 + 0.3089 z^-71 - 0.4874 z^-72
+ 0.2032 z^-73 - 0.2141 z^-74 - 0.1085 z^-75 - 0.01474 z^-76 + 0.1658 z^-77
- 0.5453 z^-78 + 0.1681 z^-79 - 0.518 z^-80 + 0.1863 z^-81 - 0.4323 z^-82
- 0.1008 z^-83 - 0.2457 z^-84 - 0.4056 z^-85 - 0.1628 z^-86 - 0.2306 z^-87
- 0.2753 z^-88 - 0.4686 z^-89 - 0.03813 z^-90 - 0.2876 z^-91 - 0.1334 z^-92
- 0.2625 z^-93 + 0.0958 z^-94 - 0.1888 z^-95 - 0.1861 z^-96

B(z) = -4.032 z^-1 + 7.582 z^-2 + 3.754 z^-3 - 0.2941 z^-4 - 5.397 z^-5 + 0.2928 z^-6
- 0.2754 z^-7 + 4.411 z^-8 - 2.212 z^-9 - 0.6602 z^-10 + 2.772 z^-11 - 2.456 z^-12
- 3.469 z^-13 + 5.75 z^-14 - 7.237 z^-15 + 13.09 z^-16 - 2.298 z^-17 - 2.15 z^-18
+ 1.944 z^-19 - 2.189 z^-20 - 7.391 z^-21 + 2.994 z^-22 + 0.1356 z^-23 - 13.61 z^-24
+ 9.545 z^-25 - 10.39 z^-26 + 12.91 z^-27 - 9.705 z^-28 + 6.911 z^-29 - 9.049 z^-30
+ 22.16 z^-31 - 21.57 z^-32 + 5.296 z^-33 + 11 z^-34 - 10.62 z^-35 + 1.269 z^-36
+ 0.3632 z^-37 + 7.623 z^-38 - 8.317 z^-39 + 24.26 z^-40 - 17.75 z^-41 + 4.961 z^-42
- 9.031 z^-43 + 3.737 z^-44 + 3.009 z^-45 - 4.8 z^-46 + 0.7521 z^-47 - 0.5381 z^-48
+ 0.9887 z^-49 - 2.876 z^-50 + 2.425 z^-51 - 4.41 z^-52 + 3.129 z^-53 + 12.94 z^-54
- 14.68 z^-55 + 0.8304 z^-56 - 8.768 z^-57 + 14.14 z^-58 - 6.045 z^-59 + 6.429 z^-60
- 8.992 z^-61 + 4.28 z^-62 - 0.7156 z^-63 - 1.85 z^-64 + 5.321 z^-65 - 11.95 z^-66
+ 10.97 z^-67 - 7.427 z^-68 + 11.18 z^-69 - 18.3 z^-70 + 10.9 z^-71 - 6.871 z^-72
+ 11.82 z^-73 - 6.819 z^-74 + 2.327 z^-75 + 2.039 z^-76 - 6.456 z^-77 + 5.07 z^-78
- 0.8658 z^-79 - 0.7433 z^-80 - 4.457 z^-81 - 0.8231 z^-82 + 4.789 z^-83
- 8.152 z^-84 + 8.838 z^-85 - 8.131 z^-86 + 16.73 z^-87 - 16.47 z^-88 + 12.78 z^-89
- 10.23 z^-90 + 5.608 z^-91 - 8.664 z^-92 + 10.42 z^-93 - 0.6398 z^-94 - 9.011 z^-95
+ 13.29 z^-96

Transfer model in z transform

-4.032 z^-1 + 7.582 z^-2 + 3.754 z^-3 - 0.2941 z^-4 - 5.397 z^-5 + 0.2928 z^-6
- 0.2754 z^-7 + 4.411 z^-8 - 2.212 z^-9 - 0.6602 z^-10 + 2.772 z^-11
- 2.456 z^-12 - 3.469 z^-13 + 5.75 z^-14 - 7.237 z^-15 + 13.09 z^-16
- 2.298 z^-17 - 2.15 z^-18 + 1.944 z^-19 - 2.189 z^-20 - 7.391 z^-21
+ 2.994 z^-22 + 0.1356 z^-23 - 13.61 z^-24 + 9.545 z^-25 - 10.39 z^-26
+ 12.91 z^-27 - 9.705 z^-28 + 6.911 z^-29 - 9.049 z^-30 + 22.16 z^-31
- 21.57 z^-32 + 5.296 z^-33 + 11 z^-34 - 10.62 z^-35 + 1.269 z^-36 + 0.3632 z^-37
+ 7.623 z^-38 - 8.317 z^-39 + 24.26 z^-40 - 17.75 z^-41 + 4.961 z^-42
- 9.031 z^-43 + 3.737 z^-44 + 3.009 z^-45 - 4.8 z^-46 + 0.7521 z^-47
- 0.5381 z^-48 + 0.9887 z^-49 - 2.876 z^-50 + 2.425 z^-51 - 4.41 z^-52
+ 3.129 z^-53 + 12.94 z^-54 - 14.68 z^-55 + 0.8304 z^-56 - 8.768 z^-57

+ 14.14 z^-58 - 6.045 z^-59 + 6.429 z^-60 - 8.992 z^-61 + 4.28 z^-62
- 0.7156 z^-63 - 1.85 z^-64 + 5.321 z^-65 - 11.95 z^-66 + 10.97 z^-67
- 7.427 z^-68 + 11.18 z^-69 - 18.3 z^-70 + 10.9 z^-71 - 6.871 z^-72 + 11.82 z^-73
- 6.819 z^-74 + 2.327 z^-75 + 2.039 z^-76 - 6.456 z^-77 + 5.07 z^-78
- 0.8658 z^-79 - 0.7433 z^-80 - 4.457 z^-81 - 0.8231 z^-82 + 4.789 z^
-83 - 8.152 z^-84 + 8.838 z^-85 - 8.131 z^-86 + 16.73 z^-87 - 16.47 z^-88
+ 12.78 z^-89 - 10.23 z^-90 + 5.608 z^-91 - 8.664 z^-92 + 10.42 z^-93
- 0.6398 z^-94 - 9.011 z^-95 + 13.29 z^-96

---

1 - 0.7313 z^-1 + 0.6747 z^-2 - 0.07717 z^-3 + 0.4125 z^-4 + 0.1185 z^-5 + 0.5476 z^-6
- 0.1168 z^-7 + 0.2645 z^-8 + 0.064 z^-9 + 0.4486 z^-10 + 0.1093 z^-11
+ 0.2261 z^-12 + 0.2727 z^-13 + 0.777 z^-14 - 0.2884 z^-15 + 0.9318 z^-16
- 0.1224 z^-17 + 0.6684 z^-18 - 0.2651 z^-19 + 0.5452 z^-20 + 0.01442 z^-21
+ 0.2391 z^-22 + 0.1968 z^-23 - 0.2227 z^-24 + 0.5923 z^-25 - 0.2458 z^-26
+ 0.0004188 z^-27 + 0.04377 z^-28 + 0.2871 z^-29 - 0.4814 z^-30 + 0.1418 z^-31
+ 0.2162 z^-32 - 0.2725 z^-33 + 0.1859 z^-34 - 0.2802 z^-35 + 0.2339 z^-36
+ 0.1416 z^-37 + 0.1764 z^-38 - 0.2862 z^-39 + 0.04004 z^-40 + 0.08527 z^-41
- 0.157 z^-42 + 0.2651 z^-43 - 0.3554 z^-44 + 0.3377 z^-45 - 0.5968 z^-46
+ 0.1829 z^-47 - 0.06365 z^-48 - 0.1697 z^-49 - 0.3472 z^-50 + 0.2315 z^-51
- 0.4388 z^-52 - 0.01694 z^-53 - 0.2347 z^-54 - 0.002039 z^-55 + 0.03309 z^-56
- 0.09773 z^-57 + 0.06969 z^-58 + 0.1614 z^-59 - 0.2326 z^-60 + 0.2576 z^-61
- 0.1355 z^-62 + 0.22 z^-63 - 0.1962 z^-64 + 0.1745 z^-65 - 0.1875 z^
-66 + 0.1123 z^-67 - 0.2706 z^-68 + 0.02671 z^-69 - 0.1323 z^-70 + 0.3089 z^-71
- 0.4874 z^-72 + 0.2032 z^-73 - 0.2141 z^-74 - 0.1085 z^-75 - 0.01474 z^-76
+ 0.1658 z^-77 - 0.5453 z^-78 + 0.1681 z^-79 - 0.518 z^-80 + 0.1863 z^-81
- 0.4323 z^-82 - 0.1008 z^-83 - 0.2457 z^-84 - 0.4056 z^-85 - 0.1628 z^-86
- 0.2306 z^-87 - 0.2753 z^-88 - 0.4686 z^-89 - 0.03813 z^-90 - 0.2876 z^-91
- 0.1334 z^-92 - 0.2625 z^-93 + 0.0958 z^-94 - 0.1888 z^-95 - 0.1861 z^-96

Transfer model in s transform

50.06 s^98 - 56.29 s^97 + 8362 s^96 - 9509 s^95 + 6.726e05 s^94 - 7.721e05 s^93
+ 3.47e07 s^92 - 4.014e07 s^91 + 1.291e09 s^90 - 1.502e09 s^89 + 3.687e10 s^88
- 4.308e10 s^87 + 8.422e11 s^86 - 9.866e11 s^85 + 1.58e13 s^84 - 1.853e13 s^83
+ 2.483e14 s^82 - 2.91e14 s^81 + 3.317e15 s^80 - 3.877e15 s^79 + 3.808e16 s^78
- 4.433e16 s^77 + 3.791e17 s^76 - 4.387e17 s^75 + 3.295e18 s^74 - 3.785e18 s^73
+ 2.515e19 s^72 - 2.862e19 s^71 + 1.693e20 s^70 - 1.905e20 s^69 + 1.009e21 s^68
- 1.12e21 s^67 + 5.337e21 s^66 - 5.834e21 s^65 + 2.512e22 s^64 - 2.697e22 s^63
+ 1.053e23 s^62 - 1.109e23 s^61 + 3.941e23 s^60 - 4.055e23 s^59 + 1.317e24 s^58
- 1.321e24 s^57 + 3.928e24 s^56 - 3.831e24 s^55 + 1.047e25 s^54 - 9.891e24 s^53
+ 2.489e25 s^52 - 2.272e25 s^51 + 5.28e25 s^50 - 4.638e25 s^49 + 9.98e25 s^48
- 8.404e25 s^47 + 1.678e26 s^46 - 1.349e26 s^45 + 2.505e26 s^44 - 1.913e26 s^43
+ 3.312e26 s^42 - 2.391e26 s^41 + 3.868e26 s^40 - 2.625e26 s^39 + 3.977e26 s^38
- 2.523e26 s^37 + 3.585e26 s^36 - 2.114e26 s^35 + 2.821e26 s^34 - 1.535e26 s^33
+ 1.928e26 s^32 - 9.609e25 s^31 + 1.137e26 s^30 - 5.151e25 s^29 + 5.745e25 s^28
- 2.346e25 s^27 + 2.466e25 s^26 - 8.993e24 s^25 + 8.907e24 s^24 - 2.872e24 s^23
+ 2.675e24 s^22 - 7.542e23 s^21 + 6.588e23 s^20 - 1.604e23 s^19 + 1.308e23 s^18
- 2.714e22 s^17 + 2.053e22 s^16 - 3.568e21 s^15 + 2.48e21 s^14 - 3.54e20 s^13
+ 2.233e20 s^12 - 2.549e19 s^11 + 1.434e19 s^10 - 1.263e18 s^9 + 6.165e17 s^8
- 3.991e16 s^7 + 1.611e16 s^6 - 7.262e14 s^5 + 2.141e14 s^4 - 6.546e12 s^3
+ 9.842e11 s^2 - 1.579e10 s + 3.25e08

---

s^99 + 2.378 s^98 + 175.8 s^97 + 396.5 s^96 + 1.487e04 s^95 + 3.182e04 s^94 + 8.067e05 s^93
+ 1.638e06 s^92 + 3.154e07 s^91 + 6.081e07 s^90 + 9.469e08 s^89 + 1.734e09 s^88
+ 2.272e10 s^87 + 3.952e10 s^86 + 4.48e11 s^85 + 7.4e11 s^84 + 7.397e12 s^83

+ 1.161e13 s^82 + 1.038e14 s^81 + 1.547e14 s^80 + 1.253e15 s^79 + 1.773e15 s^78
+ 1.311e16 s^77 + 1.761e16 s^76 + 1.199e17 s^75 + 1.528e17 s^74 + 9.625e17 s^73
+ 1.164e18 s^72 + 6.82e18 s^71 + 7.821e18 s^70 + 4.28e19 s^69 + 4.651e19 s^68
+ 2.385e20 s^67 + 2.455e20 s^66 + 1.183e21 s^65 + 1.153e21 s^64 + 5.236e21 s^63
+ 4.823e21 s^62 + 2.068e22 s^61 + 1.8e22 s^60 + 7.298e22 s^59 + 5.996e22 s^58
+ 2.302e23 s^57 + 1.783e23 s^56 + 6.492e23 s^55 + 4.733e23 s^54 + 1.636e24 s^53
+ 1.121e24 s^52 + 3.679e24 s^51 + 2.368e24 s^50 + 7.383e24 s^49 + 4.451e24 s^48
+ 1.32e25 s^47 + 7.44e24 s^46 + 2.097e25 s^45 + 1.103e25 s^44 + 2.957e25 s^43
+ 1.448e25 s^42 + 3.689e25 s^41 + 1.676e25 s^40 + 4.062e25 s^39 + 1.707e25 s^38
+ 3.932e25 s^37 + 1.523e25 s^36 + 3.334e25 s^35 + 1.185e25 s^34 + 2.464e25 s^33
+ 8.002e24 s^32 + 1.579e25 s^31 + 4.658e24 s^30 + 8.725e24 s^29 + 2.321e24 s^28
+ 4.126e24 s^27 + 9.821e23 s^26 + 1.657e24 s^25 + 3.494e23 s^24 + 5.593e23 s^23
+ 1.033e23 s^22 + 1.571e23 s^21 + 2.503e22 s^20 + 3.62e22 s^19 + 4.885e21 s^18
+ 6.738e21 s^17 + 7.524e20 s^16 + 9.929e20 s^15 + 8.912e19 s^14 + 1.13e20 s^13
+ 7.861e18 s^12 + 9.62e18 s^11 + 4.966e17 s^10 + 5.862e17 s^9 + 2.144e16 s^8
+ 2.402e16 s^7 + 5.989e14 s^6 + 5.991e14 s^5 + 9.999e12 s^4 + 7.589e12 s^3
+ 8.131e10 s^2 + 3.183e10 s + 4.315e07

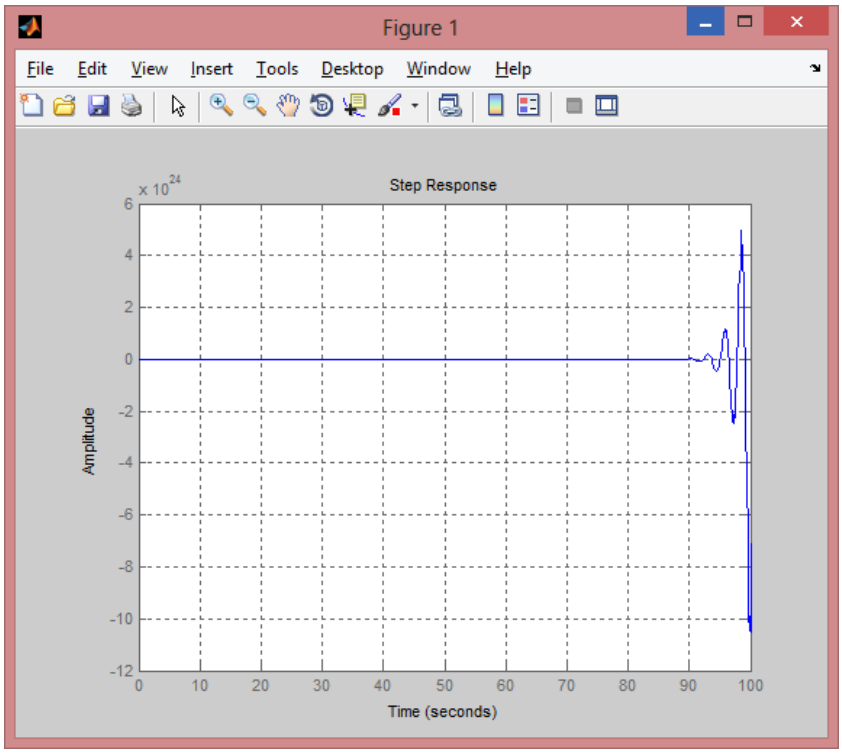

Figure 32: Step response (Level 1 - Linear)

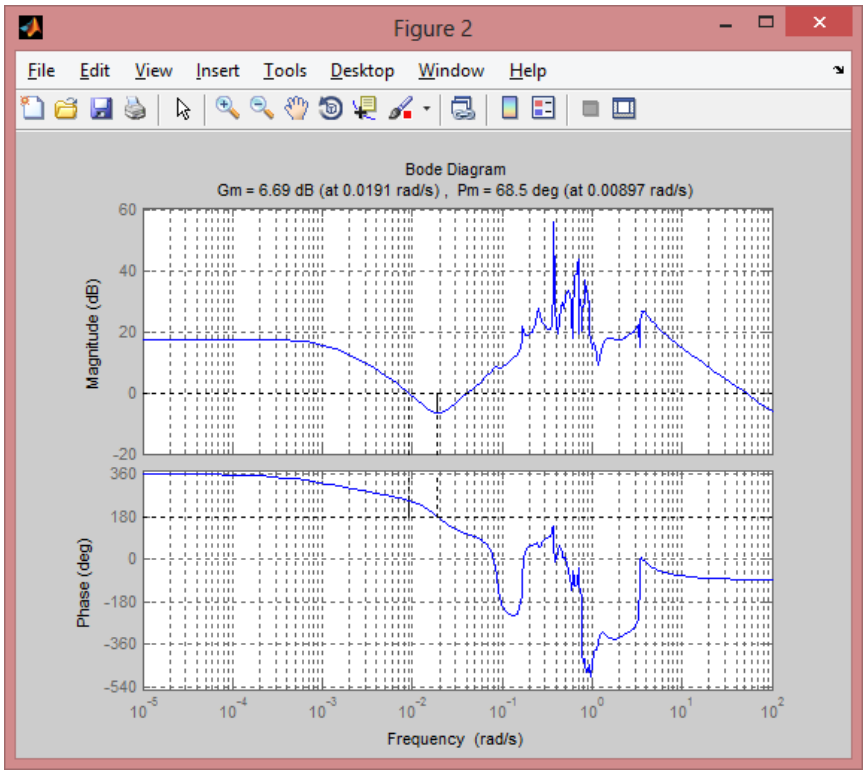

Figure 33:Bode plot (Level 1 - Linear)

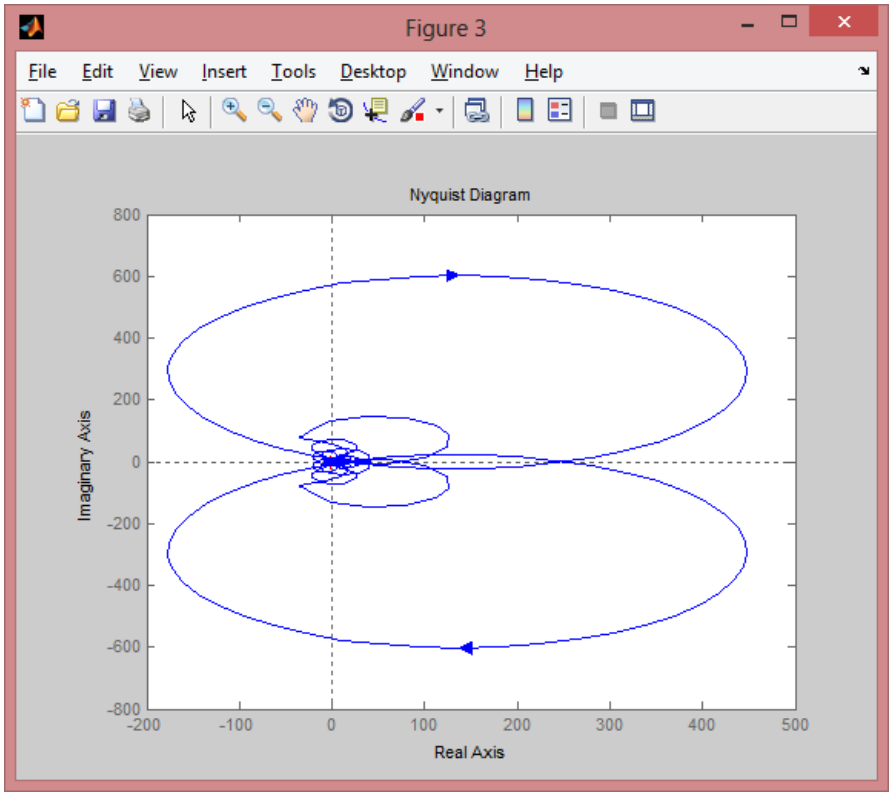

Figure 34: Nyquist plot (Level 1 - Linear)

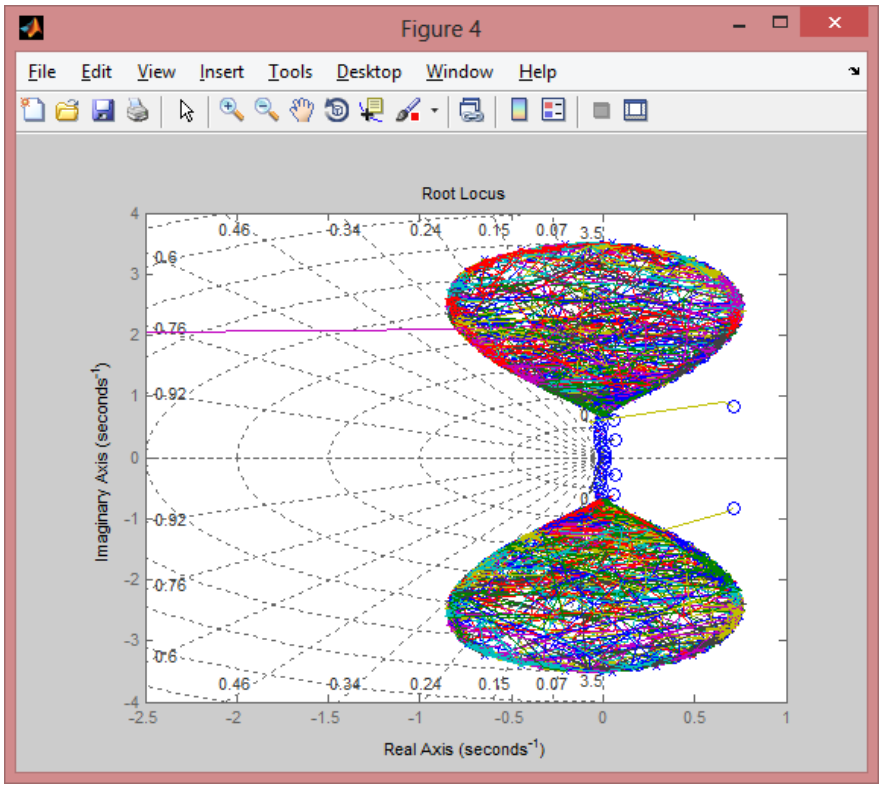

Figure 35: Root locus plot (Level 1 - Linear)

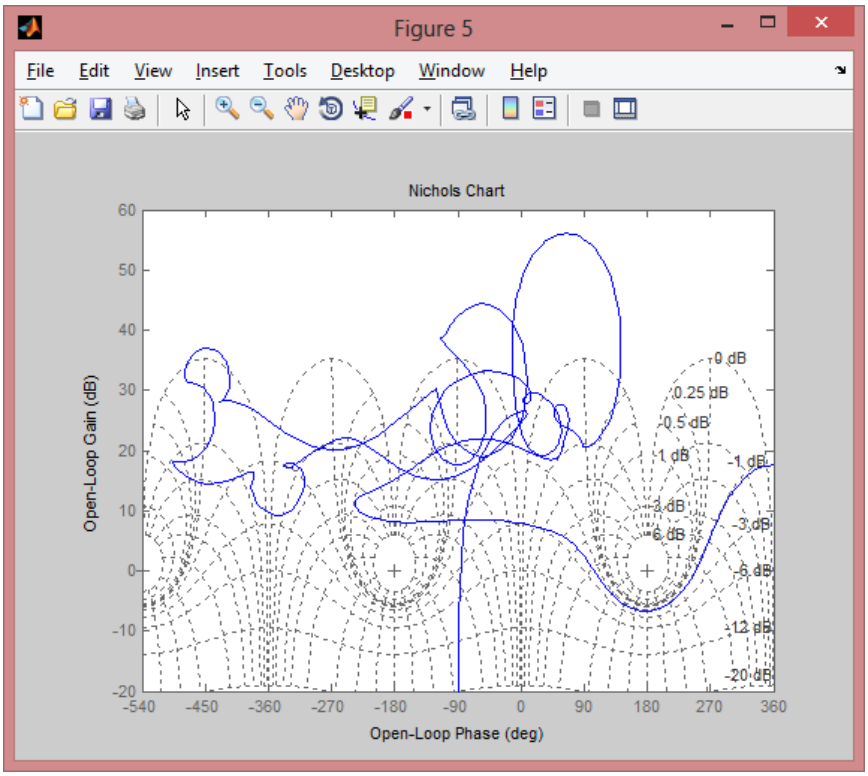

Figure 36: Nichols plot (Level 1 – Linear)

Level 2

ARX Model

Fit to estimation data: 96.38%

A(z) = 1 - 0.6685 z^-1 + 0.3489 z^-2 - 0.598 z^-3 - 0.07725 z^-4 + 0.1461 z^-5 - 0.02203 z^-6
+ 0.2935 z^-7 + 0.2175 z^-8 + 0.1274 z^-9 - 0.1225 z^-10 + 0.2118 z^-11 - 0.3887 z^-12
+ 0.353 z^-13 - 0.3557 z^-14 + 0.4064 z^-15 - 0.368 z^-16 + 0.1367 z^-17
+ 0.1353 z^-18 - 0.1422 z^-19 + 0.0006027 z^-20 - 0.2315 z^-21 + 0.5562 z^-22
- 0.06718 z^-23 + 0.5814 z^-24 - 0.1223 z^-25 - 0.3057 z^-26 - 0.3077 z^-27
- 0.2798 z^-28 - 0.4031 z^-29 + 0.6569 z^-30 + 0.3411 z^-31 + 0.2672 z^-32
- 0.00577 z^-33 - 0.6211 z^-34 - 0.08368 z^-35 - 0.102 z^-36 + 0.3279 z^-37
+ 0.1387 z^-38 + 0.08416 z^-39 + 0.1133 z^-40 - 0.243 z^-41 + 0.2047 z^-42
- 0.4344 z^-43 - 0.286 z^-44 + 0.1718 z^-45 - 0.1035 z^-46 + 0.2641 z^-47
+ 0.3671 z^-48 + 0.1037 z^-49 - 0.4474 z^-50 - 0.3116 z^-51 - 0.2868 z^-52
- 0.03658 z^-53 + 0.9033 z^-54 + 0.08868 z^-55 + 0.02752 z^-56 - 0.1778 z^-57
- 1.03 z^-58 + 0.383 z^-59 - 0.3222 z^-60 + 0.458 z^-61 + 0.1594 z^-62 + 0.05754 z^-63
- 0.06859 z^-64 - 0.07518 z^-65 + 0.07897 z^-66 + 0.07641 z^-67 - 0.0849 z^-68
- 0.2487 z^-69 - 0.2775 z^-70 - 0.1494 z^-71 + 0.639 z^-72 - 0.2764 z^-73
+ 0.4063 z^-74 - 0.4939 z^-75 - 0.1408 z^-76 - 0.0692 z^-77 + 0.1795 z^-78
+ 0.04711 z^-79 - 0.006193 z^-80 + 0.2833 z^-81 - 0.5381 z^-82 + 0.2319 z^-83
- 0.2346 z^-84 - 0.01996 z^-85 + 0.06101 z^-86 + 0.08977 z^-87 - 0.2612 z^-88
+ 0.124 z^-89 - 0.1337 z^-90 - 0.0247 z^-91 - 0.06993 z^-92 - 0.1805 z^-93
+ 0.3189 z^-94 + 0.07291 z^-95 + 0.258 z^-96 - 0.1975 z^-97 - 0.2431 z^-98

B(z) = -6.571 z^-1 + 1.691 z^-2 - 2.533 z^-3 + 1.421 z^-4 + 3.567 z^-5 + 2.654 z^
-6 + 0.7955 z^-7 + 0.4957 z^-8 - 1.156 z^-9 - 8.468 z^-10 + 3.441 z^-11 - 3.074 z^-12
+ 2.332 z^-13 + 3.892 z^-14 + 0.6175 z^-15 + 3.608 z^-16 + 0.06949 z^-17
+ 0.2684 z^-18 - 4.343 z^-19 + 1.832 z^-20 - 1.057 z^-21 + 1.42 z^-22 - 1.196 z^-23
- 2.971 z^-24 + 1.298 z^-25 + 0.3064 z^-26 - 0.4577 z^-27 + 2.239 z^-28 + 3.131 z^-29
+ 0.8125 z^-30 + 4.975 z^-31 - 11 z^-32 + 1.886 z^-33 - 6.594 z^-34 + 3.699 z^-35
+ 1.257 z^-36 + 1.173 z^-37 + 4.452 z^-38 - 4.335 z^-39 + 5.126 z^-40 - 5.931 z^-41
- 0.1399 z^-42 - 1.445 z^-43 - 3.166 z^-44 + 0.3856 z^-45 + 4.729 z^-46 - 0.6051 z^-47
+ 6.191 z^-48 - 1.854 z^-49 - 7.428 z^-50 - 0.1504 z^-51 + 0.9321 z^-52 + 1.492 z^-53
+ 8.284 z^-54 - 2.34 z^-55 - 7.051 z^-56 + 3.461 z^-57 - 4.469 z^-58 + 0.2753 z^-59
+ 4.212 z^-60 + 1.09 z^-61 - 4.307 z^-62 + 5.236 z^-63 - 2.228 z^-64 - 0.8814 z^-65
+ 4.946 z^-66 - 4.808 z^-67 - 7.706 z^-68 + 4.972 z^-69 + 1.335 z^-70 + 4.36 z^-71
+ 10.82 z^-72 - 8.421 z^-73 - 6.106 z^-74 + 0.6505 z^-75 - 5.901 z^-76 + 3.908 z^-77
+ 8.81 z^-78 - 3.076 z^-79 - 0.3897 z^-80 + 3.699 z^-81 - 5.68 z^-82 + 0.6647 z^-83
+ 3.727 z^-84 - 5.195 z^-85 - 3.265 z^-86 + 1.816 z^-87 - 1.379 z^-88 + 3.341 z^-89
+ 12.85 z^-90 - 14.78 z^-91 + 3.708 z^-92 - 3.548 z^-93 - 2.368 z^-94 + 5.456 z^-95
- 3.763 z^-96 + 2.229 z^-97 - 1.763 z^-98

Transfer model in z transform

-6.571 z^-1 + 1.691 z^-2 - 2.533 z^-3 + 1.421 z^-4 + 3.567 z^-5 + 2.654 z^-6
+ 0.7955 z^-7 + 0.4957 z^-8 - 1.156 z^-9 - 8.468 z^-10 + 3.441 z^-11
- 3.074 z^-12 + 2.332 z^-13 + 3.892 z^-14 + 0.6175 z^-15 + 3.608 z^-16
+ 0.06949 z^-17 + 0.2684 z^-18 - 4.343 z^-19 + 1.832 z^-20 - 1.057 z^
-21 + 1.42 z^-22 - 1.196 z^-23 - 2.971 z^-24 + 1.298 z^-25 + 0.3064 z^-26
- 0.4577 z^-27 + 2.239 z^-28 + 3.131 z^-29 + 0.8125 z^-30 + 4.975 z^-31
- 11 z^-32 + 1.886 z^-33 - 6.594 z^-34 + 3.699 z^-35 + 1.257 z^-36 + 1.173 z^-37
+ 4.452 z^-38 - 4.335 z^-39 + 5.126 z^-40 - 5.931 z^-41 - 0.1399 z^-42
- 1.445 z^-43 - 3.166 z^-44 + 0.3856 z^-45 + 4.729 z^-46 - 0.6051 z^-47
+ 6.191 z^-48 - 1.854 z^-49 - 7.428 z^-50 - 0.1504 z^-51 + 0.9321 z^-52
+ 1.492 z^-53 + 8.284 z^-54 - 2.34 z^-55 - 7.051 z^-56 + 3.461 z^-57

- 4.469 z^-58 + 0.2753 z^-59 + 4.212 z^-60 + 1.09 z^-61 - 4.307 z^-62
+ 5.236 z^-63 - 2.228 z^-64 - 0.8814 z^-65 + 4.946 z^-66 - 4.808 z^-67
- 7.706 z^-68 + 4.972 z^-69 + 1.335 z^-70 + 4.36 z^-71 + 10.82 z^-72
- 8.421 z^-73 - 6.106 z^-74 + 0.6505 z^-75 - 5.901 z^-76 + 3.908 z^-77
+ 8.81 z^-78 - 3.076 z^-79 - 0.3897 z^-80 + 3.699 z^-81 - 5.68 z^-82
+ 0.6647 z^-83 + 3.727 z^-84 - 5.195 z^-85 - 3.265 z^-86 + 1.816 z^-87
- 1.379 z^-88 + 3.341 z^-89 + 12.85 z^-90 - 14.78 z^-91 + 3.708 z^-92
- 3.548 z^-93 - 2.368 z^-94 + 5.456 z^-95 - 3.763 z^-96 + 2.229 z^-97
- 1.763 z^-98

---

1 - 0.6685 z^-1 + 0.3489 z^-2 - 0.598 z^-3 - 0.07725 z^-4 + 0.1461 z^-5 - 0.02203 z^-6
+ 0.2935 z^-7 + 0.2175 z^-8 + 0.1274 z^-9 - 0.1225 z^-10 + 0.2118 z^-11
- 0.3887 z^-12 + 0.353 z^-13 - 0.3557 z^-14 + 0.4064 z^-15 - 0.368 z^
-16 + 0.1367 z^-17 + 0.1353 z^-18 - 0.1422 z^-19 + 0.0006027 z^-20 - 0.2315 z^-21
+ 0.5562 z^-22 - 0.06718 z^-23 + 0.5814 z^-24 - 0.1223 z^-25 - 0.3057 z^-26
- 0.3077 z^-27 - 0.2798 z^-28 - 0.4031 z^-29 + 0.6569 z^-30 + 0.3411 z^-31
+ 0.2672 z^-32 - 0.00577 z^-33 - 0.6211 z^-34 - 0.08368 z^-35 - 0.102 z^-36
+ 0.3279 z^-37 + 0.1387 z^-38 + 0.08416 z^-39 + 0.1133 z^-40 - 0.243 z^-41
+ 0.2047 z^-42 - 0.4344 z^-43 - 0.286 z^-44 + 0.1718 z^-45 - 0.1035 z^-46
+ 0.2641 z^-47 + 0.3671 z^-48 + 0.1037 z^-49 - 0.4474 z^-50 - 0.3116 z^-51
- 0.2868 z^-52 - 0.03658 z^-53 + 0.9033 z^-54 + 0.08868 z^-55 + 0.02752 z^-56
- 0.1778 z^-57 - 1.03 z^-58 + 0.383 z^-59 - 0.3222 z^-60 + 0.458 z^-61
+ 0.1594 z^-62 + 0.05754 z^-63 - 0.06859 z^-64 - 0.07518 z^-65 + 0.07897 z^-66
+ 0.07641 z^-67 - 0.0849 z^-68 - 0.2487 z^-69 - 0.2775 z^-70 - 0.1494 z^-71
+ 0.639 z^-72 - 0.2764 z^-73 + 0.4063 z^-74 - 0.4939 z^-75 - 0.1408 z^-76
- 0.0692 z^-77 + 0.1795 z^-78 + 0.04711 z^-79 - 0.006193 z^-80 + 0.2833 z^-81
- 0.5381 z^-82 + 0.2319 z^-83 - 0.2346 z^-84 - 0.01996 z^-85 + 0.06101 z^-86
+ 0.08977 z^-87 - 0.2612 z^-88 + 0.124 z^-89 - 0.1337 z^-90 - 0.0247 z^-91
- 0.06993 z^-92 - 0.1805 z^-93 + 0.3189 z^-94 + 0.07291 z^-95 + 0.258 z^-96
- 0.1975 z^-97 - 0.2431 z^-98

Transfer model in s transform

-7.618 s^100 - 3.324 s^99 - 1358 s^98 - 680.8 s^97 - 1.165e05 s^96 - 6.498e04 s^95
- 6.411e06 s^94 - 3.888e06 s^93 - 2.542e08 s^92 - 1.648e08 s^91 - 7.739e09 s^90
- 5.298e09 s^89 - 1.884e11 s^88 - 1.347e11 s^87 - 3.768e12 s^86 - 2.79e12 s^85
- 6.312e13 s^84 - 4.805e13 s^83 - 8.992e14 s^82 - 6.994e14 s^81 - 1.102e16 s^80
- 8.709e15 s^79 - 1.171e17 s^78 - 9.364e16 s^77 - 1.087e18 s^76 - 8.762e17 s^75
- 8.875e18 s^74 - 7.177e18 s^73 - 6.395e19 s^72 - 5.173e19 s^71 - 4.083e20 s^70
- 3.293e20 s^69 - 2.317e21 s^68 - 1.858e21 s^67 - 1.171e22 s^66 - 9.311e21 s^65
- 5.283e22 s^64 - 4.153e22 s^63 - 2.129e23 s^62 - 1.651e23 s^61 - 7.671e23 s^60
- 5.853e23 s^59 - 2.473e24 s^58 - 1.852e24 s^57 - 7.131e24 s^56 - 5.231e24 s^55
- 1.839e25 s^54 - 1.318e25 s^53 - 4.237e25 s^52 - 2.962e25 s^51 - 8.716e25 s^50
- 5.927e25 s^49 - 1.598e26 s^48 - 1.055e26 s^47 - 2.607e26 s^46 - 1.665e26 s^45
- 3.776e26 s^44 - 2.328e26 s^43 - 4.843e26 s^42 - 2.874e26 s^41 - 5.482e26 s^40
- 3.121e26 s^39 - 5.458e26 s^38 - 2.97e26 s^37 - 4.758e26 s^36 - 2.465e26 s^35
- 3.616e26 s^34 - 1.775e26 s^33 - 2.382e26 s^32 - 1.101e26 s^31 - 1.351e26 s^30
- 5.843e25 s^29 - 6.549e25 s^28 - 2.63e25 s^27 - 2.691e25 s^26 - 9.933e24 s^25
- 9.277e24 s^24 - 3.111e24 s^23 - 2.652e24 s^22 - 7.966e23 s^21 - 6.198e23 s^20
- 1.639e23 s^19 - 1.165e23 s^18 - 2.653e22 s^17 - 1.723e22 s^16 - 3.289e21 s^15
- 1.957e21 s^14 - 3.019e20 s^13 - 1.65e20 s^12 - 1.955e19 s^11 - 9.872e18 s^10
- 8.313e17 s^9 - 3.932e17 s^8 - 2.047e16 s^7 - 9.442e15 s^6 - 2.188e14 s^5
- 1.148e14 s^4 - 3.201e10 s^3 - 4.825e11 s^2 + 3.485e09 s - 1.908e08

---

s^101 + 2.02 s^100 + 179.1 s^99 + 344 s^98 + 1.544e04 s^97 + 2.823e04 s^96 + 8.548e05 s^95

+ 1.487e06 s^94 + 3.413e07 s^93 + 5.648e07 s^92 + 1.048e09 s^91 + 1.65e09 s^90
+ 2.574e10 s^89 + 3.857e10 s^88 + 5.199e11 s^87 + 7.412e11 s^86 + 8.805e12 s^85
+ 1.194e13 s^84 + 1.269e14 s^83 + 1.637e14 s^82 + 1.574e15 s^81 + 1.931e15 s^80
+ 1.695e16 s^79 + 1.977e16 s^78 + 1.596e17 s^77 + 1.77e17 s^76 + 1.322e18 s^75
+ 1.393e18 s^74 + 9.674e18 s^73 + 9.679e18 s^72 + 6.277e19 s^71 + 5.963e19 s^70
+ 3.622e20 s^69 + 3.265e20 s^68 + 1.863e21 s^67 + 1.593e21 s^66 + 8.56e21 s^65
+ 6.934e21 s^64 + 3.515e22 s^63 + 2.698e22 s^62 + 1.292e23 s^61 + 9.384e22 s^60
+ 4.25e23 s^59 + 2.92e23 s^58 + 1.252e24 s^57 + 8.128e23 s^56 + 3.3e24 s^55
+ 2.023e24 s^54 + 7.779e24 s^53 + 4.5e24 s^52 + 1.638e25 s^51 + 8.934e24 s^50
+ 3.078e25 s^49 + 1.581e25 s^48 + 5.152e25 s^47 + 2.488e25 s^46 + 7.663e25 s^45
+ 3.477e25 s^44 + 1.01e26 s^43 + 4.302e25 s^42 + 1.177e26 s^41 + 4.697e25 s^40
+ 1.208e26 s^39 + 4.511e25 s^38 + 1.087e26 s^37 + 3.793e25 s^36 + 8.543e25 s^35
+ 2.78e25 s^34 + 5.83e25 s^33 + 1.766e25 s^32 + 3.434e25 s^31 + 9.665e24 s^30
+ 1.733e25 s^29 + 4.522e24 s^28 + 7.439e24 s^27 + 1.794e24 s^26 + 2.689e24 s^25
+ 5.979e23 s^24 + 8.097e23 s^23 + 1.654e23 s^22 + 2.006e23 s^21 + 3.749e22 s^20
+ 4.026e22 s^19 + 6.853e21 s^18 + 6.435e21 s^17 + 9.907e20 s^16 + 8.017e20 s^15
+ 1.106e20 s^14 + 7.587e19 s^13 + 9.233e18 s^12 + 5.281e18 s^11 + 5.528e17 s^10
+ 2.591e17 s^9 + 2.233e16 s^8 + 8.455e15 s^7 + 5.539e14 s^6 + 1.678e14 s^5
+ 7.161e12 s^4 + 1.727e12 s^3 + 3.273e10 s^2 + 6.327e09 s - 2.52e07

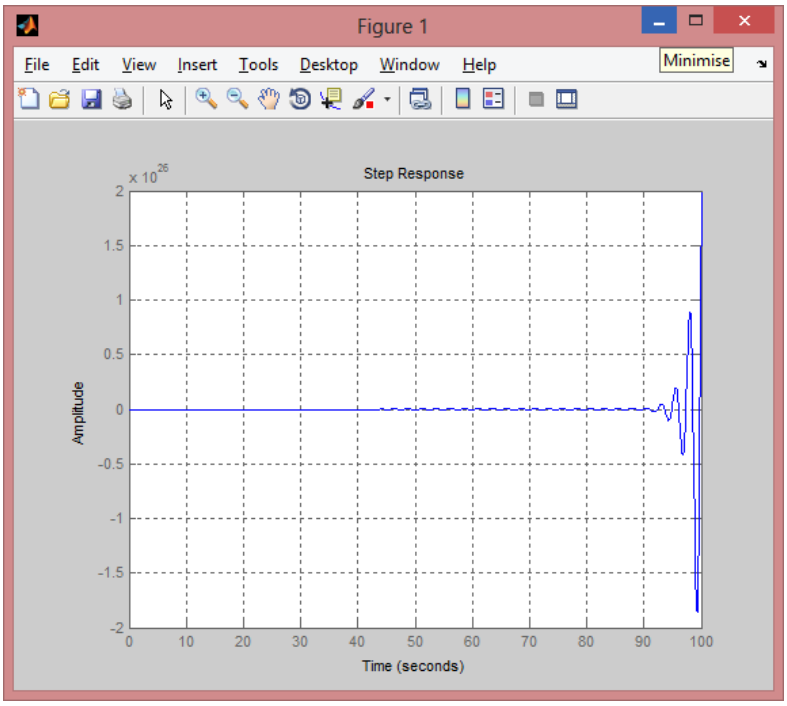

Figure 37: Step response (Level 2 - Linear)

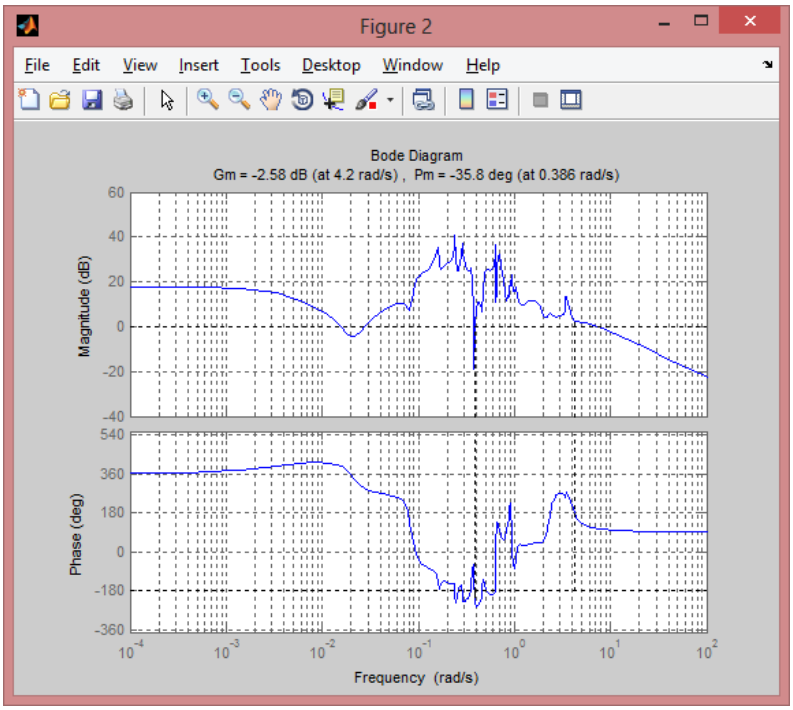

Figure 38: Bode plot (Level 2 - Linear)

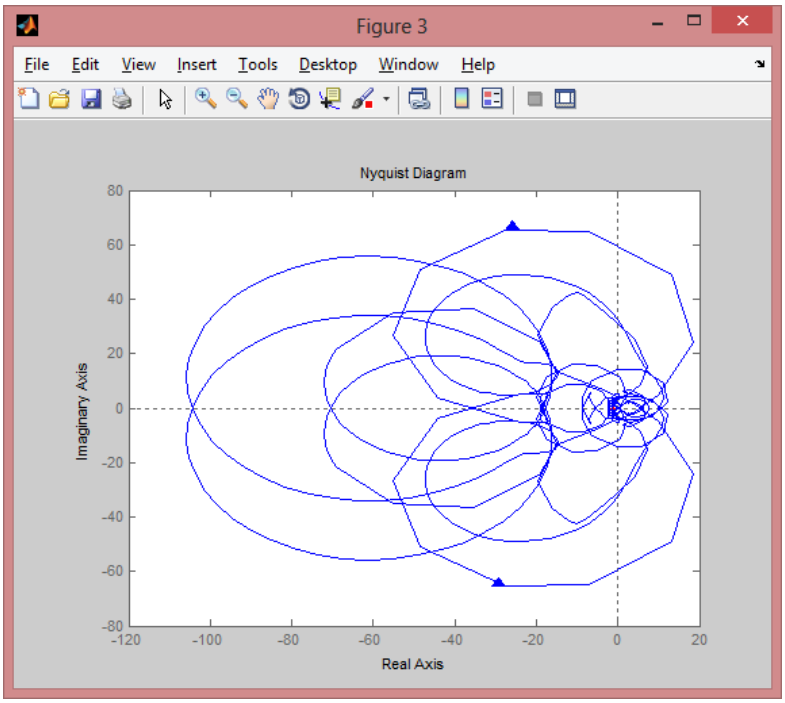

Figure 39: Nyquist plot (Level 2 - Linear)

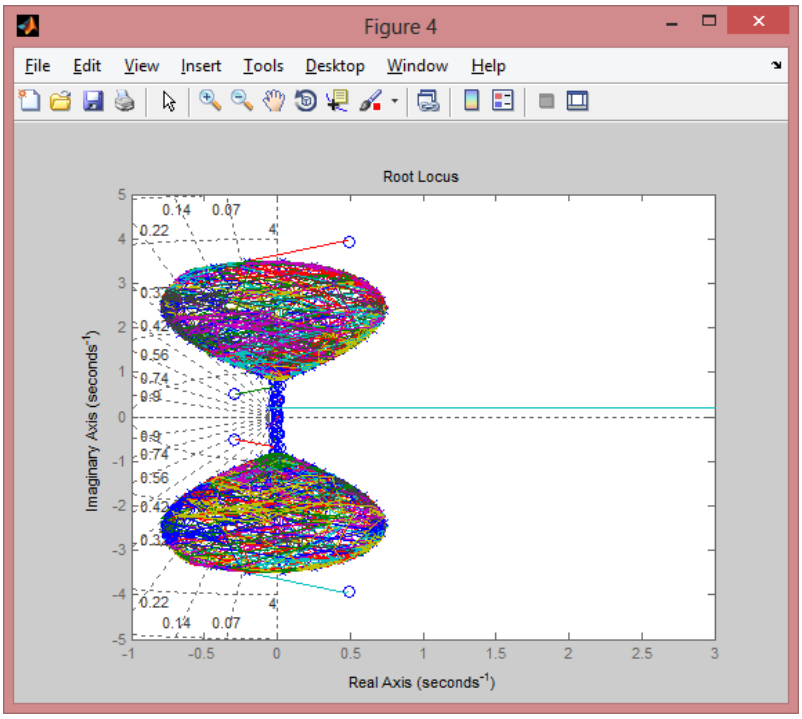

Figure 40: Root locus plot (Level 2 - Linear)

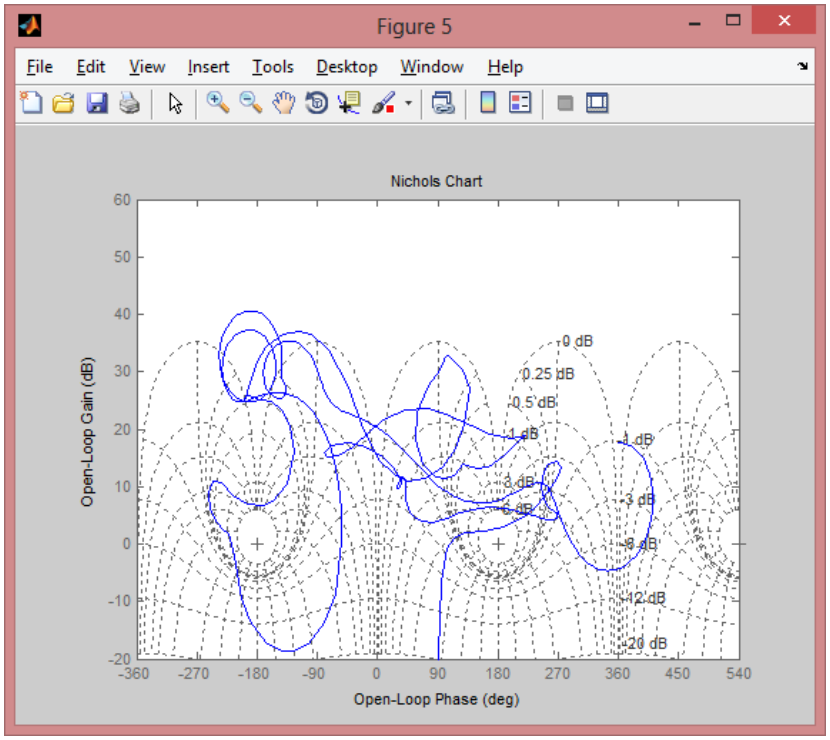

Figure 41: Nichols plot (Level 2 - Linear)

Level 3

ARX Model

Fit to estimation data: 96.56%

A(z) = 1 - 1.862 z^-1 + 1.43 z^-2 - 1.319 z^-3 + 1.259 z^-4 - 0.6792 z^-5 + 0.5849 z^-6
- 0.3336 z^-7 - 0.06455 z^-8 + 0.1403 z^-9 - 0.4693 z^-10 + 0.9719 z^-11
- 1.031 z^-12 + 0.8843 z^-13 - 0.6046 z^-14 + 0.171 z^-15 + 0.3403 z^-16
- 0.6744 z^-17 + 0.6249 z^-18 - 0.6668 z^-19 + 0.4576 z^-20 - 0.04767 z^-21
+ 0.222 z^-22 - 0.3304 z^-23 + 0.03553 z^-24 + 0.1729 z^-25 - 0.4189 z^-26
+ 0.4965 z^-27 - 0.07702 z^-28 - 0.1195 z^-29 - 0.1686 z^-30 + 0.4092 z^-31
- 0.1689 z^-32 - 0.1277 z^-33 + 0.3092 z^-34 - 0.1152 z^-35 - 0.4899 z^-36
+ 0.6683 z^-37 - 0.6632 z^-38 + 0.6406 z^-39 - 0.3452 z^-40 + 0.2532 z^-41
- 0.4474 z^-42 + 0.47 z^-43 - 0.1408 z^-44 - 0.05819 z^-45 - 0.04178 z^-46
- 0.462 z^-47 + 0.8012 z^-48 - 0.6322 z^-49 + 0.525 z^-50 - 0.3255 z^-51
+ 0.1296 z^-52 - 0.08628 z^-53 - 0.04858 z^-54 + 0.1171 z^-55 - 0.3361 z^
-56 + 0.8286 z^-57 - 0.7898 z^-58 + 0.6231 z^-59 - 0.8364 z^-60 + 1.123 z^-61
- 1.582 z^-62 + 1.712 z^-63 - 1.325 z^-64 + 1.263 z^-65 - 1.144 z^-66 + 0.9522 z^-67
- 0.6771 z^-68 + 0.3813 z^-69 + 0.05039 z^-70 - 0.3139 z^-71 + 0.4328 z^-72
- 0.7879 z^-73 + 1.032 z^-74 - 0.7986 z^-75 + 0.3861 z^-76 + 0.08029 z^-77
- 0.02528 z^-78 - 0.2185 z^-79 + 0.1544 z^-80 + 0.1209 z^-81 - 0.1733 z^-82
+ 0.239 z^-83 - 0.2857 z^-84 + 0.6098 z^-85 - 0.9363 z^-86 + 1.087 z^-87
- 1.062 z^-88 + 0.6422 z^-89 - 0.4246 z^-90 + 1.122 z^-91 - 0.9207 z^-92
+ 0.2801 z^-93 + 0.02006 z^-94 - 0.417 z^-95 + 0.3997 z^-96

B(z) = 0.1189 z^-1 + 5.632 z^-2 + 0.9657 z^-3 - 8.802 z^-4 + 11.9 z^-5 - 5.492 z^
-6 - 0.5488 z^-7 + 7.009 z^-8 - 3.636 z^-9 - 4.565 z^-10 + 2.524 z^-11 - 1.956 z^-12
- 1.215 z^-13 + 9.647 z^-14 - 4.471 z^-15 - 2.474 z^-16 - 1.468 z^-17 + 0.843 z^-18
- 1.487 z^-19 + 4.749 z^-20 - 7.396 z^-21 + 3.297 z^-22 + 1.505 z^-23 - 2.615 z^-24
- 3.402 z^-25 - 5.31 z^-26 + 0.9203 z^-27 - 1.397 z^-28 + 15.74 z^-29 - 14.06 z^-30
+ 8.599 z^-31 + 4.525 z^-32 - 9.01 z^-33 + 3.591 z^-34 - 6.309 z^-35 + 3.607 z^-36
+ 0.2435 z^-37 + 3.864 z^-38 - 1.171 z^-39 - 0.1494 z^-40 + 6.302 z^-41 - 0.9 z^-42
- 5.34 z^-43 - 5.1 z^-44 + 2.545 z^-45 - 1.244 z^-46 + 7.942 z^-47 - 0.1414 z^-48
- 5.213 z^-49 + 1.78 z^-50 - 9.902 z^-51 - 1.431 z^-52 + 4.955 z^-53 - 2.831 z^-54
+ 3.544 z^-55 - 5.834 z^-56 + 8.895 z^-57 + 3.69 z^-58 - 7.89 z^-59 - 8.622 z^-60
+ 11.18 z^-61 - 7.089 z^-62 + 2.151 z^-63 + 13.61 z^-64 - 10.92 z^-65 + 9.904 z^-66
- 3.484 z^-67 + 3.94 z^-68 - 10.01 z^-69 + 3.93 z^-70 + 13.72 z^-71 - 6.882 z^-72
- 2.171 z^-73 + 3.766 z^-74 - 0.1583 z^-75 - 7.029 z^-76 - 2.103 z^-77 - 3.627 z^-78
+ 6.525 z^-79 + 2.679 z^-80 - 3.645 z^-81 - 1.315 z^-82 + 4.894 z^-83 - 7.687 z^-84
+ 5.576 z^-85 - 14.03 z^-86 + 9.397 z^-87 + 0.07331 z^-88 - 1.215 z^-89 + 1.917 z^-90
- 8.66 z^-91 + 16.23 z^-92 - 3.642 z^-93 + 2.263 z^-94 - 11.65 z^-95 + 10.61 z^-96

Transfer model in z transform

0.1189 z^-1 + 5.632 z^-2 + 0.9657 z^-3 - 8.802 z^-4 + 11.9 z^-5 - 5.492 z^-6
- 0.5488 z^-7 + 7.009 z^-8 - 3.636 z^-9 - 4.565 z^-10 + 2.524 z^-11 - 1.956 z^-12
- 1.215 z^-13 + 9.647 z^-14 - 4.471 z^-15 - 2.474 z^-16 - 1.468 z^-17
+ 0.843 z^-18 - 1.487 z^-19 + 4.749 z^-20 - 7.396 z^-21 + 3.297 z^-22
+ 1.505 z^-23 - 2.615 z^-24 - 3.402 z^-25 - 5.31 z^-26 + 0.9203 z^-27
- 1.397 z^-28 + 15.74 z^-29 - 14.06 z^-30 + 8.599 z^-31 + 4.525 z^-32
- 9.01 z^-33 + 3.591 z^-34 - 6.309 z^-35 + 3.607 z^-36 + 0.2435 z^-37
+ 3.864 z^-38 - 1.171 z^-39 - 0.1494 z^-40 + 6.302 z^-41 - 0.9 z^-42
- 5.34 z^-43 - 5.1 z^-44 + 2.545 z^-45 - 1.244 z^-46 + 7.942 z^-47 - 0.1414 z^-48
- 5.213 z^-49 + 1.78 z^-50 - 9.902 z^-51 - 1.431 z^-52 + 4.955 z^-53
- 2.831 z^-54 + 3.544 z^-55 - 5.834 z^-56 + 8.895 z^-57 + 3.69 z^-58
- 7.89 z^-59 - 8.622 z^-60 + 11.18 z^-61 - 7.089 z^-62 + 2.151 z^-63

+ 13.61 z^-64 - 10.92 z^-65 + 9.904 z^-66 - 3.484 z^-67 + 3.94 z^-68
- 10.01 z^-69 + 3.93 z^-70 + 13.72 z^-71 - 6.882 z^-72 - 2.171 z^-73
+ 3.766 z^-74 - 0.1583 z^-75 - 7.029 z^-76 - 2.103 z^-77 - 3.627 z^-78
+ 6.525 z^-79 + 2.679 z^-80 - 3.645 z^-81 - 1.315 z^-82 + 4.894 z^-83
- 7.687 z^-84 + 5.576 z^-85 - 14.03 z^-86 + 9.397 z^-87 + 0.07331 z^-88
- 1.215 z^-89 + 1.917 z^-90 - 8.66 z^-91 + 16.23 z^-92 - 3.642 z^-93
+ 2.263 z^-94 - 11.65 z^-95 + 10.61 z^-96

---

1 - 1.862 z^-1 + 1.43 z^-2 - 1.319 z^-3 + 1.259 z^-4 - 0.6792 z^-5 + 0.5849 z^-6
- 0.3336 z^-7 - 0.06455 z^-8 + 0.1403 z^-9 - 0.4693 z^-10 + 0.9719 z^
-11 - 1.031 z^-12 + 0.8843 z^-13 - 0.6046 z^-14 + 0.171 z^-15 + 0.3403 z^-16
- 0.6744 z^-17 + 0.6249 z^-18 - 0.6668 z^-19 + 0.4576 z^-20 - 0.04767 z^-21
+ 0.222 z^-22 - 0.3304 z^-23 + 0.03553 z^-24 + 0.1729 z^-25 - 0.4189 z^-26
+ 0.4965 z^-27 - 0.07702 z^-28 - 0.1195 z^-29 - 0.1686 z^-30 + 0.4092 z^-31
- 0.1689 z^-32 - 0.1277 z^-33 + 0.3092 z^-34 - 0.1152 z^-35 - 0.4899 z^-36
+ 0.6683 z^-37 - 0.6632 z^-38 + 0.6406 z^-39 - 0.3452 z^-40 + 0.2532 z^-41
- 0.4474 z^-42 + 0.47 z^-43 - 0.1408 z^-44 - 0.05819 z^-45 - 0.04178 z^-46
- 0.462 z^-47 + 0.8012 z^-48 - 0.6322 z^-49 + 0.525 z^-50 - 0.3255 z^
-51 + 0.1296 z^-52 - 0.08628 z^-53 - 0.04858 z^-54 + 0.1171 z^-55 - 0.3361 z^-56
+ 0.8286 z^-57 - 0.7898 z^-58 + 0.6231 z^-59 - 0.8364 z^-60 + 1.123 z^-61
- 1.582 z^-62 + 1.712 z^-63 - 1.325 z^-64 + 1.263 z^-65 - 1.144 z^-66
+ 0.9522 z^-67 - 0.6771 z^-68 + 0.3813 z^-69 + 0.05039 z^-70 - 0.3139 z^-71
+ 0.4328 z^-72 - 0.7879 z^-73 + 1.032 z^-74 - 0.7986 z^-75 + 0.3861 z^-76
+ 0.08029 z^-77 - 0.02528 z^-78 - 0.2185 z^-79 + 0.1544 z^-80 + 0.1209 z^-81
- 0.1733 z^-82 + 0.239 z^-83 - 0.2857 z^-84 + 0.6098 z^-85 - 0.9363 z^-86
+ 1.087 z^-87 - 1.062 z^-88 + 0.6422 z^-89 - 0.4246 z^-90 + 1.122 z^-91
- 0.9207 z^-92 + 0.2801 z^-93 + 0.02006 z^-94 - 0.417 z^-95 + 0.3997 z^-96

Transfer model in s transform

-14.91 s^97 + 27.36 s^96 - 2420 s^95 + 4374 s^94 - 1.89e05 s^93 + 3.366e05 s^92
- 9.462e06 s^91 + 1.66e07 s^90 - 3.413e08 s^89 + 5.9e08 s^88 - 9.451e09 s^87
+ 1.61e10 s^86 - 2.09e11 s^85 + 3.51e11 s^84 - 3.795e12 s^83 + 6.281e12 s^82
- 5.765e13 s^81 + 9.408e13 s^80 - 7.435e14 s^79 + 1.197e15 s^78 - 8.233e15 s^77
+ 1.307e16 s^76 - 7.895e16 s^75 + 1.237e17 s^74 - 6.601e17 s^73 + 1.02e18 s^72
- 4.839e18 s^71 + 7.384e18 s^70 - 3.123e19 s^69 + 4.706e19 s^68 - 1.781e20 s^67
+ 2.651e20 s^66 - 8.994e20 s^65 + 1.323e21 s^64 - 4.032e21 s^63 + 5.865e21 s^62
- 1.606e22 s^61 + 2.311e22 s^60 - 5.692e22 s^59 + 8.107e22 s^58 - 1.795e23 s^57
+ 2.532e23 s^56 - 5.038e23 s^55 + 7.044e23 s^54 - 1.258e24 s^53 + 1.744e24 s^52
- 2.79e24 s^51 + 3.842e24 s^50 - 5.494e24 s^49 + 7.521e24 s^48 - 9.586e24 s^47
+ 1.306e25 s^46 - 1.479e25 s^45 + 2.009e25 s^44 - 2.013e25 s^43 + 2.729e25 s^42
- 2.409e25 s^41 + 3.268e25 s^40 - 2.526e25 s^39 + 3.436e25 s^38 - 2.311e25 s^37
+ 3.162e25 s^36 - 1.837e25 s^35 + 2.535e25 s^34 - 1.261e25 s^33 + 1.761e25 s^32
- 7.433e24 s^31 + 1.055e25 s^30 - 3.734e24 s^29 + 5.411e24 s^28 - 1.586e24 s^27
+ 2.358e24 s^26 - 5.638e23 s^25 + 8.648e23 s^24 - 1.66e23 s^23 + 2.641e23 s^22
- 3.996e22 s^21 + 6.628e22 s^20 - 7.746e21 s^19 + 1.345e22 s^18 - 1.187e21 s^17
+ 2.162e21 s^16 - 1.403e20 s^15 + 2.683e20 s^14 - 1.238e19 s^13 + 2.484e19 s^12
- 7.76e17 s^11 + 1.636e18 s^10 - 3.162e16 s^9 + 7.161e16 s^8 - 6.966e14 s^7
+ 1.87e15 s^6 - 4.777e12 s^5 + 2.417e13 s^4 - 1.176e10 s^3 + 1.129e11 s^2
- 1.112e09 s + 6.295e07

---

s^98 + 1.273 s^97 + 166 s^96 + 201.9 s^95 + 1.327e04 s^94 + 1.54e04 s^93 + 6.797e05 s^92
+ 7.534e05 s^91 + 2.509e07 s^90 + 2.654e07 s^89 + 7.109e08 s^88 + 7.177e08 s^87
+ 1.61e10 s^86 + 1.55e10 s^85 + 2.992e11 s^84 + 2.748e11 s^83 + 4.656e12 s^82
+ 4.075e12 s^81 + 6.154e13 s^80 + 5.131e13 s^79 + 6.987e14 s^78 + 5.546e14 s^77
+ 6.874e15 s^76 + 5.191e15 s^75 + 5.901e16 s^74 + 4.236e16 s^73 + 4.445e17 s^72

+ 3.03e17 s^71 + 2.951e18 s^70 + 1.908e18 s^69 + 1.732e19 s^68 + 1.062e19 s^67
+ 9.019e19 s^66 + 5.231e19 s^65 + 4.173e20 s^64 + 2.287e20 s^63 + 1.719e21 s^62
+ 8.887e20 s^61 + 6.306e21 s^60 + 3.071e21 s^59 + 2.063e22 s^58 + 9.445e21 s^57
+ 6.017e22 s^56 + 2.584e22 s^55 + 1.564e23 s^54 + 6.286e22 s^53 + 3.624e23 s^52
+ 1.359e23 s^51 + 7.47e23 s^50 + 2.606e23 s^49 + 1.368e24 s^48 + 4.425e23 s^47
+ 2.224e24 s^46 + 6.643e23 s^45 + 3.198e24 s^44 + 8.787e23 s^43 + 4.06e24 s^42
+ 1.021e24 s^41 + 4.536e24 s^40 + 1.039e24 s^39 + 4.442e24 s^38 + 9.203e23 s^37
+ 3.798e24 s^36 + 7.067e23 s^35 + 2.821e24 s^34 + 4.674e23 s^33 + 1.81e24 s^32
+ 2.643e23 s^31 + 9.969e23 s^30 + 1.266e23 s^29 + 4.678e23 s^28 + 5.086e22 s^27
+ 1.855e23 s^26 + 1.689e22 s^25 + 6.154e22 s^24 + 4.555e21 s^23 + 1.689e22 s^22
+ 9.719e20 s^21 + 3.788e21 s^20 + 1.576e20 s^19 + 6.831e20 s^18 + 1.791e19 s^17
+ 9.73e19 s^16 + 1.115e18 s^15 + 1.071e19 s^14 - 2.637e16 s^13 + 8.853e17 s^12
- 1.344e16 s^11 + 5.306e16 s^10 - 1.385e15 s^9 + 2.193e15 s^8 - 7.531e13 s^7
+ 5.801e13 s^6 - 2.245e12 s^5 + 8.699e11 s^4 - 3.254e10 s^3 + 5.891e09 s^2
- 1.669e08 s + 7.951e06

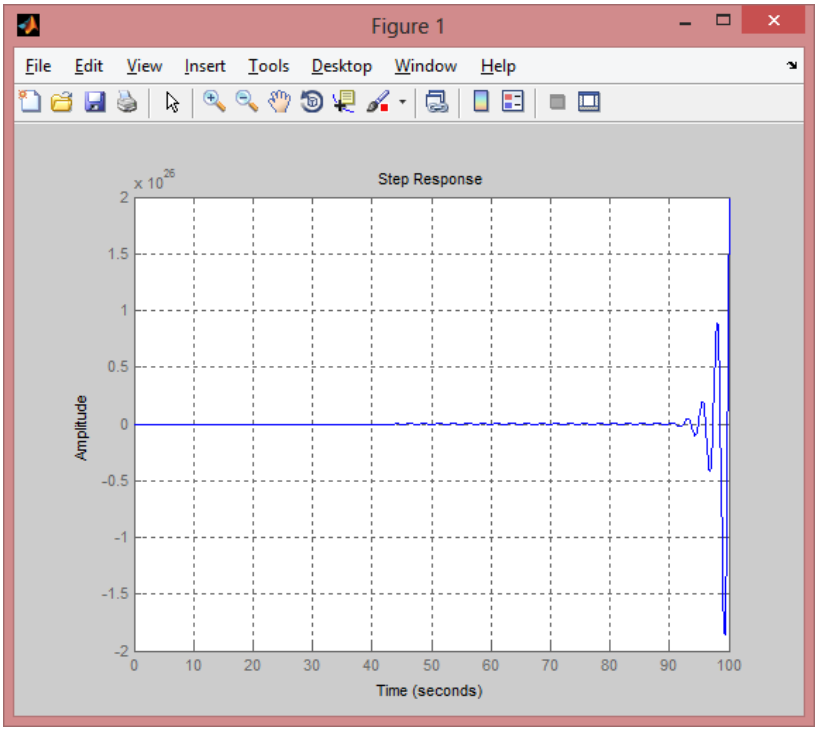

Figure 42: Step response (Level 3 - Linear)

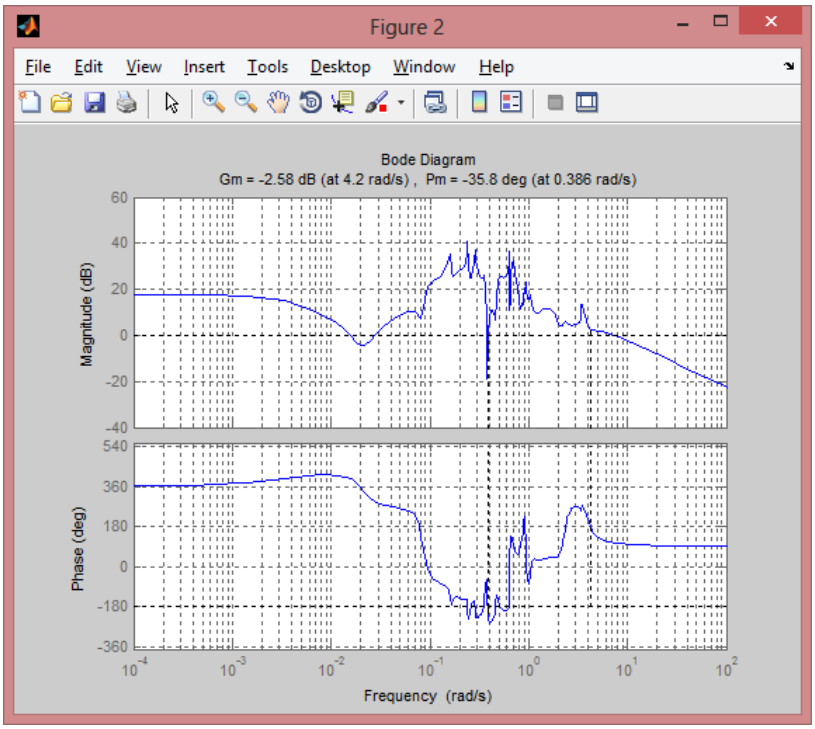

Figure 43: Bode plot (Level 3 - Linear)

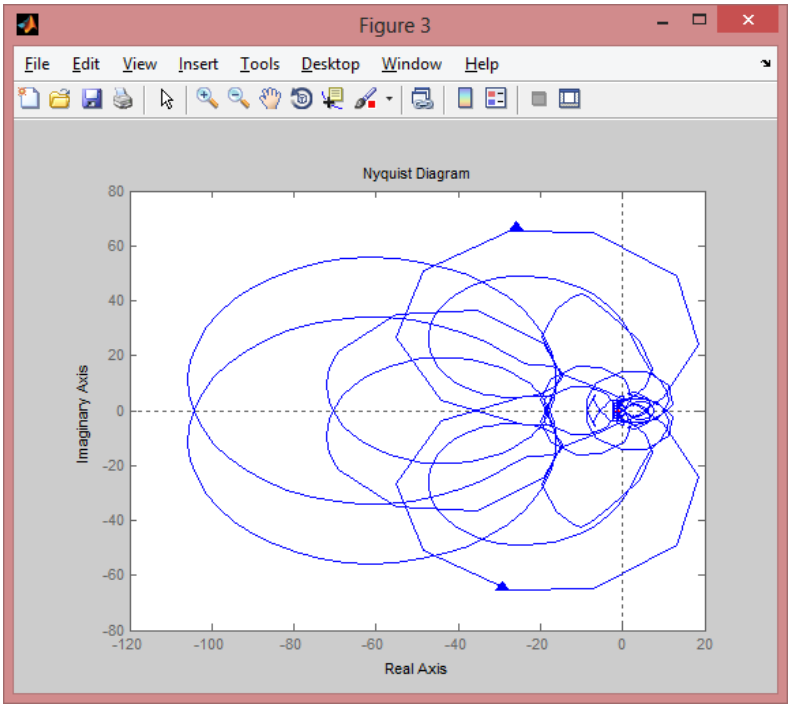

Figure 44: Nyquist plot (Level 3 - Linear)

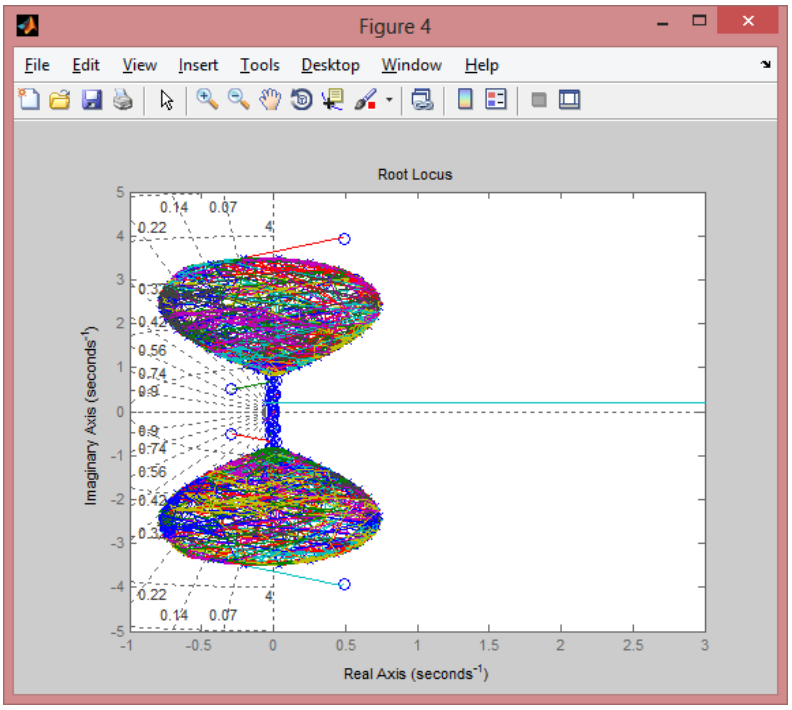

Figure 45: Root locus plot (Level 3 - Linear)

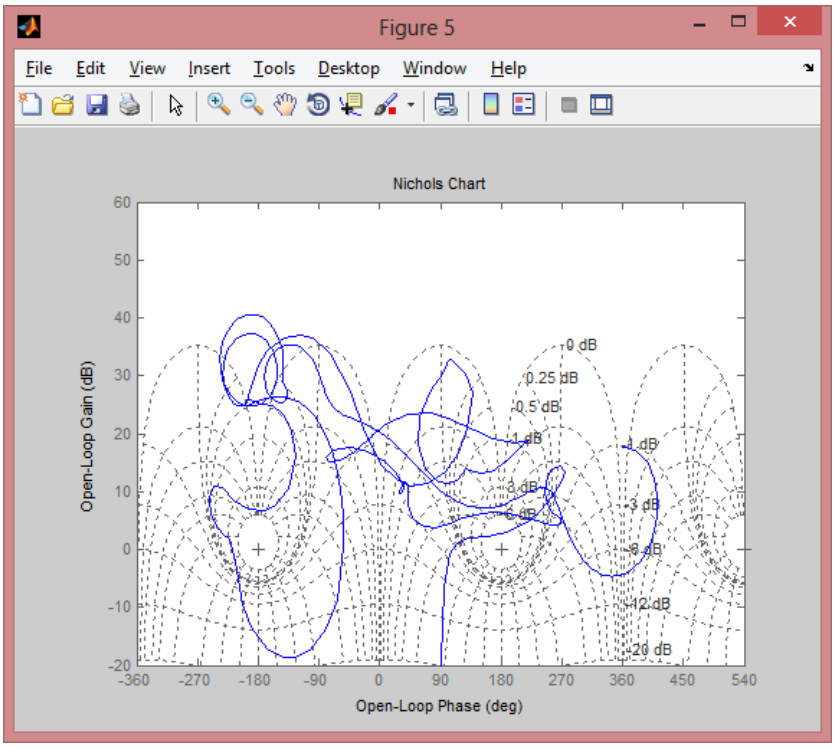

Figure 46: Nichols plot (Level 3 - Linear)

Level 4

ARX Model

Fit to estimation data: 99.27%

A(z) = 1 - 2.758 z^-1 + 3.035 z^-2 - 2.064 z^-3 + 1.673 z^-4 - 1.849 z^-5 + 1.945 z^-6
- 1.782 z^-7 + 1.309 z^-8 - 1.048 z^-9 + 1.472 z^-10 - 1.468 z^-11 + 0.9451 z^-12
- 1.004 z^-13 + 1.507 z^-14 - 1.924 z^-15 + 2.118 z^-16 - 2.071 z^-17 + 1.862 z^-18
- 1.568 z^-19 + 1.031 z^-20 - 0.6019 z^-21 + 0.6929 z^-22 - 0.8181 z^-23
+ 0.654 z^-24 - 0.2174 z^-25 - 0.3064 z^-26 + 0.614 z^-27 - 0.8178 z^-28
+ 1.136 z^-29 - 1.492 z^-30 + 1.829 z^-31 - 1.884 z^-32 + 1.787 z^-33 - 2.147 z^-34
+ 2.896 z^-35 - 3.023 z^-36 + 2.399 z^-37 - 1.913 z^-38 + 1.894 z^-39 - 2.003 z^-40
+ 2.307 z^-41 - 2.856 z^-42 + 3.272 z^-43 - 3.244 z^-44 + 2.828 z^-45 - 2.49 z^-46
+ 2.558 z^-47 - 2.9 z^-48 + 3.359 z^-49 - 3.683 z^-50 + 3.569 z^-51 - 3.028 z^-52
+ 2.433 z^-53 - 2.174 z^-54 + 2.219 z^-55 - 2.316 z^-56 + 2.501 z^-57 - 2.983 z^-58
+ 3.209 z^-59 - 2.71 z^-60 + 1.819 z^-61 - 1.106 z^-62 + 1.184 z^-63 - 1.929 z^-64
+ 2.578 z^-65 - 2.715 z^-66 + 2.367 z^-67 - 1.845 z^-68 + 1.54 z^-69 - 1.611 z^-70
+ 1.914 z^-71 - 2.078 z^-72 + 1.779 z^-73 - 1.369 z^-74 + 1.141 z^-75 - 0.7098 z^-76
+ 0.1316 z^-77 + 0.09247 z^-78 + 0.06408 z^-79 - 0.3258 z^-80 + 0.4397 z^
-81 - 0.3172 z^-82 + 0.2244 z^-83 - 0.2174 z^-84 + 0.08287 z^-85 - 0.02526 z^-86
+ 0.1566 z^-87 - 0.2311 z^-88 + 0.1242 z^-89 + 0.1454 z^-90 - 0.4831 z^-91
+ 0.6173 z^-92 - 0.3407 z^-93 + 0.03626 z^-94

B(z) = -0.3668 z^-1 + 1.55 z^-2 - 0.7461 z^-3 - 0.8526 z^-4 + 1.909 z^-5 - 0.9978 z^-6
- 0.4748 z^-7 - 0.2412 z^-8 - 0.3374 z^-9 - 0.1837 z^-10 - 0.1343 z^-11 - 0.3242 z^-12
+ 1.128 z^-13 - 0.6182 z^-14 + 0.09095 z^-15 - 0.7948 z^-16 + 1.472 z^-17
+ 1.356 z^-18 - 1.936 z^-19 + 1.004 z^-20 + 0.214 z^-21 - 0.3433 z^-22 - 0.645 z^-23
+ 2.492 z^-24 - 0.8257 z^-25 + 1.67 z^-26 - 2.906 z^-27 + 1.227 z^-28 + 0.9149 z^-29
- 0.9506 z^-30 + 0.2126 z^-31 + 1.154 z^-32 - 1.862 z^-33 + 1.239 z^-34 - 1.875 z^-35
+ 1.314 z^-36 - 1.946 z^-37 + 0.8336 z^-38 - 0.8039 z^-39 - 0.5104 z^-40
- 0.8709 z^-41 + 2.453 z^-42 - 1.881 z^-43 + 1.408 z^-44 - 1.466 z^-45 + 0.688 z^-46
- 1.176 z^-47 + 2.351 z^-48 - 1.743 z^-49 + 0.1432 z^-50 - 0.1788 z^-51 - 0.6493 z^-52
+ 0.7451 z^-53 + 1.339 z^-54 - 2.959 z^-55 + 2.914 z^-56 - 0.5988 z^-57 + 0.01981 z^-58
- 0.422 z^-59 + 1.742 z^-60 - 1.244 z^-61 + 0.3854 z^-62 - 0.01518 z^-63
- 0.5178 z^-64 + 0.5963 z^-65 - 0.03505 z^-66 + 1.668 z^-67 - 3.311 z^-68
- 0.1631 z^-69 + 2.427 z^-70 - 0.8458 z^-71 - 0.8302 z^-72 + 0.1821 z^-73
- 1.45 z^-74 + 1.908 z^-75 - 1.08 z^-76 + 1.485 z^-77 + 1.003 z^-78 + 0.08719 z^-79
- 2.628 z^-80 + 2.544 z^-81 - 0.6879 z^-82 + 1.074 z^-83 - 1.004 z^-84 + 1.398 z^-85
- 1.584 z^-86 + 0.3624 z^-87 - 1.084 z^-88 + 1.987 z^-89 + 0.08412 z^-90
- 1.193 z^-91 + 0.2706 z^-92 - 1.199 z^-93 + 0.7303 z^-94

Transfer model in z transform

-0.3668 z^-1 + 1.55 z^-2 - 0.7461 z^-3 - 0.8526 z^-4 + 1.909 z^-5 - 0.9978 z^
-6 - 0.4748 z^-7 - 0.2412 z^-8 - 0.3374 z^-9 - 0.1837 z^-10 - 0.1343 z^-11
- 0.3242 z^-12 + 1.128 z^-13 - 0.6182 z^-14 + 0.09095 z^-15 - 0.7948 z^-16
+ 1.472 z^-17 + 1.356 z^-18 - 1.936 z^-19 + 1.004 z^-20 + 0.214 z^-21
- 0.3433 z^-22 - 0.645 z^-23 + 2.492 z^-24 - 0.8257 z^-25 + 1.67 z^-26
- 2.906 z^-27 + 1.227 z^-28 + 0.9149 z^-29 - 0.9506 z^-30 + 0.2126 z^
-31 + 1.154 z^-32 - 1.862 z^-33 + 1.239 z^-34 - 1.875 z^-35 + 1.314 z^-36
- 1.946 z^-37 + 0.8336 z^-38 - 0.8039 z^-39 - 0.5104 z^-40 - 0.8709 z^-41
+ 2.453 z^-42 - 1.881 z^-43 + 1.408 z^-44 - 1.466 z^-45 + 0.688 z^-46
- 1.176 z^-47 + 2.351 z^-48 - 1.743 z^-49 + 0.1432 z^-50 - 0.1788 z^-51
- 0.6493 z^-52 + 0.7451 z^-53 + 1.339 z^-54 - 2.959 z^-55 + 2.914 z^-56
- 0.5988 z^-57 + 0.01981 z^-58 - 0.422 z^-59 + 1.742 z^-60 - 1.244 z^
-61 + 0.3854 z^-62 - 0.01518 z^-63 - 0.5178 z^-64 + 0.5963 z^-65 - 0.03505 z^-66

+ 1.668 z^-67 - 3.311 z^-68 - 0.1631 z^-69 + 2.427 z^-70 - 0.8458 z^-71
- 0.8302 z^-72 + 0.1821 z^-73 - 1.45 z^-74 + 1.908 z^-75 - 1.08 z^-76
+ 1.485 z^-77 + 1.003 z^-78 + 0.08719 z^-79 - 2.628 z^-80 + 2.544 z^-81
- 0.6879 z^-82 + 1.074 z^-83 - 1.004 z^-84 + 1.398 z^-85 - 1.584 z^-86
+ 0.3624 z^-87 - 1.084 z^-88 + 1.987 z^-89 + 0.08412 z^-90 - 1.193 z^
-91 + 0.2706 z^-92 - 1.199 z^-93 + 0.7303 z^-94

---

1 - 2.758 z^-1 + 3.035 z^-2 - 2.064 z^-3 + 1.673 z^-4 - 1.849 z^-5 + 1.945 z^
-6 - 1.782 z^-7 + 1.309 z^-8 - 1.048 z^-9 + 1.472 z^-10 - 1.468 z^-11
+ 0.9451 z^-12 - 1.004 z^-13 + 1.507 z^-14 - 1.924 z^-15 + 2.118 z^-16
- 2.071 z^-17 + 1.862 z^-18 - 1.568 z^-19 + 1.031 z^-20 - 0.6019 z^-21
+ 0.6929 z^-22 - 0.8181 z^-23 + 0.654 z^-24 - 0.2174 z^-25 - 0.3064 z^-26
+ 0.614 z^-27 - 0.8178 z^-28 + 1.136 z^-29 - 1.492 z^-30 + 1.829 z^-31
- 1.884 z^-32 + 1.787 z^-33 - 2.147 z^-34 + 2.896 z^-35 - 3.023 z^-36
+ 2.399 z^-37 - 1.913 z^-38 + 1.894 z^-39 - 2.003 z^-40 + 2.307 z^-41
- 2.856 z^-42 + 3.272 z^-43 - 3.244 z^-44 + 2.828 z^-45 - 2.49 z^-46
+ 2.558 z^-47 - 2.9 z^-48 + 3.359 z^-49 - 3.683 z^-50 + 3.569 z^-51 - 3.028 z^-52
+ 2.433 z^-53 - 2.174 z^-54 + 2.219 z^-55 - 2.316 z^-56 + 2.501 z^-57
- 2.983 z^-58 + 3.209 z^-59 - 2.71 z^-60 + 1.819 z^-61 - 1.106 z^-62
+ 1.184 z^-63 - 1.929 z^-64 + 2.578 z^-65 - 2.715 z^-66 + 2.367 z^-67
- 1.845 z^-68 + 1.54 z^-69 - 1.611 z^-70 + 1.914 z^-71 - 2.078 z^-72
+ 1.779 z^-73 - 1.369 z^-74 + 1.141 z^-75 - 0.7098 z^-76 + 0.1316 z^-77
+ 0.09247 z^-78 + 0.06408 z^-79 - 0.3258 z^-80 + 0.4397 z^-81 - 0.3172 z^-82
+ 0.2244 z^-83 - 0.2174 z^-84 + 0.08287 z^-85 - 0.02526 z^-86 + 0.1566 z^-87
- 0.2311 z^-88 + 0.1242 z^-89 + 0.1454 z^-90 - 0.4831 z^-91 + 0.6173 z^-92
- 0.3407 z^-93 + 0.03626 z^-94

Transfer model in s transform

-4.038 s^95 + 1.503 s^94 - 635.5 s^93 + 244.3 s^92 - 4.807e04 s^91 + 1.904e04 s^90
- 2.328e06 s^89 + 9.486e05 s^88 - 8.113e07 s^87 + 3.395e07 s^86 - 2.168e09 s^85
+ 9.299e08 s^84 - 4.62e10 s^83 + 2.03e10 s^82 - 8.069e11 s^81 + 3.627e11 s^80
- 1.177e13 s^79 + 5.41e12 s^78 - 1.456e14 s^77 + 6.836e13 s^76 - 1.544e15 s^75
+ 7.398e14 s^74 - 1.415e16 s^73 + 6.916e15 s^72 - 1.128e17 s^71 + 5.624e16 s^70
- 7.868e17 s^69 + 3.999e17 s^68 - 4.82e18 s^67 + 2.497e18 s^66 - 2.602e19 s^65
+ 1.374e19 s^64 - 1.24e20 s^63 + 6.673e19 s^62 - 5.231e20 s^61 + 2.868e20 s^60
- 1.954e21 s^59 + 1.092e21 s^58 - 6.463e21 s^57 + 3.685e21 s^56 - 1.894e22 s^55
+ 1.102e22 s^54 - 4.911e22 s^53 + 2.92e22 s^52 - 1.125e23 s^51 + 6.851e22 s^50
- 2.275e23 s^49 + 1.421e23 s^48 - 4.043e23 s^47 + 2.601e23 s^46 - 6.295e23 s^45
+ 4.194e23 s^44 - 8.542e23 s^43 + 5.937e23 s^42 - 1.003e24 s^41 + 7.357e23 s^40
- 1.011e24 s^39 + 7.949e23 s^38 - 8.607e23 s^37 + 7.454e23 s^36 - 6.057e23 s^35
+ 6.034e23 s^34 - 3.373e23 s^33 + 4.189e23 s^32 - 1.333e23 s^31 + 2.475e23 s^30
- 2.127e22 s^29 + 1.233e23 s^28 + 1.753e22 s^27 + 5.117e22 s^26 + 1.904e22 s^25
+ 1.742e22 s^24 + 1.068e22 s^23 + 4.755e21 s^22 + 4.198e21 s^21 + 1.006e21 s^20
+ 1.23e21 s^19 + 1.548e20 s^18 + 2.713e20 s^17 + 1.473e19 s^16 + 4.456e19 s^15
+ 2.436e17 s^14 + 5.308e18 s^13 - 1.568e17 s^12 + 4.394e17 s^11 - 2.39e16 s^10
+ 2.365e16 s^9 - 1.623e15 s^8 + 7.455e14 s^7 - 4.891e13 s^6 + 1.181e13 s^5
- 2.534e11 s^4 + 8.3e10 s^3 + 8.379e09 s^2 - 8.336e07 s + 5.907e06

---

s^96 + 3.445 s^95 + 162.3 s^94 + 541.5 s^93 + 1.266e04 s^92 + 4.09e04 s^91 + 6.319e05 s^90
+ 1.977e06 s^89 + 2.269e07 s^88 + 6.879e07 s^87 + 6.244e08 s^86 + 1.835e09 s^85
+ 1.371e10 s^84 + 3.902e10 s^83 + 2.465e11 s^82 + 6.803e11 s^81 + 3.705e12 s^80
+ 9.908e12 s^79 + 4.72e13 s^78 + 1.223e14 s^77 + 5.153e14 s^76 + 1.294e15 s^75
+ 4.865e15 s^74 + 1.184e16 s^73 + 3.998e16 s^72 + 9.428e16 s^71 + 2.876e17 s^70
+ 6.569e17 s^69 + 1.818e18 s^68 + 4.022e18 s^67 + 1.014e19 s^66 + 2.171e19 s^65
+ 4.997e19 s^64 + 1.036e20 s^63 + 2.182e20 s^62 + 4.378e20 s^61 + 8.455e20 s^60

+ 1.641e21 s^59 + 2.908e21 s^58 + 5.456e21 s^57 + 8.883e21 s^56 + 1.611e22 s^55
+ 2.409e22 s^54 + 4.221e22 s^53 + 5.8e22 s^52 + 9.813e22 s^51 + 1.238e23 s^50
+ 2.022e23 s^49 + 2.34e23 s^48 + 3.685e23 s^47 + 3.908e23 s^46 + 5.935e23 s^45
+ 5.756e23 s^44 + 8.423e23 s^43 + 7.454e23 s^42 + 1.051e24 s^41 + 8.461e23 s^40
+ 1.148e24 s^39 + 8.385e23 s^38 + 1.094e24 s^37 + 7.222e23 s^36 + 9.06e23 s^35
+ 5.378e23 s^34 + 6.484e23 s^33 + 3.442e23 s^32 + 3.986e23 s^31 + 1.88e23 s^30
+ 2.09e23 s^29 + 8.686e22 s^28 + 9.274e22 s^27 + 3.365e22 s^26 + 3.45e22 s^25
+ 1.081e22 s^24 + 1.064e22 s^23 + 2.838e21 s^22 + 2.685e21 s^21 + 6.002e20 s^20
+ 5.46e20 s^19 + 1.003e20 s^18 + 8.786e19 s^17 + 1.296e19 s^16 + 1.094e19 s^15
+ 1.261e18 s^14 + 1.024e18 s^13 + 8.969e16 s^12 + 6.972e16 s^11 + 4.516e15 s^10
+ 3.29e15 s^9 + 1.554e14 s^8 + 1.008e14 s^7 + 3.489e12 s^6 + 1.81e12 s^5
+ 4.712e10 s^4 + 1.614e10 s^3 + 3.448e08 s^2 + 5.614e07 s + 8.413e05

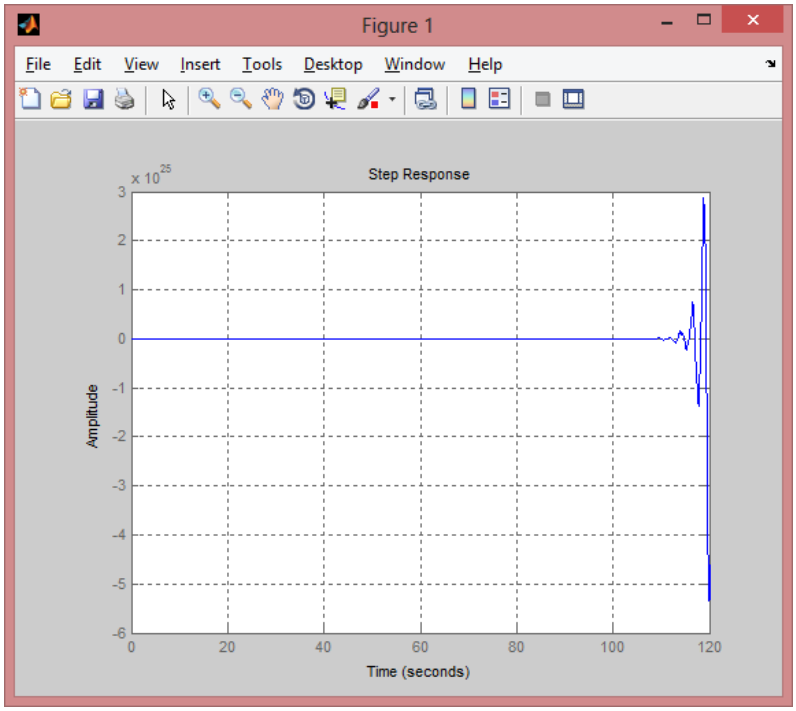

Figure 47: Step response (Level 4 - Linear)

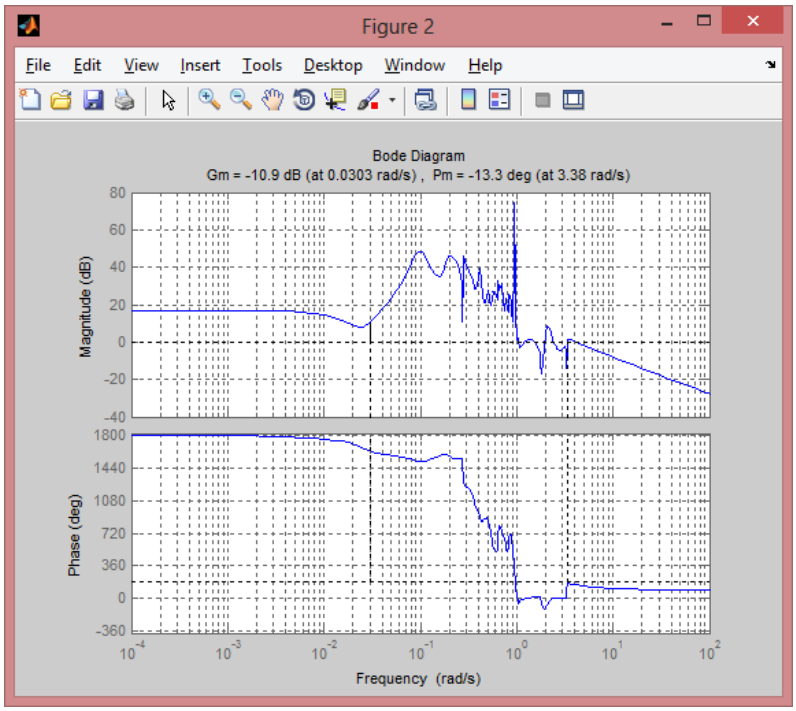

Figure 48: Bode plot (Level 4 - Linear)

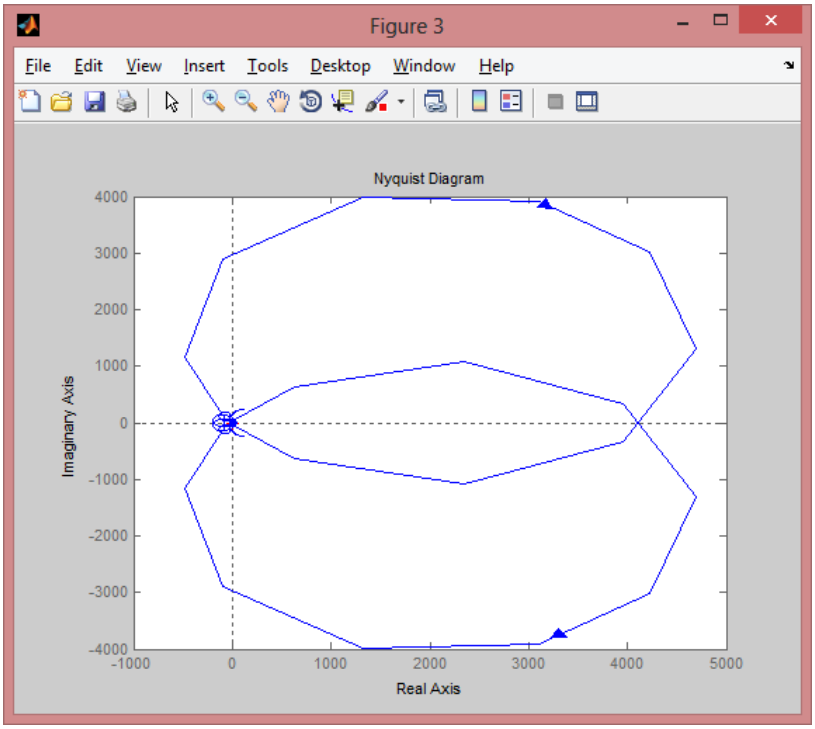

Figure 49: Nyquist plot (Level 4 - Linear)

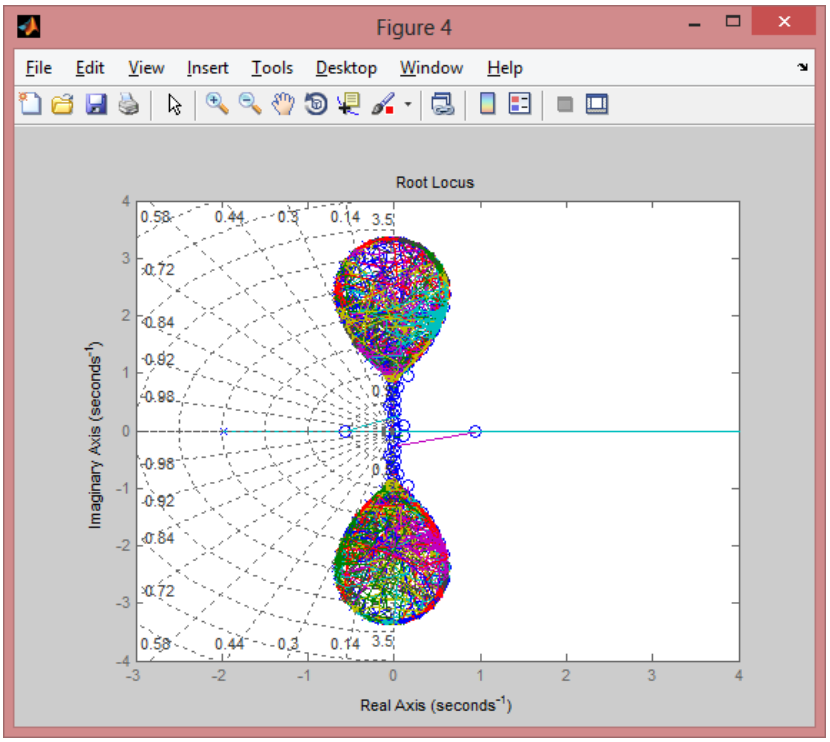

Figure 50: Root locus plot (Level 4 - Linear)

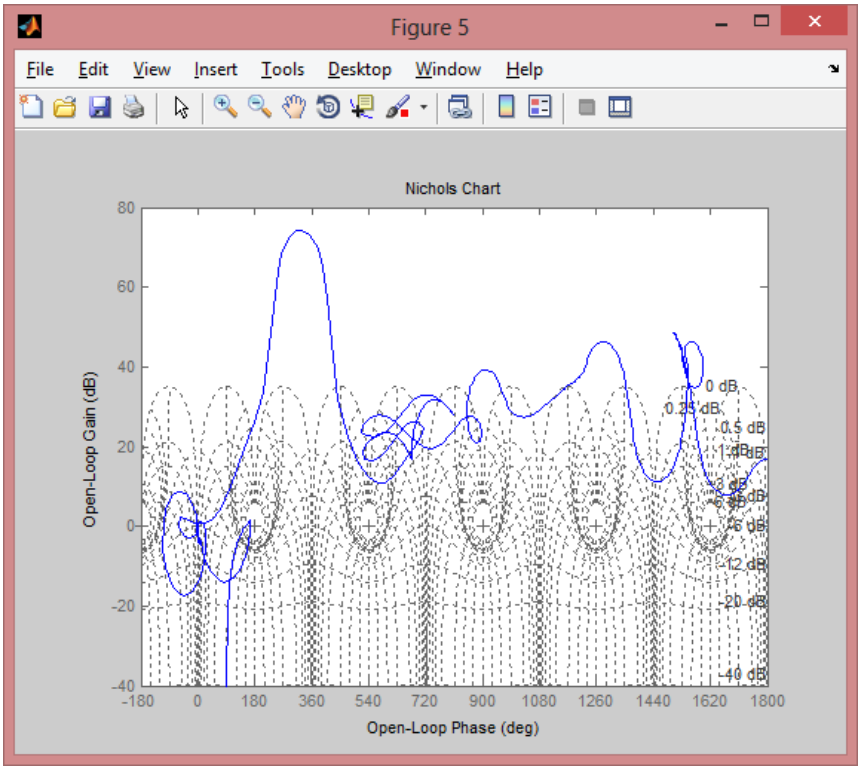

Figure 51: Nichols plot (Level 4 - Linear)

Flow 1

ARX Model

Fit to estimation data: 91.16%

A(z) = 1 - 0.7942 z^-1 + 0.744 z^-2 - 0.5596 z^-3 + 0.6528 z^-4 - 0.2351 z^-5 - 0.02419 z^-6
+ 0.5431 z^-7 - 0.5036 z^-8 + 0.1467 z^-9 - 0.1201 z^-10 + 0.3908 z^-11 - 0.3557 z^-12
+ 0.2089 z^-13 - 0.3731 z^-14 + 0.2633 z^-15 - 0.4104 z^-16 + 0.5862 z^-17
- 0.0402 z^-18 - 0.07447 z^-19 + 0.01548 z^-20 + 0.1038 z^-21 - 0.2137 z^
-22 + 0.3335 z^-23 - 0.4779 z^-24 + 0.3363 z^-25 - 0.5622 z^-26 + 0.4093 z^-27
+ 0.0455 z^-28 - 0.4577 z^-29 + 0.04848 z^-30 + 0.02371 z^-31 + 0.1465 z^
-32 - 0.08332 z^-33 + 0.03335 z^-34 + 0.1626 z^-35 - 0.7028 z^-36 + 0.2039 z^-37
- 0.04858 z^-38 - 0.08626 z^-39 + 0.02029 z^-40 - 0.1712 z^-41 + 0.09656 z^-42
- 0.2567 z^-43 + 0.2669 z^-44 - 0.2123 z^-45 + 0.1526 z^-46 - 0.5805 z^-47
+ 0.5119 z^-48 - 0.4808 z^-49 + 0.2926 z^-50 - 0.3213 z^-51 + 0.54 z^-52
- 0.08684 z^-53 - 0.1147 z^-54 + 0.4472 z^-55 - 0.4788 z^-56 + 0.2959 z^-57
- 0.09558 z^-58 + 0.3138 z^-59 - 0.1883 z^-60 + 0.2951 z^-61 + 0.0559 z^-62
- 0.05072 z^-63 - 0.2795 z^-64 + 0.2624 z^-65 - 0.2488 z^-66 + 0.2059 z^-67
- 0.3904 z^-68 + 0.4495 z^-69 - 0.5329 z^-70 + 0.2941 z^-71 - 0.02337 z^-72
+ 0.1742 z^-73 - 0.2255 z^-74 - 0.2982 z^-75 + 0.2465 z^-76 - 0.04078 z^-77
+ 0.2086 z^-78 - 0.0893 z^-79 + 0.3988 z^-80 - 0.6076 z^-81 + 0.5509 z^-82
- 0.843 z^-83 + 0.5156 z^-84 - 0.4791 z^-85 + 0.4477 z^-86 - 0.1286 z^-87
+ 0.044 z^-88 + 0.2722 z^-89 - 0.3096 z^-90 + 0.01944 z^-91 - 0.1473 z^-92
+ 0.1167 z^-93 + 0.1635 z^-94 - 0.3025 z^-95 + 0.636 z^-96 - 0.3552 z^-97
+ 0.3592 z^-98 - 0.3699 z^-99

B(z) = -0.8872 z^-1 + 3.884 z^-2 + 5.149 z^-3 + 0.009992 z^-4 - 0.07676 z^-5 - 3.838 z^-6
+ 1.701 z^-7 - 3.046 z^-8 - 0.5509 z^-9 + 4.936 z^-10 - 2.9 z^-11 - 4.089 z^-12
+ 2.949 z^-13 - 0.9717 z^-14 + 1.018 z^-15 - 2.043 z^-16 + 2.241 z^-17 - 0.3241 z^-18
- 7.428 z^-19 + 5.783 z^-20 + 4.171 z^-21 - 0.8533 z^-22 - 6.643 z^-23 + 2.703 z^-24
- 1.75 z^-25 + 1.053 z^-26 - 7.253 z^-27 + 14.35 z^-28 - 12 z^-29 + 8.958 z^-30
- 8.743 z^-31 + 0.5068 z^-32 - 2.254 z^-33 + 7.097 z^-34 - 0.3167 z^-35 - 0.246 z^-36
+ 1.21 z^-37 + 3.863 z^-38 - 7.633 z^-39 + 2.285 z^-40 - 0.9063 z^-41 - 4.386 z^-42
- 0.4647 z^-43 - 0.4604 z^-44 + 8.371 z^-45 - 3.813 z^-46 - 1.648 z^-47 + 2.952 z^-48
+ 5.914 z^-49 - 5.086 z^-50 + 1.761 z^-51 - 4.105 z^-52 - 3.321 z^-53 - 1.233 z^-54
+ 7.813 z^-55 + 1.073 z^-56 + 6.068 z^-57 - 4.292 z^-58 - 1.707 z^-59 - 4.052 z^-60
+ 0.148 z^-61 + 4.24 z^-62 - 6.742 z^-63 + 8.002 z^-64 - 2.682 z^-65 + 1.418 z^-66
- 5.139 z^-67 + 0.7784 z^-68 + 1.955 z^-69 - 4.887 z^-70 - 2.636 z^-71 + 9.958 z^-72
- 8.916 z^-73 + 7.382 z^-74 + 0.1719 z^-75 + 2.864 z^-76 - 0.7472 z^-77 - 7.423 z^-78
+ 2.131 z^-79 - 1.446 z^-80 - 3.829 z^-81 + 8.958 z^-82 - 0.403 z^-83 + 5.397 z^-84
- 5.929 z^-85 - 0.4922 z^-86 - 6.207 z^-87 - 4.617 z^-88 + 9.575 z^-89 - 3.152 z^-90
+ 5.488 z^-91 - 2.912 z^-92 + 1.584 z^-93 + 1.752 z^-94 + 1.156 z^-95 - 2.686 z^-96
- 2.018 z^-97 - 4.747 z^-98 + 6.96 z^-99

Transfer model in z transform

-1.24 z^-1 + 5.957 z^-2 + 6.112 z^-3 - 1.244 z^-4 + 1.748 z^-5 - 4.316 z^-6
- 0.884 z^-7 + 1.981 z^-8 - 0.9048 z^-9 + 1.914 z^-10 + 0.9065 z^-11
- 4.908 z^-12 - 0.1253 z^-13 + 1.252 z^-14 + 0.9728 z^-15 - 2.403 z^-16
+ 0.1791 z^-17 + 0.5952 z^-18 - 6.893 z^-19 + 5.385 z^-20 + 6.553 z^-21
- 1.349 z^-22 - 3.49 z^-23 - 3.205 z^-24 - 2.23 z^-25 + 4.559 z^
-26 - 8.062 z^-27 + 8.094 z^-28 - 2.959 z^-29 + 0.2357 z^-30 - 4.673 z^-31
+ 2.802 z^-32 - 1.925 z^-33 - 0.721 z^-34 + 5.783 z^-35 - 3.756 z^-36
- 2.946 z^-37 + 8.047 z^-38 - 3.804 z^-39 - 3.586 z^-40 + 0.9866 z^-41

- 2.314 z^-42 - 1.526 z^-43 - 3.154 z^-44 + 8.461 z^-45 + 2.011 z^-46
- 5.654 z^-47 - 0.1161 z^-48 + 8.444 z^-49 - 2.538 z^-50 - 3.679 z^-51
+ 0.3106 z^-52 - 3.959 z^-53 - 4.762 z^-54 + 8.042 z^-55 + 5.737 z^-56
+ 2.744 z^-57 - 2.005 z^-58 - 1.663 z^-59 - 2.974 z^-60 - 1.114 z^-61
+ 3.935 z^-62 - 4.342 z^-63 + 3.996 z^-64 - 1.694 z^-65 + 2.55 z^-66
- 0.5279 z^-67 - 4.66 z^-68 + 3.142 z^-69 - 4.236 z^-70 - 7.231 z^-71
+ 8.871 z^-72 - 2.02 z^-73 + 1.487 z^-74 + 2.449 z^-75 + 2.378 z^-76
+ 2.335 z^-77 - 8.252 z^-78 - 1.67 z^-79 + 1.133 z^-80 - 3.411 z^-81
+ 6.222 z^-82 + 3.931 z^-83 + 5.612 z^-84 - 8.628 z^-85 - 3.032 z^-86
+ 0.6706 z^-87 - 7.118 z^-88 + 4.808 z^-89 + 1.167 z^-90 + 1.08 z^-91
- 2.843 z^-92 + 1.981 z^-93 + 6.818 z^-94 - 0.4828 z^-95 - 2.931 z^-96
+ 0.09127 z^-97 - 9.205 z^-98 + 0.5413 z^-99 + 9.492 z^-100

---

1 - 0.5453 z^-1 + 0.4684 z^-2 - 0.1144 z^-3 + 0.2907 z^-4 + 0.3072 z^-5
- 0.05758 z^-6 + 0.3838 z^-7 - 0.1929 z^-8 + 0.1256 z^-9 - 0.1204 z^-10
+ 0.4019 z^-11 - 0.02635 z^-12 - 0.1255 z^-13 - 0.2041 z^-14 + 0.2812 z^-15
- 0.2857 z^-16 + 0.4089 z^-17 + 0.3576 z^-18 - 0.3339 z^-19 + 0.0052 z^-20
+ 0.2878 z^-21 - 0.1531 z^-22 + 0.183 z^-23 - 0.2386 z^-24 + 0.1453 z^-25
- 0.2341 z^-26 + 0.06636 z^-27 + 0.3253 z^-28 - 0.3475 z^-29 - 0.1312 z^-30
- 0.1659 z^-31 + 0.2884 z^-32 - 0.0531 z^-33 - 0.3453 z^-34 + 0.4209 z^-35
- 0.639 z^-36 - 0.3194 z^-37 + 0.2516 z^-38 + 0.01549 z^-39 - 0.2534 z^-40
- 0.2556 z^-41 + 0.1601 z^-42 - 0.2492 z^-43 + 0.07459 z^-44 + 0.003714 z^-45
- 0.096 z^-46 - 0.5022 z^-47 + 0.2102 z^-48 - 0.2933 z^-49 + 0.1825 z^-50
- 0.3087 z^-51 + 0.1145 z^-52 + 0.2761 z^-53 - 0.3061 z^-54 + 0.2572 z^-55
- 0.1177 z^-56 + 0.02109 z^-57 - 0.1625 z^-58 + 0.363 z^-59 + 0.06703 z^-60
+ 0.0268 z^-61 + 0.1807 z^-62 + 0.1088 z^-63 - 0.3225 z^-64 + 0.04343 z^-65
+ 0.0823 z^-66 + 0.05098 z^-67 - 0.4994 z^-68 + 0.3183 z^-69 - 0.1259 z^-70
+ 0.001928 z^-71 + 0.02048 z^-72 + 0.1278 z^-73 - 0.08229 z^-74
- 0.56 z^-75 + 0.207 z^-76 + 0.2088 z^-77 + 0.01815 z^-78 + 0.07659 z^-79
+ 0.4943 z^-80 - 0.5999 z^-81 + 0.1748 z^-82 - 0.3473 z^-83 + 0.1868 z^-84
- 0.1729 z^-85 - 0.0114 z^-86 + 0.1449 z^-87 - 0.1107 z^-88 + 0.22 z^-89
- 0.216 z^-90 + 0.1128 z^-91 - 0.3174 z^-92 - 0.002813 z^-93 + 0.2851 z^-94
- 0.3797 z^-95 + 0.3891 z^-96 + 0.0663 z^-97 + 0.1734 z^-98 - 0.2306 z^-99

Transfer model in s transform

7.254 s^98 - 21.62 s^97 + 1159 s^96 - 3355 s^95 + 8.907e04 s^94 - 2.506e05 s^93
+ 4.392e06 s^92 - 1.2e07 s^91 + 1.561e08 s^90 - 4.137e08 s^89 + 4.262e09 s^88
- 1.095e10 s^87 + 9.305e10 s^86 - 2.317e11 s^85 + 1.669e12 s^84 - 4.02e12 s^83
+ 2.506e13 s^82 - 5.838e13 s^81 + 3.2e14 s^80 - 7.198e14 s^79 + 3.513e15 s^78
- 7.618e15 s^77 + 3.344e16 s^76 - 6.982e16 s^75 + 2.78e17 s^74 - 5.578e17 s^73
+ 2.03e18 s^72 - 3.906e18 s^71 + 1.308e19 s^70 - 2.408e19 s^69 + 7.457e19 s^68
- 1.311e20 s^67 + 3.776e20 s^66 - 6.323e20 s^65 + 1.701e21 s^64 - 2.705e21 s^63
+ 6.831e21 s^62 - 1.028e22 s^61 + 2.447e22 s^60 - 3.474e22 s^59 + 7.829e22 s^58
- 1.044e23 s^57 + 2.237e23 s^56 - 2.789e23 s^55 + 5.707e23 s^54 - 6.62e23 s^53
+ 1.3e24 s^52 - 1.395e24 s^51 + 2.64e24 s^50 - 2.604e24 s^49 + 4.775e24 s^48
- 4.298e24 s^47 + 7.681e24 s^46 - 6.255e24 s^45 + 1.096e25 s^44 - 7.999e24 s^43
+ 1.385e25 s^42 - 8.952e24 s^41 + 1.545e25 s^40 - 8.723e24 s^39 + 1.516e25 s^38
- 7.354e24 s^37 + 1.303e25 s^36 - 5.321e24 s^35 + 9.764e24 s^34 - 3.271e24 s^33
+ 6.347e24 s^32 - 1.684e24 s^31 + 3.556e24 s^30 - 7.122e23 s^29 + 1.705e24 s^28
- 2.391e23 s^27 + 6.94e23 s^26 - 5.962e22 s^25 + 2.374e23 s^24 - 9.03e21 s^23
+ 6.744e22 s^22 + 1.846e20 s^21 + 1.57e22 s^20 + 5.626e20 s^19 + 2.945e21 s^18
+ 1.789e20 s^17 + 4.359e20 s^16 + 3.365e19 s^15 + 4.96e19 s^14 + 4.223e18 s^13
+ 4.191e18 s^12 + 3.562e17 s^11 + 2.509e17 s^10 + 1.946e16 s^9 + 9.948e15 s^8
+ 6.367e14 s^7 + 2.352e14 s^6 + 1.071e13 s^5 + 2.752e12 s^4 + 6.411e10 s^3
+ 1.003e10 s^2 - 9.016e06 s + 1.798e06

---

s^99 + 0.9946 s^98 + 161 s^97 + 157.1 s^96 + 1.249e04 s^95 + 1.194e04 s^94 + 6.22e05 s^93
+ 5.826e05 s^92 + 2.234e07 s^91 + 2.049e07 s^90 + 6.166e08 s^89 + 5.535e08 s^88
+ 1.362e10 s^87 + 1.196e10 s^86 + 2.472e11 s^85 + 2.122e11 s^84 + 3.761e12 s^83
+ 3.154e12 s^82 + 4.868e13 s^81 + 3.985e13 s^80 + 5.42e14 s^79 + 4.328e14 s^78
+ 5.236e15 s^77 + 4.077e15 s^76 + 4.421e16 s^75 + 3.354e16 s^74 + 3.28e17 s^73
+ 2.424e17 s^72 + 2.149e18 s^71 + 1.545e18 s^70 + 1.247e19 s^69 + 8.717e18 s^68
+ 6.428e19 s^67 + 4.368e19 s^66 + 2.951e20 s^65 + 1.947e20 s^64 + 1.208e21 s^63
+ 7.737e20 s^62 + 4.418e21 s^61 + 2.743e21 s^60 + 1.443e22 s^59 + 8.685e21 s^58
+ 4.215e22 s^57 + 2.456e22 s^56 + 1.1e23 s^55 + 6.204e22 s^54 + 2.565e23 s^53
+ 1.399e23 s^52 + 5.34e23 s^51 + 2.814e23 s^50 + 9.91e23 s^49 + 5.045e23 s^48
+ 1.637e24 s^47 + 8.046e23 s^46 + 2.403e24 s^45 + 1.139e24 s^44 + 3.127e24 s^43
+ 1.43e24 s^42 + 3.596e24 s^41 + 1.585e24 s^40 + 3.644e24 s^39 + 1.547e24 s^38
+ 3.241e24 s^37 + 1.325e24 s^36 + 2.519e24 s^35 + 9.909e23 s^34 + 1.702e24 s^33
+ 6.441e23 s^32 + 9.947e23 s^31 + 3.617e23 s^30 + 4.991e23 s^29 + 1.743e23 s^28
+ 2.134e23 s^27 + 7.148e22 s^26 + 7.706e22 s^25 + 2.471e22 s^24 + 2.325e22 s^23
+ 7.122e21 s^22 + 5.789e21 s^21 + 1.688e21 s^20 + 1.172e21 s^19 + 3.237e20 s^18
+ 1.894e20 s^17 + 4.919e19 s^16 + 2.39e19 s^15 + 5.777e18 s^14 + 2.289e18 s^13
+ 5.071e17 s^12 + 1.602e17 s^11 + 3.184e16 s^10 + 7.798e15 s^9 + 1.344e15 s^8
+ 2.457e14 s^7 + 3.473e13 s^6 + 4.483e12 s^5 + 4.681e11 s^4 + 3.841e10 s^3
+ 2.279e09 s^2 + 7.334e07 s + 4.898e05

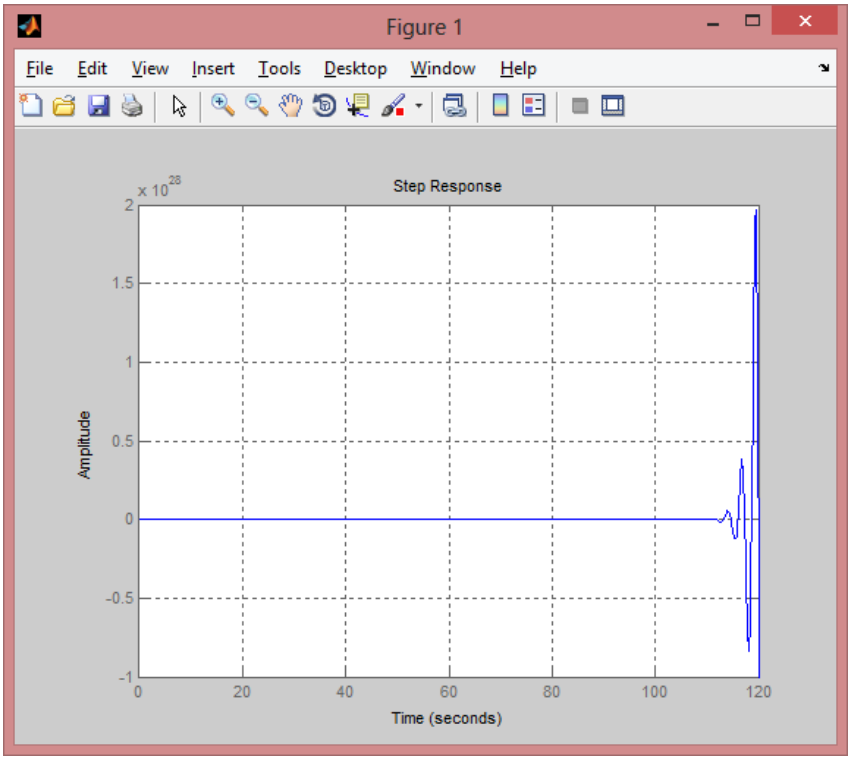

Figure 52: Step response (Flow 1 - Linear)

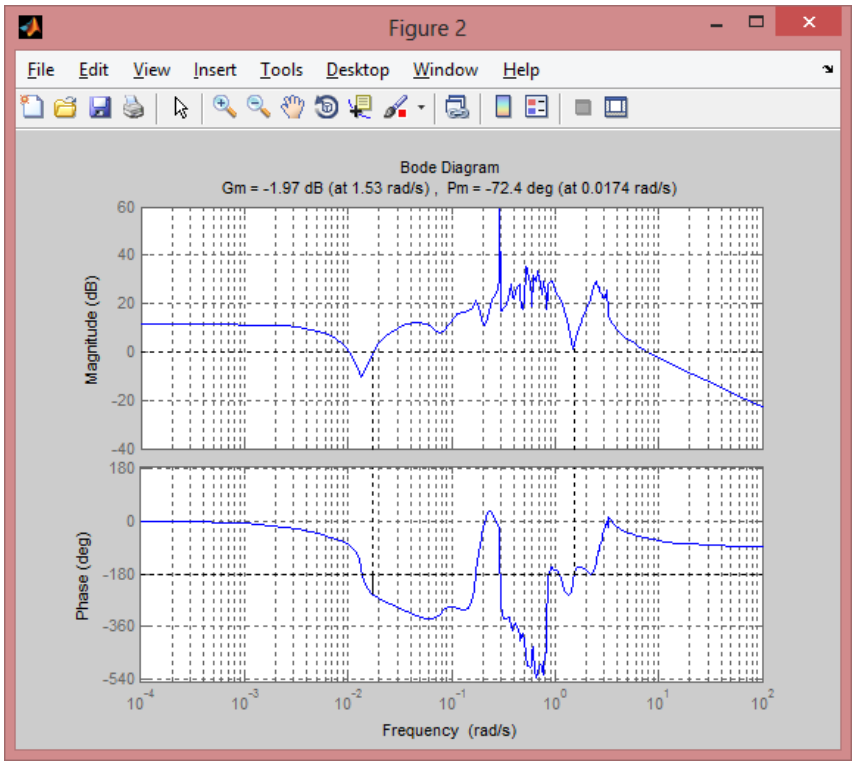

Figure 53: Bode plot (Flow 1 - Linear)

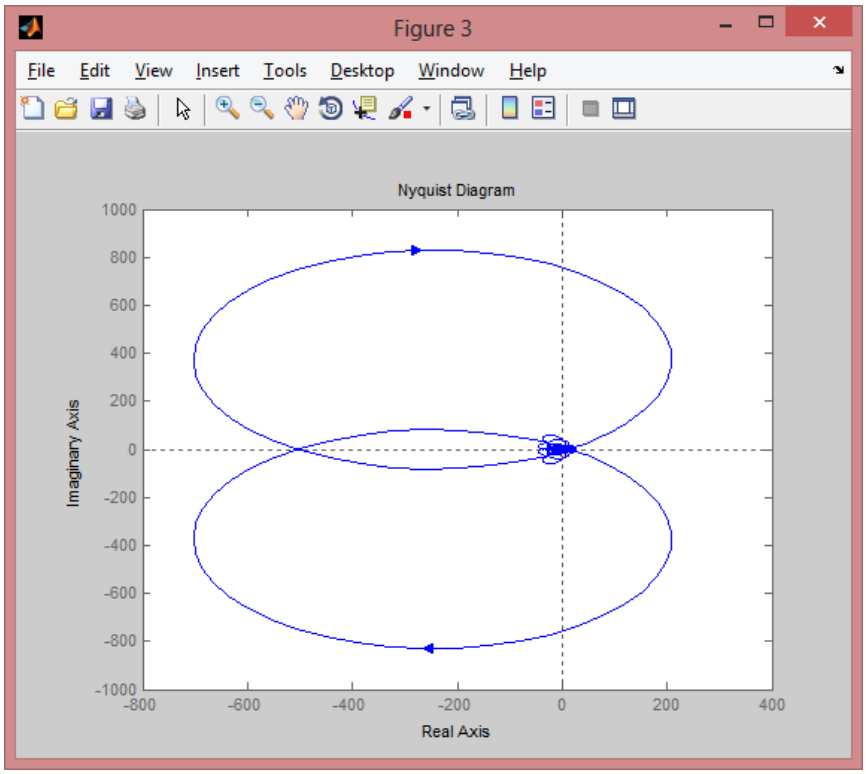

Figure 54: Nyquist plot (Flow 1 - Linear)

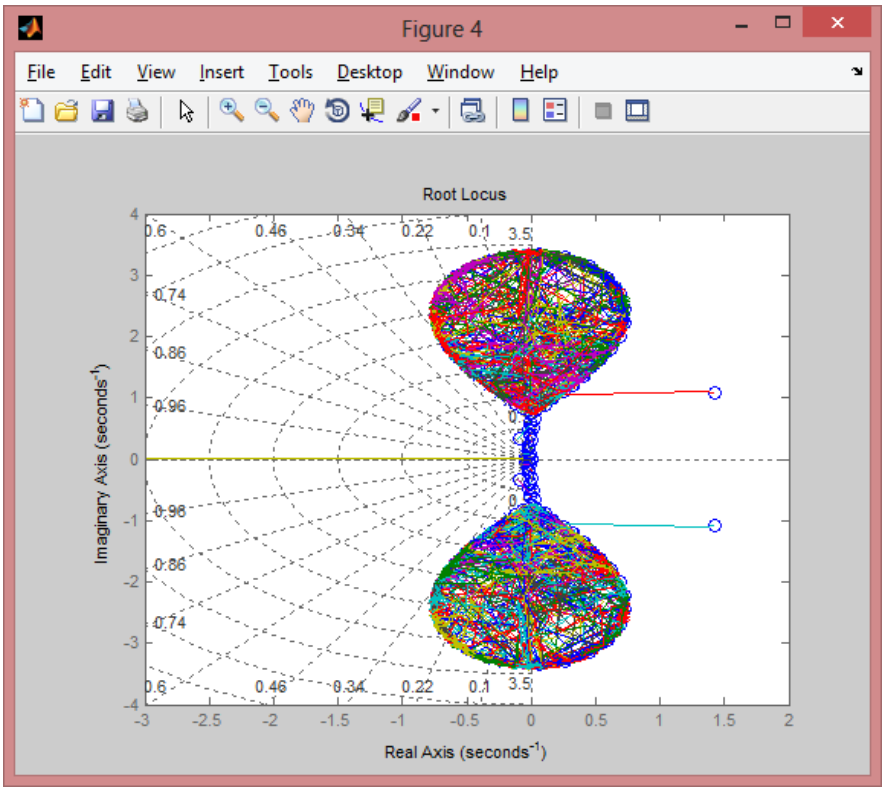

Figure 55: Root locus plot (Flow 1 - Linear)

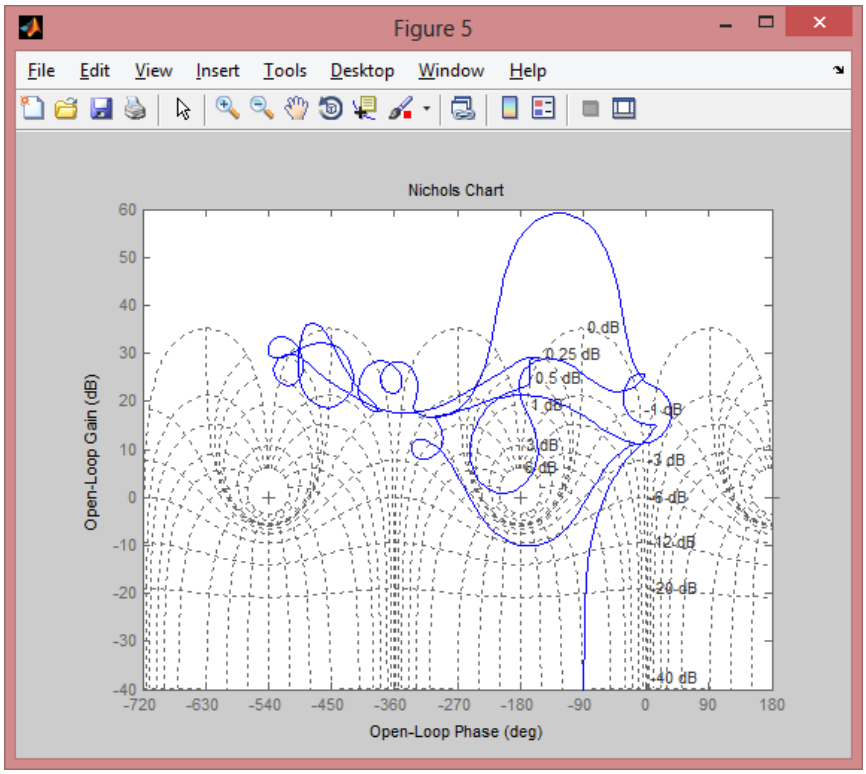

Figure 56: Nichols plot (Flow 2 - Linear)

Flow 2

ARX Model

Fit to estimation data: 94.31%

A(z) = 1 - 1.208 z^-1 + 0.5238 z^-2 - 0.3481 z^-3 + 0.007538 z^-4 + 0.4 z^-5 - 0.6188 z^-6
+ 0.6287 z^-7 - 0.5012 z^-8 + 0.1692 z^-9 + 0.1731 z^-10 + 0.1482 z^-11 - 0.3591 z^-12
- 0.1581 z^-13 + 0.09164 z^-14 - 0.02059 z^-15 + 0.2773 z^-16 - 0.5588 z^
-17 + 0.6637 z^-18 - 0.1358 z^-19 - 0.6919 z^-20 + 0.6968 z^-21 - 0.07265 z^-22
- 0.4608 z^-23 + 0.3692 z^-24 + 0.2142 z^-25 - 0.298 z^-26 - 0.02084 z^-27
+ 0.2501 z^-28 - 0.4069 z^-29 + 0.2097 z^-30 - 0.3278 z^-31 + 0.4683 z^-32
- 0.3552 z^-33 - 0.2342 z^-34 + 0.5979 z^-35 - 0.4965 z^-36 + 0.2252 z^-37
+ 0.2927 z^-38 - 0.3112 z^-39 - 0.03641 z^-40 + 0.2688 z^-41 - 0.142 z^-42
- 0.01683 z^-43 - 0.1288 z^-44 - 0.07955 z^-45 + 0.1251 z^-46 - 0.4733 z^
-47 + 0.4679 z^-48 + 0.1563 z^-49 - 0.7457 z^-50 + 0.9564 z^-51 - 0.724 z^-52
+ 0.1979 z^-53 + 0.05811 z^-54 - 0.08836 z^-55 + 0.05758 z^-56 - 0.001113 z^-57
+ 0.04553 z^-58 - 0.1205 z^-59 + 0.1273 z^-60 - 0.4313 z^-61 + 0.5365 z^-62
- 0.3497 z^-63 + 0.3192 z^-64 - 0.02306 z^-65 - 0.1712 z^-66 + 0.2101 z^-67
- 0.3375 z^-68 + 0.3735 z^-69 - 0.1811 z^-70 - 0.3029 z^-71 + 0.1108 z^-72
- 0.01312 z^-73 + 0.1717 z^-74 - 0.1248 z^-75 + 0.02845 z^-76 - 0.1648 z^
-77 + 0.122 z^-78 + 0.2139 z^-79 - 0.3364 z^-80 + 0.4 z^-81 - 0.5845 z^-82
+ 0.6707 z^-83 - 0.8196 z^-84 + 0.9071 z^-85 - 0.7894 z^-86 + 0.594 z^-87
- 0.3803 z^-88 - 0.1821 z^-89 + 0.3442 z^-90 - 0.3723 z^-91 + 0.5724 z^-92
- 0.2059 z^-93 + 0.02049 z^-94

B(z) = -0.7035 z^-1 - 2.69 z^-2 + 1.02 z^-3 + 1.285 z^-4 - 1.224 z^-5 + 2.525 z^-6
- 1.784 z^-7 + 1.444 z^-8 - 1.066 z^-9 + 0.3187 z^-10 + 0.5476 z^-11 - 1.87 z^-12
+ 0.8136 z^-13 - 0.1418 z^-14 + 2.398 z^-15 - 0.5373 z^-16 + 1.028 z^-17
+ 0.2654 z^-18 - 2.102 z^-19 + 1.471 z^-20 - 1.309 z^-21 + 0.7626 z^-22 - 0.3842 z^-23
- 1.908 z^-24 + 2.809 z^-25 - 0.9354 z^-26 - 1.301 z^-27 + 2.86 z^-28 - 2.775 z^-29
- 0.7321 z^-30 + 1.788 z^-31 + 0.4154 z^-32 - 2.223 z^-33 + 1.867 z^-34 + 0.5121 z^-35
+ 0.711 z^-36 - 2.476 z^-37 + 1.695 z^-38 + 0.1682 z^-39 - 2.299 z^-40 + 0.7867 z^-41
+ 0.1827 z^-42 + 0.1447 z^-43 - 1.89 z^-44 + 2.697 z^-45 - 0.2955 z^-46 - 1.317 z^-47
+ 1.4 z^-48 + 1.363 z^-49 - 2.54 z^-50 - 0.5157 z^-51 + 2.149 z^-52 - 1.847 z^-53
+ 1.437 z^-54 + 1.525 z^-55 - 0.935 z^-56 - 0.1482 z^-57 + 1.152 z^-58 - 0.03997 z^-59
- 2.729 z^-60 + 1.119 z^-61 + 1.201 z^-62 - 1.757 z^-63 + 0.02226 z^-64 + 1.804 z^-65
- 0.8669 z^-66 - 1.589 z^-67 + 0.9883 z^-68 + 0.309 z^-69 - 1.014 z^-70 - 0.8868 z^-71
+ 2.402 z^-72 + 0.2852 z^-73 - 0.1342 z^-74 + 0.8976 z^-75 - 0.1967 z^-76
- 0.6689 z^-77 - 0.6256 z^-78 + 1.093 z^-79 - 0.4379 z^-80 - 0.6593 z^-81
+ 1.747 z^-82 - 0.3432 z^-83 - 0.6338 z^-84 + 0.3717 z^-85 - 0.1584 z^-86
- 0.717 z^-87 - 0.5798 z^-88 - 0.687 z^-89 + 0.621 z^-90 + 2.036 z^-91 - 2.26 z^-92
+ z^-93 - 0.8921 z^-94

Transfer model in z transform

-0.7035 z^-1 - 2.69 z^-2 + 1.02 z^-3 + 1.285 z^-4 - 1.224 z^-5 + 2.525 z^-6 - 1.784 z^-7
+ 1.444 z^-8 - 1.066 z^-9 + 0.3187 z^-10 + 0.5476 z^-11 - 1.87 z^-12
+ 0.8136 z^-13 - 0.1418 z^-14 + 2.398 z^-15 - 0.5373 z^-16 + 1.028 z^
-17 + 0.2654 z^-18 - 2.102 z^-19 + 1.471 z^-20 - 1.309 z^-21 + 0.7626 z^-22
- 0.3842 z^-23 - 1.908 z^-24 + 2.809 z^-25 - 0.9354 z^-26 - 1.301 z^-27
+ 2.86 z^-28 - 2.775 z^-29 - 0.7321 z^-30 + 1.788 z^-31 + 0.4154 z^-32
- 2.223 z^-33 + 1.867 z^-34 + 0.5121 z^-35 + 0.711 z^-36 - 2.476 z^-37
+ 1.695 z^-38 + 0.1682 z^-39 - 2.299 z^-40 + 0.7867 z^-41 + 0.1827 z^
-42 + 0.1447 z^-43 - 1.89 z^-44 + 2.697 z^-45 - 0.2955 z^-46 - 1.317 z^-47
+ 1.4 z^-48 + 1.363 z^-49 - 2.54 z^-50 - 0.5157 z^-51 + 2.149 z^-52 - 1.847 z^-53
+ 1.437 z^-54 + 1.525 z^-55 - 0.935 z^-56 - 0.1482 z^-57 + 1.152 z^-58

- 0.03997 z^-59 - 2.729 z^-60 + 1.119 z^-61 + 1.201 z^-62 - 1.757 z^-63
+ 0.02226 z^-64 + 1.804 z^-65 - 0.8669 z^-66 - 1.589 z^-67 + 0.9883 z^-68
+ 0.309 z^-69 - 1.014 z^-70 - 0.8868 z^-71 + 2.402 z^-72 + 0.2852 z^-73
- 0.1342 z^-74 + 0.8976 z^-75 - 0.1967 z^-76 - 0.6689 z^-77 - 0.6256 z^-78
+ 1.093 z^-79 - 0.4379 z^-80 - 0.6593 z^-81 + 1.747 z^-82 - 0.3432 z^
-83 - 0.6338 z^-84 + 0.3717 z^-85 - 0.1584 z^-86 - 0.717 z^-87 - 0.5798 z^-88
- 0.687 z^-89 + 0.621 z^-90 + 2.036 z^-91 - 2.26 z^-92 + z^-93 - 0.8921 z^-94

---

1 - 1.208 z^-1 + 0.5238 z^-2 - 0.3481 z^-3 + 0.007538 z^-4 + 0.4 z^-5 - 0.6188 z^-6
+ 0.6287 z^-7 - 0.5012 z^-8 + 0.1692 z^-9 + 0.1731 z^-10 + 0.1482 z^-11
- 0.3591 z^-12 - 0.1581 z^-13 + 0.09164 z^-14 - 0.02059 z^-15 + 0.2773 z^-16
- 0.5588 z^-17 + 0.6637 z^-18 - 0.1358 z^-19 - 0.6919 z^-20 + 0.6968 z^-21
- 0.07265 z^-22 - 0.4608 z^-23 + 0.3692 z^-24 + 0.2142 z^-25 - 0.298 z^-26
- 0.02084 z^-27 + 0.2501 z^-28 - 0.4069 z^-29 + 0.2097 z^-30 - 0.3278 z^-31
+ 0.4683 z^-32 - 0.3552 z^-33 - 0.2342 z^-34 + 0.5979 z^-35 - 0.4965 z^-36
+ 0.2252 z^-37 + 0.2927 z^-38 - 0.3112 z^-39 - 0.03641 z^-40 + 0.2688 z^-41
- 0.142 z^-42 - 0.01683 z^-43 - 0.1288 z^-44 - 0.07955 z^-45 + 0.1251 z^-46
- 0.4733 z^-47 + 0.4679 z^-48 + 0.1563 z^-49 - 0.7457 z^-50 + 0.9564 z^-51
- 0.724 z^-52 + 0.1979 z^-53 + 0.05811 z^-54 - 0.08836 z^-55 + 0.05758 z^-56
- 0.001113 z^-57 + 0.04553 z^-58 - 0.1205 z^-59 + 0.1273 z^-60 - 0.4313 z^-61
+ 0.5365 z^-62 - 0.3497 z^-63 + 0.3192 z^-64 - 0.02306 z^-65 - 0.1712 z^-66
+ 0.2101 z^-67 - 0.3375 z^-68 + 0.3735 z^-69 - 0.1811 z^-70 - 0.3029 z^-71
+ 0.1108 z^-72 - 0.01312 z^-73 + 0.1717 z^-74 - 0.1248 z^-75 + 0.02845 z^-76
- 0.1648 z^-77 + 0.122 z^-78 + 0.2139 z^-79 - 0.3364 z^-80 + 0.4 z^-81
- 0.5845 z^-82 + 0.6707 z^-83 - 0.8196 z^-84 + 0.9071 z^-85 - 0.7894 z^-86
+ 0.594 z^-87 - 0.3803 z^-88 - 0.1821 z^-89 + 0.3442 z^-90 - 0.3723 z^-91
+ 0.5724 z^-92 - 0.2059 z^-93 + 0.02049 z^-94

Transfer model in s transform

7.556 s^95 - 1.982 s^94 + 1191 s^93 - 345.7 s^92 + 9.017e04 s^91 - 2.888e04 s^90
+ 4.37e06 s^89 - 1.539e06 s^88 + 1.523e08 s^87 - 5.886e07 s^86 + 4.067e09 s^85
- 1.721e09 s^84 + 8.658e10 s^83 - 4.006e10 s^82 + 1.51e12 s^81 - 7.626e11 s^80
+ 2.198e13 s^79 - 1.211e13 s^78 + 2.71e14 s^77 - 1.628e14 s^76 + 2.861e15 s^75
- 1.872e15 s^74 + 2.609e16 s^73 - 1.86e16 s^72 + 2.068e17 s^71 - 1.606e17 s^70
+ 1.432e18 s^69 - 1.213e18 s^68 + 8.701e18 s^67 - 8.037e18 s^66 + 4.652e19 s^65
- 4.693e19 s^64 + 2.193e20 s^63 - 2.42e20 s^62 + 9.133e20 s^61 - 1.105e21 s^60
+ 3.36e21 s^59 - 4.467e21 s^58 + 1.093e22 s^57 - 1.602e22 s^56 + 3.138e22 s^55
- 5.099e22 s^54 + 7.946e22 s^53 - 1.439e23 s^52 + 1.77e23 s^51 - 3.601e23 s^50
+ 3.458e23 s^49 - 7.98e23 s^48 + 5.891e23 s^47 - 1.564e24 s^46 + 8.692e23 s^45
- 2.706e24 s^44 + 1.099e24 s^43 - 4.122e24 s^42 + 1.169e24 s^41 - 5.514e24 s^40
+ 1.013e24 s^39 - 6.456e24 s^38 + 6.639e23 s^37 - 6.588e24 s^36 + 2.494e23 s^35
- 5.834e24 s^34 - 8.003e22 s^33 - 4.458e24 s^32 - 2.403e23 s^31 - 2.921e24 s^30
- 2.464e23 s^29 - 1.63e24 s^28 - 1.735e23 s^27 - 7.678e23 s^26 - 9.307e22 s^25
- 3.023e23 s^24 - 3.917e22 s^23 - 9.838e22 s^22 - 1.3e22 s^21 - 2.609e22 s^20
- 3.382e21 s^19 - 5.544e21 s^18 - 6.785e20 s^17 - 9.251e20 s^16 - 1.026e20 s^15
- 1.181e20 s^14 - 1.128e19 s^13 - 1.116e19 s^12 - 8.583e17 s^11 - 7.451e17 s^10
- 4.161e16 s^9 - 3.29e16 s^8 - 1.109e15 s^7 - 8.651e14 s^6 - 1.119e13 s^5
- 1.129e13 s^4 + 2.95e10 s^3 - 5.107e10 s^2 + 1.899e08 s - 1.213e07

---

s^96 + 4.052 s^95 + 166 s^94 + 648.6 s^93 + 1.325e04 s^92 + 4.99e04 s^91 + 6.777e05 s^90
+ 2.459e06 s^89 + 2.494e07 s^88 + 8.719e07 s^87 + 7.044e08 s^86 + 2.371e09 s^85
+ 1.588e10 s^84 + 5.146e10 s^83 + 2.937e11 s^82 + 9.154e11 s^81 + 4.542e12 s^80
+ 1.361e13 s^79 + 5.961e13 s^78 + 1.717e14 s^77 + 6.714e14 s^76 + 1.856e15 s^75
+ 6.546e15 s^74 + 1.737e16 s^73 + 5.564e16 s^72 + 1.415e17 s^71 + 4.145e17 s^70

+ 1.009e18 s^69 + 2.718e18 s^68 + 6.329e18 s^67 + 1.575e19 s^66 + 3.502e19 s^65
+ 8.08e19 s^64 + 1.714e20 s^63 + 3.68e20 s^62 + 7.437e20 s^61 + 1.49e21 s^60
+ 2.863e21 s^59 + 5.365e21 s^58 + 9.791e21 s^57 + 1.72e22 s^56 + 2.975e22 s^55
+ 4.91e22 s^54 + 8.028e22 s^53 + 1.247e23 s^52 + 1.924e23 s^51 + 2.817e23 s^50
+ 4.088e23 s^49 + 5.652e23 s^48 + 7.696e23 s^47 + 1.006e24 s^46 + 1.281e24 s^45
+ 1.584e24 s^44 + 1.88e24 s^43 + 2.202e24 s^42 + 2.427e24 s^41 + 2.695e24 s^40
+ 2.747e24 s^39 + 2.895e24 s^38 + 2.714e24 s^37 + 2.716e24 s^36 + 2.331e24 s^35
+ 2.216e24 s^34 + 1.73e24 s^33 + 1.564e24 s^32 + 1.104e24 s^31 + 9.49e23 s^30
+ 6.005e23 s^29 + 4.912e23 s^28 + 2.763e23 s^27 + 2.15e23 s^26 + 1.065e23 s^25
+ 7.88e22 s^24 + 3.398e22 s^23 + 2.389e22 s^22 + 8.853e21 s^21 + 5.905e21 s^20
+ 1.852e21 s^19 + 1.169e21 s^18 + 3.051e20 s^17 + 1.815e20 s^16 + 3.859e19 s^15
+ 2.149e19 s^14 + 3.629e18 s^13 + 1.872e18 s^12 + 2.433e17 s^11 + 1.143e17 s^10
+ 1.097e16 s^9 + 4.55e15 s^8 + 3.043e14 s^7 + 1.054e14 s^6 + 4.505e12 s^5
+ 1.126e12 s^4 + 2.687e10 s^3 + 2.339e09 s^2 + 1.335e07 s - 1.421e07

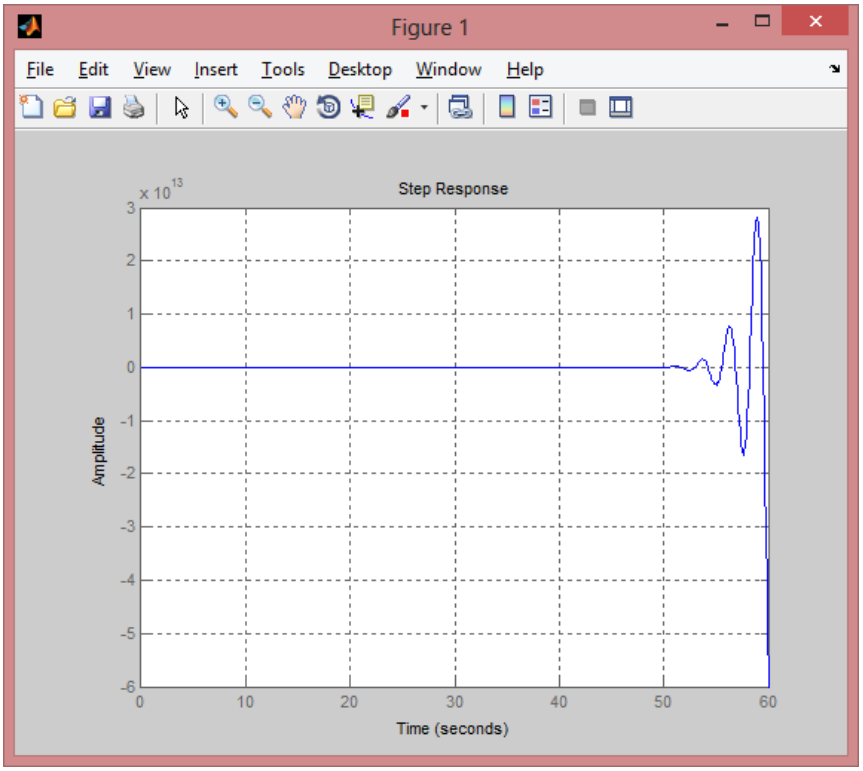

Figure 57: Step response (Flow 2 - Linear)

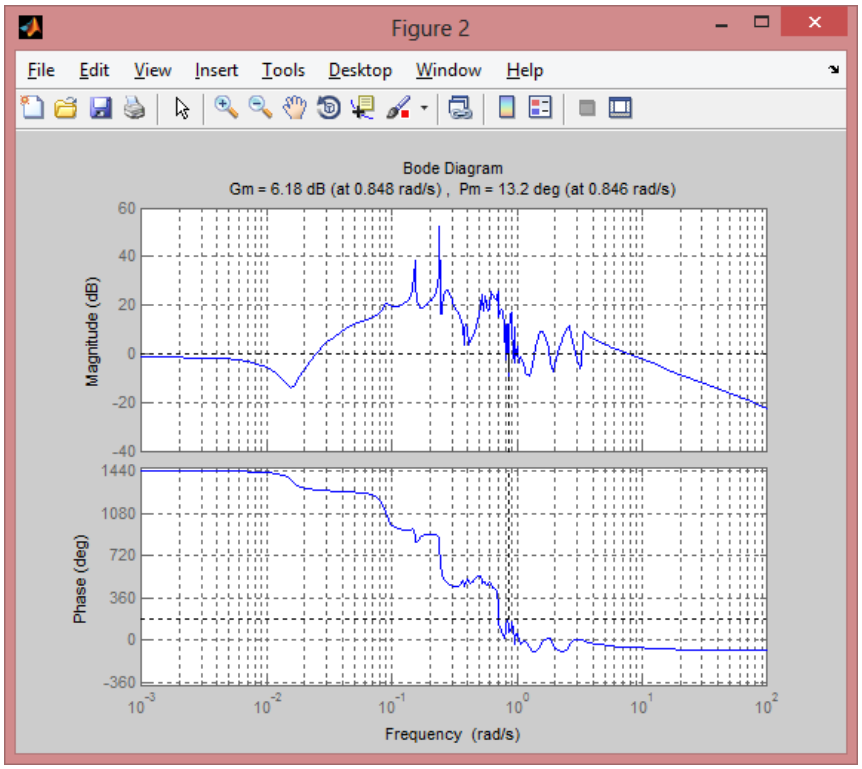

Figure 58: Bode plot (Flow 2 - Linear)

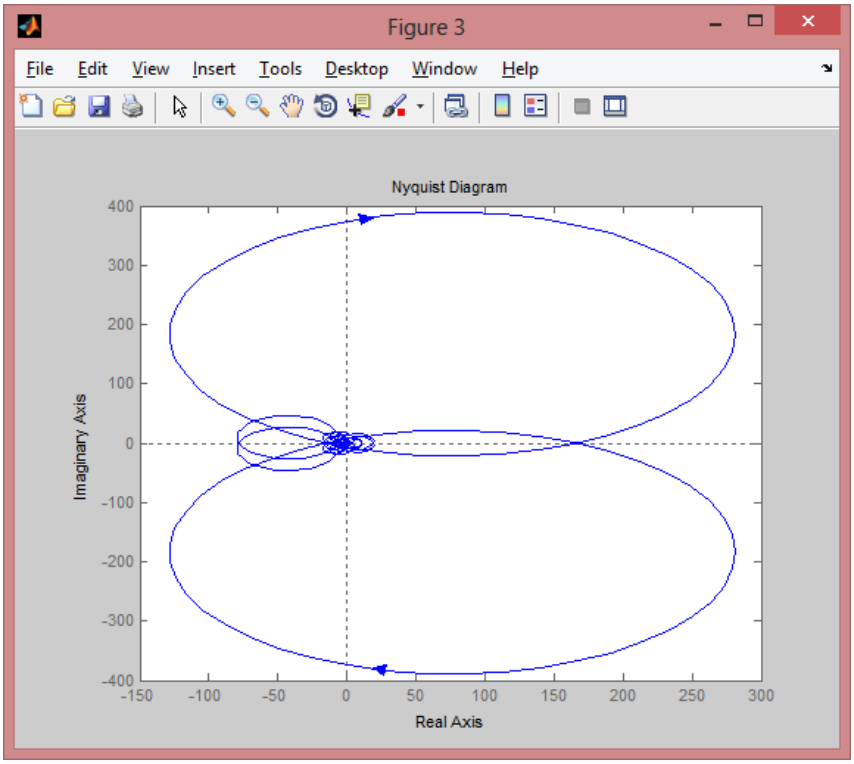

Figure 59: Nyquist plot (Flow 2 - Linear)

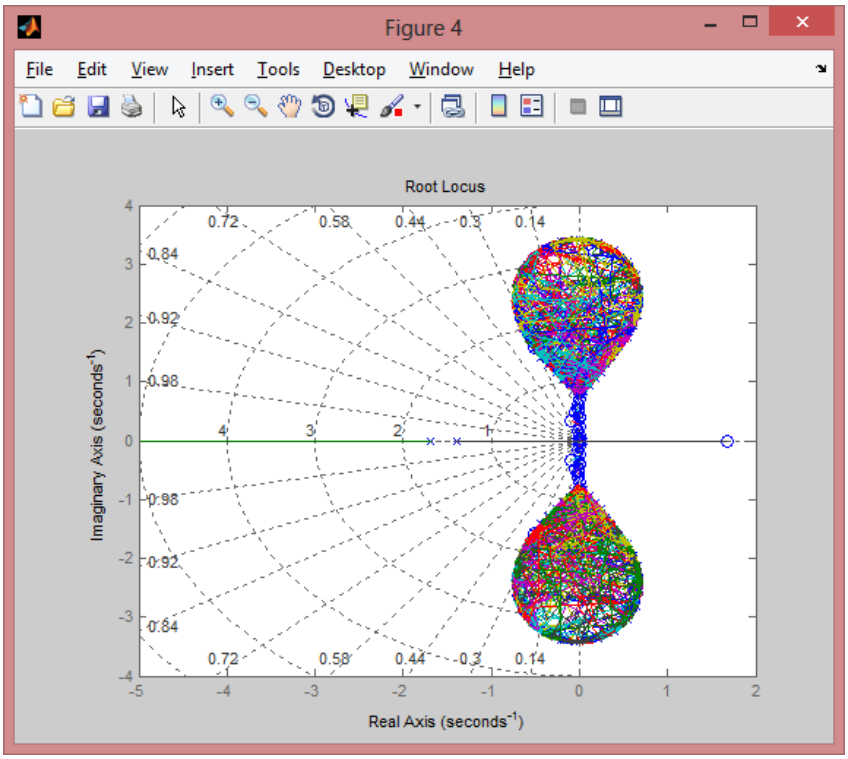

Figure 60: Root locus plot (Flow 2 - Linear)

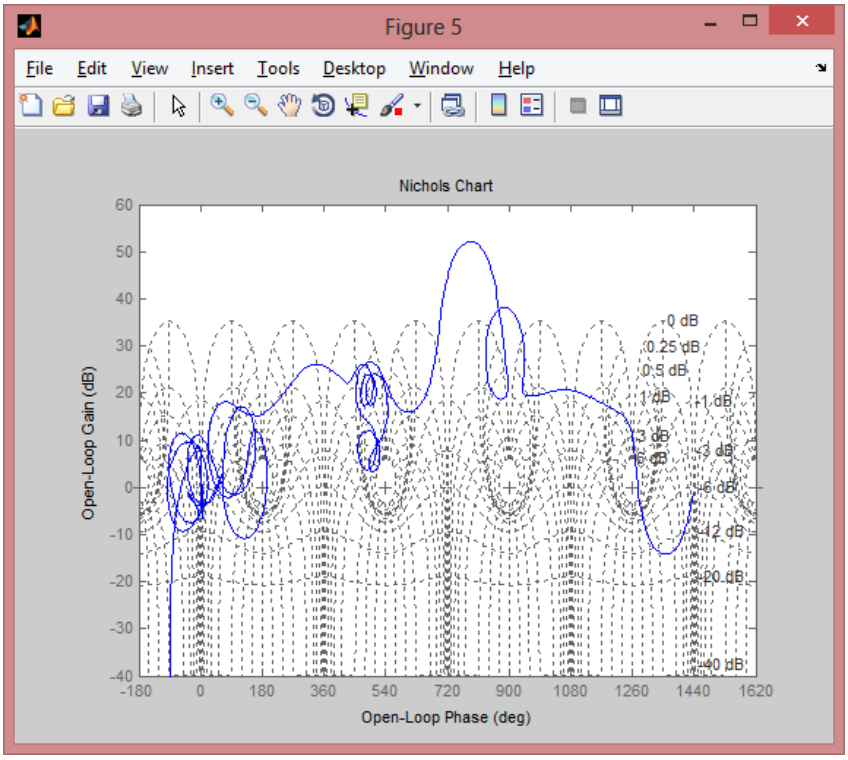

Figure 61: Nichols plot (Flow 2 - Linear)

Pressure 1

ARX Model

Fit to estimation data: 90.04%

A(z) = 1 - 0.597 z^-1 + 0.05056 z^-2 + 0.02716 z^-3 + 0.07335 z^-4 - 0.3212 z^-5
+ 0.3931 z^-6 - 0.1151 z^-7 + 0.2283 z^-8 - 0.3553 z^-9 - 0.2882 z^-10 + 0.4856 z^-11
- 0.1797 z^-12 - 0.2107 z^-13 + 0.2413 z^-14 + 0.01242 z^-15 - 0.05856 z^
-16 - 0.2445 z^-17 + 0.4197 z^-18 + 0.09188 z^-19 + 0.04252 z^-20 + 0.0006754 z^-21
+ 0.1829 z^-22 + 0.5227 z^-23 - 0.3844 z^-24 + 0.1485 z^-25 - 0.04837 z^-26
- 0.1148 z^-27 + 0.06222 z^-28 - 0.1011 z^-29 - 0.3062 z^-30 + 0.3347 z^-31
- 0.4621 z^-32 + 0.3123 z^-33 - 0.1748 z^-34 - 0.3406 z^-35 + 0.4998 z^-36
- 0.05372 z^-37 - 0.4079 z^-38 + 0.6931 z^-39 - 0.2816 z^-40 + 0.203 z^-41
- 0.1135 z^-42 - 0.01777 z^-43 - 0.2386 z^-44 + 0.472 z^-45 - 0.5006 z^-46
+ 0.4316 z^-47 + 0.4129 z^-48 - 0.6254 z^-49 - 0.01133 z^-50 + 0.02227 z^
-51 - 0.3016 z^-52 + 0.148 z^-53 + 0.1012 z^-54 - 0.5536 z^-55 + 0.6578 z^-56
- 0.8496 z^-57 + 0.1153 z^-58 + 0.4015 z^-59 - 0.3408 z^-60 + 0.4159 z^-61
- 0.1244 z^-62 - 0.309 z^-63 + 0.693 z^-64 - 0.4597 z^-65 - 0.02519 z^-66
+ 0.1919 z^-67 - 0.08317 z^-68 - 0.1053 z^-69 - 0.07641 z^-70 - 0.2914 z^
-71 + 0.5666 z^-72 - 0.4906 z^-73 + 0.1777 z^-74 + 0.1212 z^-75 + 0.2594 z^-76
- 0.132 z^-77 - 0.13 z^-78 + 0.5147 z^-79 - 0.6346 z^-80 + 0.4181 z^-81 - 0.7714 z^-82
+ 0.599 z^-83 - 0.3254 z^-84 - 0.07701 z^-85 + 0.2708 z^-86 + 0.3799 z^-87
- 0.443 z^-88 + 0.06215 z^-89 - 0.08143 z^-90 - 0.4688 z^-91 - 0.4822 z^-92
+ 0.403 z^-93 + 0.4273 z^-94 + 0.4303 z^-95 - 0.468 z^-96

B(z) = 281.5 z^-1 - 433.9 z^-2 + 117.6 z^-3 - 11.33 z^-4 + 291 z^-5 - 12.66 z^-6
- 170 z^-7 + 304.1 z^-8 + 150.6 z^-9 - 194.2 z^-10 - 282.7 z^-11 + 465.6 z^-12
- 284.9 z^-13 - 35.2 z^-14 - 203.8 z^-15 + 180.6 z^-16 + 334.4 z^-17 - 552.2 z^-18
+ 555.3 z^-19 - 76.46 z^-20 - 166.6 z^-21 - 152.5 z^-22 - 328 z^-23 + 845.6 z^-24
- 1454 z^-25 + 1249 z^-26 + 611.8 z^-27 - 241.1 z^-28 + 259.7 z^-29 - 1265 z^-30
+ 900.9 z^-31 + 300.1 z^-32 - 710.7 z^-33 + 474.9 z^-34 + 80.66 z^-35 - 570.8 z^-36
+ 654.5 z^-37 - 941.4 z^-38 + 778.6 z^-39 - 134 z^-40 - 609 z^-41 + 951.6 z^-42
- 664.6 z^-43 + 22.39 z^-44 + 560.4 z^-45 - 890 z^-46 + 1075 z^-47 - 1103 z^-48
+ 1002 z^-49 - 1086 z^-50 + 1256 z^-51 - 1370 z^-52 + 1321 z^-53 - 273.7 z^-54
- 416.9 z^-55 + 196.7 z^-56 + 231 z^-57 - 595.2 z^-58 + 67.22 z^-59 - 135.7 z^-60
+ 146 z^-61 + 945.7 z^-62 - 1310 z^-63 + 454.7 z^-64 - 130.7 z^-65 - 417.3 z^-66
+ 883.5 z^-67 - 504.4 z^-68 - 44.72 z^-69 + 708.1 z^-70 - 956.1 z^-71 + 444.6 z^-72
- 23.88 z^-73 + 10.84 z^-74 + 288.6 z^-75 - 616.8 z^-76 + 89.87 z^-77 + 449.5 z^-78
- 908.2 z^-79 + 836.3 z^-80 - 278.8 z^-81 + 501.1 z^-82 - 483.3 z^-83 - 288.7 z^-84
+ 695.2 z^-85 - 416.8 z^-86 + 523 z^-87 - 1017 z^-88 + 1278 z^-89 - 1074 z^-90
+ 350.4 z^-91 - 214.6 z^-92 + 562 z^-93 - 412.7 z^-94 + 222.3 z^-95 - 430.5 z^-96

Transfer model in z function

281.5 z^-1 - 433.9 z^-2 + 117.6 z^-3 - 11.33 z^-4 + 291 z^-5 - 12.66 z^-6 - 170 z^-7
+ 304.1 z^-8 + 150.6 z^-9 - 194.2 z^-10 - 282.7 z^-11 + 465.6 z^-12 - 284.9 z^-13
- 35.2 z^-14 - 203.8 z^-15 + 180.6 z^-16 + 334.4 z^-17 - 552.2 z^-18
+ 555.3 z^-19 - 76.46 z^-20 - 166.6 z^-21 - 152.5 z^-22 - 328 z^-23 + 845.6 z^-24
- 1454 z^-25 + 1249 z^-26 + 611.8 z^-27 - 241.1 z^-28 + 259.7 z^-29 - 1265 z^-30
+ 900.9 z^-31 + 300.1 z^-32 - 710.7 z^-33 + 474.9 z^-34 + 80.66 z^-35
- 570.8 z^-36 + 654.5 z^-37 - 941.4 z^-38 + 778.6 z^-39 - 134 z^-40 - 609 z^-41
+ 951.6 z^-42 - 664.6 z^-43 + 22.39 z^-44 + 560.4 z^-45 - 890 z^-46 + 1075 z^-47
- 1103 z^-48 + 1002 z^-49 - 1086 z^-50 + 1256 z^-51 - 1370 z^-52 + 1321 z^-53
- 273.7 z^-54 - 416.9 z^-55 + 196.7 z^-56 + 231 z^-57 - 595.2 z^-58 + 67.22 z^-59
- 135.7 z^-60 + 146 z^-61 + 945.7 z^-62 - 1310 z^-63 + 454.7 z^-64 - 130.7 z^-65
- 417.3 z^-66 + 883.5 z^-67 - 504.4 z^-68 - 44.72 z^-69 + 708.1 z^-70

- 956.1 z^-71 + 444.6 z^-72 - 23.88 z^-73 + 10.84 z^-74 + 288.6 z^-75
- 616.8 z^-76 + 89.87 z^-77 + 449.5 z^-78 - 908.2 z^-79 + 836.3 z^-80
- 278.8 z^-81 + 501.1 z^-82 - 483.3 z^-83 - 288.7 z^-84 + 695.2 z^-85
- 416.8 z^-86 + 523 z^-87 - 1017 z^-88 + 1278 z^-89 - 1074 z^-90 + 350.4 z^-91
- 214.6 z^-92 + 562 z^-93 - 412.7 z^-94 + 222.3 z^-95 - 430.5 z^-96

---

1 - 0.597 z^-1 + 0.05056 z^-2 + 0.02716 z^-3 + 0.07335 z^-4 - 0.3212 z^-5 + 0.3931 z^-6
- 0.1151 z^-7 + 0.2283 z^-8 - 0.3553 z^-9 - 0.2882 z^-10 + 0.4856 z^-11
- 0.1797 z^-12 - 0.2107 z^-13 + 0.2413 z^-14 + 0.01242 z^-15 - 0.05856 z^-16
- 0.2445 z^-17 + 0.4197 z^-18 + 0.09188 z^-19 + 0.04252 z^-20 + 0.0006754 z^-21
+ 0.1829 z^-22 + 0.5227 z^-23 - 0.3844 z^-24 + 0.1485 z^-25 - 0.04837 z^-26
- 0.1148 z^-27 + 0.06222 z^-28 - 0.1011 z^-29 - 0.3062 z^-30 + 0.3347 z^-31
- 0.4621 z^-32 + 0.3123 z^-33 - 0.1748 z^-34 - 0.3406 z^-35 + 0.4998 z^-36
- 0.05372 z^-37 - 0.4079 z^-38 + 0.6931 z^-39 - 0.2816 z^-40 + 0.203 z^-41
- 0.1135 z^-42 - 0.01777 z^-43 - 0.2386 z^-44 + 0.472 z^-45 - 0.5006 z^-46
+ 0.4316 z^-47 + 0.4129 z^-48 - 0.6254 z^-49 - 0.01133 z^-50 + 0.02227 z^-51
- 0.3016 z^-52 + 0.148 z^-53 + 0.1012 z^-54 - 0.5536 z^-55 + 0.6578 z^-56
- 0.8496 z^-57 + 0.1153 z^-58 + 0.4015 z^-59 - 0.3408 z^-60 + 0.4159 z^-61
- 0.1244 z^-62 - 0.309 z^-63 + 0.693 z^-64 - 0.4597 z^-65 - 0.02519 z^-66
+ 0.1919 z^-67 - 0.08317 z^-68 - 0.1053 z^-69 - 0.07641 z^-70 - 0.2914 z^-71
+ 0.5666 z^-72 - 0.4906 z^-73 + 0.1777 z^-74 + 0.1212 z^-75 + 0.2594 z^-76
- 0.132 z^-77 - 0.13 z^-78 + 0.5147 z^-79 - 0.6346 z^-80 + 0.4181 z^-81
- 0.7714 z^-82 + 0.599 z^-83 - 0.3254 z^-84 - 0.07701 z^-85 + 0.2708 z^-86
+ 0.3799 z^-87 - 0.443 z^-88 + 0.06215 z^-89 - 0.08143 z^-90 - 0.4688 z^-91
- 0.4822 z^-92 + 0.403 z^-93 + 0.4273 z^-94 + 0.4303 z^-95 - 0.468 z^-96

Transfer model in s function

-663.5 s^96 + 1717 s^95 - 1.024e05 s^94 + 2.652e05 s^93 - 7.611e06 s^92 + 1.971e07 s^91
- 3.625e08 s^90 + 9.386e08 s^89 - 1.244e10 s^88 + 3.219e10 s^87 - 3.277e11 s^86
+ 8.469e11 s^85 - 6.898e12 s^84 + 1.779e13 s^83 - 1.192e14 s^82 + 3.067e14 s^81
- 1.725e15 s^80 + 4.421e15 s^79 - 2.121e16 s^78 + 5.408e16 s^77 - 2.241e17 s^76
+ 5.677e17 s^75 - 2.052e18 s^74 + 5.159e18 s^73 - 1.64e19 s^72 + 4.086e19 s^71
- 1.151e20 s^70 + 2.835e20 s^69 - 7.121e20 s^68 + 1.732e21 s^67 - 3.899e21 s^66
+ 9.34e21 s^65 - 1.895e22 s^64 + 4.46e22 s^63 - 8.188e22 s^62 + 1.889e23 s^61
- 3.152e23 s^60 + 7.109e23 s^59 - 1.082e24 s^58 + 2.379e24 s^57 - 3.316e24 s^56
+ 7.08e24 s^55 - 9.067e24 s^54 + 1.874e25 s^53 - 2.212e25 s^52 + 4.411e25 s^51
- 4.812e25 s^50 + 9.223e25 s^49 - 9.323e25 s^48 + 1.711e26 s^47 - 1.606e26 s^46
+ 2.811e26 s^45 - 2.456e26 s^44 + 4.082e26 s^43 - 3.323e26 s^42 + 5.226e26 s^41
- 3.969e26 s^40 + 5.88e26 s^39 - 4.167e26 s^38 + 5.795e26 s^37 - 3.832e26 s^36
+ 4.98e26 s^35 - 3.069e26 s^34 + 3.715e26 s^33 - 2.13e26 s^32 + 2.393e26 s^31
- 1.272e26 s^30 + 1.322e26 s^29 - 6.485e25 s^28 + 6.216e25 s^27 - 2.798e25 s^26
+ 2.468e25 s^25 - 1.011e25 s^24 + 8.19e24 s^23 - 3.02e24 s^22 + 2.245e24 s^21
- 7.346e23 s^20 + 5.012e23 s^19 - 1.429e23 s^18 + 8.955e22 s^17 - 2.175e22 s^16
+ 1.253e22 s^15 - 2.517e21 s^14 + 1.335e21 s^13 - 2.135e20 s^12 + 1.044e20 s^11
- 1.264e19 s^10 + 5.682e18 s^9 - 4.876e17 s^8 + 2.001e17 s^7 - 1.1e16 s^6
+ 4.081e15 s^5 - 1.166e14 s^4 + 4.069e13 s^3 - 2.831e11 s^2 + 1.468e11 s
+ 7.056e07

---

s^97 + 0.7503 s^96 + 161.7 s^95 + 119.1 s^94 + 1.258e04 s^93 + 9102 s^92 + 6.278e05 s^91
+ 4.458e05 s^90 + 2.258e07 s^89 + 1.574e07 s^88 + 6.235e08 s^87 + 4.264e08 s^86
+ 1.376e10 s^85 + 9.234e09 s^84 + 2.493e11 s^83 + 1.642e11 s^82 + 3.782e12 s^81
+ 2.443e12 s^80 + 4.872e13 s^79 + 3.088e13 s^78 + 5.392e14 s^77 + 3.353e14 s^76
+ 5.171e15 s^75 + 3.155e15 s^74 + 4.326e16 s^73 + 2.591e16 s^72 + 3.175e17 s^71
+ 1.866e17 s^70 + 2.053e18 s^69 + 1.185e18 s^68 + 1.174e19 s^67 + 6.655e18 s^66
+ 5.95e19 s^65 + 3.314e19 s^64 + 2.679e20 s^63 + 1.467e20 s^62 + 1.073e21 s^61

+ 5.78e20 s^60 + 3.827e21 s^59 + 2.029e21 s^58 + 1.216e22 s^57 + 6.35e21 s^56
+ 3.442e22 s^55 + 1.772e22 s^54 + 8.68e22 s^53 + 4.408e22 s^52 + 1.948e23 s^51
+ 9.768e22 s^50 + 3.887e23 s^49 + 1.926e23 s^48 + 6.884e23 s^47 + 3.373e23 s^46
+ 1.08e24 s^45 + 5.238e23 s^44 + 1.498e24 s^43 + 7.196e23 s^42 + 1.831e24 s^41
+ 8.716e23 s^40 + 1.966e24 s^39 + 9.279e23 s^38 + 1.848e24 s^37 + 8.645e23 s^36
+ 1.513e24 s^35 + 7.015e23 s^34 + 1.074e24 s^33 + 4.931e23 s^32 + 6.57e23 s^31
+ 2.982e23 s^30 + 3.441e23 s^29 + 1.54e23 s^28 + 1.531e23 s^27 + 6.733e22 s^26
+ 5.737e22 s^25 + 2.466e22 s^24 + 1.792e22 s^23 + 7.47e21 s^22 + 4.61e21 s^21
+ 1.845e21 s^20 + 9.631e20 s^19 + 3.648e20 s^18 + 1.606e20 s^17 + 5.647e19 s^16
+ 2.094e19 s^15 + 6.655e18 s^14 + 2.077e18 s^13 + 5.758e17 s^12 + 1.516e17 s^11
+ 3.485e16 s^10 + 7.765e15 s^9 + 1.382e15 s^8 + 2.622e14 s^7 + 3.283e13 s^6
+ 5.318e12 s^5 + 4.124e11 s^4 + 5.491e10 s^3 + 2.187e09 s^2 + 2.003e08 s
+ 6.166e05

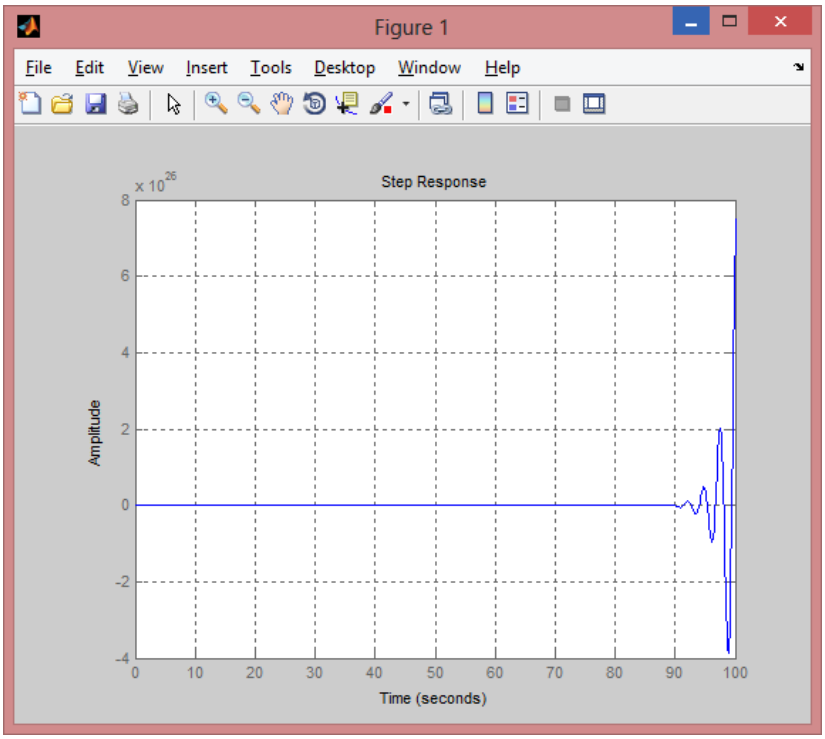

Figure 62: Step response (Pressure 1 - Linear)

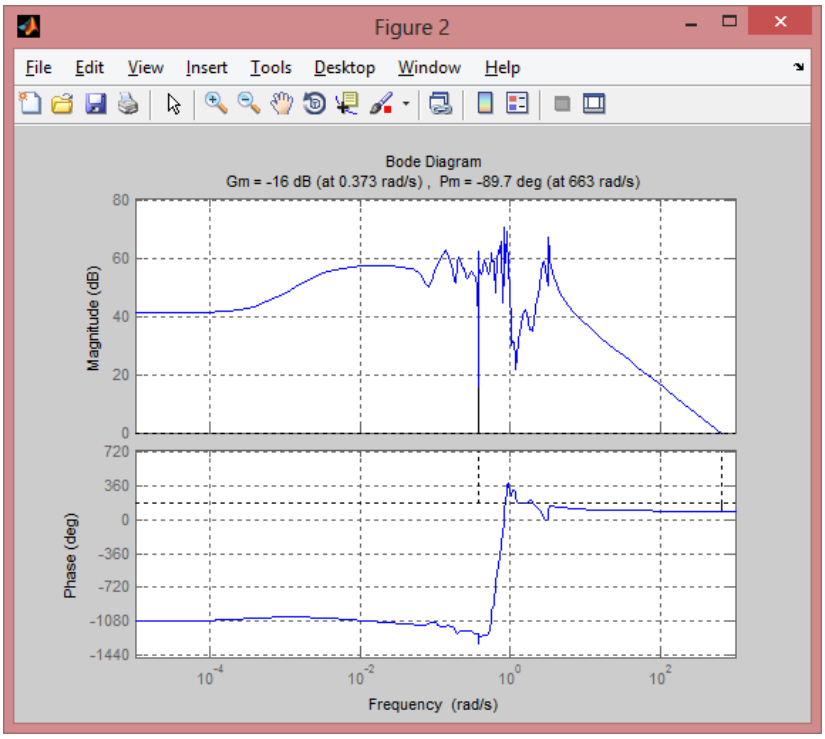

Figure 63: Step response (Pressure 1 - Linear)

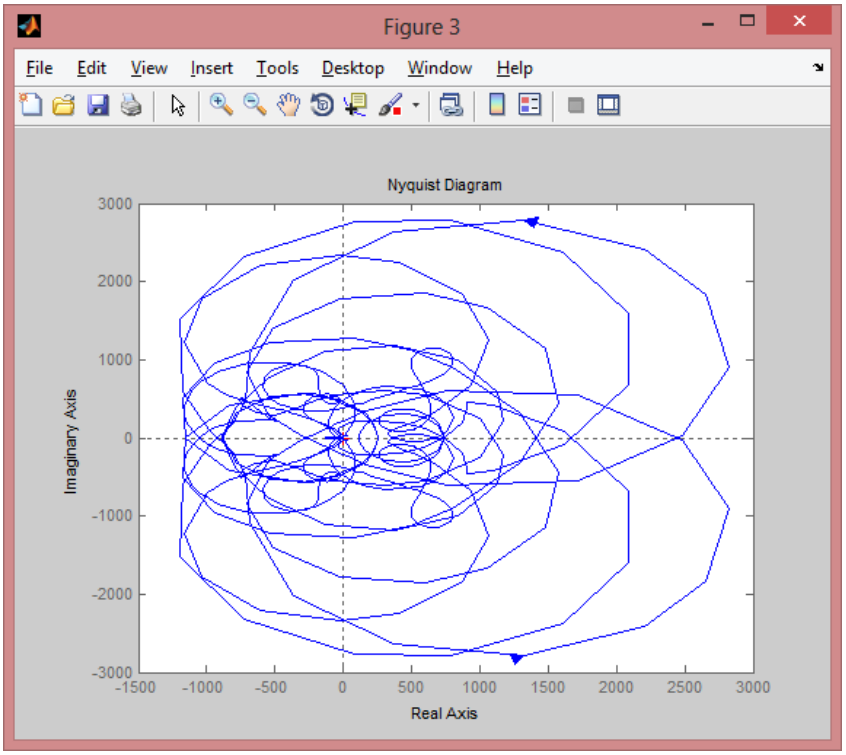

Figure 64: Nyquist plot (Pressure 1 - Linear)

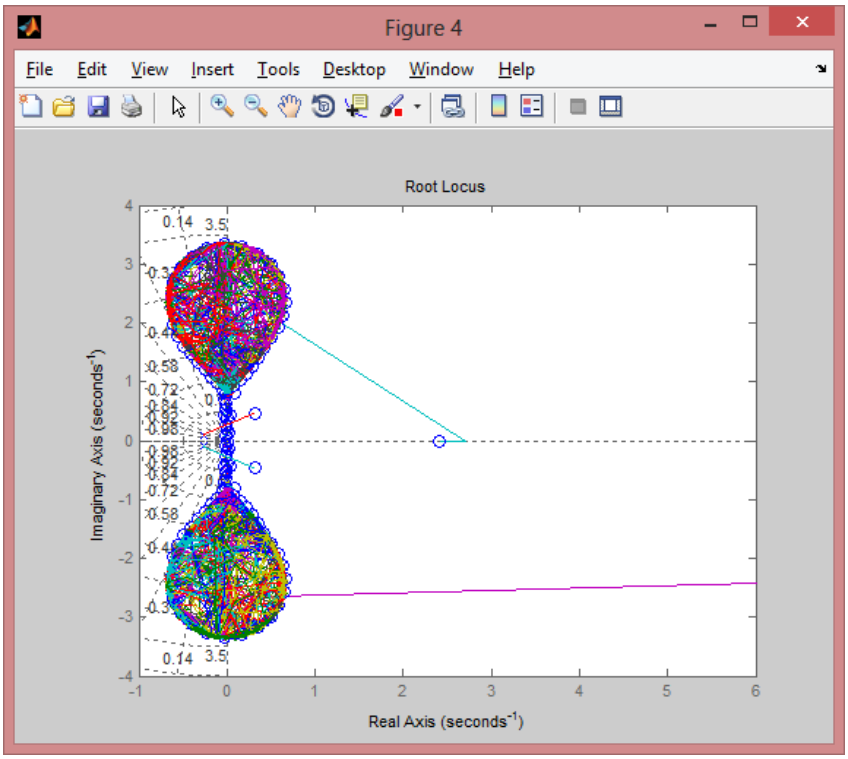

Figure 65: Root locus plot (Pressure 1 - Linear)

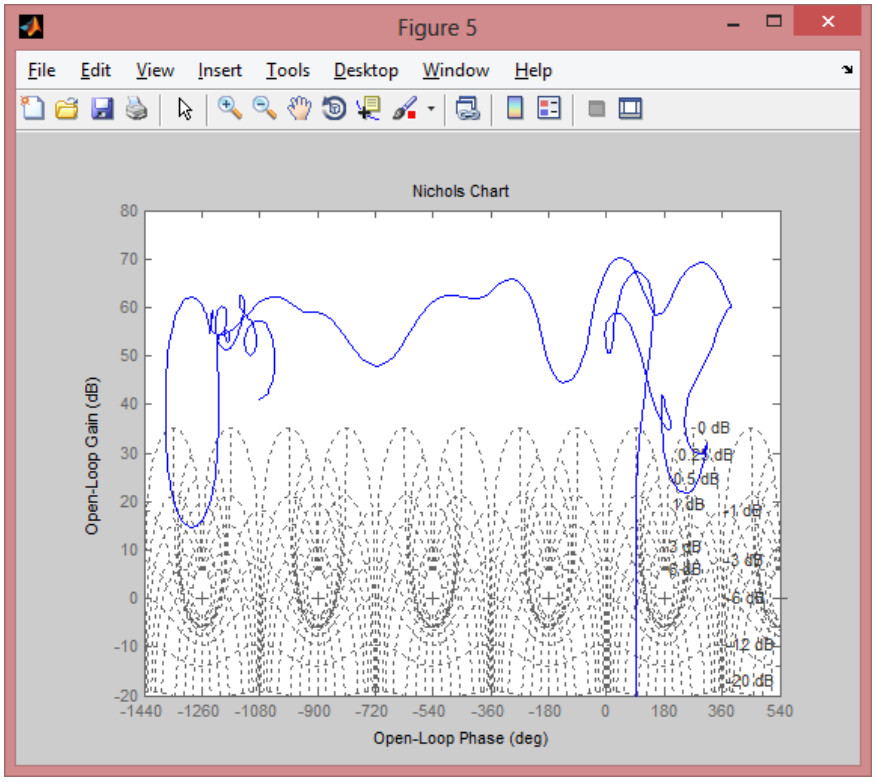

Figure 66: Nichols plot (Pressure 1 - Linear)

APPENDIX 2

NON-LINEAR SYSTEM IDENTIFICATION

Temperature 1

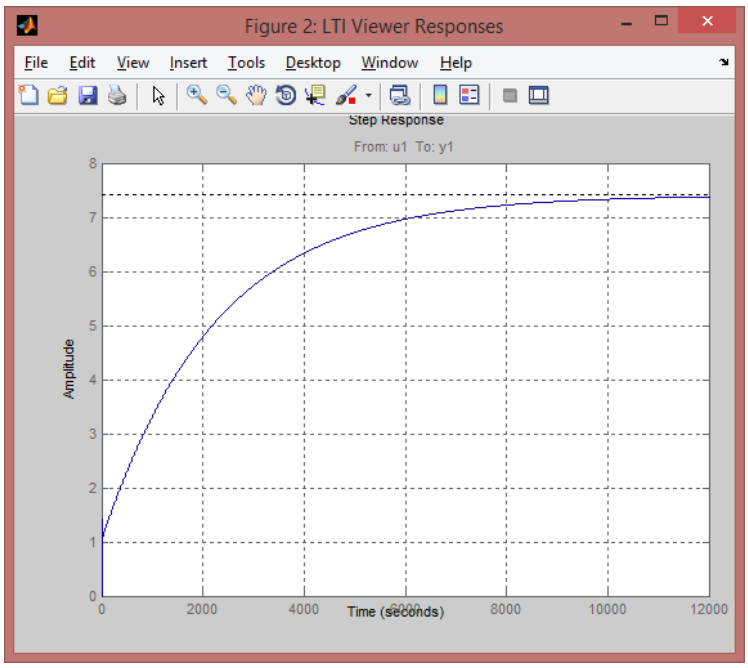

Figure 67: Step response (Temperature 1 - Nonlinear)

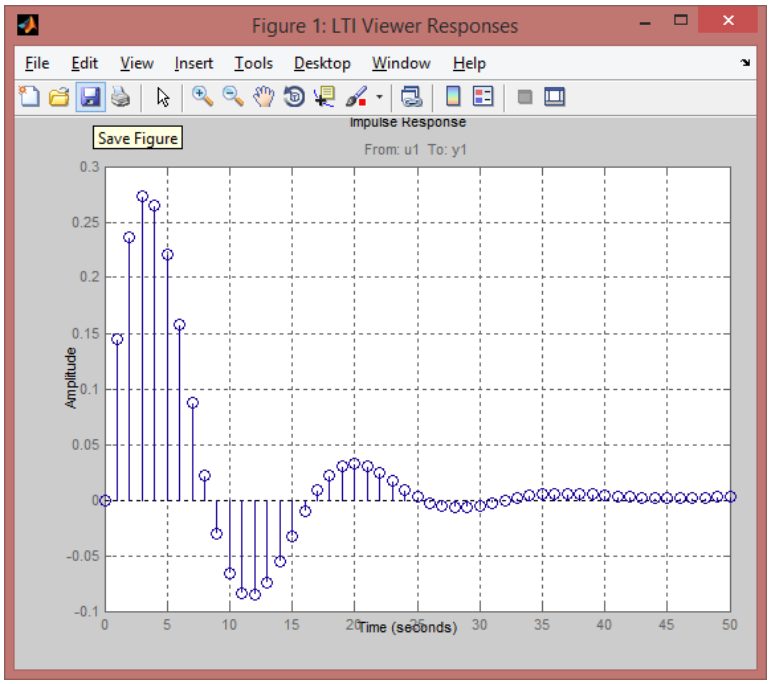

Figure 68: Impulse response (Temperature 1 - Nonlinear)

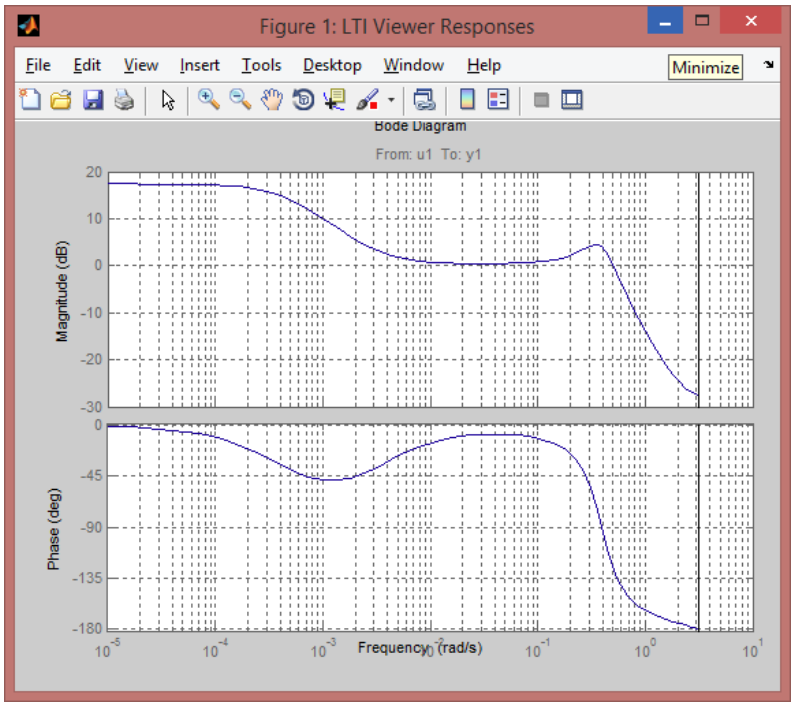

Figure 69: Bode plot (Temperature 1 - Nonlinear)

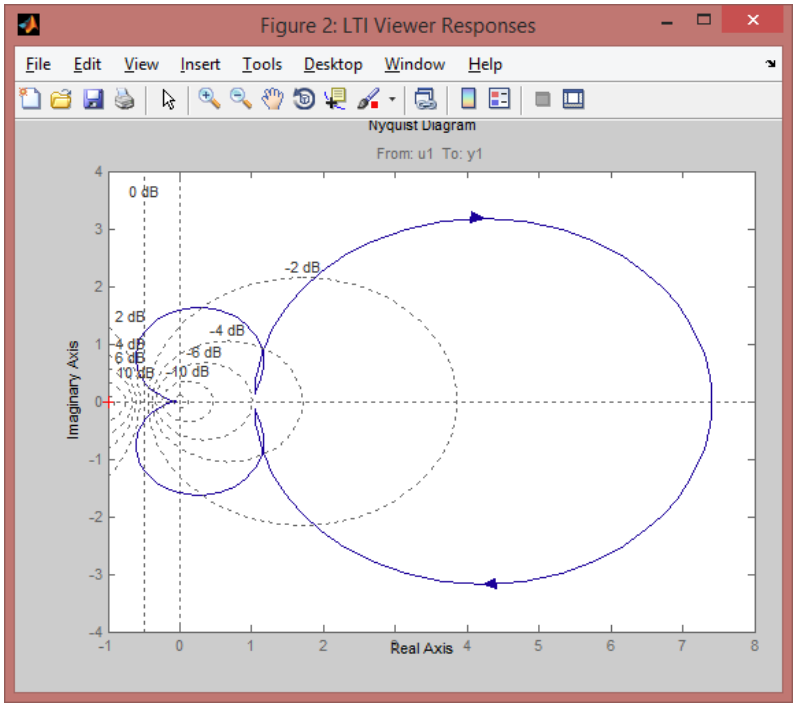

Figure 70: Nyquist plot (Temperature 1 - Nonlinear)

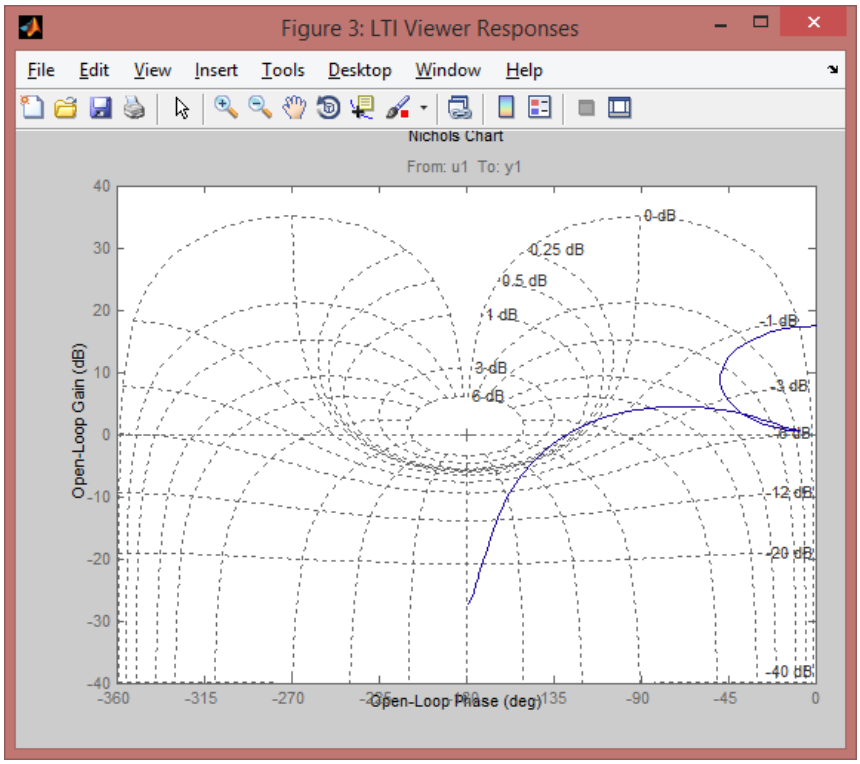

Figure 71: Nichols plot (Temperature 1 - Nonlinear)

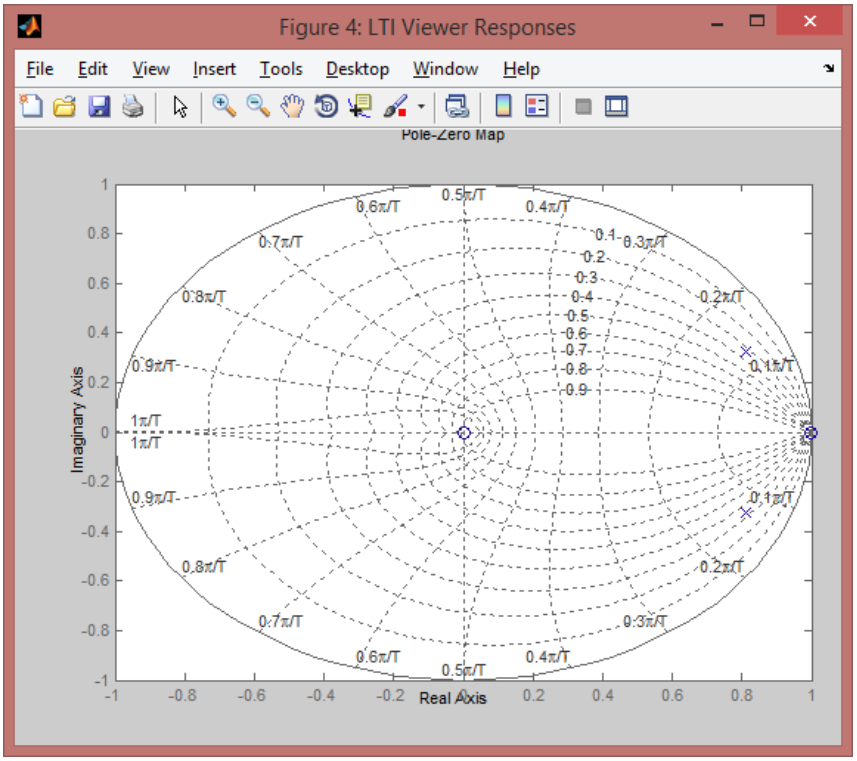

Figure 72: Poles/zero plot (Temperature 1 - Nonlinear)

Temperature 2

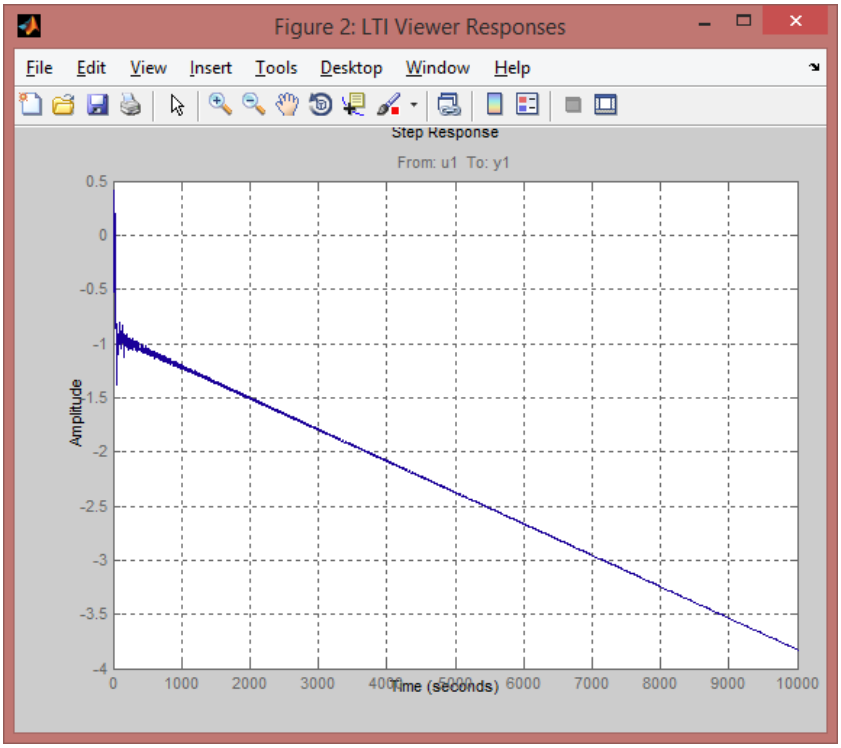

Figure 73: Step response (Temperature 2 - Nonlinear)

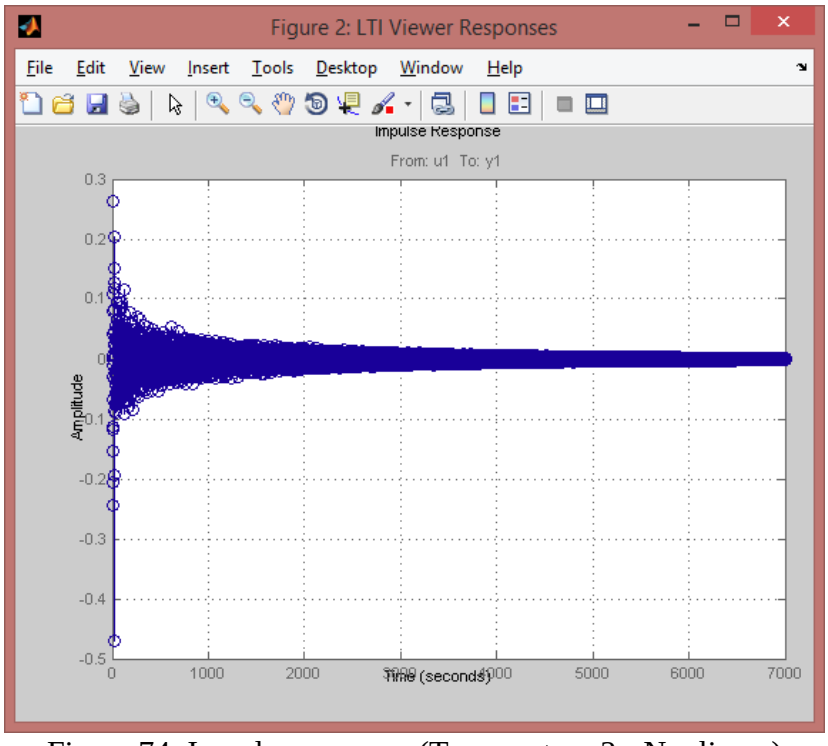

Figure 74: Impulse response (Temperature 2 - Nonlinear)

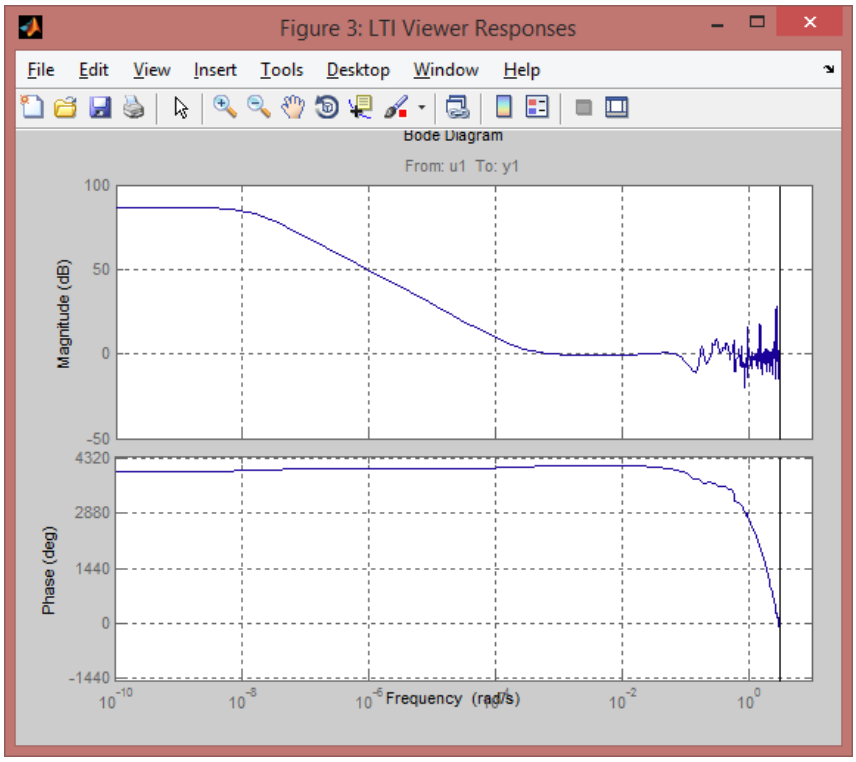

Figure 75: Bode plot (Temperature 2 - Nonlinear)

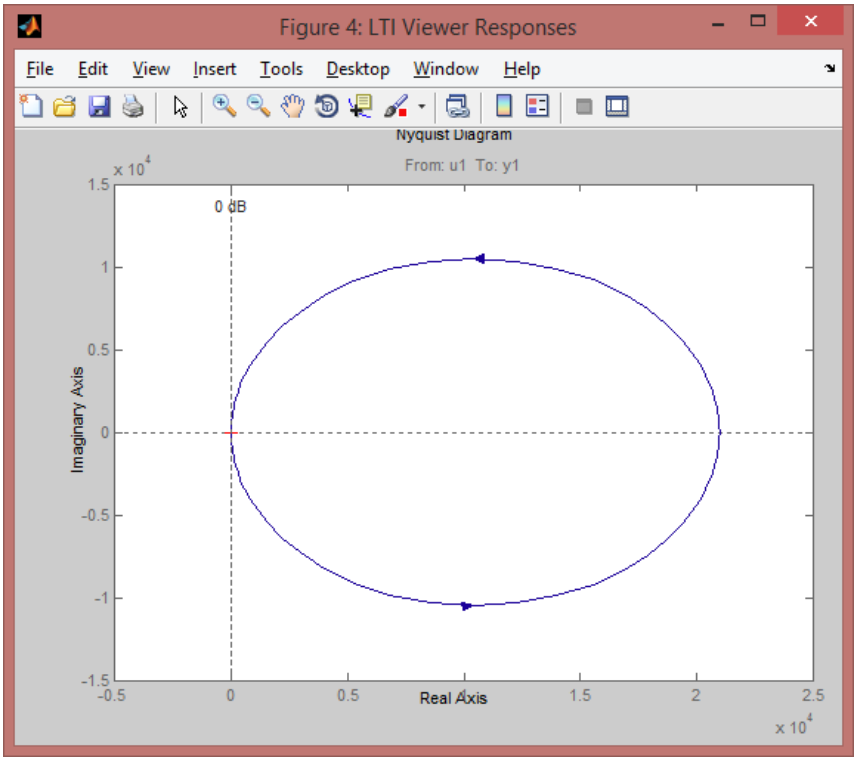

Figure 76: Nyquist plot (Temperature 2 - Nonlinear)

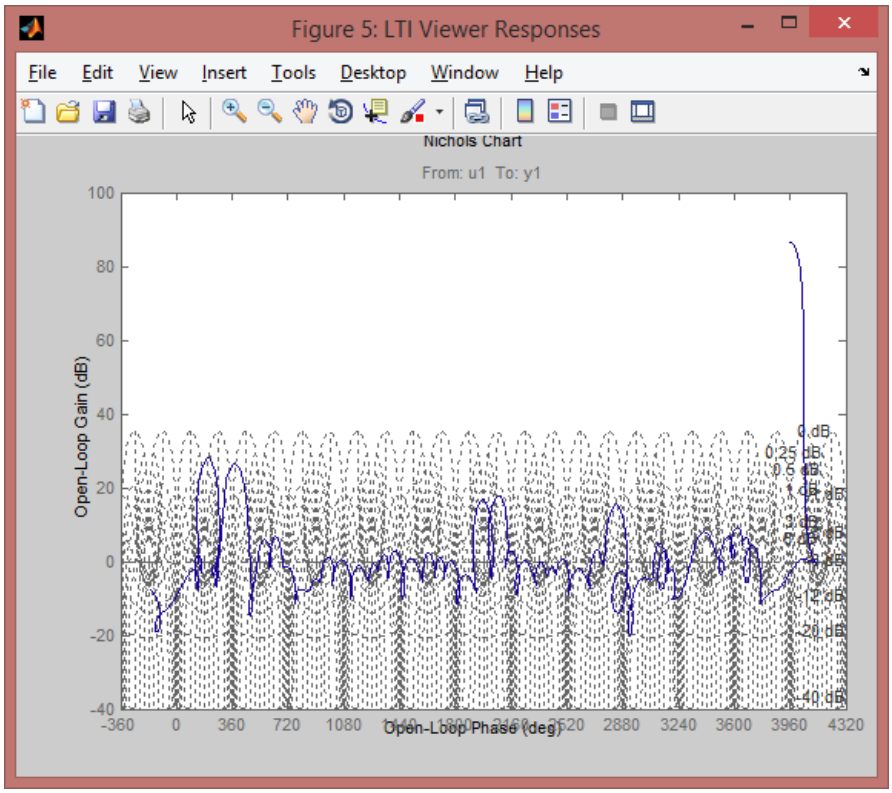

Figure 77: Nichols plot (Temperature 2 - Nonlinear)

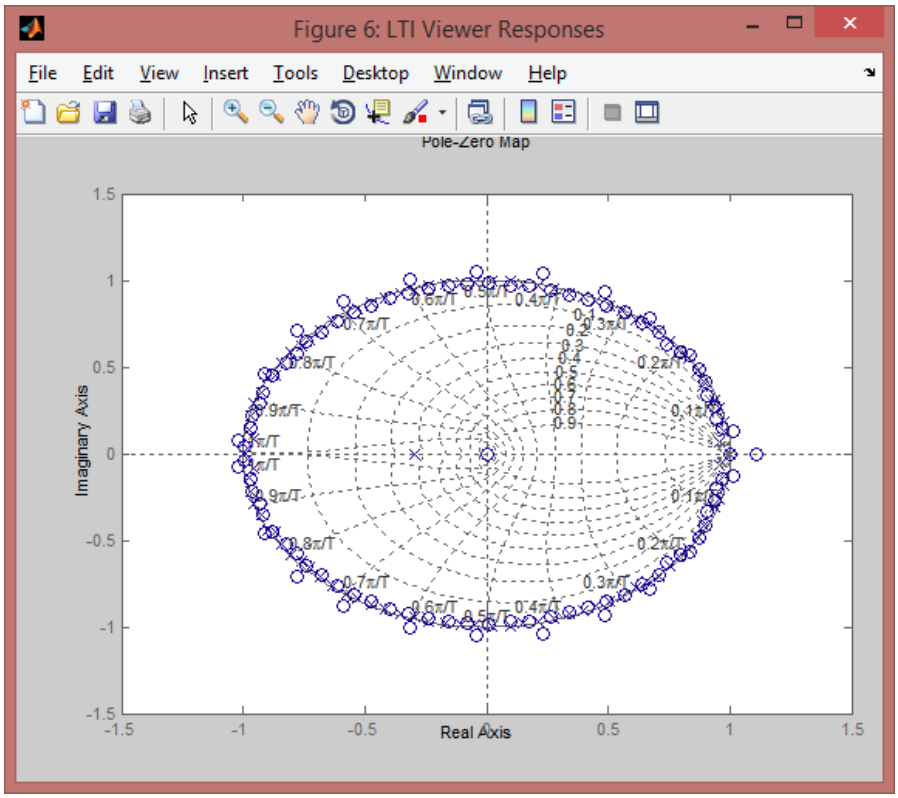

Figure 78: Poles/zero plot (Temperature 2 - Nonlinear)

Temperature 3

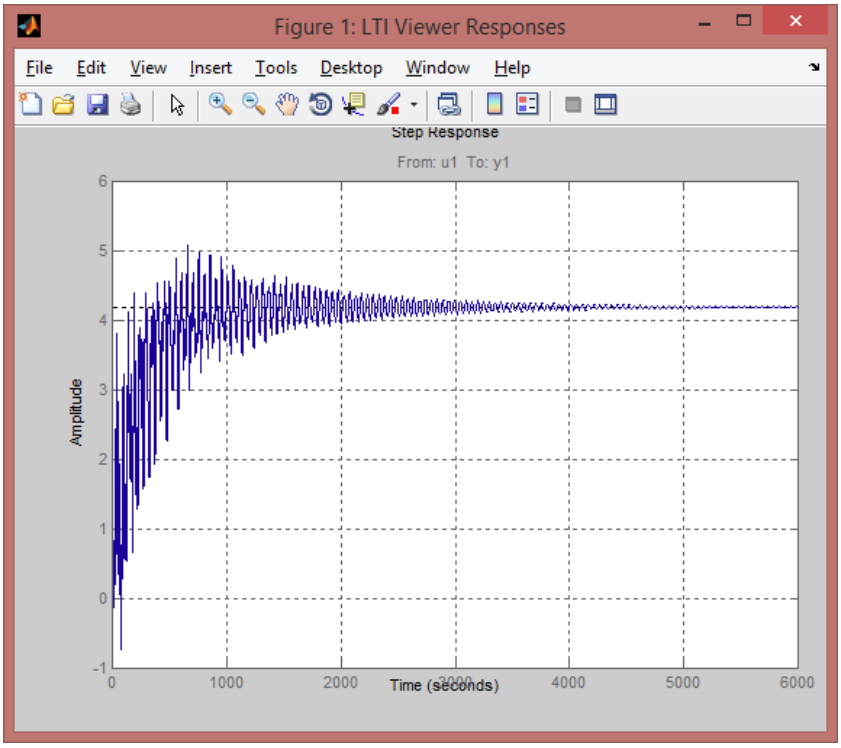

Figure 79: Step response (Temperature 3 - Nonlinear)

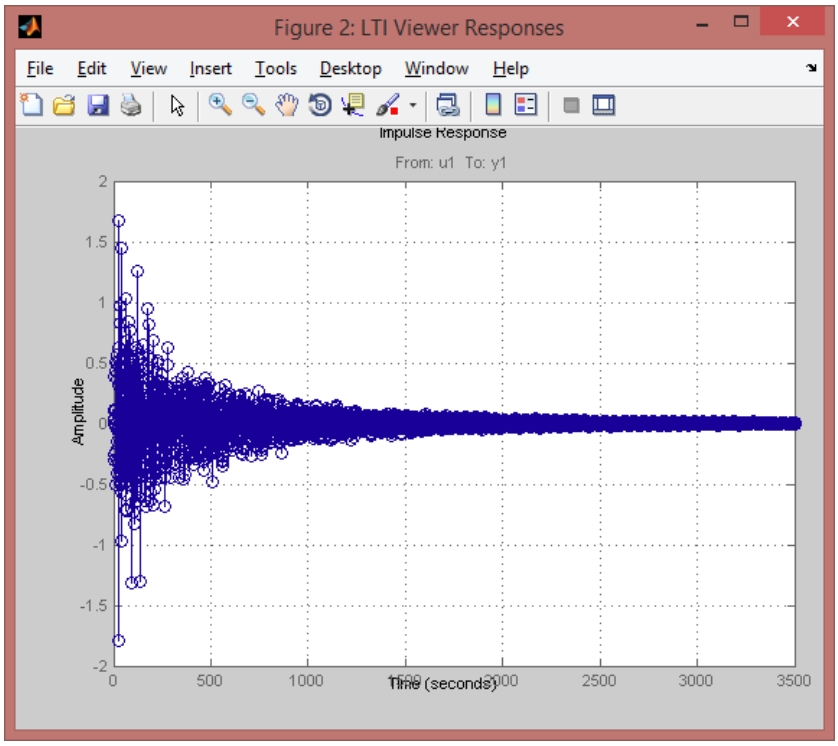

Figure 80: Impulse response (Temperature 3 - Nonlinear)

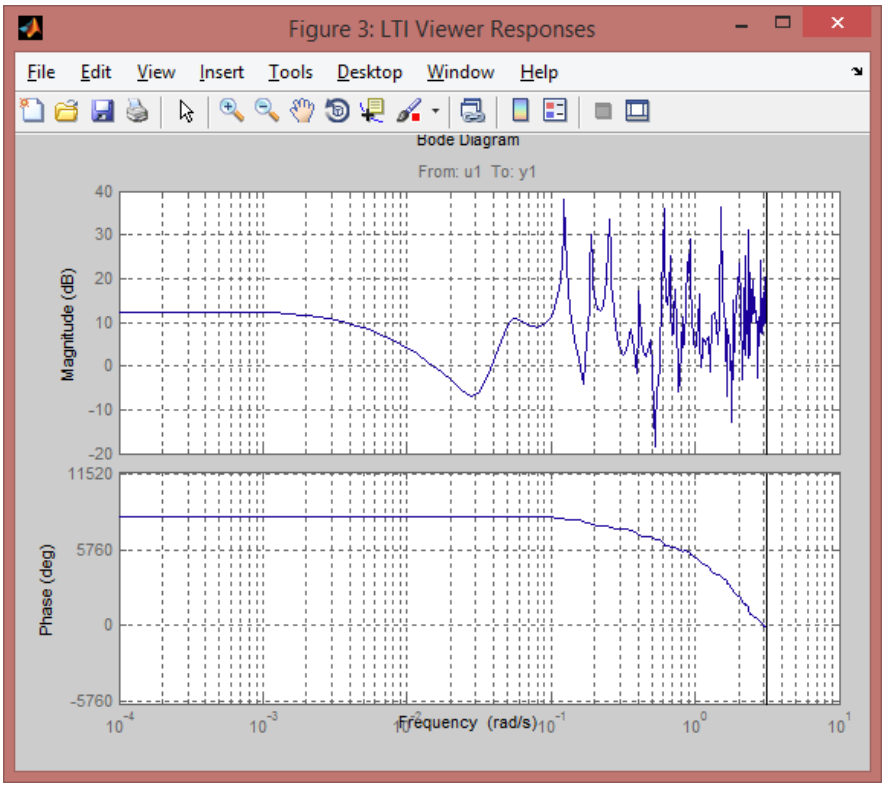

Figure 81: Bode plot (Temperature 3 - Nonlinear)

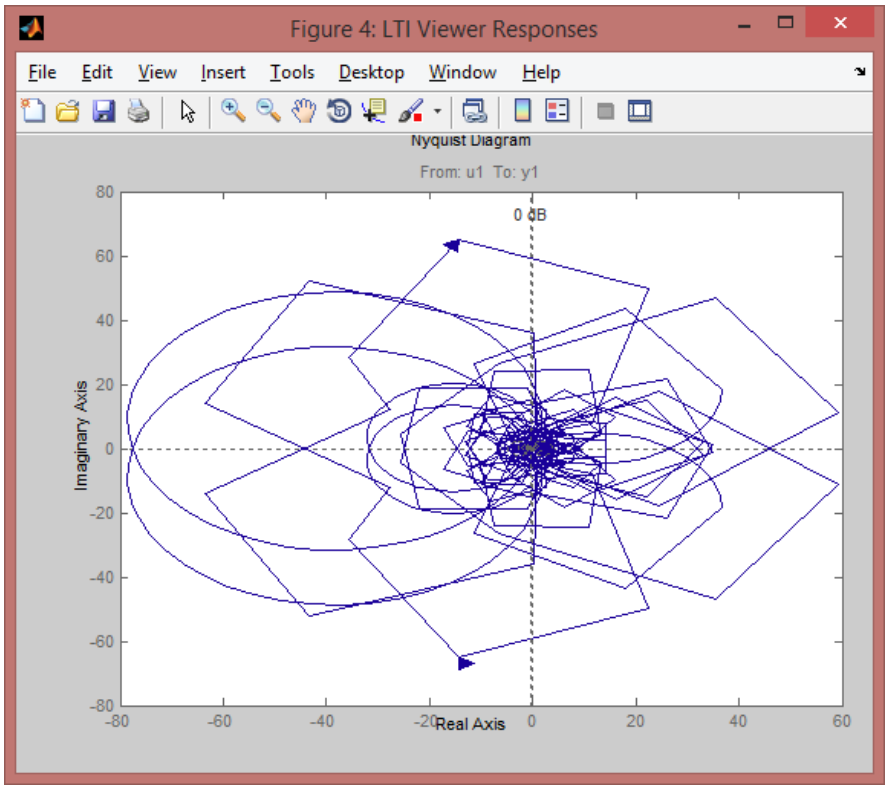

Figure 82: Nyquist plot (Temperature 3 - Nonlinear)

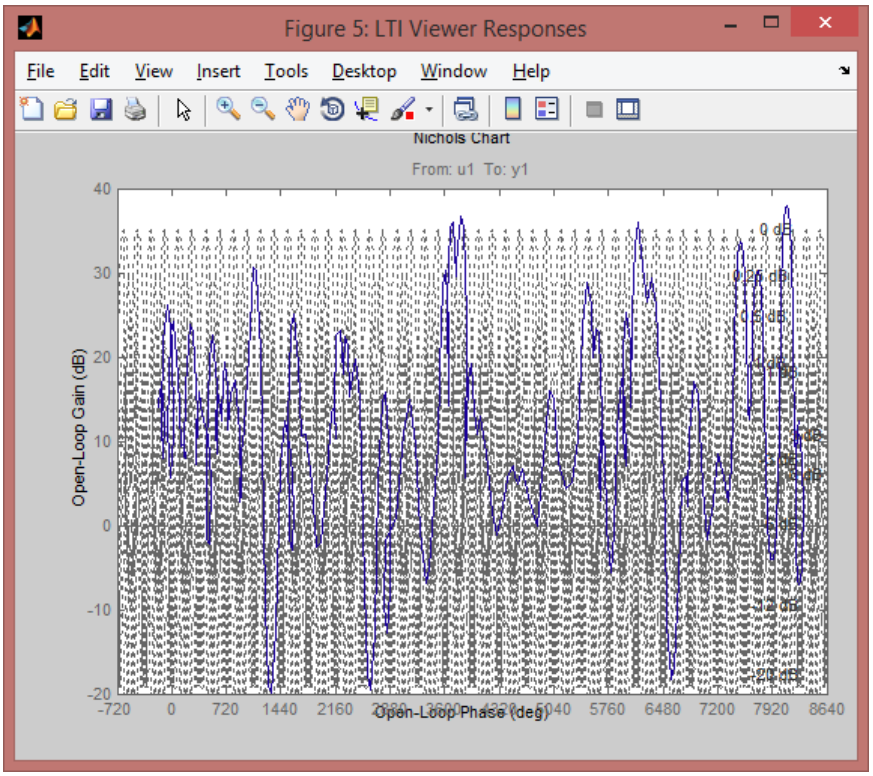

Figure 83: Nichols plot (Temperature 3 - Nonlinear)

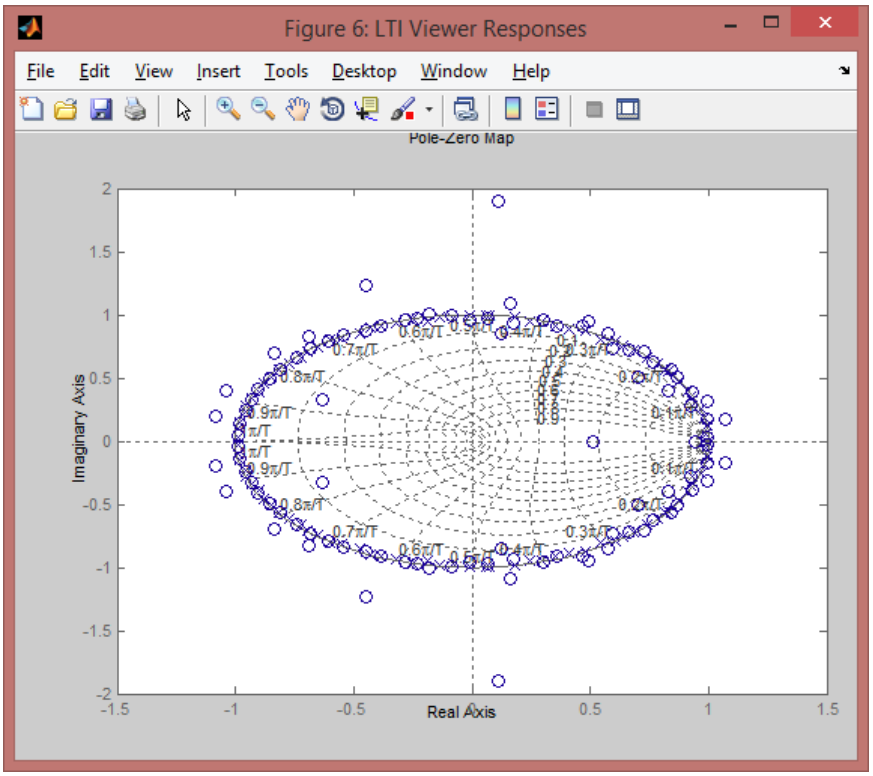

Figure 84: Poles/zero plot (Temperature 3 - Nonlinear)

Temperature 4

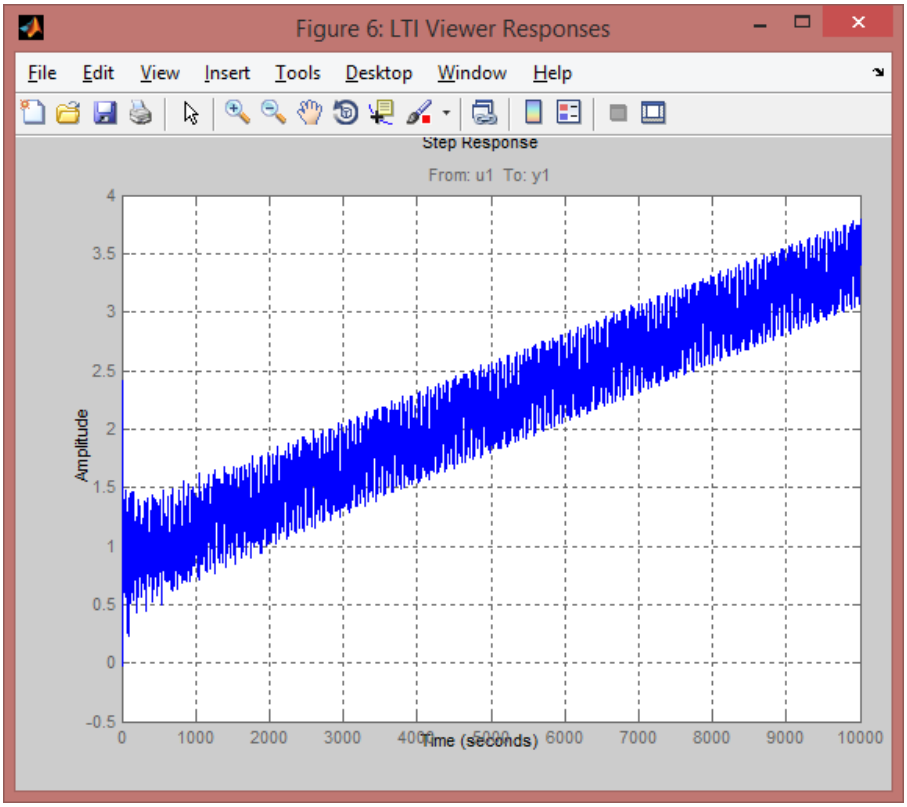

Figure 85: Step response (Temperature 4 - Nonlinear)

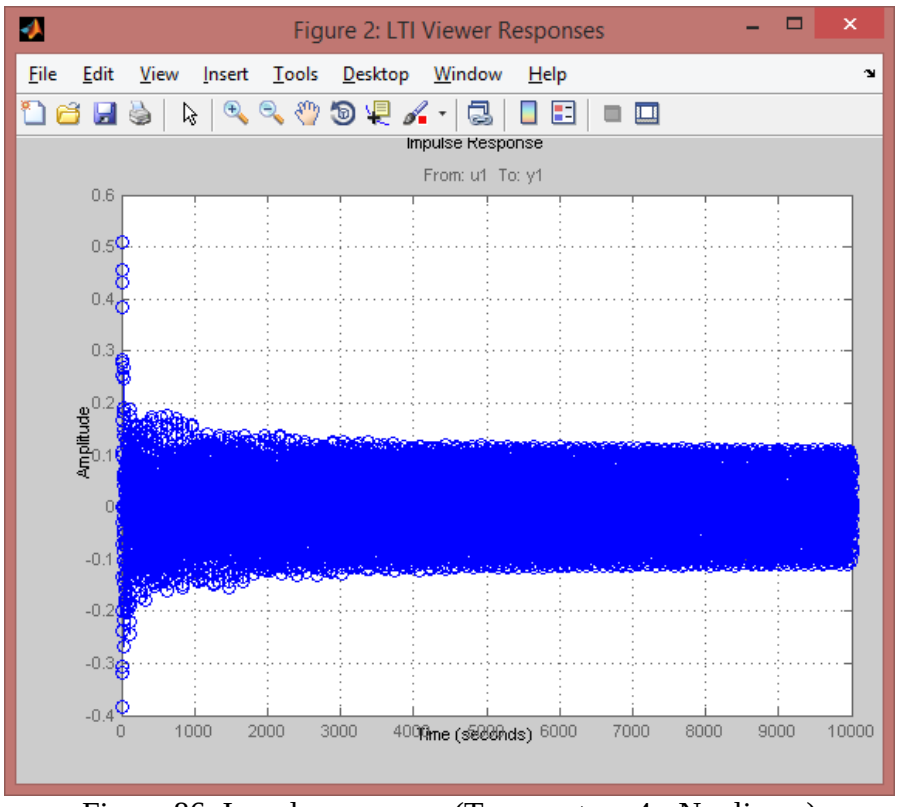

Figure 86: Impulse response (Temperature 4 - Nonlinear)

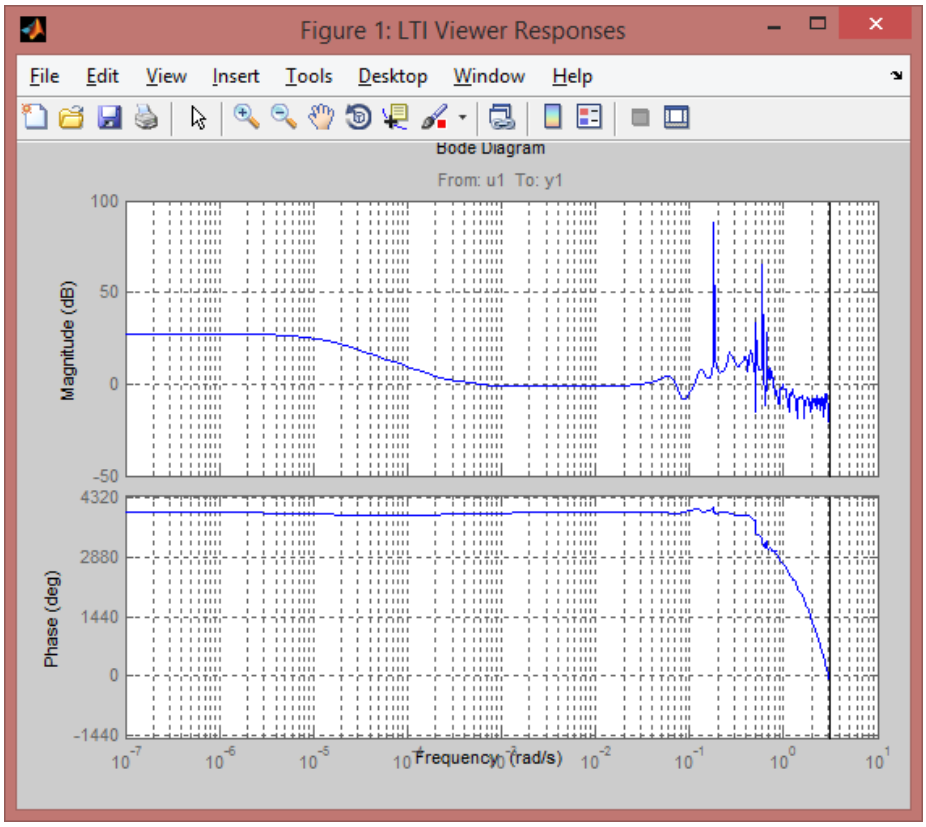

Figure 87: Bode plot (Temperature 4 – Nonlinear)

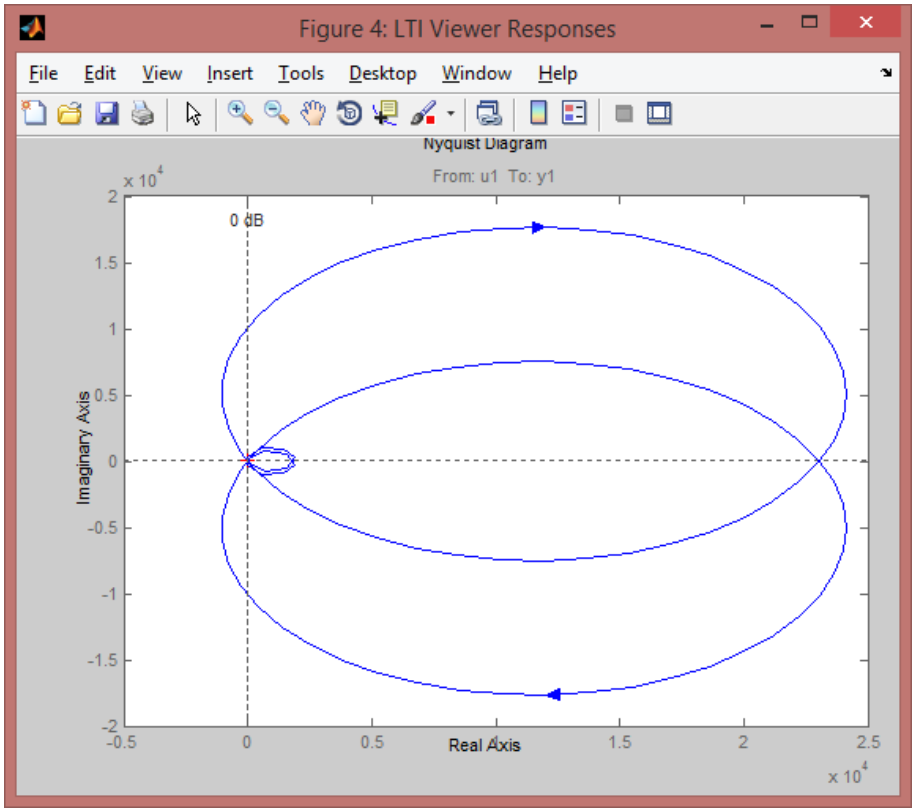

Figure 88: Nyquist plot (Temperature 4 - Nonlinear)

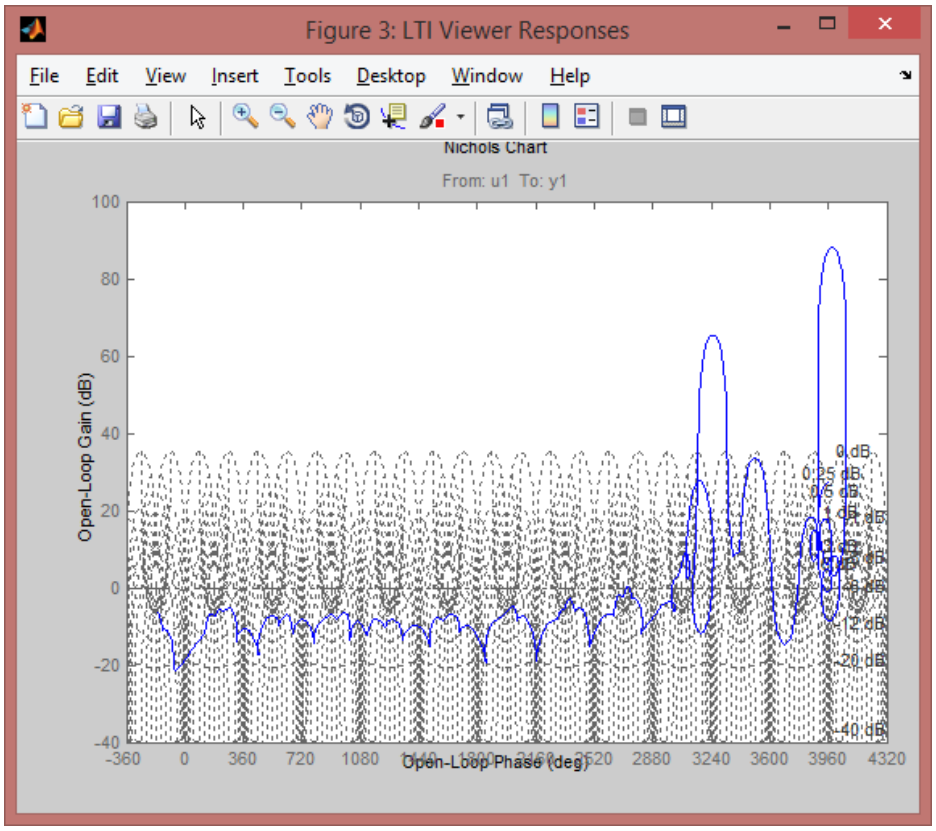

Figure 89: Nichols plot (Temperature 4 - Nonlinear)

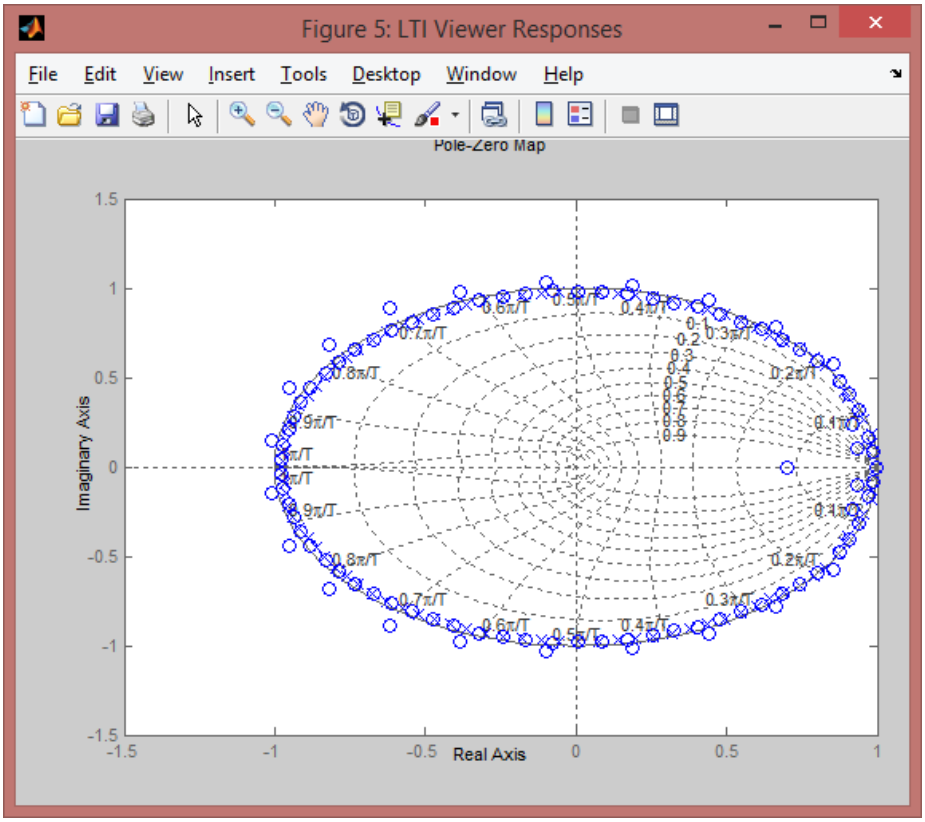

Figure 90: Poles/zero plot (Temperature 4 - Nonlinear)

Temperature 5

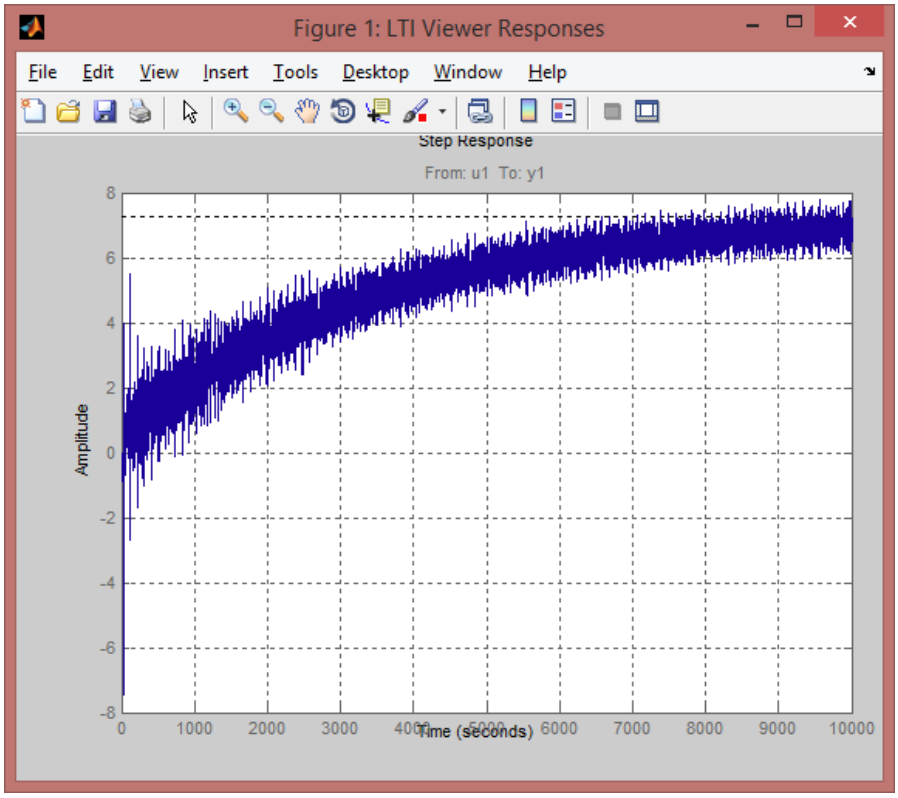

Figure 91: Step response (Temperature 5 - Nonlinear)

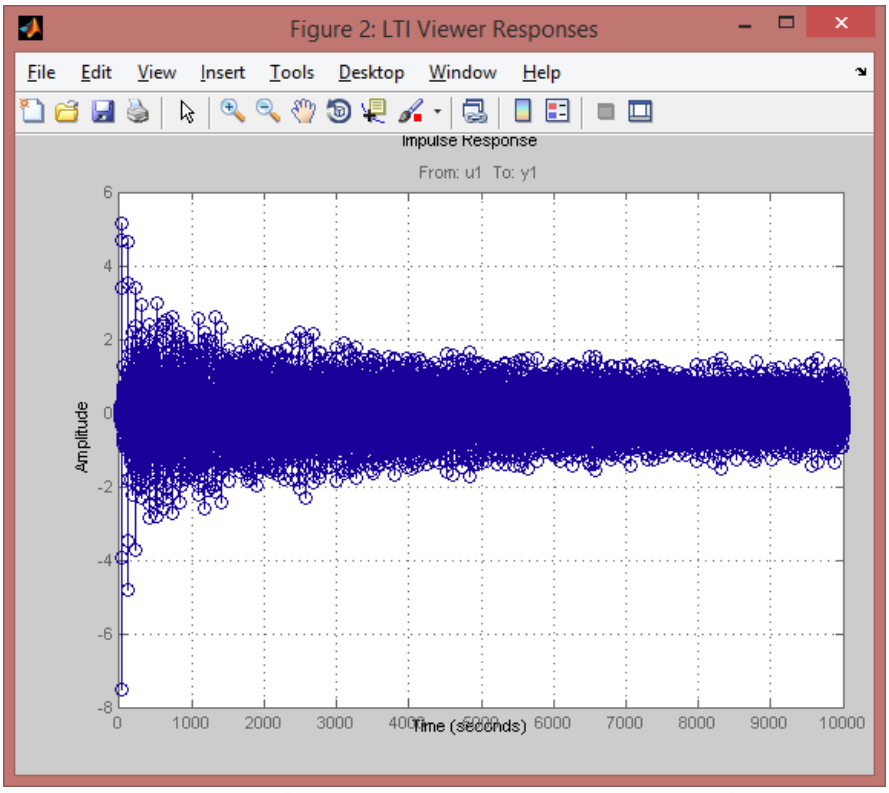

Figure 92: Impulse response (Temperature 5 - Nonlinear)

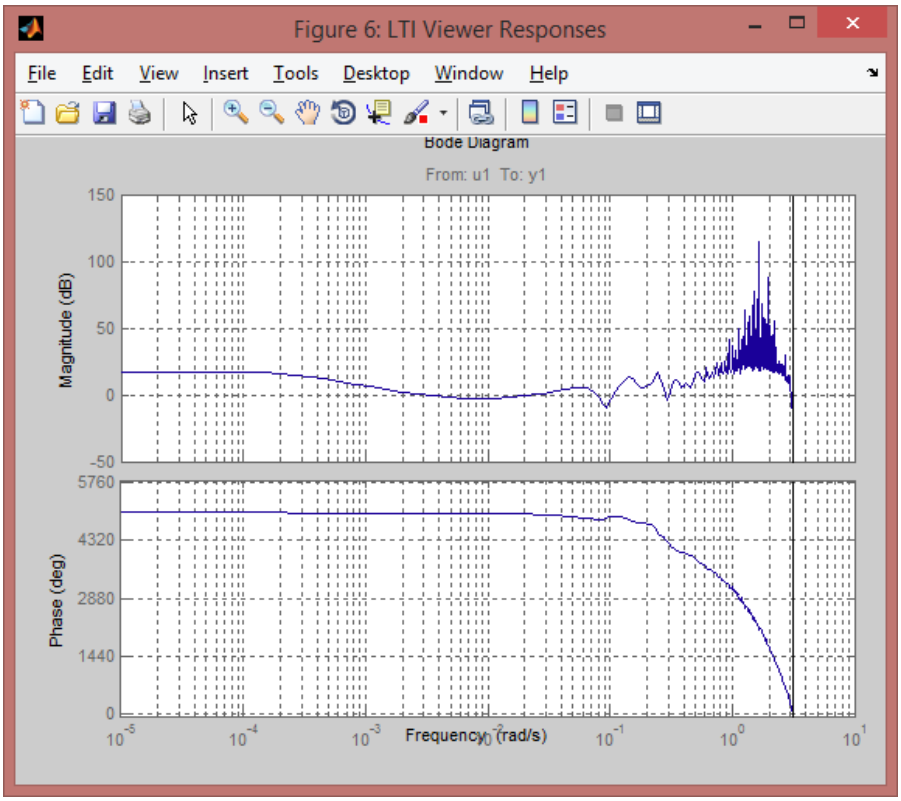

Figure 93: Bode plot (Temperature 5 - Nonlinear)

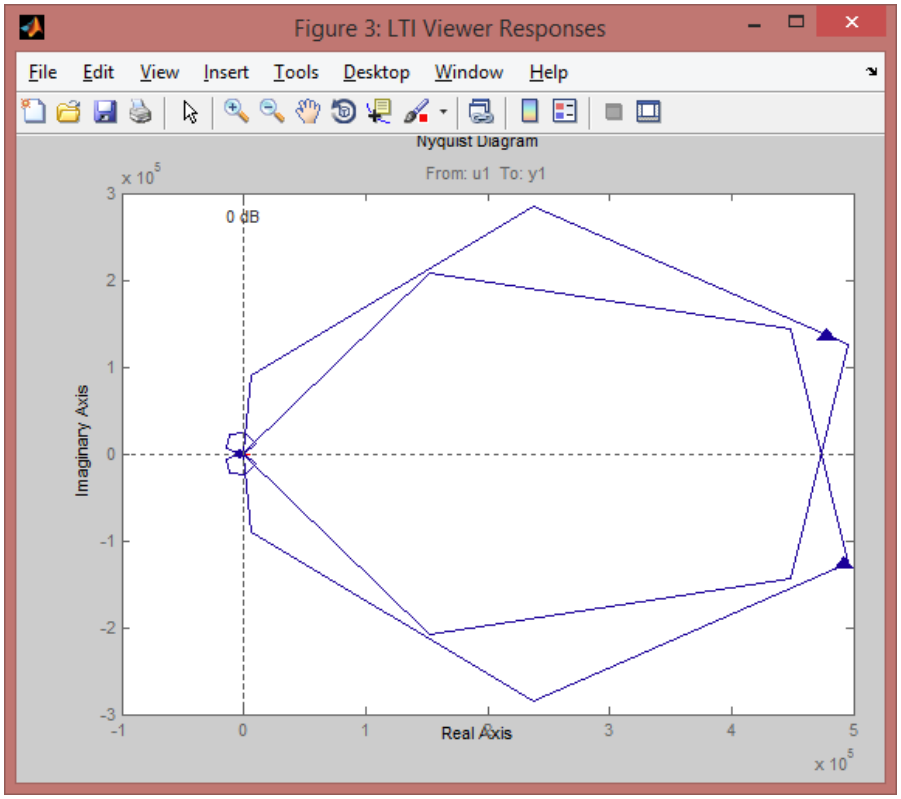

Figure 94: Nyquist plot (Temperature 5 - Nonlinear)

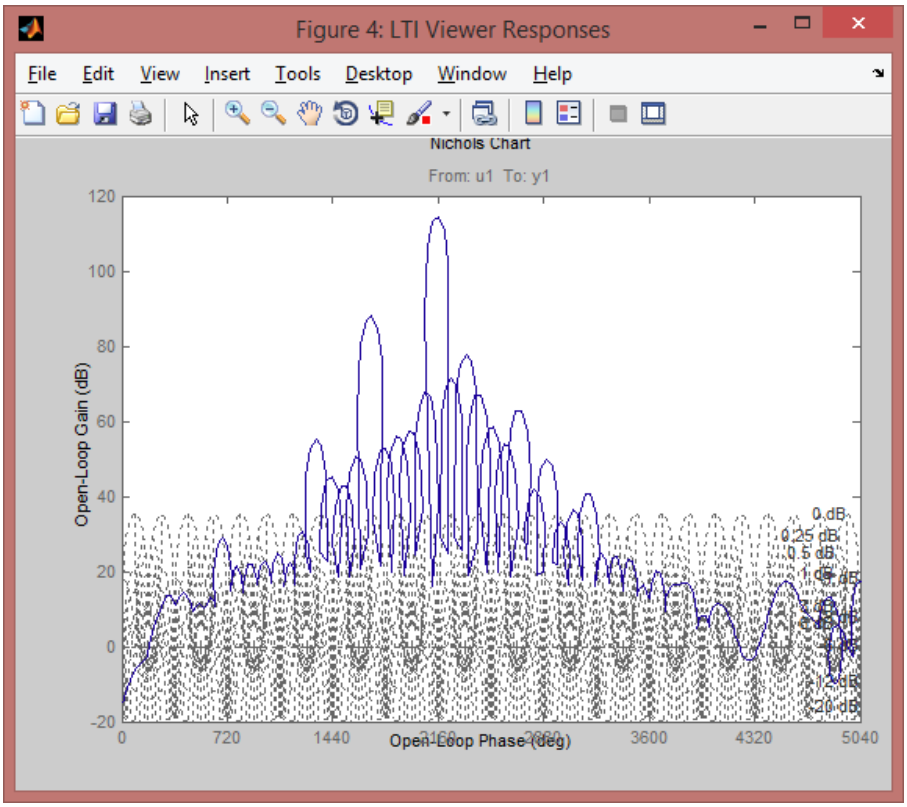

Figure 95: Nichols plot (Temperature 5 - Nonlinear)

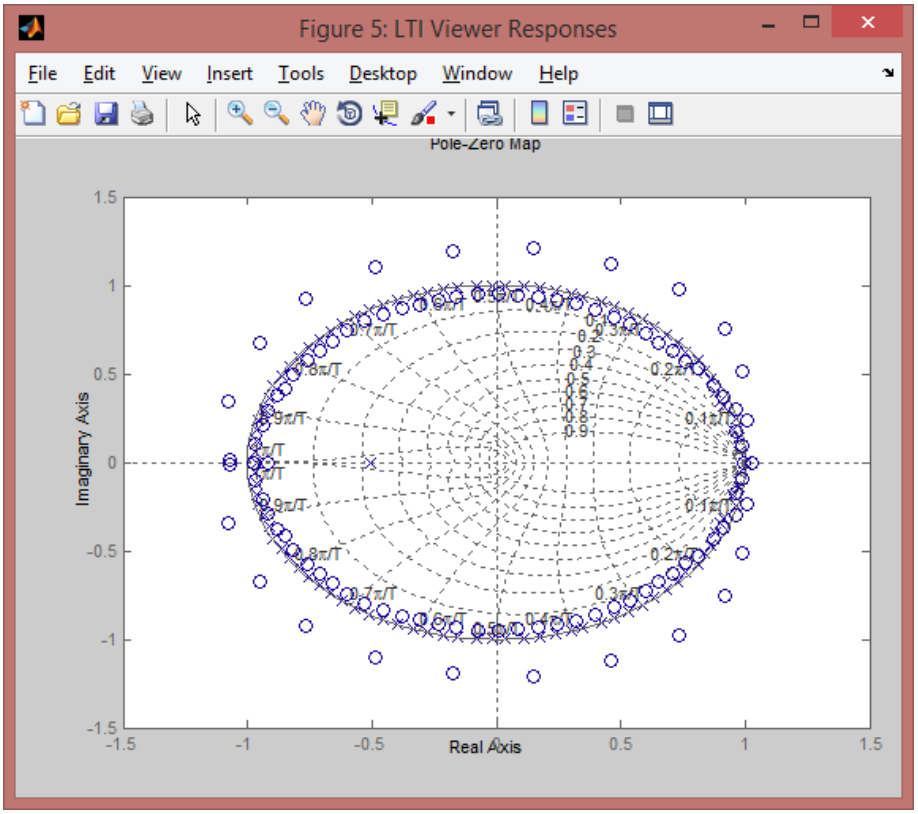

Figure 96: Poles/zero plot (Temperature 5 - Nonlinear)

Temperature 6

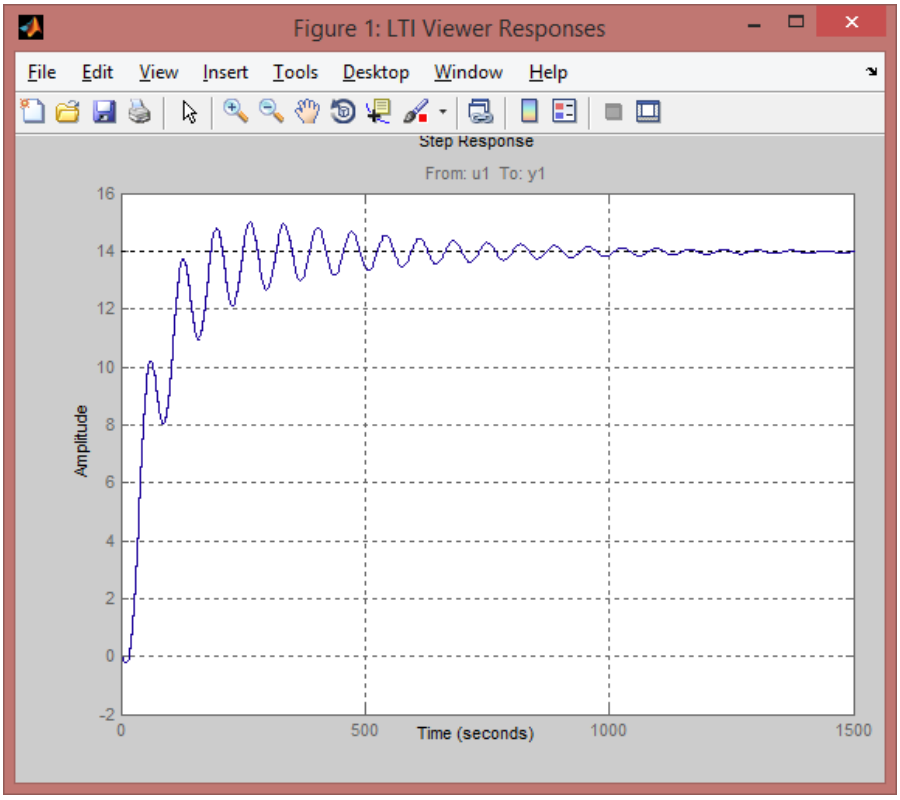

Figure 97: Step response (Temperature 6 - Nonlinear)

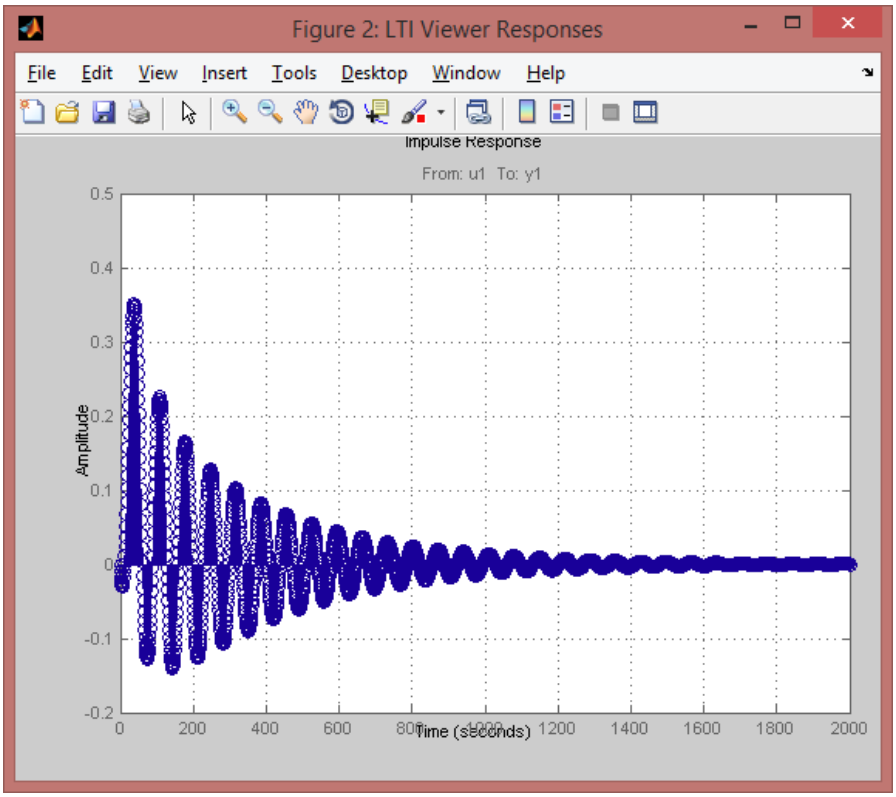

Figure 98: Impulse response (Temperature 6 - Nonlinear)

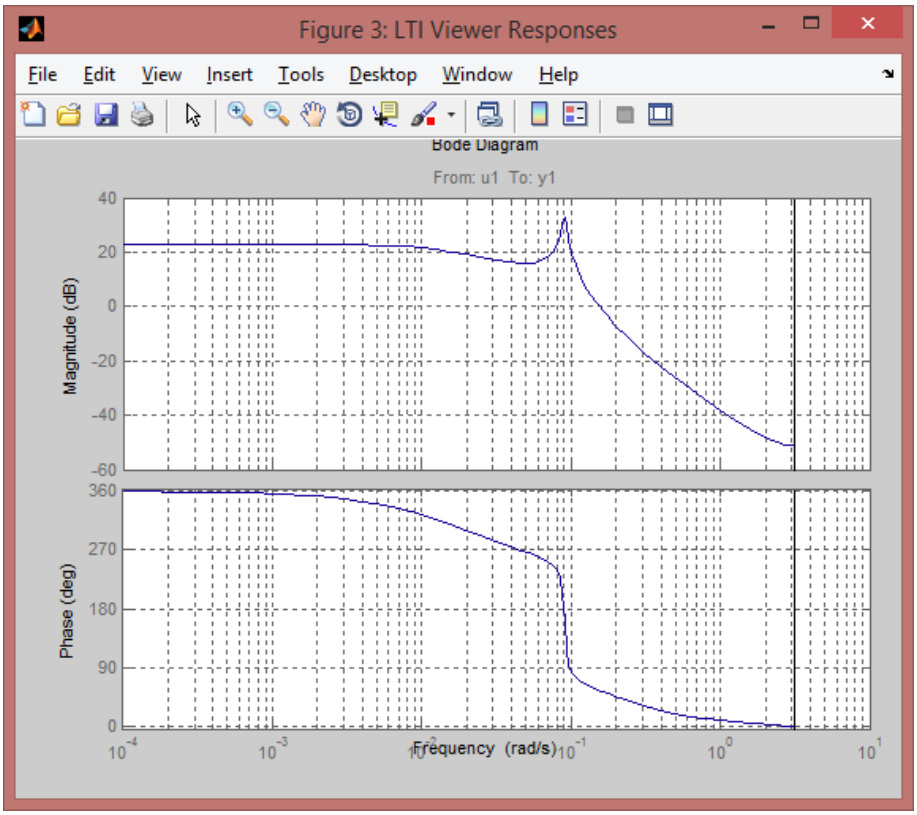

Figure 99: Bode plot (Temperature 6 - Nonlinear)

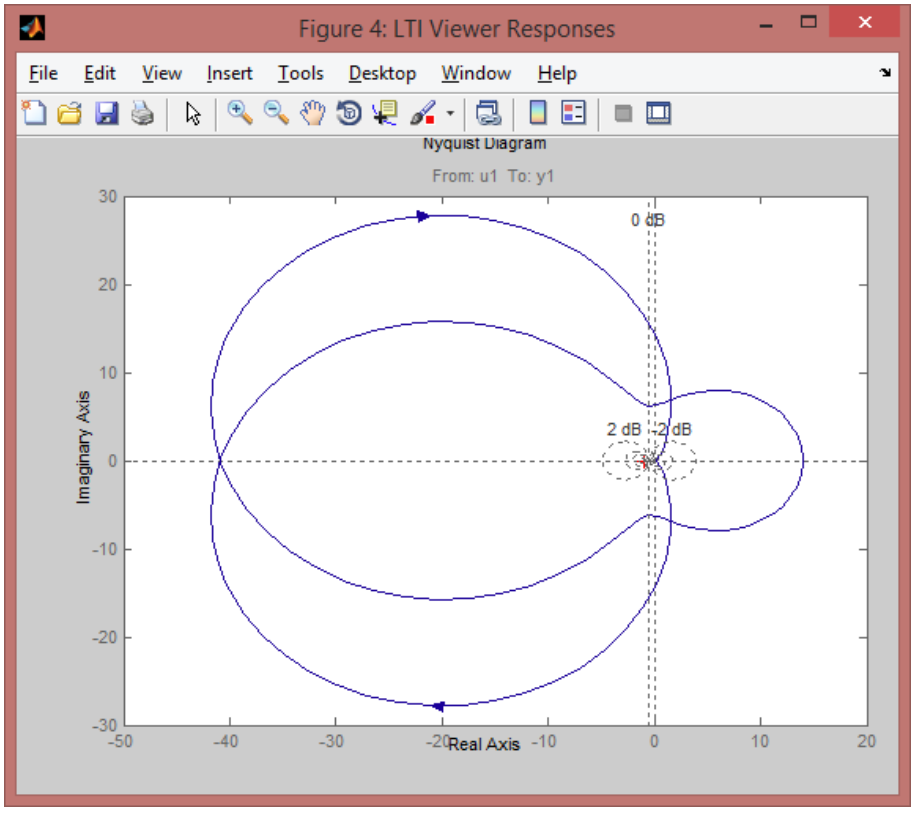

Figure 100: Nyquist plot (Temperature 6 - Nonlinear)

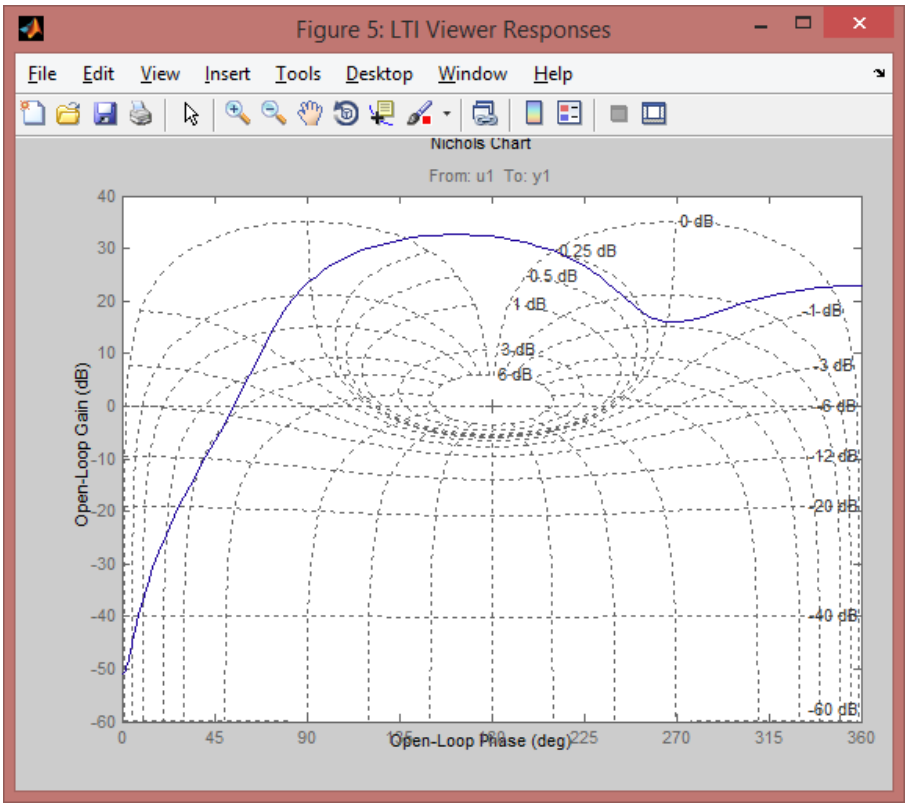

Figure 101: Nichols plot (Temperature 6 - Nonlinear)

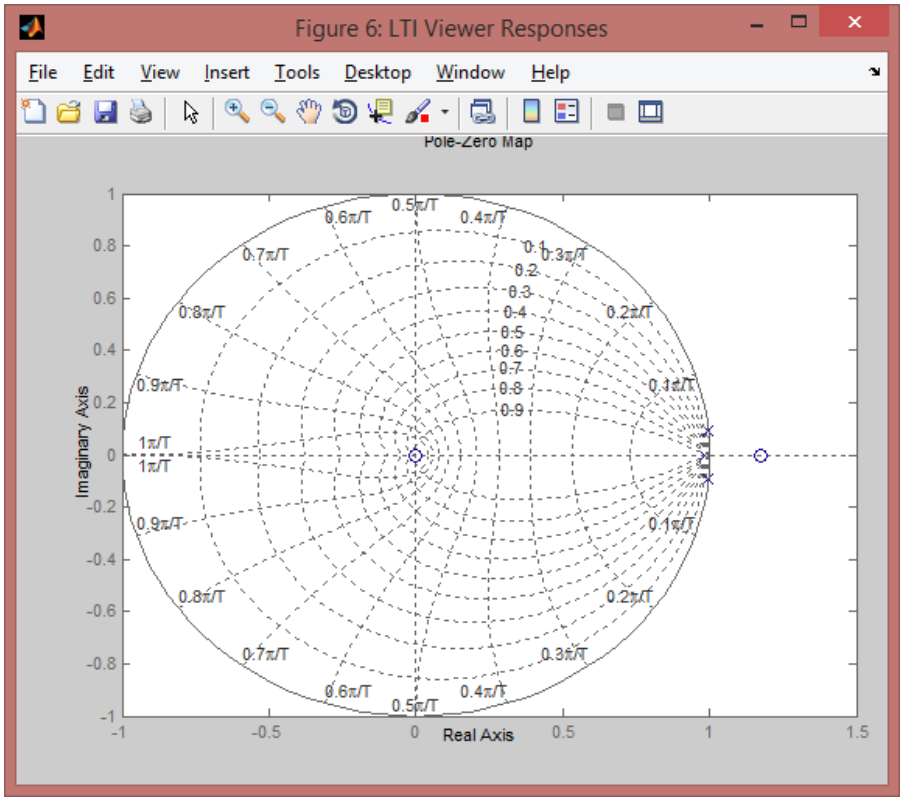

Figure 102: Poles/zero plot (Temperature 6 - Nonlinear)

Level 1

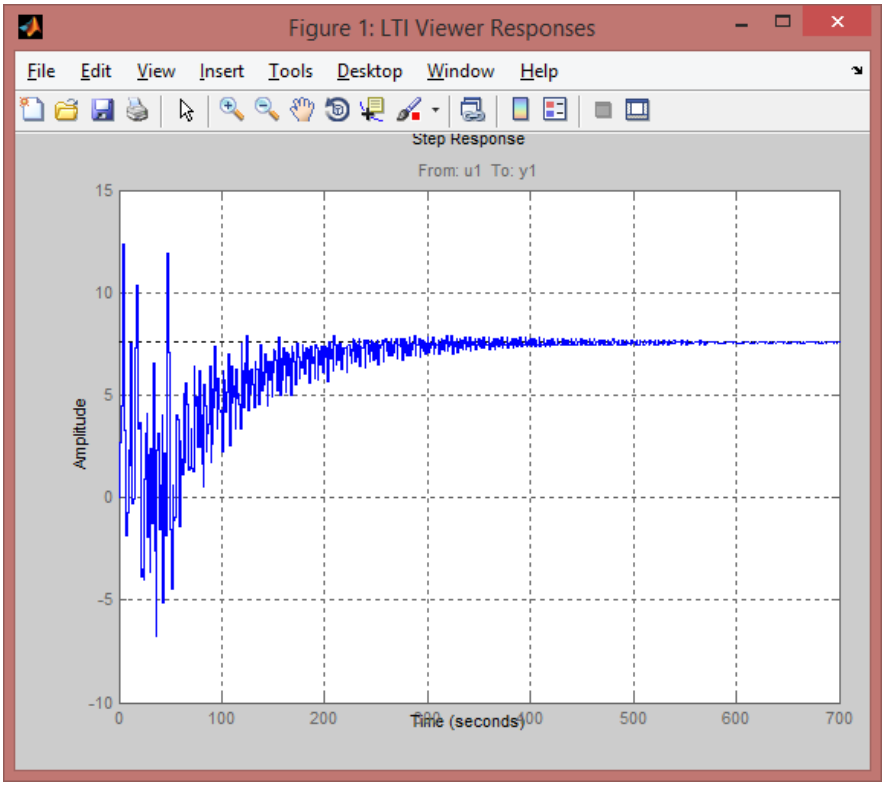

Figure 103: Step response (Level 1 - Nonlinear)

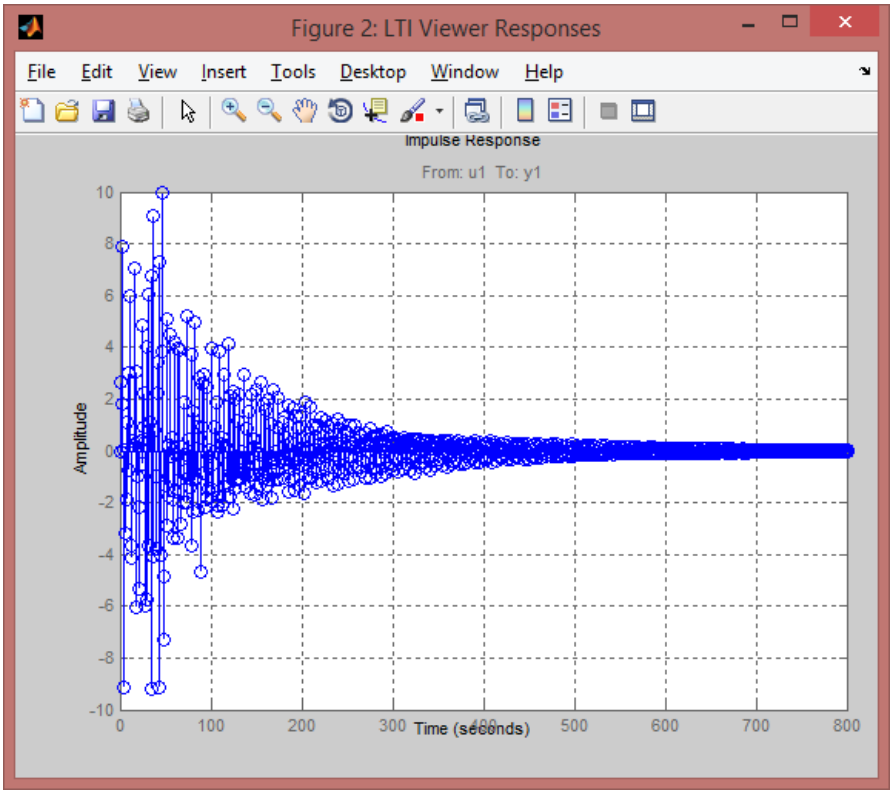

Figure 104: Impulse plot (Level 1 - Nonlinear)

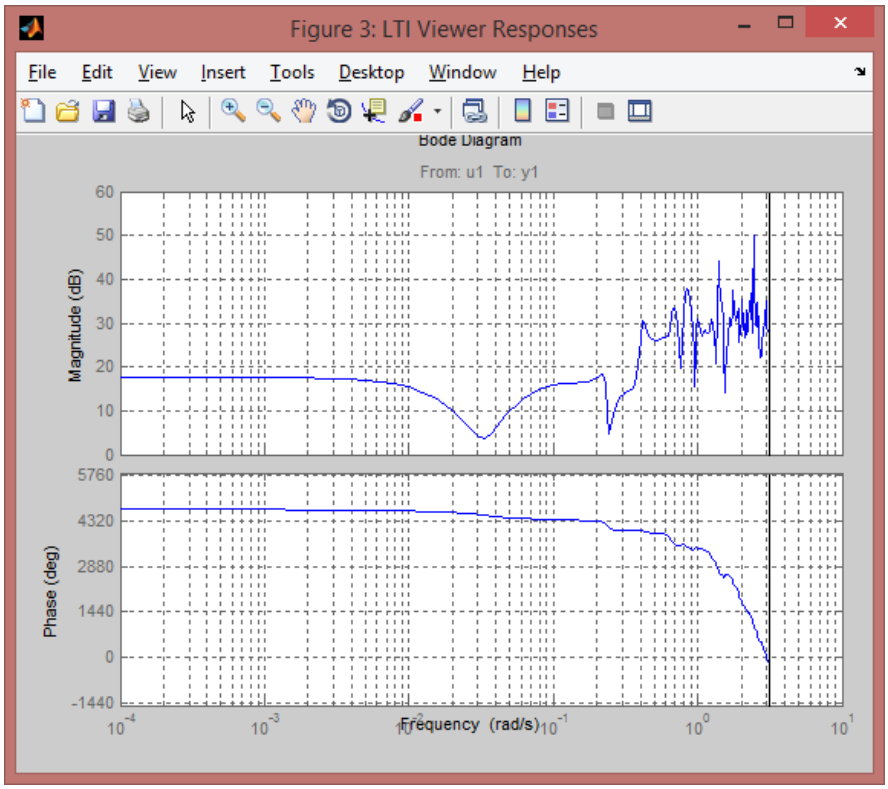

Figure 105: Bode plot (Level 1 - Nonlinear)

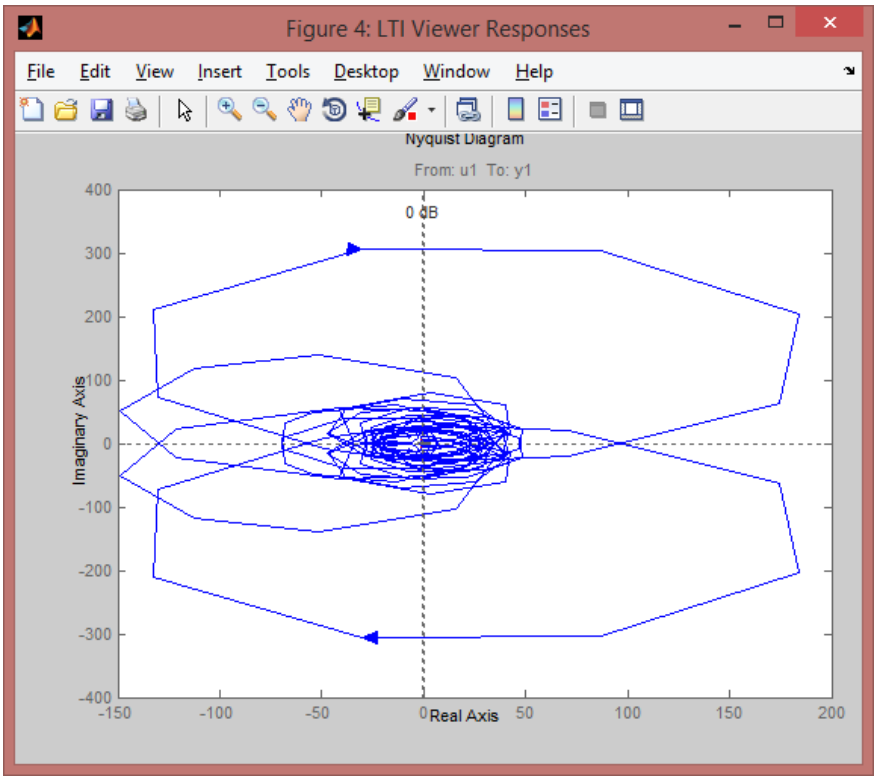

Figure 106: Nyquist plot (Level 1 - Nonlinear)

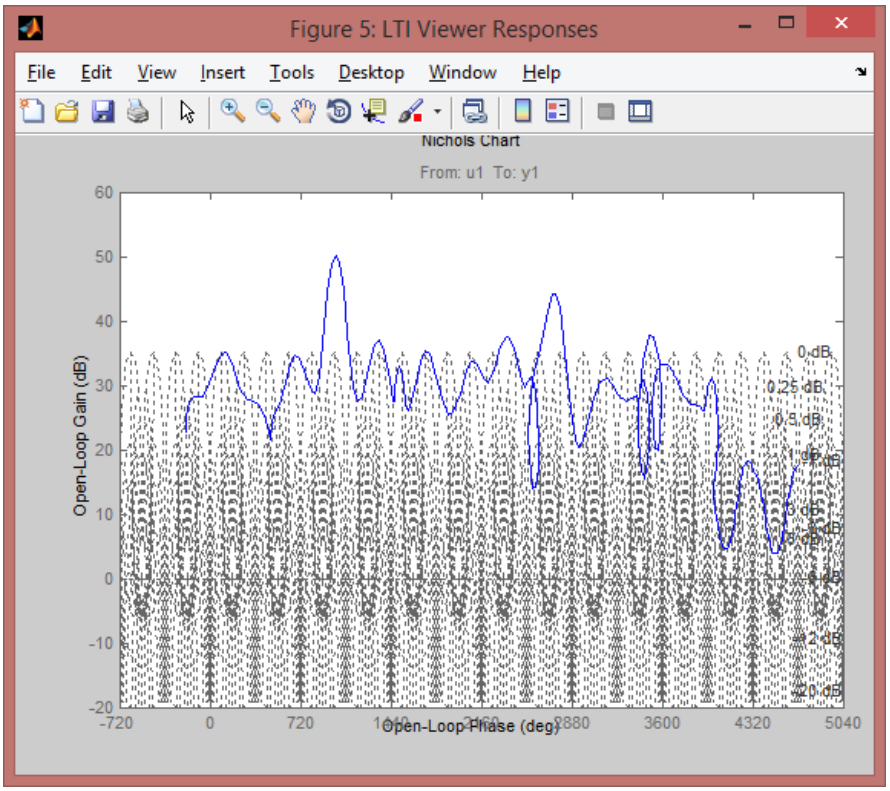

Figure 107: Nichols plot (Level 1 - Nonlinear)

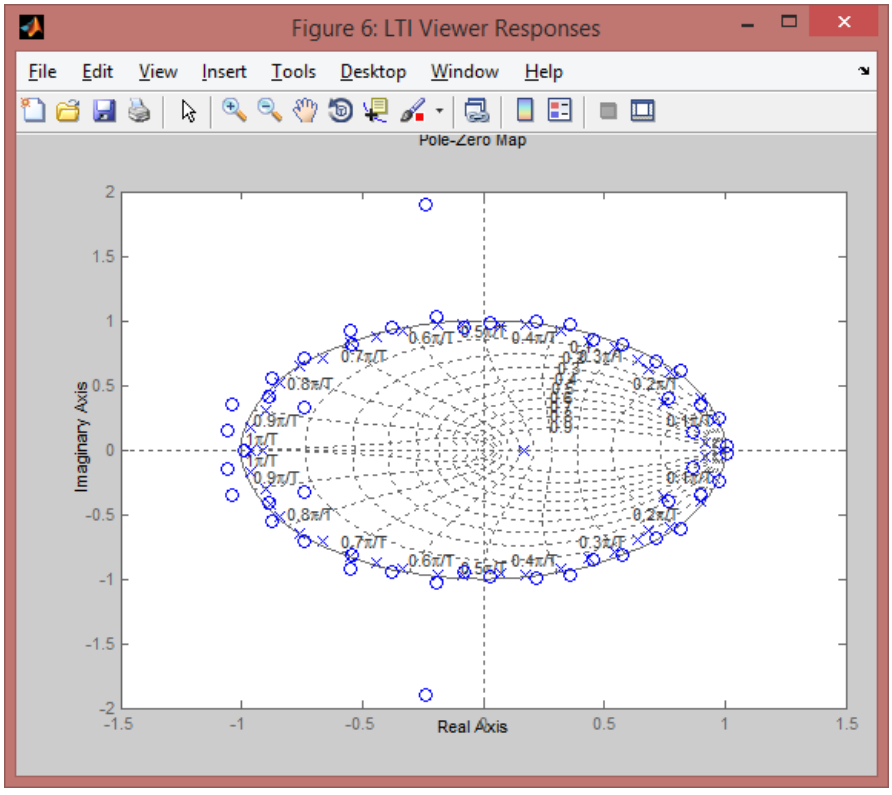

Figure 108: Poles/zero plot (Level 1 - Nonlinear)

Level 2

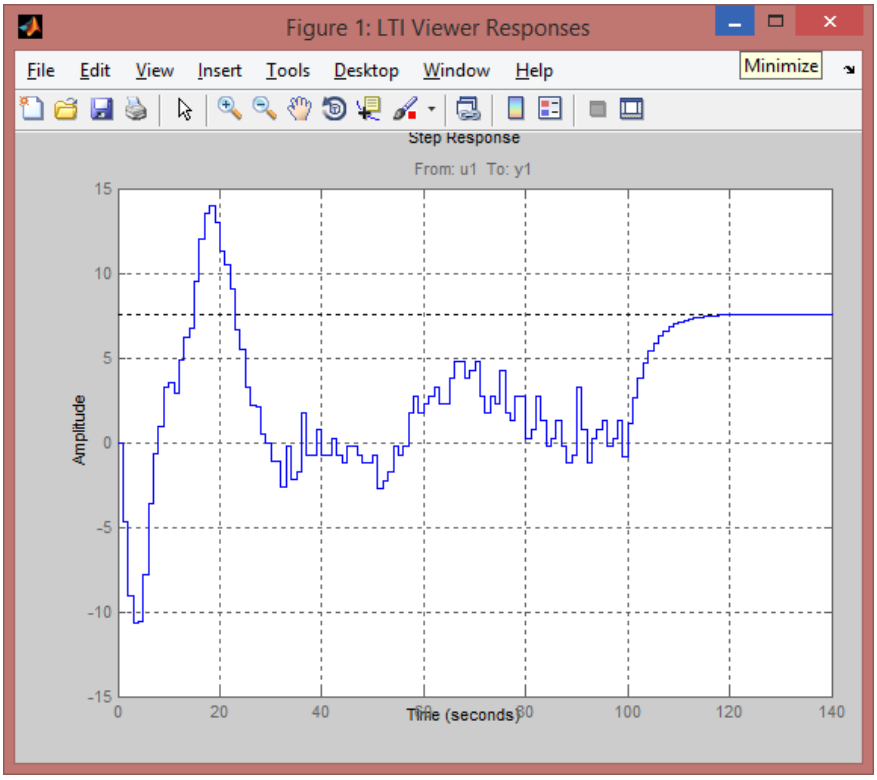

Figure 109: Step response (Level 2 - Nonlinear)

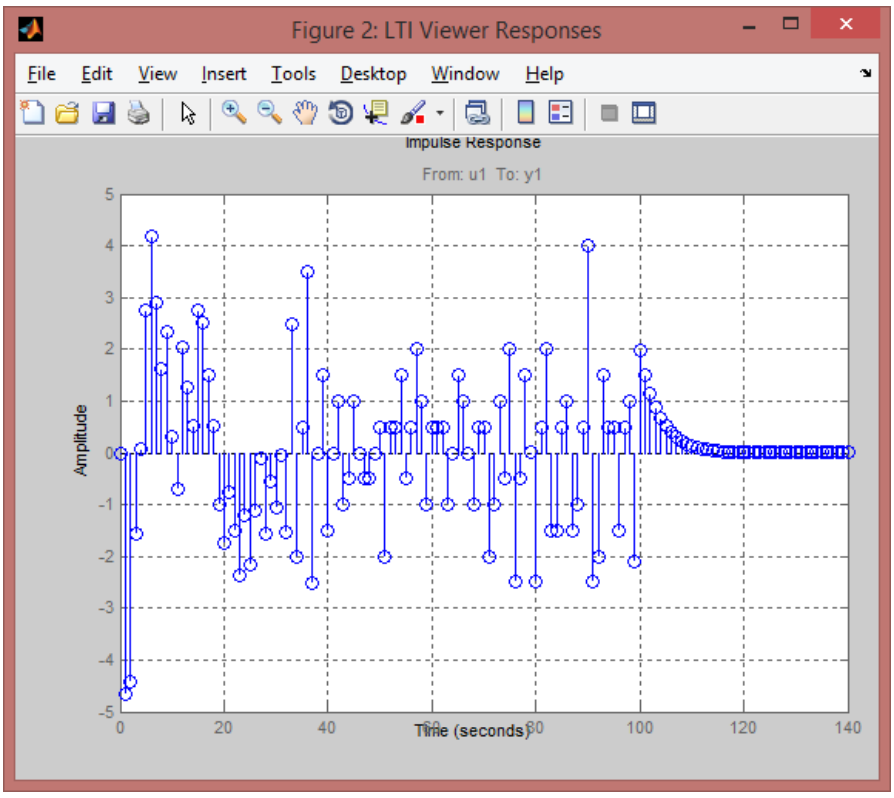

Figure 110: Impulse response (Level 2 - Nonlinear)

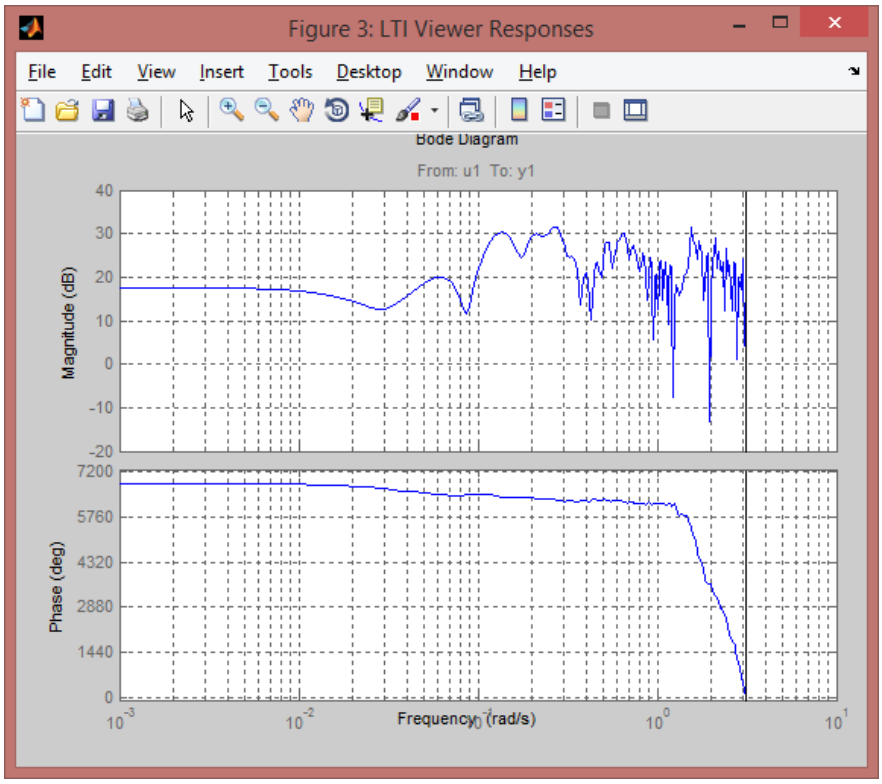

Figure 111: Bode plot (Level 2 - Nonlinear)

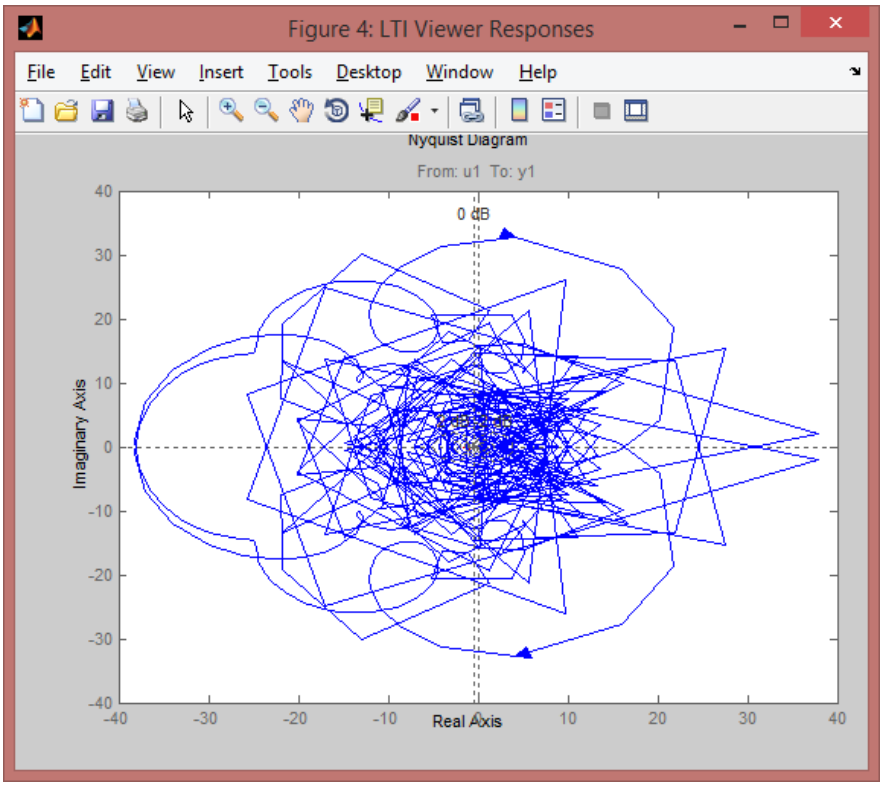

Figure 112: Nyquist plot (Level 2 - Nonlinear)

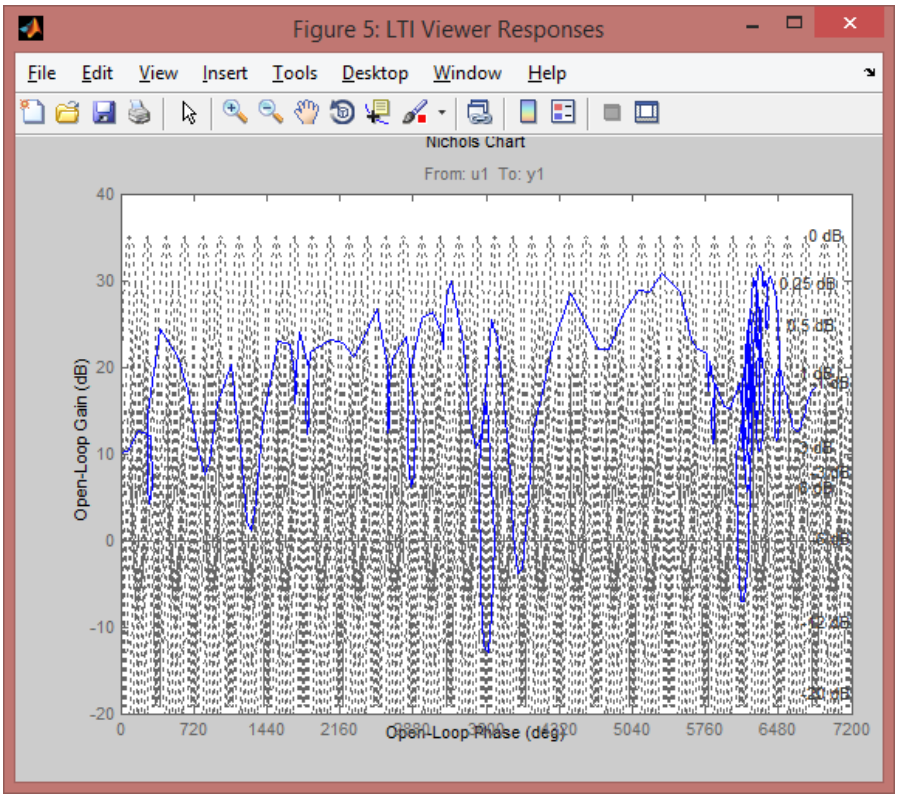

Figure 113: Nichols plot (Level 2 - Nonlinear)

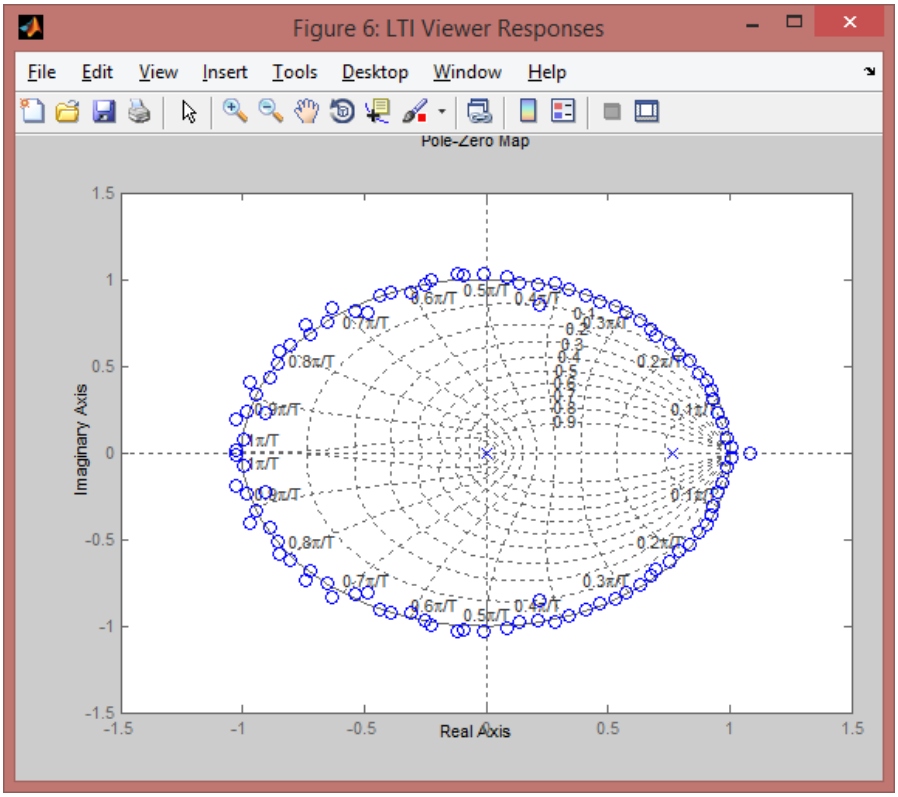

Figure 114: Poles/zero plot (Level 2 - Nonlinear)

Level 3

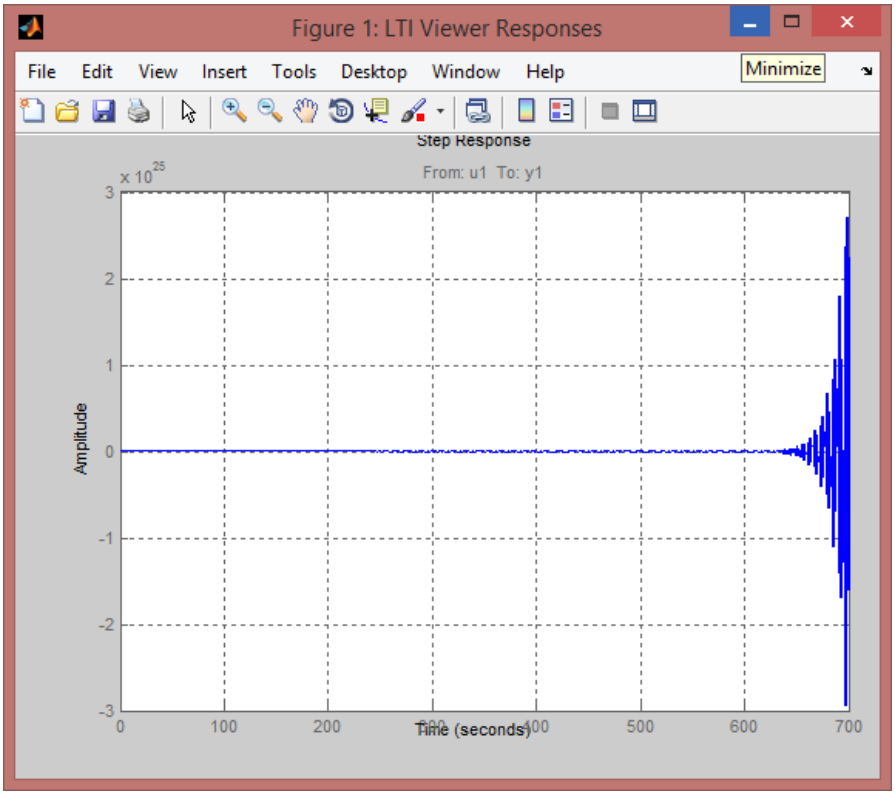

Figure 115: Step response (Level 3 - Nonlinear)

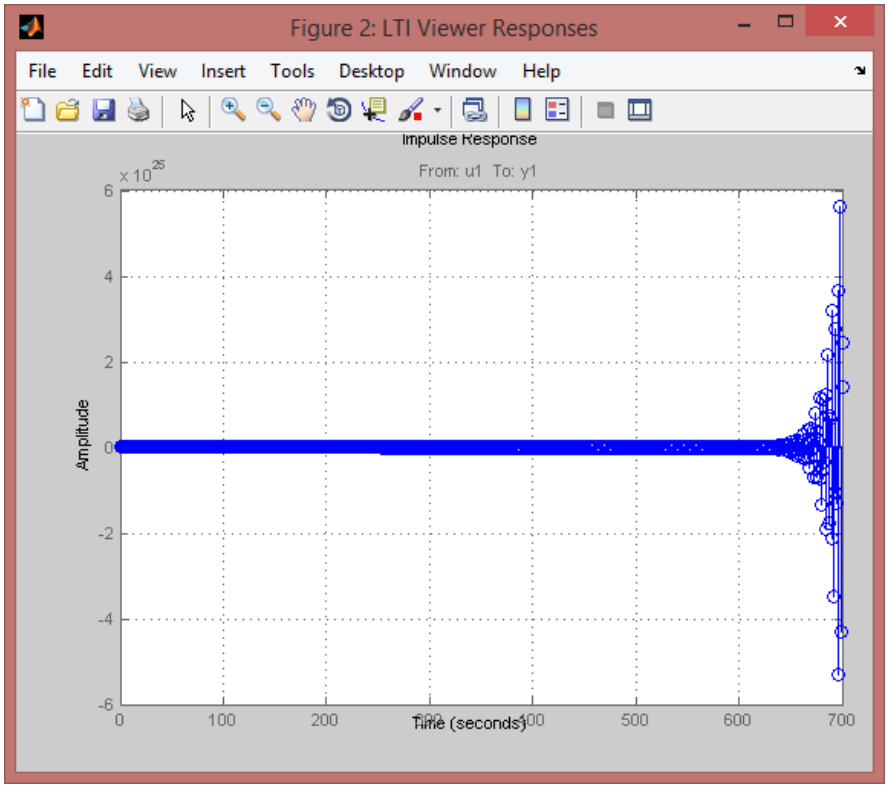

Figure 116: Impulse plot (Level 3 - Nonlinear)

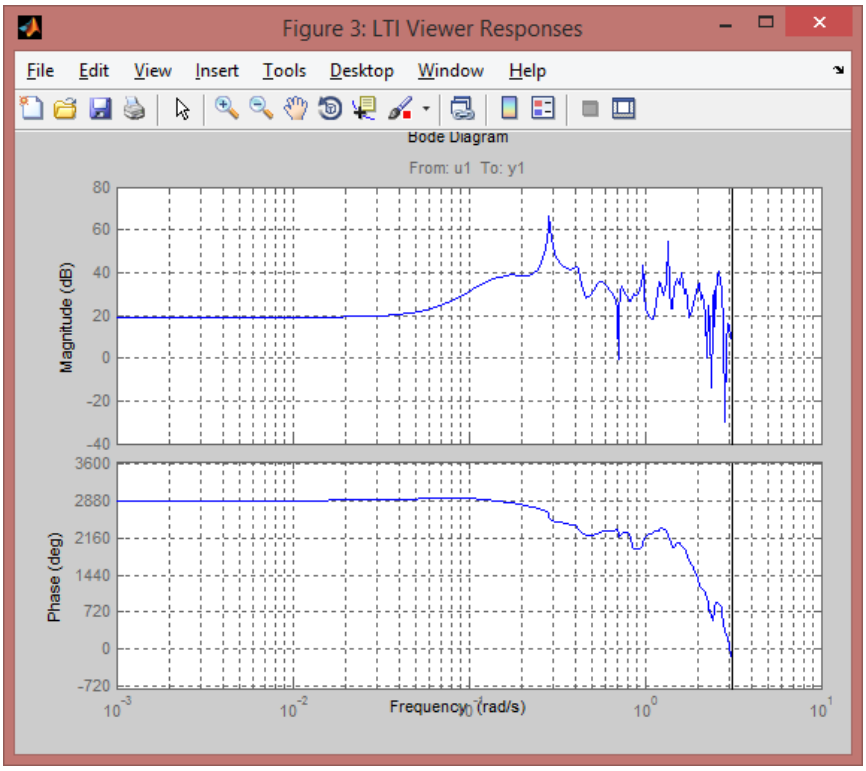

Figure 117: Bode plot (Level 3 - Nonlinear)

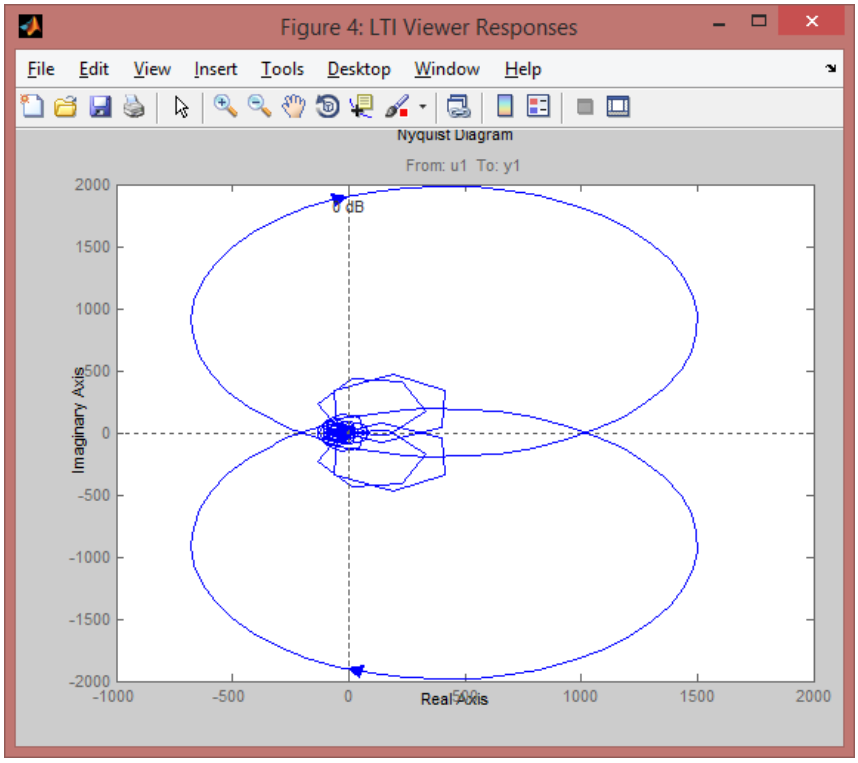

Figure 118: Nyquist plot (Level 3 - Nonlinear)

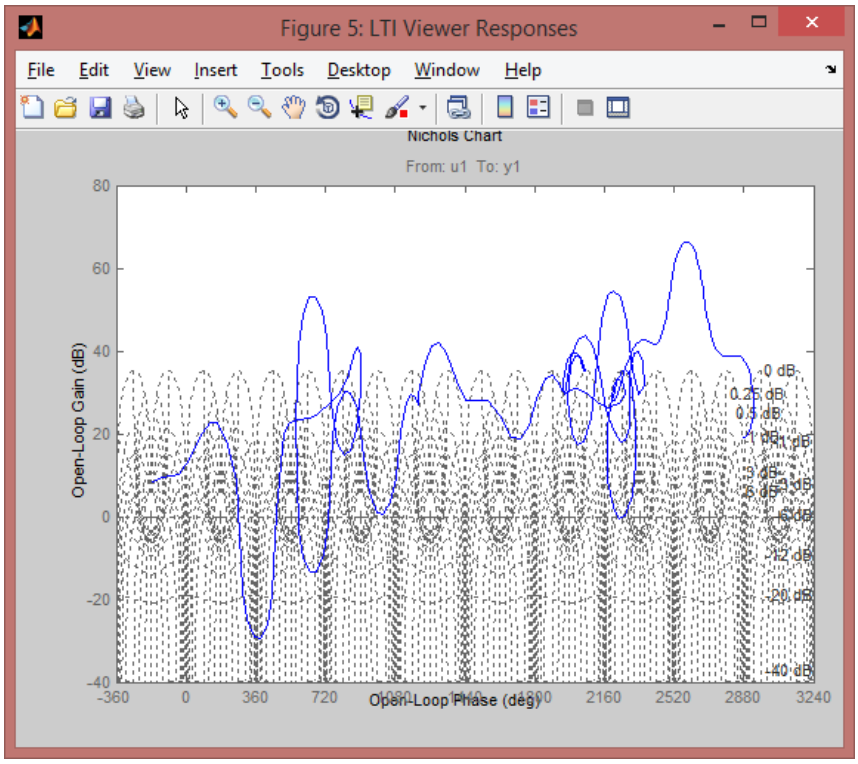

Figure 119: Nichols plot (Level 3 - Nonlinear)

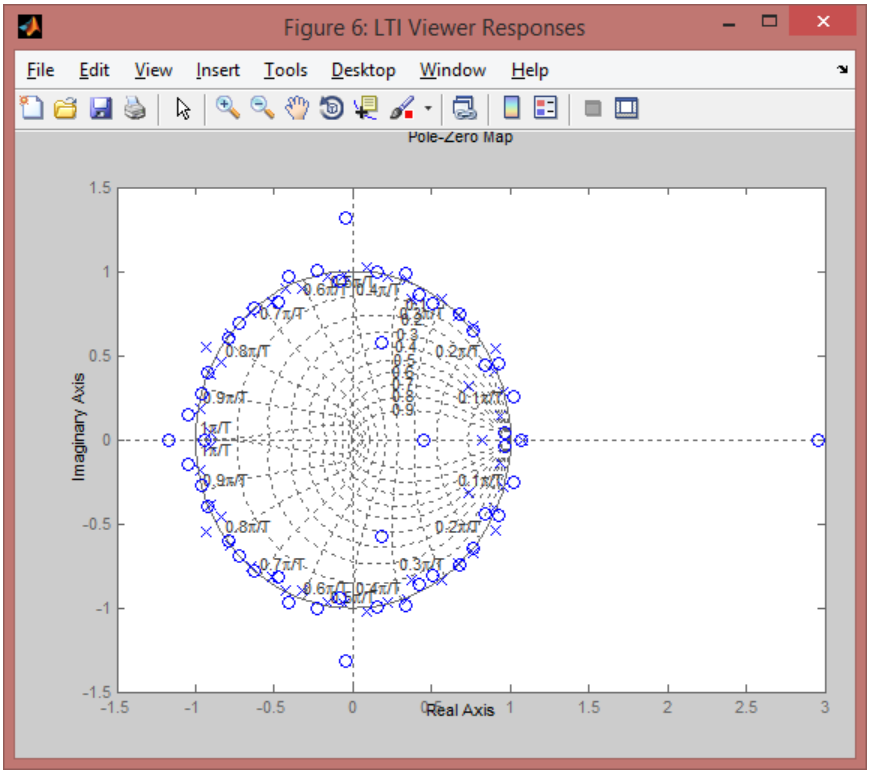

Figure 120: Poles/zero plot (Level 3 - Nonlinear)

Level 4

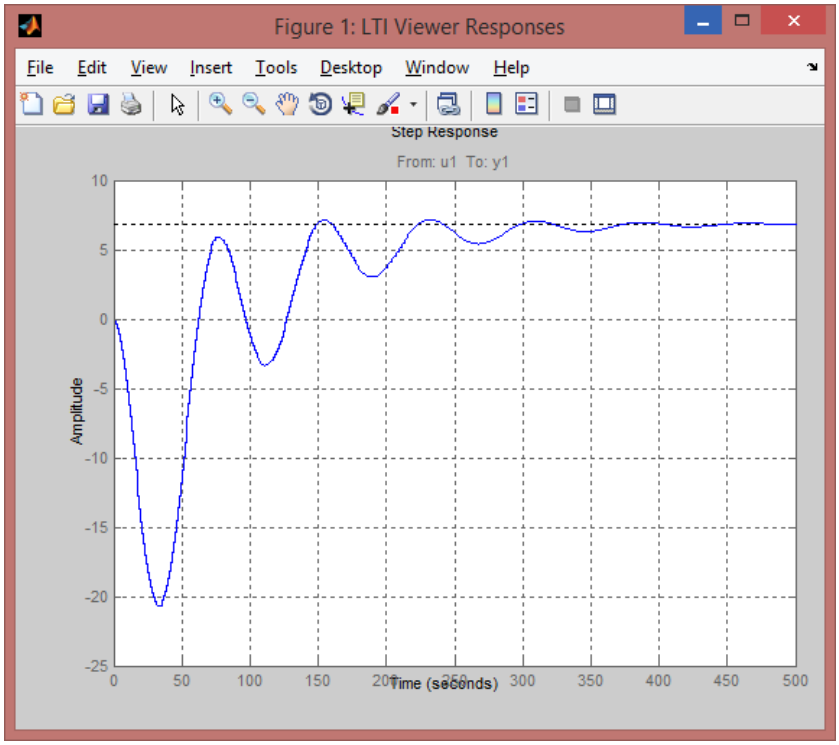

Figure 121: Step response (Level 4 - Nonlinear)

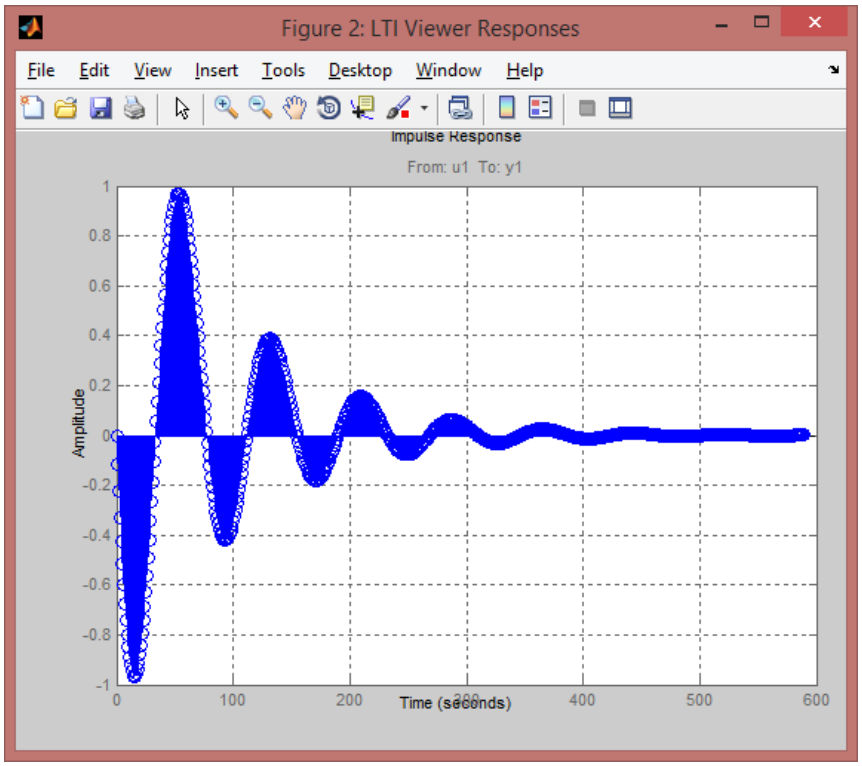

Figure 122: Impulse response (Level 4 - Nonlinear)

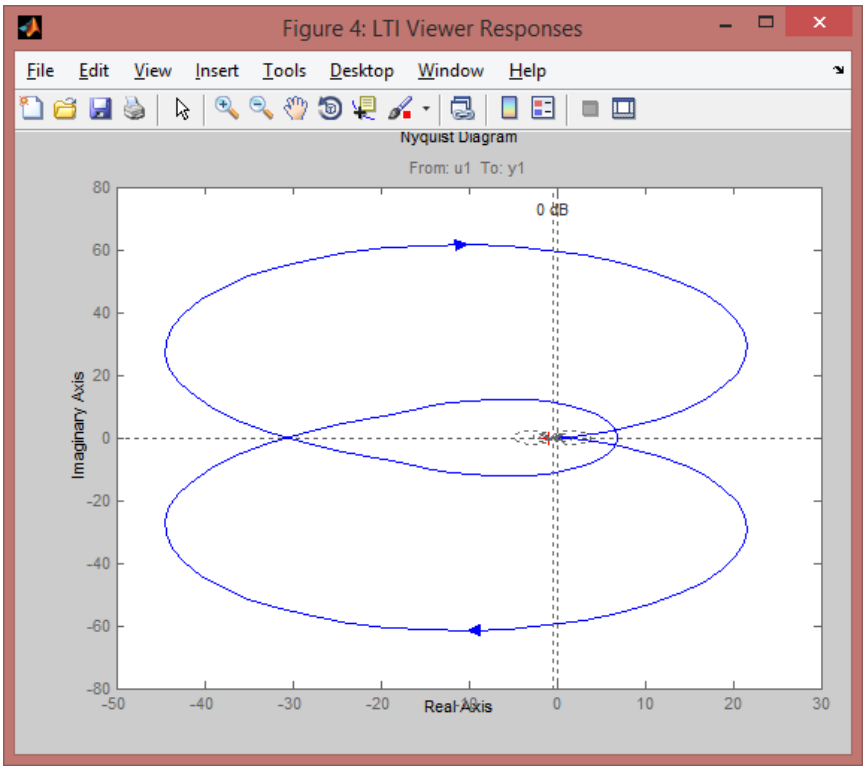

Figure 123: Bode plot (Level 4 - Nonlinear)

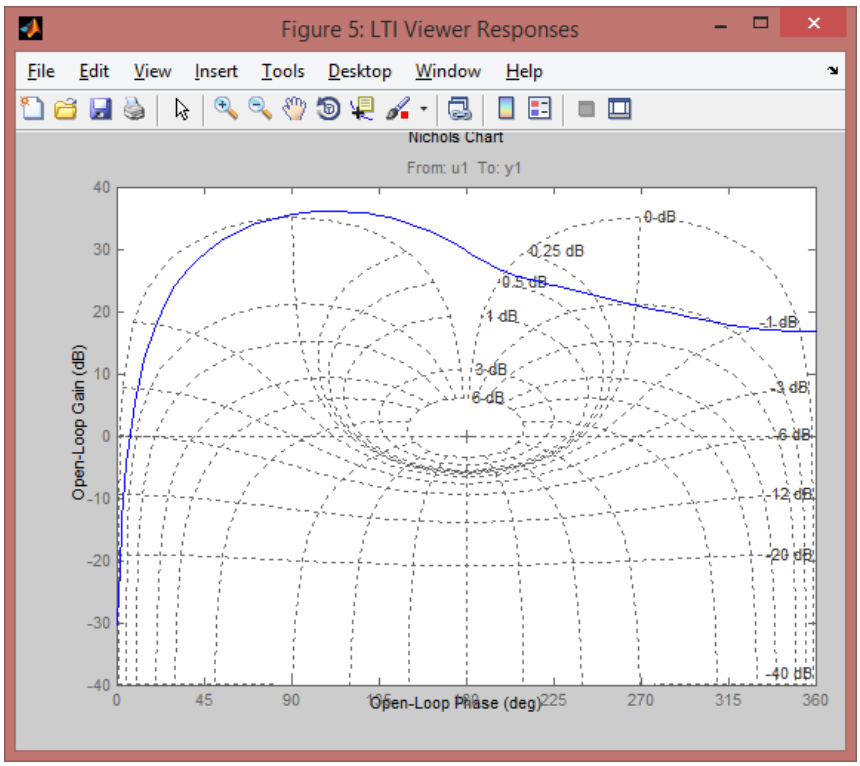

Figure 124: Nyquist plot (Level 4 - Nonlinear)

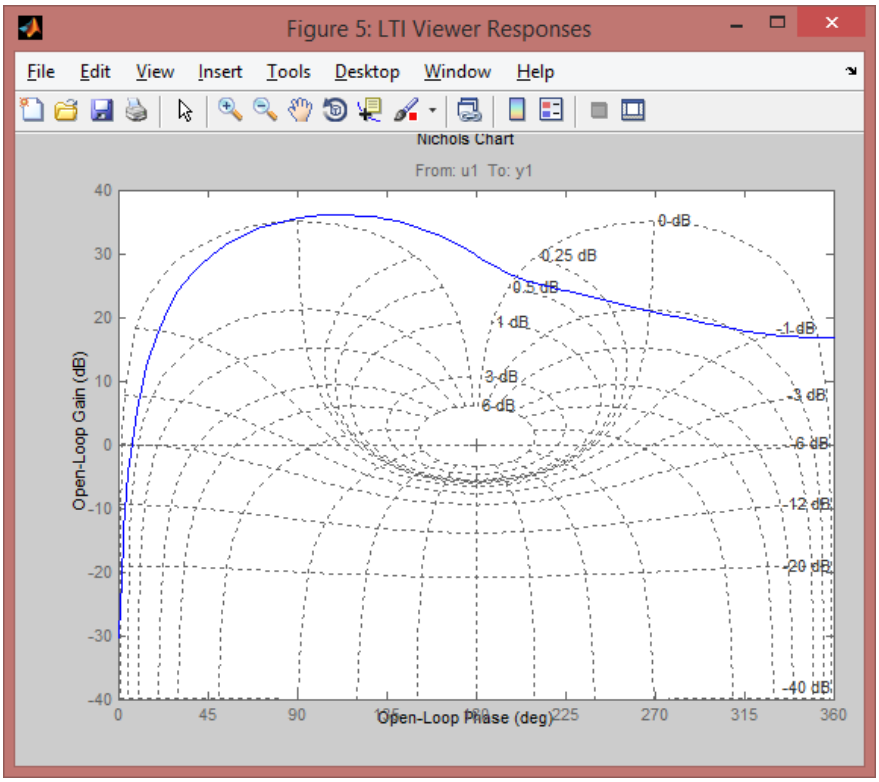

Figure 125: Nichols plot (Level 4 - Nonlinear)

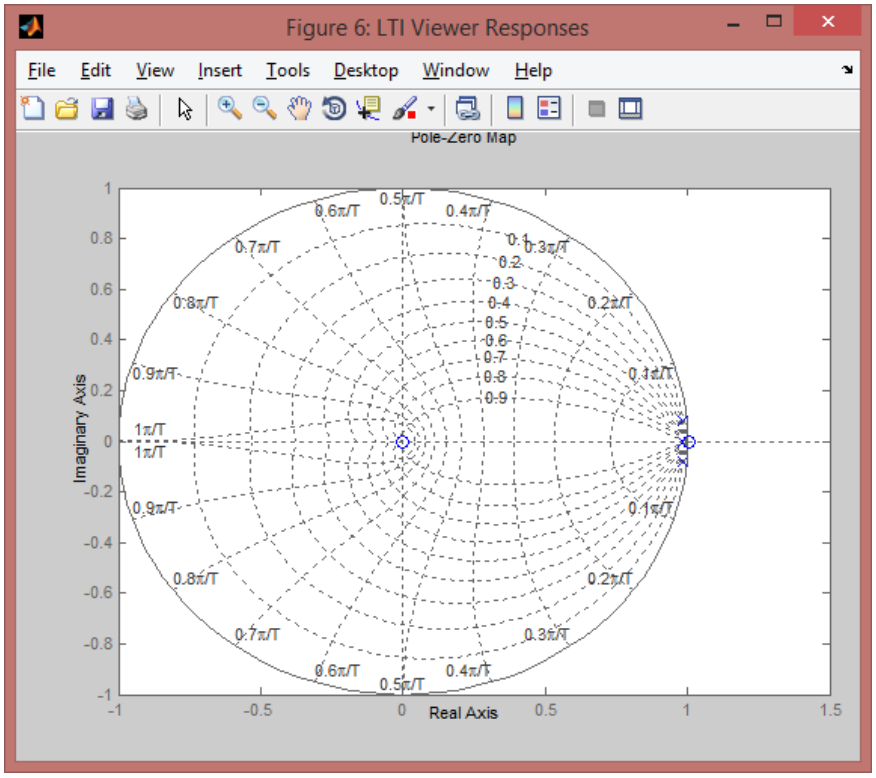

Figure 126: Poles/zero plot (Level 4 - Nonlinear)

Flow 1

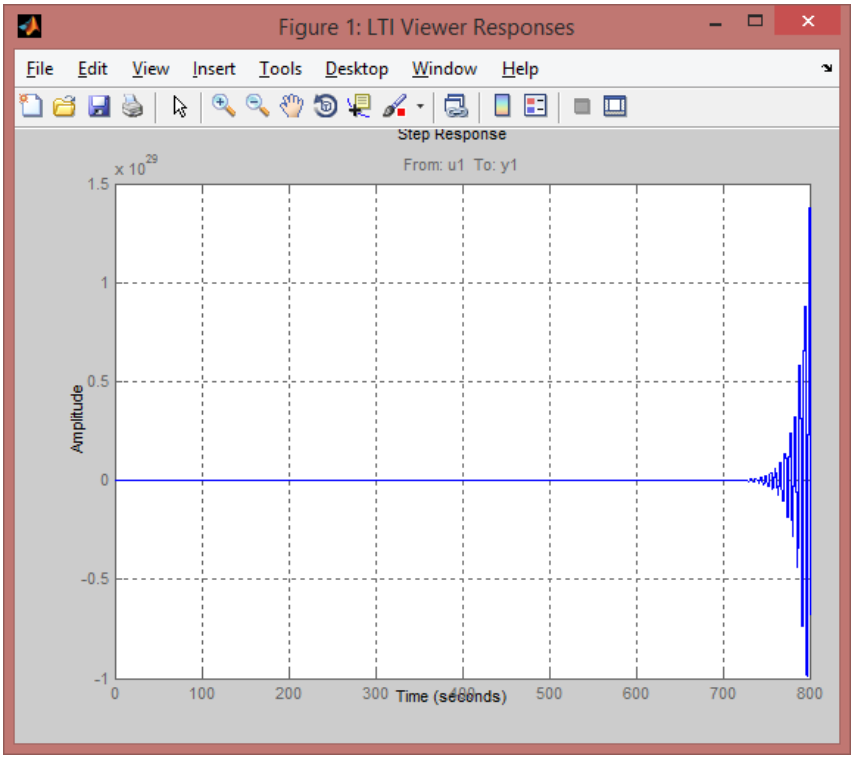

Figure 127: Step response (Flow 1 - Nonlinear)

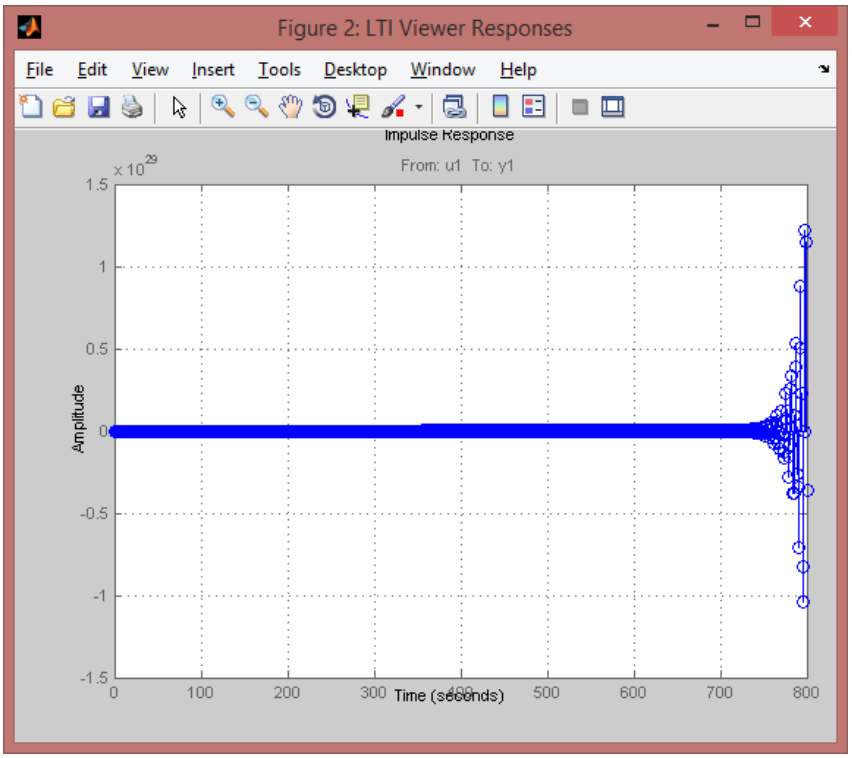

Figure 128: Impulse response (Flow 1 - Nonlinear)

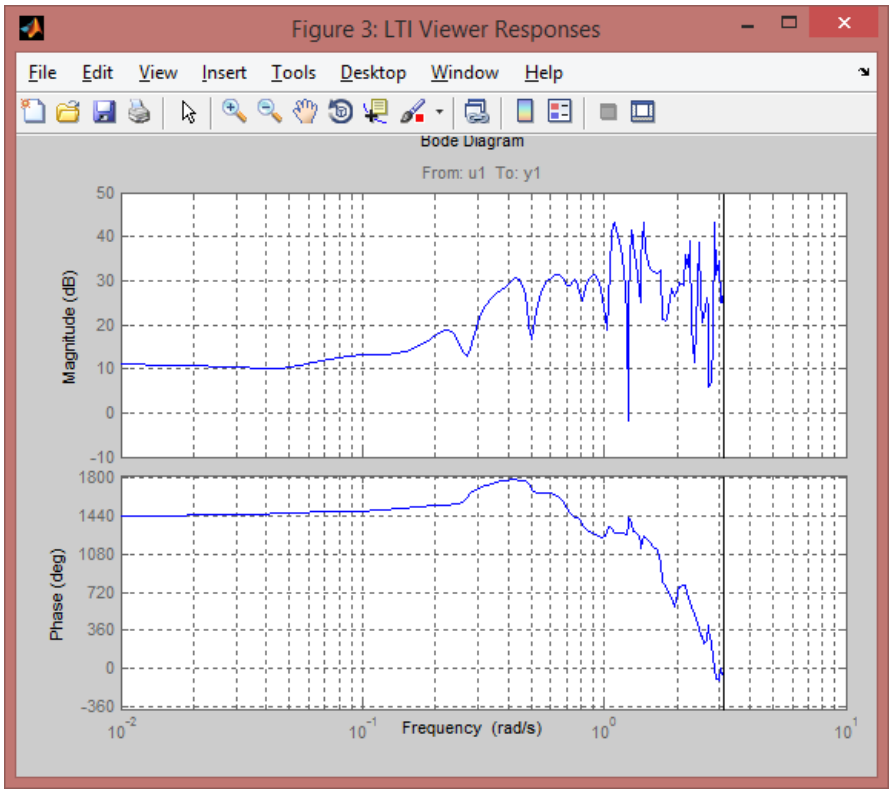

Figure 129: Bode plot (Flow 1 - Nonlinear)

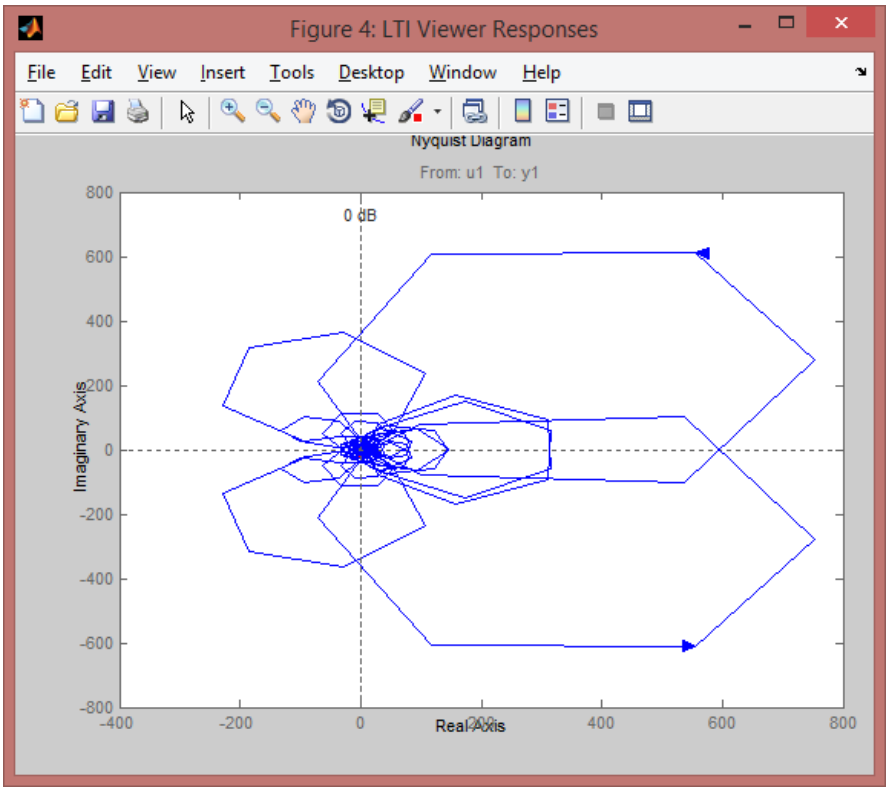

Figure 130: Nyquist plot (Flow 1 - Nonlinear)

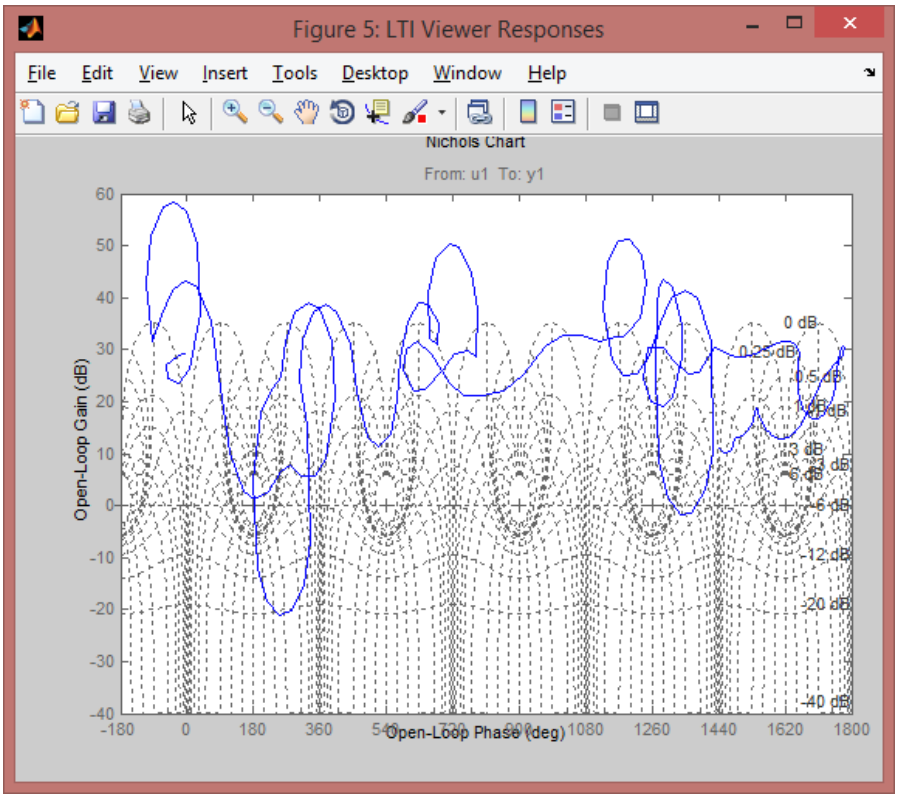

Figure 131: Nichols plot (Flow 1 - Nonlinear)

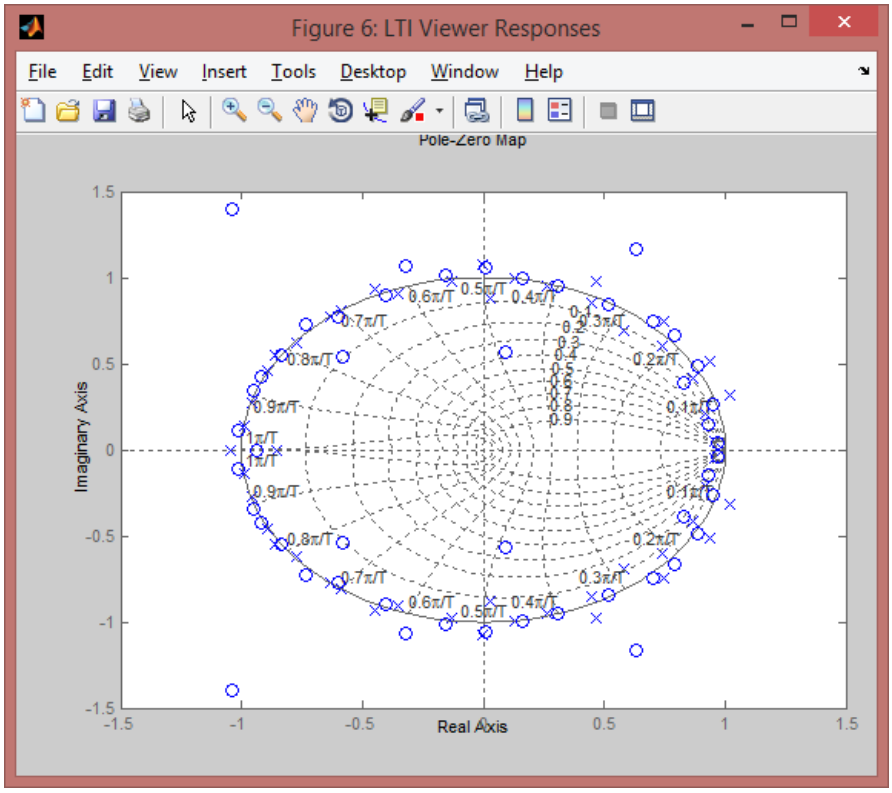

Figure 132: Poles/zero plot (Flow 1 - Nonlinear)

Flow 2

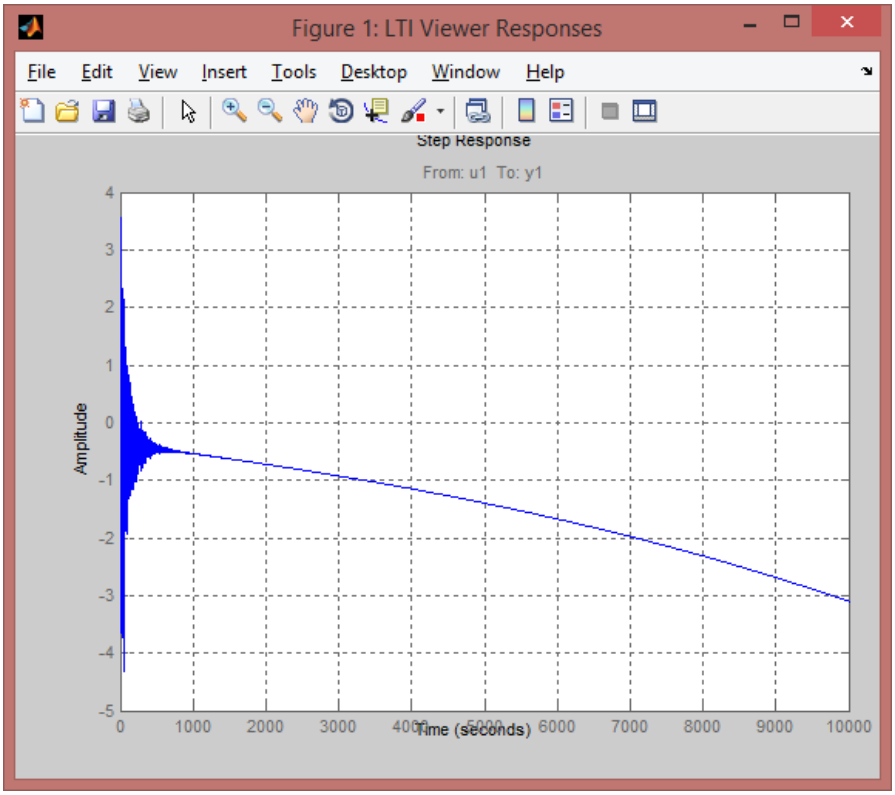

Figure 133: Step response (Flow 2 - Nonlinear)

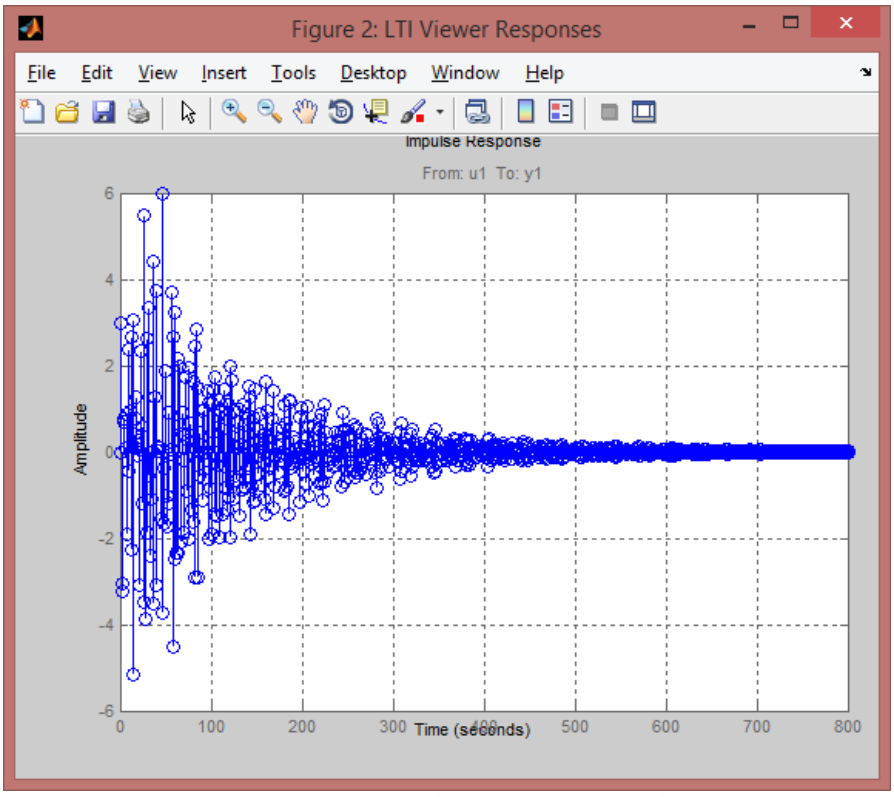

Figure 134: Impulse plot (Flow 2 - Nonlinear)

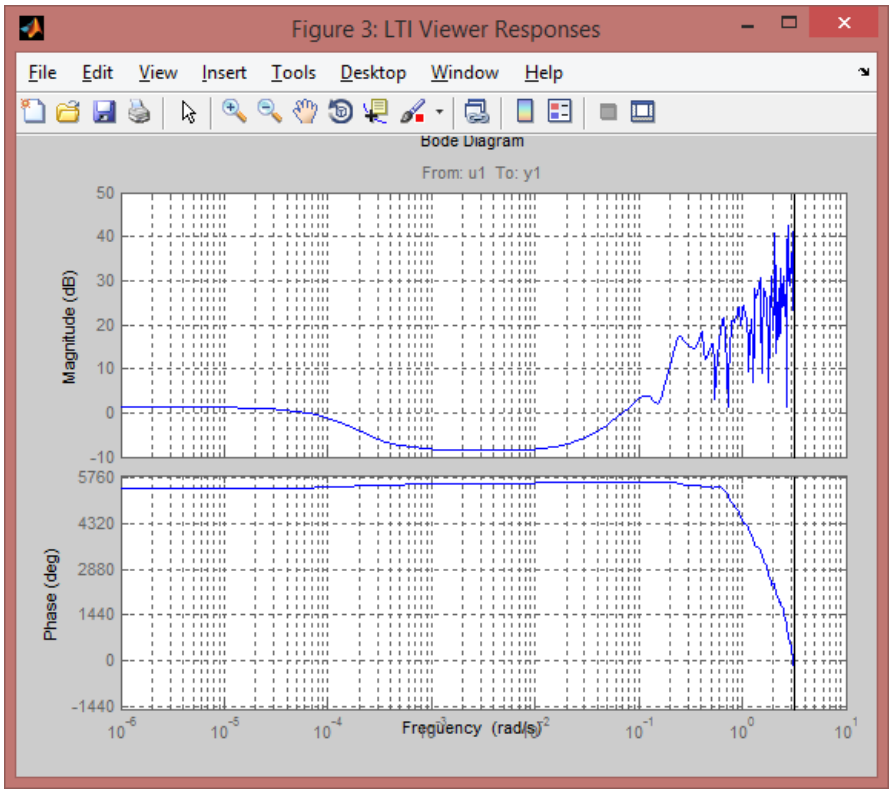

Figure 135: Bode plot (Flow 2 - Nonlinear)

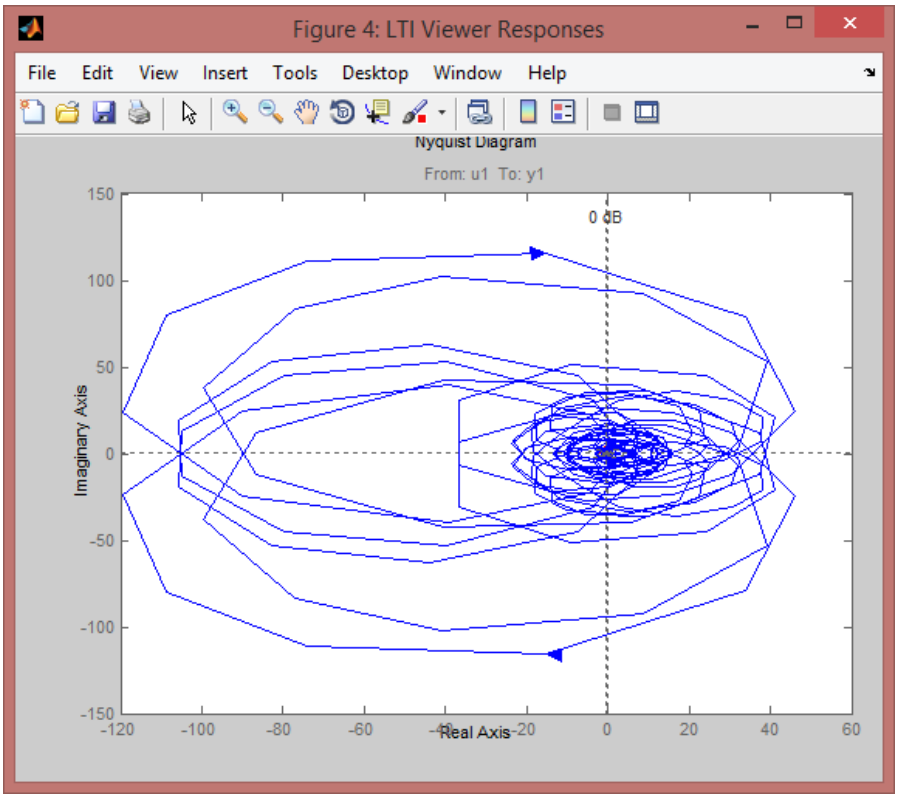

Figure 136: Nyquist plot (Flow 2 - Nonlinear)

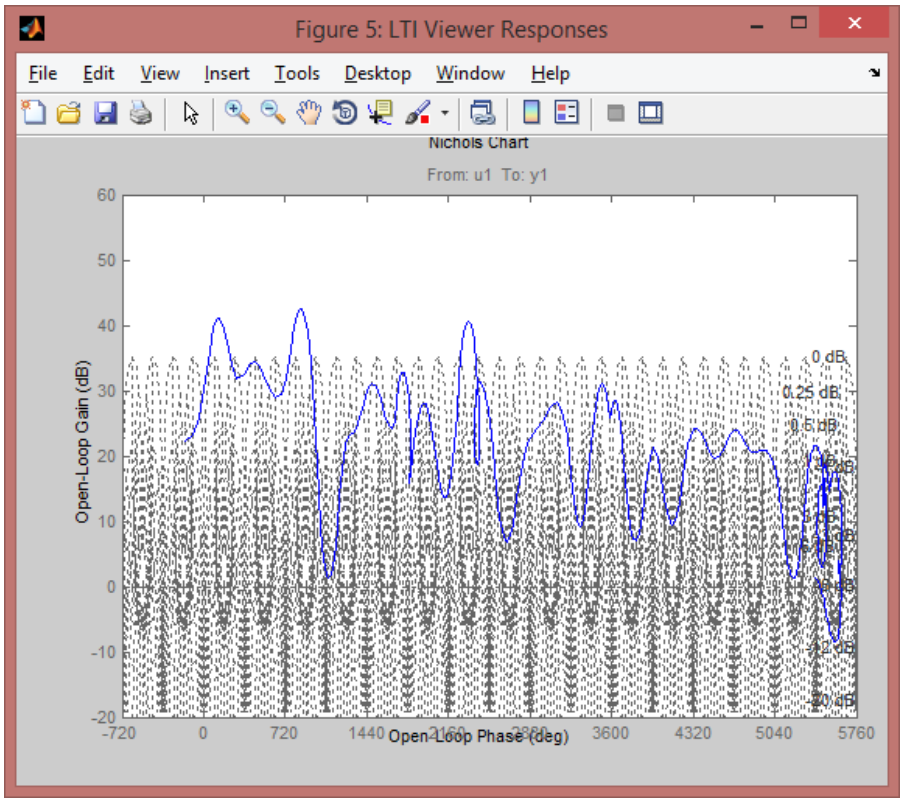

Figure 137: Nichols plot (Flow 2 - Nonlinear)

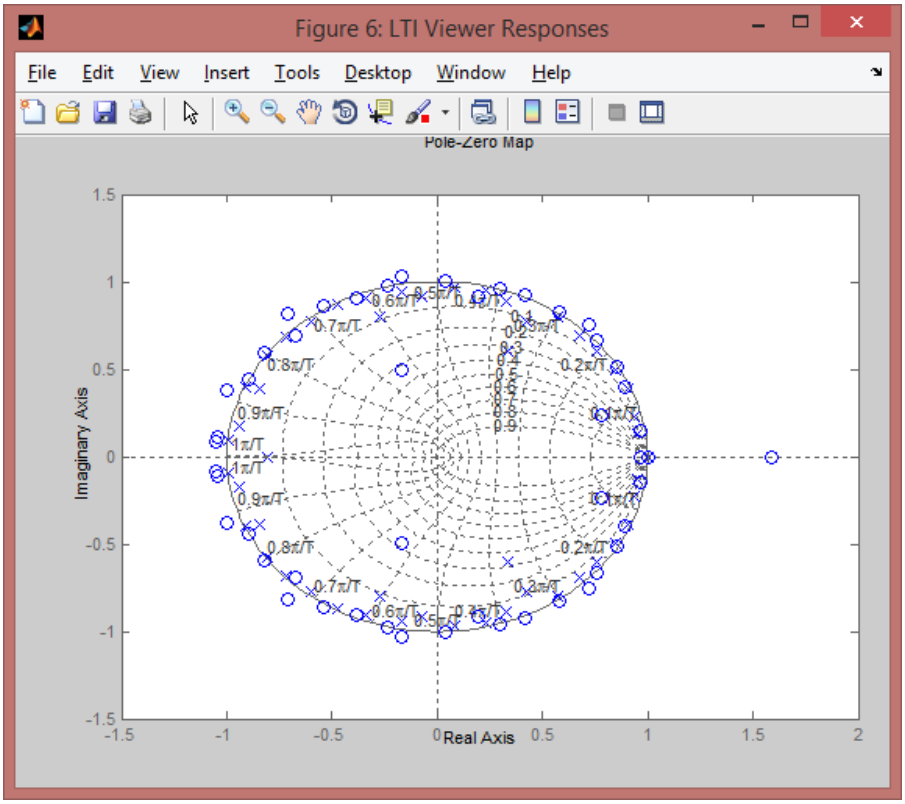

Figure 138: Poles/zero plot (Flow 2 - Nonlinear)

Pressure 1

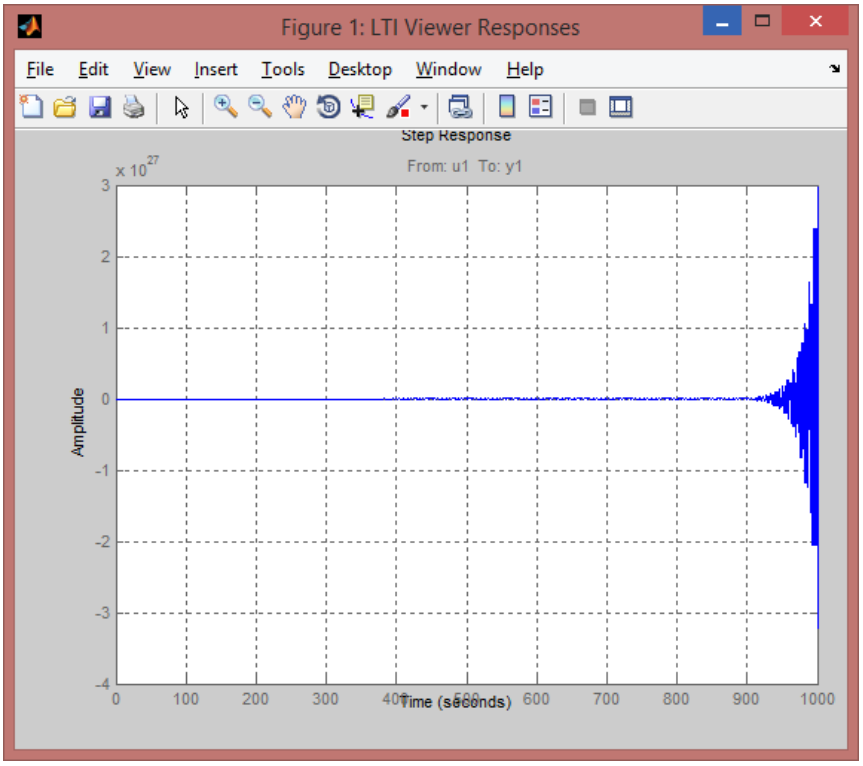

Figure 139: Step response (Pressure 1 - Nonlinear)

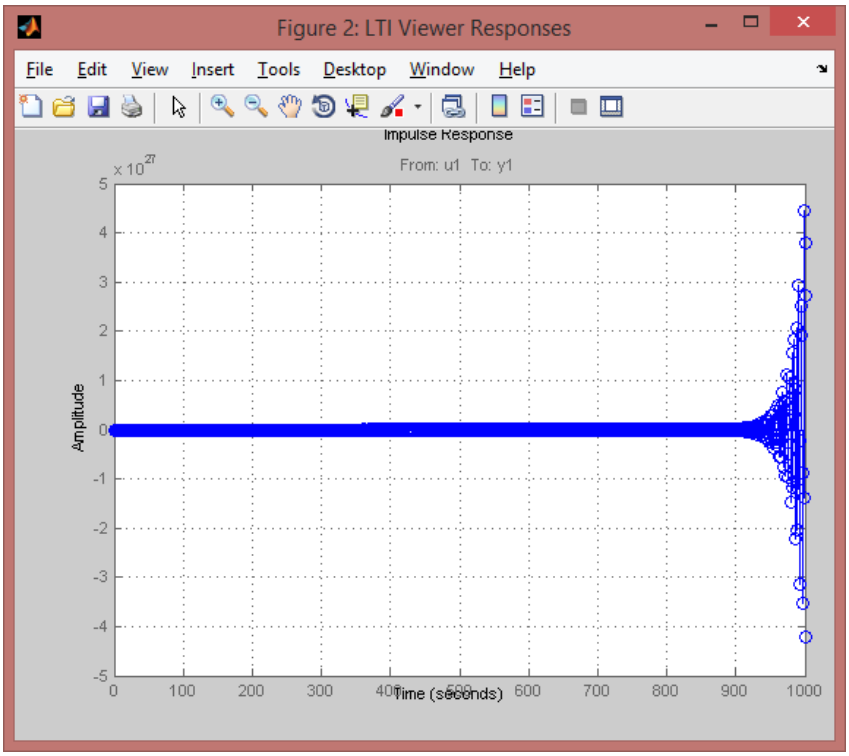

Figure 140: Impulse response (Pressure 1 - Nonlinear)

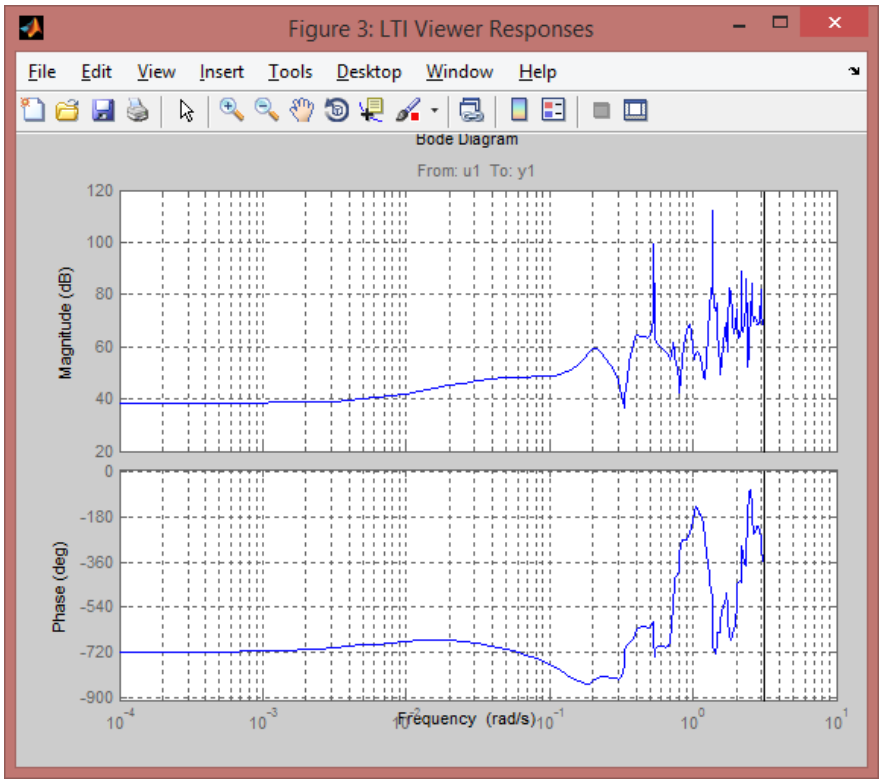

Figure 141: Bode plot (Pressure 1 - Nonlinear)

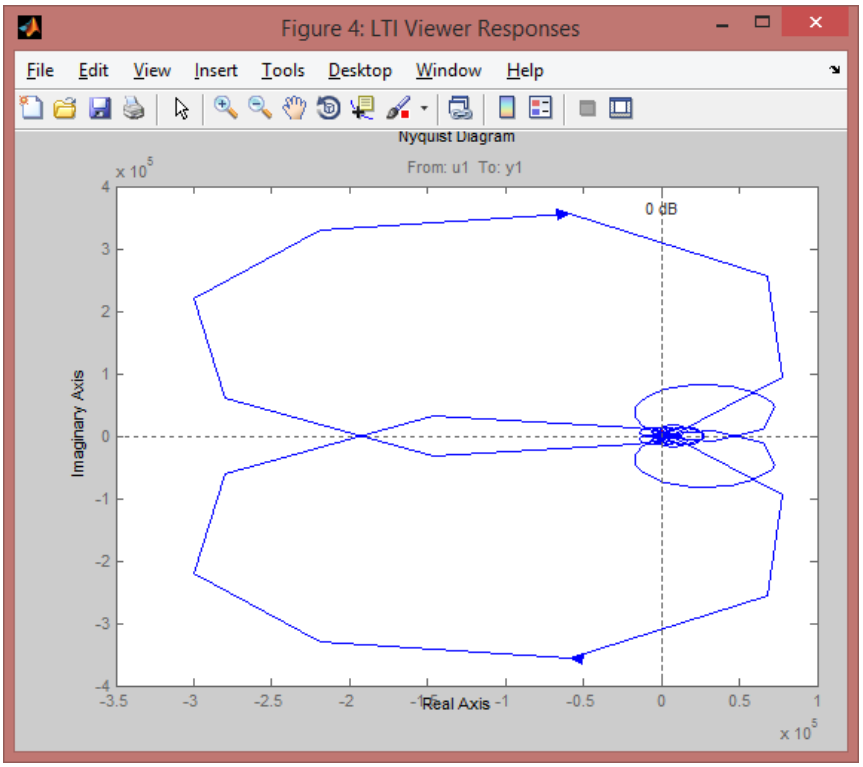

Figure 142: Nyquist plot (Pressure 1 - Nonlinear)

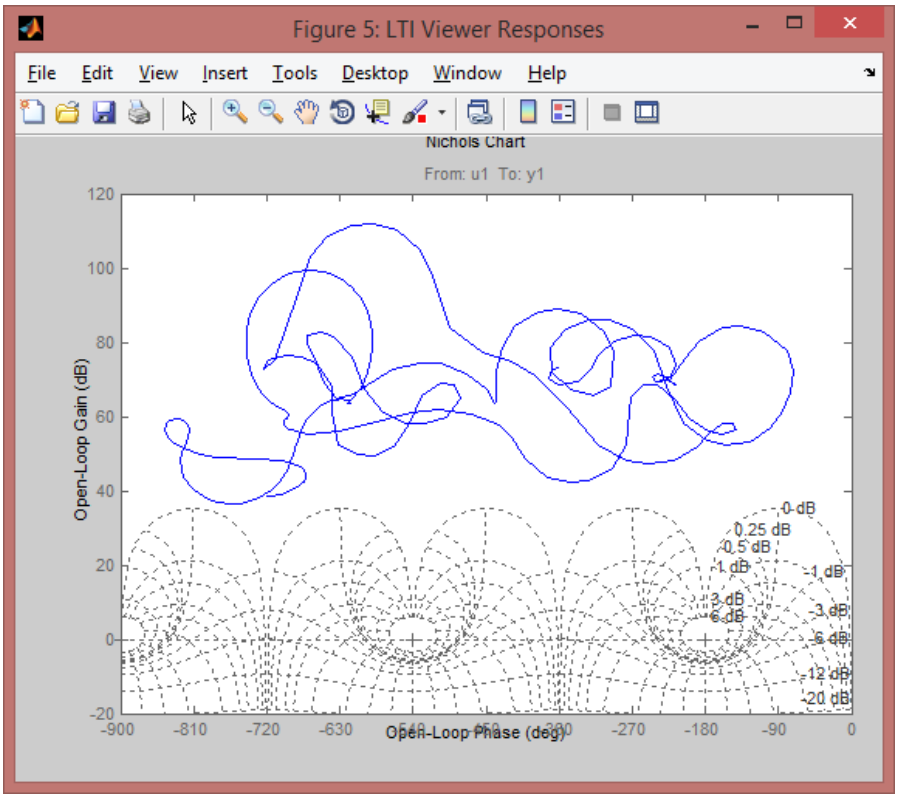

Figure 143: Nichols plot (Pressure 1 - Nonlinear)

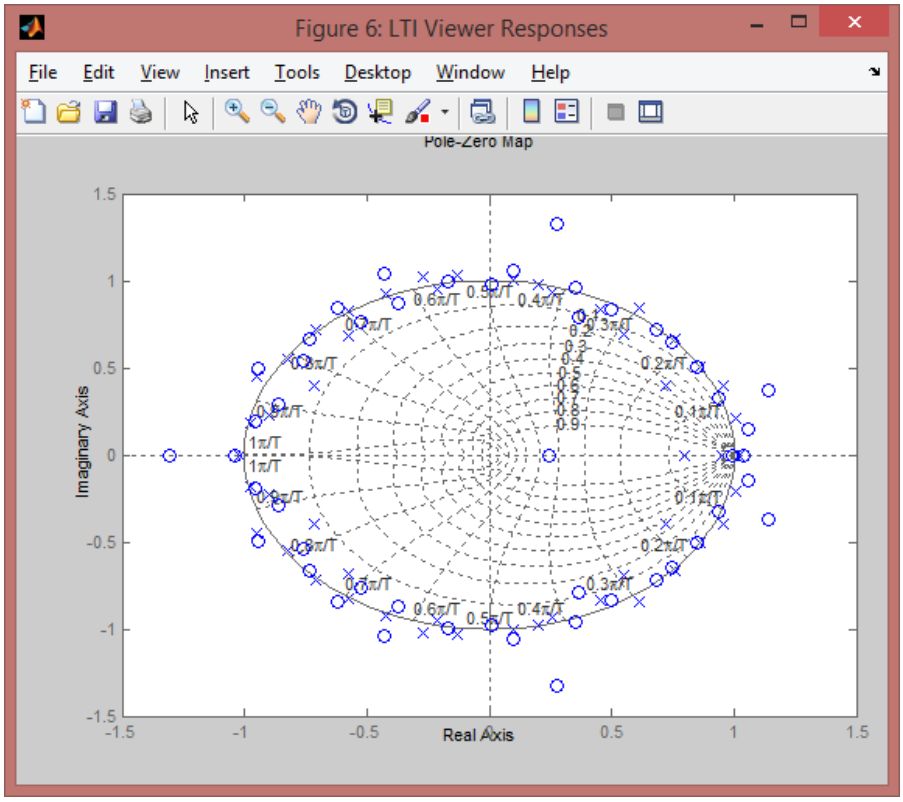

Figure 144: Poles/zero plot (Pressure 1 - Nonlinear)